DISSERTATION | DOCTORAL THESIS

Titel | Title

Functional and evolutionary ecology of the giant ciliate Zoothamnium niveum thiotrophic mutualism

verfasst von | submitted by

Salvador Espada Hinojosa

angestrebter akademischer Grad | in partial fulfilment of the requirements for the degree of

Doctor of Philosophy (PhD)

Wien | Vienna, 2024

Dedicated to the memory of Agustín Antúnez Corrales

and Francisco Macías Ruíz (Paco Bicis)

with whom I shared the SymbioGroup

1

Acknowledgment

Abstract

Interspecific cooperation requires understanding of commodities exchanged between partners. The giant ciliate *Zoothamnium niveum* and its ectosymbiont *Candidatus* Thiobius zoothamnicola is the only sulfur-oxidizing, chemoautotrophic (thiotrophic) association that can be cultivated under controlled conditions. In this study, we corroborate that the symbiont performs sulfide oxidation to gain energy for carbon fixation, and demonstrate the transfer of organic carbon to the host through milking (considered a byproduct benefit) and farming (costly to the symbiont). Further, we recapitulated the breakdown of the association experimentally. When colonies were maintained under oxic conditions without sulfide, colonies and swarmers died in less than 2 days. The reproductive effort of the colonies was maintained during this time, despite a decrease in released swarmers. In another suite of experiments, we show that swarmers disperse in the oxic water column and settle onto sulfide emitting surfaces rapidly. If they do not encounter sulfide, they lose the symbiont within 48 h. Without symbionts, the swarmers grow into a colony whose shape differs from that of symbiotic colonies, being the only case of polyphenism in a mutualism as of yet. Aposymbiotic colonies can live with sulfide, but grow to smaller maximum sizes than under oxic conditions, indicating a detoxification role of the symbionts as an additional byproduct benefit provided to the host. We further show that *Candidatus* Thiobius zoothamnicola has a reduced genome compared to a free-living close relative, in line with theoretical predictions for a vertically transmitted symbiont. Lactate, acetate and urea are possible additional byproduct benefits that could be provided by the host to the symbiont. Finally, we closed the genome of *Candidatus* Endoriftia persephone, the endosymbiont of the deep-sea tubeworm *Riftia pachyptila*. This has in comparison a more versatile metabolism, consistent with its horizontally transmitted symbiont lifestyle. Overall, the giant ciliate mutualism exhibits several byproduct commodities that come without costs and therefore likely allowed the emergence of this mutualism.

Zusammenfassung

Wesentlich für das Verständnis mutualistischer Symbiosen ist jenes über die ausgetauschten Produkte die der Kooperation zwischen den Partnern zugrunde liegen. Der Riesenziliat *Zoothamnium niveum* und sein Ektosymbiont *Candidatus* Thiobius zoothamnicola ist die einzige schwefeloxidierende, chemoautotrophe (thiotrophe) Assoziation, die unter kontrollierten Bedingungen kultiviert werden kann. In dieser Studie bestätigen wir, dass der Symbiont Sulfidoxidation betreibt, um Energie für die Kohlenstofffixierung zu gewinnen, und zeigen den Transfer von organischem Kohlenstoff an den Wirt durch Melken (als Nebenprodukt) und Züchten (kostspielig für den Symbionten). Weiters wurde der Zusammenbruch der Assoziation experimentell untersucht. Unter sauerstoffarmen Bedingungen ohne Sulfid starben sowohl die Kolonien als auch die Schwärmer in weniger als 2 Tagen. Die Fortpflanzungsfähigkeit der Kolonien blieb während dieser Zeit erhalten, es wurden jedoch weniger Schwärmer freigesetzt. In einer weiteren Versuchsreihe zeigen wir, dass sich die Schwärmer in der oxischen Wassersäule ausbreiten und sich schnell an sulfidhaltigen Oberflächen niederlassen. Ohne Sulfid verlieren sie ihre Symbionten innerhalb von 48 Stunden und wachsen zu einer anderen Kolonieform heran als mit Symbionten. Bisher ist das die einzige Beobachtung von Polyphenismus in einer mutualistischen Symbiose. Auch aposymbiotische Kolonien können mit Sulfid leben, erreichen aber eine geringere Maximalgröße als unter oxischen Bedingungen, was auf eine Entgiftungsfunktion der Symbionten als zusätzlichen Vorteil für den Wirt hinweist. Weiters zeigen wir das *Candidatus* Thiobius zoothamnicola im Vergleich zu einem freilebenden nahen Verwandten eine geringere Genomgröße aufweist, was den theoretischen Vorhersagen für einen vertikal übertragenen Symbionten entspricht. Laktat, Acetat und Harnstoff sind mögliche zusätzliche Nebenprodukte, die dem Symbionten vom Wirt zur Verfügung gestellt werden könnten. Zusätzlich schlossen wir das Genom von *Candidatus* Endoriftia persephone, dem Endosymbiont vom Tiefsee Riesen-Röhrenwurm *Riftia pachyptila*. Im Vergleich hat dieser einen vielseitigeren Stoffwechsel, was mit seiner horizontal übertragenen Lebensweise als Symbiont übereinstimmt. Insgesamt weist der Mutualismus der Riesenzilien mehrere Nebenprodukte auf, die keine Kosten verursachen und daher eine *de novo* Evolution für diesen Mutualismus begünstigen.

Table of contents

Introduction

Symbiosis, the living together of unlike organisms (de Bary 1879), plays a key role in the evolution of life. The description of symbiosis in terms of costs and benefits is widespread, whether limited to mutualistic relationships with benefits to the partners, as defined by Pierre-Joseph van Beneden (1876), or more commonly used for associations involving two or more species living in physical contact with each other at least temporarily (de Bary 1879). When harmful effects reduce the number of offspring of a partner while enhancing the reproductive output of the other partner, the relationship is termed parasitic.

Mutualism between microbial symbionts and eukaryote hosts is of fundamental ecological and evolutionary importance (Douglas 2010, McFall-Ngai et al. 2013, Bronstein 2015). Such beneficial associations thrive in virtually every ecosystem on Earth, from tropical rainforests to high altitudes on mountains, from shallow-water corals reefs to deep-sea hydrothermal vents. What was once considered an evolutionary oddity is now well recognized as ubiquitous in nature (see Sapp 2004). Virtually all animals live with more or less complex microbial communities in their intestinal tracts, including humans. Most vascular plants associate with microbes on or in their roots. Most microbial symbionts are bacteria, many are microalgae, and a few are archaea (Douglas 2010). Such microbe – eukaryote mutualisms are remarkably diverse with respect to the number of microbial partners, cooperative traits, symbiont location on or in the host, specificity for a certain range of partner species, dependence on the partner, and mode of symbiont transmission from one host generation to the next (Bright and Bulgheresi 2010, Douglas 2010, Bronstein 2015).

Cooperative traits are central for the interacting partners according to the accrued costs of producing benefits for the partner and their impact on the receiving partner. The degree of cooperativeness (from highly cooperative to uncooperative) of a single genotype may vary with environmental context (Jones et al. 2015). Most often partners trade in several, different, and often complementary goods and services (Janzen 1985) that one partner needs and the other can provide. Such cooperative traits may be morphological, physiological or behavioral commodities. They serve to categorize mutualisms into three

categories according to their main function, transportation (dispersal, mobility), protection, or nutrition (Douglas 2010, Bronstein 2015). Cooperative traits may have evolved at least partially because of their beneficial effect on the partner (West et al. 2007). Alternatively, they may have evolved as selfish traits that incidentally benefit the partner (byproduct benefits, West-Eberhard 1975, Connor 1986, Sachs et al. 2004). Both adaptive cooperative traits involve costs to produce them, either as benefits for the partner with costs to oneself (costly benefits) or as benefits to oneself that exceed the costs (byproduct benefits, Hauert et al. 2006). Trait loss in the receiving partner may be the result of compensation of trait function by the providing partner (Connor 1995, Ellers et al. 2012).

Theory predicts that benefits are provided at a cost to increase the partner's fitness without guarantee of reciprocation (Trivers 1971). Therefore, each partner faces the temptation to shirk the costly investments in the other and instead allocate all resources to their own offspring. However, both partners are better off mutually cooperating than mutually shirking. This creates a social dilemma, a conflict of interest between individual partners and the associated pair, that has attracted much attention in evolutionary biology (Bergstrom et al. 2003, Sachs et al. 2004, Lehmann and Keller 2006, Foster and Wenseleers 2006, West et al. 2007, Gardner and Foster 2008, Leigh 2010, Bshary and Bronstein 2011, Werner et al. 2014, West et al. 2015). Also, evolutionary game theory models mutualism but uses a game theory approach, in its simplest constellation with two partners (a host and a symbiont) and two adaptive strategies (cooperate and defect), thus referred to as a 2x2 game. The cooperator provides benefits to the partner and the defector (cheater) does not or only at reduced levels (Mar and Denis 1994, Roberts and Sherratt 1998, Doebeli and Knowlton 1998, Killingback and Doebeli 1998, Killingback et al. 1999, Killingback and Doebeli 2002).

The evolutionary outcome of 2x2 games depends on the costs to provide benefits. In the Prisoner's Dilemma costs exceed the benefits to self and hence cheaters dominate over cooperators (Trivers 1971, Axelrod and Hamilton 1981, Doebeli and Knowlton 1998, Roberts and Sherrat 1998, Killingback et al. 1999, Hauert et al. 2006). In contrast, in byproduct mutualism, the benefits to oneself exceed the costs, allowing cooperators to outcompete cheaters (Hauert et al. 2006). In this case, selfish traits that incidentally benefit the partner are exchanged between both partners (West-Eberhard 1975, Brown 1983, Connor 1986,

Sachs et al. 2004). In pseudo-reciprocity one partner provides an incidental byproduct benefit to other, who reciprocates with a costly benefit to the actor (Connor 1986, 1995). In this asymmetric situation (Sachs et al. 2004), cooperators providing a byproduct benefit outcompete cheaters, while cooperators, providing costly benefits, are dominated by cheaters. Therefore, neither the reciprocity in the Prisoner's dilemma nor pseudo-reciprocity allows for cooperation to evolve unless mechanisms promote cooperators to interact more often with each other than with noncooperators (Trivers 1971, Hamilton 1975).

Positive assortment between the focal genotype and phenotypes with cooperative traits is identified as the most fundamental requirement for the evolution of mutualism (Queller 1985, Fletcher and Doebeli 2009). The cooperative symbiont genotype must receive more benefits from the host individual than less or non-cooperative symbiont genotypes. Likewise, the cooperative host genotype must receive more benefits from the individuals of the symbiont population than less or non-cooperative host genotypes. To increase its frequency in a population of individuals with different levels of cooperativeness, the cooperative genotype must be overcompensated for its benefits provided to the partner by receiving benefits from the partner (Queller 1985, Fletcher and Doebeli 2009).

Positive assortment may arise in microbe – eukaryote mutualism through different mechanisms: 1) Partner choice, where symbiont recruitment in horizontally transmitted symbionts is through preferential selection of cooperating symbionts from the environment (Bull and Rice 1991, Noe and Hammerstein 1994, Sachs et al. 2004, Foster and Kokko 2006). Signaling or screening are identified as two ways of symbiont recruitment (Archetti et al. 2011). 2) The loner strategy with limited dispersal describes optional interactions and provides an escape hatch out of states of mutual defection (Hauert et al. 2002, Semmann et al. 2003, Izquierdo et al. 2010). Such non-participating loners are facultative partners that have the option to leave (or ostracize the other) and to revert to an aposymbiotic life at least for some time (Hauert et al. 2008). 3) Partner fidelity feedback, allows the partners to adjust their response to the received benefits (Doebeli and Knowlton 1998, Fletcher and Zwick 2006), thus promoting positive feedbacks that may result in coupling of fitness (Bull and Rice 1991, Frank 1996, Sachs et al. 2004). 4) Punishment requires a separate

mechanism, which enables punishers to inflict costs on the cheater at costs to themselves (Boyd and Richerson 1992, Clutton-Brock and Parker 1995, Boyd et al. 2010, Hauert et al. 2007, Hauert et al. 2008). Punishment creates a so-called second order dilemma because cooperators that do not punish (and hence have higher fitness) outperform the punishers with higher costs (resulting in lower fitness) (Yamagishi 1986, Clutton-Brock and Parker 1995, Boyd and Richerson 1992, Sigmund et al. 2001, Boyd et al. 2010). Also, punishment (as well as cooperation) is more likely to occur and persist if interactions are voluntary with facultative partners rather than only obligate partners (Hauert et al. 2008). In this case four strategies are possible – to cooperate, to defect, to be a loner, or to punish (Hauert et al. 2008).

Regardless of the development of a theoretical framework, there has been little connection between theory and empirical research so far, aside from a few microbe-eukaryote model systems in plants, e.g. legumes (Kiers and Denison 2008, Sachs et al. 2013, Werner et al. 2015) and mycorrhiza (Kiers and Denison 2008, Kiers et al. 2011). The main reason is probably that most symbiotic mutualisms cannot be maintained for a longer time under laboratory conditions let alone cultivated and, furthermore, in many of them the partners cannot be separated to grow and reproduce without the other. The lack of cultivation is the case in all but one of the thiotrophic symbioses, associations between sulfur-oxidizing, chemoautotrophic bacteria and animal or unicellular eukaryote hosts (Cavanaugh 2006, Dubilier et al. 2008, Sogin et al. 2021). The thiotrophic mutualism between the giant ciliate *Zoothamnium niveum* and a single bacterial partner is the exception and the main topic of my thesis.

I will introduce my work (subdivided in six chapters, two publications as first author and four as co-author) in the theoretical framework of evolutionary game theory to show how it influenced empirical research. Studies on the colonial ciliate *Zoothamnium niveum* spans centuries of science. Naturalists described the species as snowy white already in the early 19th century (Hemprich and Ehrenberg, 1831). In the second half of the 20th century, electron microscopy fully revealed the nature of this microbial symbiosis consisting of two partners (Bauer-Nebelsick et al., 1996a, b). Now, molecular techniques and metagenomic approaches enable to elucidate potential functions and interactions in this binary

relationship between the colonial ciliate and a monospecific population of the bacterial ectosymbionts *Candidatus* Thiobius zoothamnicola (Rinke et al. 2006) covering the host.

Chapter 1 reviews the knowledge about the symbiosis between *Zoothamnium niveum* and *Candidatus* Thiobius zoothamnicola at the time of starting the PhD project (**Bright et al. 2014**). The review shows that both partners belong to higher taxa prone to establish symbiosis. The colonial host cell typology includes dividing cells (terminal zooids), feeding zooids (microzooids), and dispersal stages (called macrozooids during development on the colony, called swarmers once they detach). The bacterial symbiont can be specifically visualized through fluorescence *in situ* hybridization, showing that the ectosymbiont covers in a perfect monolayer the colonies and the swarmers. Symbiont transmission is vertical when symbiotic swarmers leave the colony to disperse in the water column and settle at sulfide-emitting surfaces to found new colonies. The geographical distribution is extremely widespread in temperate and tropical regions all around the world, in habitats of decaying organic matter in marine shallow waters. Cultivation of the association under controlled concentrations of oxygen and sulfide revealed that fitness was higher with low sulfide than with high sulfide concentrations. The exchange of commodities between partners is proposed as byproduct benefits in both directions, with the colonial ciliate facilitating access to oxygen and sulfide to the bacterial symbiont by its self-serving behavior of contractions and expansion and ciliary beating, and the symbiont providing fixed organic carbon leaking from the symbiont passively and taken up by the host. This association therefore is postulated as putative byproduct mutualism.

Chapter 2 investigates the nutritional exchange between partners in the *Zoothamnium niveum* symbiosis (**Volland et al. 2018**). Previous work on the symbiosis of the giant tubeworm *Riftia pachyptila* (Bright et al. 2000) had shown with ^{14}C bicarbonate pulse-chase experiments and tissue autoradiography the action of both milking (leakage of low molecular weight organic carbon molecules from the symbiont into host cells) and farming (digestion of symbiont cells by host cells). In contrast, symbiosis between the ciliate *Kenthrophoros* spp. with the gammaproteobacterium *Candidatus* Kentron has been proposed to perform chemoheterotrophy based on the absence of canonic genes for autotrophic CO_2 fixation (Seah et al. 2019). The nutritional relationship between the two

partners in the *Zoothamnium niveum* symbiosis is characterized through the use of ^{14}C bicarbonate experiments and tissue autoradiography and ^{13}C bicarbonate experiments and NanoSIMS, addressing whether the symbiont is the site of organic carbon incorporation, and whether there is direct uptake by the host of organic compounds released by the symbiont cells and/or host digestion.

Chapter 3 investigates the fate of both partners under sulfide deficiency (**Espada-Hinojosa et al. 2022**). Sulfide, key in all thiotrophic associations and also in the *Zoothamnium niveum* symbiosis, however, is known to be variable in time and space (Bright et al. 2014). While sulfide leaks from disturbed mangrove peat surfaces on which the symbiosis grows, the leakage ceases when the area gets overgrown by microbes (Ott et al. 1998). During wood or seagrass degradation sulfide is only produced during a short time and therefore restricts the presence of the symbiosis to this time period (Laurent et al. 2009). We studied in detail the response of the symbiont and how long the colonies and their swarmers survive under sulfide starvation. Because many organisms increase their effort in reproduction when faced with adversity (Stelzer 2001), we specifically studied whether the ciliate colony responds also with additional production of swarmers. For such experimental studies the ciliate symbiosis is highly suited because they have much shorter generation times than animals.

Chapter 4 describes an unexpected discovery in the course of experimental work (**Bright et al. 2019**) for which the first indications were already produced during cultivations published in 2007 (Rinke et al. 2007). It was found that growth and reproduction of colonies happens also when sulfide is absent, but is much lower than under oxic conditions supplemented with sulfide (Rinke et al. 2007). This phenomenon was not explained at that time. During new cultivation experiments we performed during my PhD we observed the occurrence of strange pale colonies next to the typical white colonies in flow through experiments under oxic and sulfide supplemented conditions. The white color of *Zoothamnium niveum* is due to the elemental sulfur granules that is stored in the periplasm of the symbionts (Maurin et al. 2010). While our aim was to answer the question why did colonies turn pale under sulfidic conditions and whether they were still covered with symbionts, we also were puzzled with the fact that they looked different. Therefore, we performed a suite of experiments and discovered an unexpected phenomenon, a polyphenism in *Zoothamnium niveum*.

Polyphenism, a special type of phenotypic plasticity with discrete phenotypes, is well known in parasitic, competitive and predator-prey relationships, as in the case of the water flea *Daphnia lumholtzi* (Agrawal 2001). These water fleas grow a sharp helmet and an extended tail spine when exposed to fish predators, but do not have these morphological features when the predator is absent. In Chapter 4 we investigated the fate of the symbionts on swarmers in the absence of sulfide, what triggers settlement in the giant ciliate symbiosis and studied whether it is possible that swarmers settle under oxic conditions and also grow (Bright et al. 2019). We show that presence of sulfide during swarmer dispersal leads to continuation of symbiosis, while lack of sulfide leads to loss of the symbiont in swarmers that triggers polyphenism in the colony. Thus, we can find a symbiotic morphotype (often white) and an aposymbiotic morphotype (pale), the latter maintaining the ancestral form of its close relatives and showing a reduced fitness. This indicates that for the host, the loner strategy may be an option. To our knowledge, this is the first described case of polyphenism in a mutualism.

Chapter 5 and 6 cover bacterial genomics to evaluate the potential functional capabilities of three thiotrophic bacteria (**De Oliveira et al. 2022, Espada-Hinojosa et al. 2024**). Chapter 5 includes *Candidatus* Thiobius zoothamnicola (the symbiont of *Zoothamnium niveum*), and a free-living close relative, the Milos ODIII6 strain, cultivated but not currently formally described (Espada-Hinojosa et al. 2024). *Candidatus* Endoriftia persephone, the symbiont of the giant tubeworm *Riftia pachyptila*, belongs to the same family Sedimenticolaceae (Slobodkina et al. 2023). In Chapter 6, we report the closing of its genome. A coarser-grained functional description with the aggregation of metabolic pathways into functional traits for major bioelement fluxes (CHNOPS) is presented in both chapters.

References

Agrawal, Anurag A. (2001). "Phenotypic plasticity in the interactions and evolution of species". Science 294(5541):321–326. doi:10.1126/science.1060701.

Archetti, Marco, Francisco Úbeda, Drew Fudenberg, Jerry Green, Naomi E. Pierce, and Douglas W. Yu (2011). "Let the right one in: a microeconomic approach to partner choice in mutualisms". The American Naturalist 177(1):75–85. doi:10.1086/657622.

Axelrod, Robert, and William D. Hamilton (1981). "The evolution of cooperation". Science 211:1390–1396.

de Bary, Heinrich Anton (1879). "Die Erscheinung der Symbiose". Strassburg, Germany (now: Strasbourg, France): Karl J. Trübner. p. 5.

Bauer-Nebelsick, Monika, Christian F. Bardele, and Jörg A. Ott (1996a). "Electron microscopic studies on *Zoothamnium niveum* (Hemprich & Ehrenberg, 1831) Ehrenberg 1838 (Oligohymenophora, Peritrichida), a ciliate with ectosymbiotic, chemoautotrophic bacteria". European Journal of Protistology 32:202–215. doi:10.1016/S0932-4739(96)80020-4.

Bauer-Nebelsick, Monika, Christian F. Bardele, and Jörg A. Ott (1996b). "Redescription of *Zoothamnium niveum* (Hemprich & Ehrenberg, 1831) Ehrenberg, 1838 (Oligohymenophora, Peritrichida), a ciliate with ectosymbiotic, chemoautotrophic bacteria". European Journal of Protistology 32: 18–30. doi:10.1016/S0932-4739(96)80036-8.

Bergstrom, Carl T., Judith L. Bronstein, Redouan Bshary, Richard C. Connor, Martin Daly, Steven A. Frank, Herbert Gintis, Laurent Keller, Olof Leimar, Ronald Noë, and David C. Queller (2003). "Group Report: Interspecific Mutualism. Puzzles and Predictions". In Genetic and Cultural Evolution of Cooperation, P. Hammerstein (ed.). MIT Press, Cambridge.

Boyd, Robert, and Peter J Richerson (1992). "Punishment allows the evolution of cooperation (or anything else) in sizable groups". Ethology and Sociobiology 13(3):171–195. doi:10.1016/0162-3095(92)90032-Y.

Boyd, Robert, Herbert Gintis, and Samuel Bowles (2010). "Coordinated punishment of defectors sustains cooperation and can proliferate when rare". Science 328(5978):617–620. doi:10.1126/science.1183665.

Bright, Monika, H. Keckeis, and C. R. Fisher (2000). "An autoradiographic examination of carbon fixation, transfer and utilization in the *Riftia pachyptila* symbiosis". Marine Biology 136:621–632. doi:10.1007/s002270050722.

Bright, Monika, and Silvia Bulgheresi (2010). "A complex journey: transmission of microbial symbionts". Nature Reviews Microbiology 8:218–230.

Bright, Monika, Salvador Espada-Hinojosa, Ilias Lagkouvardos, and Jean-Marie Volland (2014). "The giant ciliate *Zoothamnium niveum* and its thiotrophic epibiont *Candidatus* Thiobios zoothamnicoli: a model system to study interspecies cooperation". Frontiers in Microbiology 5. doi:10.3389/fmicb.2014.00145.

Bright, Monika, Salvador Espada-Hinojosa, Jean-Marie Volland, Judith Drexel, Julia Kesting, Ingrid Kolar, Denny Morchner, et al. (2019). "Thiotrophic bacterial symbiont induces polyphenism in giant ciliate host *Zoothamnium niveum*". Scientific Reports 9(1): 15081. doi:10.1038/s41598-019-51511-3.

Bronstein, Judith (2015). "Mutualism". Oxford University Press, Oxford.

Brown, Jerram L. (1983). "Cooperation—A Biologist's Dilemma'. In Advances in the Study of Behavior, Robert A. Hinde Colin Beer Jay S. Rosenblatt and Busnel Marie-Claire (eds.), Volume 13:1–37. Academic Press, Cambridge. doi:10.1016/S0065-3454(08)60284-3.

Bshary, Redouan, and Judith L. Bronstein (2011). "A general scheme to predict partner control mechanisms in pairwise cooperative interactions between unrelated individuals". Ethology 117(4):271–283. doi:10.1111/j.1439-0310.2011.01882.x.

Bull, J. J., and W. R. Rice (1991). "Distinguishing mechanisms for the evolution of cooperation". Journal of Theoretical Biology 149:63–74. doi:10.1016/S0022-5193(05)80072-4.

Cavanaugh, Colleen M., Zoe P. McKiness, Irene L. G. Newton, and Frank J. Stewart (2006). "Marine chemosynthetic symbioses". In The Prokaryotes, 1:475–507. Springer, Berlin. doi:10.1007/978-3-642-30194-0_21.

Clutton-Brock, T., Parker, G. (1995). "Punishment in animal societies". Nature 373:209–216. doi:10.1038/373209a0.

Connor, Richard C. (1986). "Pseudo-reciprocity: Investing in mutualism". Animal Behaviour 34:1562–1584. doi: 10.1016/S0003-3472(86)80225-1.

Connor, Richard C. (1995). "The benefits of mutualism: a conceptual framework". Biological Reviews 70(3):427–457. doi:10.1111/j.1469-185X.1995.tb01196.x.

Doebeli, Michael, and Nancy Knowlton (1998). "The evolution of interspecific mutualisms". Proceedings of the National Academy of Sciences of USA 95:8676–8680. doi: 10.1073/pnas.95.15.8676.

Douglas, Angela E. (December 2014). "The Symbiotic Habit". Princeton University Press, Princeton.

Dubilier, Nicole, Claudia Bergin, and Christian Lott (2008). "Symbiotic diversity in marine animals: the art of harnessing chemosynthesis". Nature Reviews Microbiology 6:725–740. doi:10.1038/nrmicro1992.

Ellers, Jacintha, E. Toby Kiers, Cameron R. Currie, Bradon R. McDonald, and Bertanne Visser (2012). "Ecological interactions drive evolutionary loss of traits". Ecology Letters 15(10):1071–1082. doi:10.1111/j.1461-0248.2012.01830.x.

Espada-Hinojosa, Salvador, Judith Drexel, Julia Kesting, Edwin Kniha, Iason Pifeas, Lukas Schuster, Jean-Marie Volland, Helena C. Zambalos, and Monika Bright (2022). "Host-symbiont stress response to lack-of-sulfide in the giant ciliate mutualism". PLOS ONE 17(2):e0254910. doi:10.1371/journal.pone.0254910.

Espada-Hinojosa, Salvador, Clarissa Karthäuser, Abhishek Srivastava, Lukas Schuster, Teresa Winter, André Luiz De Oliveira, Frederik Schulz, Matthias Horn, Stefan Sievert, and Monika Bright (2024). "Comparative genomics of a vertically transmitted thiotrophic bacterial ectosymbiont and its close free-living relative". Molecular Ecology Resources 24(1):e13889. doi:10.1111/1755-0998.13889.

Fletcher, Jeffrey A, and Michael Doebeli (2009). "A simple and general explanation for the evolution of altruism". Proceedings of the Royal Society of London B: Biological Sciences 276(1654):13–19. doi:10.1098/rspb.2008.0829.

Fletcher, Jeffrey A., and Martin Zwick (2006). "Unifying the theories of inclusive fitness and reciprocal altruism". The American Naturalist 168(2):252–262. doi:10.1086/506529.

Foster, Kevin R., and Hanna Kokko (2006). "Cheating can stabilize cooperation in mutualisms". Proceedings of the Royal Society B 273:2233–2239. doi:10.1098/rspb.2006.3571.

Foster, K. R., and T. Wenseleers (2006). "A general model for the evolution of mutualisms". Journal of Evolutionary Biology 19(4):1283–1293. doi:10.1111/j.1420-9101.2005.01073.x.

Frank, Steven A. (1996). "Host-symbiont conflict over the mixing of symbiotic lineages". Proceedings - Royal Society of London. Biological sciences 263:339–344. doi:10.1098/rspb.1996.0052.

Gardner, Andy, and Kevin R. Foster (2008). "The evolution and ecology of cooperation - History and concepts". In Ecology of social evolution, J. Korb and J. Heinze (eds.), 1–36. Springer-Verlag, Berlin.

Hamilton, W. D. (1975). "Innate Social Aptitudes of Man: An Approach from Evolutionary Genetics". In Biosocial Anthropology, R. Fox (ed.), 133-153. Malaby Press, London.

Hauert, Christoph, Silvia Del Monte, Josef Hofbauer, and Karl Sigmund (2002). "Volunteering as red queen mechanism for cooperation in public goods games". Science 296:1129–1132. doi:10.1126/science.1070582.

Hauert, Christoph, Franziska Michor, Martin A. Nowak, and Michael Doebeli (2006). "Synergy and discounting of cooperation in social dilemmas". Journal of Theoretical Biology 239(2):195–202. doi:10.1016/j.jtbi.2005.08.040.

Hauert, Christoph, Arne Traulsen, Hannelore Brandt, Martin A. Nowak, and Karl Sigmund (2007). "Via freedom to coercion: the emergence of costly punishment". Science 316(5833):1905–1907. doi:10.1126/science.1141588.

Hauert, Christoph, Joe Yuichiro Wakano, and Michael Doebeli (2008). "Ecological public goods games: cooperation and bifurcation". Theoretical Population Biology 73(2):257–263. doi:10.1016/j.tpb.2007.11.007.

Hemprich, F. W., and C. G. Ehrenberg (1831). "Evertebrata I. Phytozoa". In Simbolae physicae. Abhandlungen der Akademie der Wissenchaften zu Berlin, Berlin.

Izquierdo S. S., Izquierdo L. R., Vega-Redondo F. (2010). "The option to leave: conditional dissociation in the evolution of cooperation". Journal of Theoretical Biolology 267(1):76–84. doi:10.1016/j.jtbi.2010.07.039.

Janzen, D. H. (1985). "The natural history of mutualisms". In The biology of mutualism. D. H. Boucher (ed.). Croom Helm, London.

Jones, Emily I., Michelle E. Afkhami, Erol Akçay, Judith L. Bronstein, Redouan Bshary, Megan E. Frederickson, Katy D. Heath, et al. (2015). "Cheaters must prosper: reconciling theoretical and empirical perspectives on cheating in mutualism". Ecology Letters 18(11):1270–1284. doi:10.1111/ele.12507.

Kiers, E. Toby, and R. Ford Denison (2008). "Sanctions, cooperation, and the stability of plant-rhizosphere mutualisms". Annual Review of Ecology, Evolution and Systematics 39:215–236. doi:10.1146/annurev.ecolsys.39.110707.173423.

Kiers, E. Toby, R. Ford Denison, Atsushi Kawakita, and Edward Allen Herre (2011). "The biological reality of host sanctions and partner fidelity". Proceedings of the National Academy of Sciences of USA 108(3):E17. doi:10.1073/pnas.1014546108.

Killingback, Timothy, and Michael Doebeli (1998). "Self-organized criticality in spatial evolutionary game theory". Journal of Theoretical Biology 191(3):335–340. doi: 10.1006/jtbi.1997.0602.

Killingback, T., M. Doebeli, and N. Knowlton (1999). "Variable investment, the continuous prisoner's dilemma, and the origin of cooperation". Proceedings of the Royal Society of London. Series B: Biological Sciences 266, (1430):1723–1728. doi:10.1098/rspb.1999.0838.

Killingback, Timothy, and Michael Doebeli (2002). "The continuous prisoner's dilemma and the evolution of cooperation through reciprocal altruism with variable investment". The American Naturalist 160(4):421–438. doi:10.1086/342070.

Laurent, Mélina C. Z., Olivier Gros, Jean-Pierre Brulport, Françoise Gaill, and Nadine Le Bris (2009). "Sunken wood habitat for thiotrophic symbiosis in mangrove swamps". Marine Environmental Research 67:83–88. doi:10.1016/j.marenvres.2008.11.006.

Lehmann, L., and L. Keller (2006). "The evolution of cooperation and altruism - a general framework and a classification of models". Journal of Evolutionary Biology 19:1365–1376. doi: 10.1111/j.1420-9101.2006.01119.x.

Leigh, E. G. Jr. (2010). "The evolution of mutualism". Journal of Evolutionary Biology 23:2507–2528. doi:10.1111/j.1420-9101.2010.02114.x.

Mar, Gary, and Paul St. Denis (1994). "Chaos in cooperation: continuous-valued Prisoner's Dilemmas in infinite-valued logic". International journal of bifurcation and chaos 4(4):943–958. doi:10.1142/S0218127494000678.

Maurin, Leslie C., David Himmel, Jean-Louis Mansot, and Olivier Gros (2010). "Raman microspectrometry as a powerful tool for a quick screening of thiotrophy: An application on mangrove swamp meiofauna of Guadeloupe (F.W.I.)". Marine Environmental Research 69(5):382–389. doi:10.1016/j.marenvres.2010.02.001.

McFall-Ngai, Margaret, Michael G. Hadfield, Thomas C. G. Bosch, Hannah V. Carey, Tomislav Domazet-Lošo, Angela E. Douglas, Nicole Dubilier, et al. (2013). "Animals in a bacterial world, a new imperative for the life sciences". Proceedings of the National Academy of Sciences of USA 110(9):3229–3236. doi:10.1073/pnas.1218525110.

Noe, Ronald, and Peter Hammerstein (1994). "Biological markets: supply and demand determine the effect of partner choice in cooperation, mutualism and mating". Behavioral Ecology and Sociobiology 35:1–11. doi:10.1007/BF00167053.

De Oliveira, André Luiz, Abhishek Srivastava, Salvador Espada-Hinojosa, and Monika Bright (2022). "The complete and closed genome of the facultative generalist *Candidatus* Endoriftia persephone from deep-sea hydrothermal vents". Molecular Ecology Resources 22(8): 3106–3123. doi:10.1111/1755-0998.13668.

Ott, Jörg A., Monika Bright, and Friederich Schiemer (1998). "The ecology of a novel symbiosis between a marine peritrich ciliate and chemoautotrophic bacteria". P.S.Z.N.: Marine Ecology 19(3):229–243. doi:10.1111/j.1439-0485.1998.tb00464.x.

Queller, David C. (1985). "Kinship, reciprocity and synergism in the evolution of social behaviour". Nature 318(6044):366–367. doi:10.1038/318366a0.

Rinke, Christian, Stephan Schmitz-Esser, Kilian Stoecker, Andrea D. Nussbaumer, Dávid A. Molnár, Katrina Vanura, Michael Wagner, Matthias Horn, Jörg A. Ott, and Monika Bright (2006). "'*Candidatus* Thiobios zoothamnicoli', an ectosymbiotic bacterium covering the giant marine ciliate *Zoothamnium niveum*". Applied and Environmental Microbiology 72(3):2014–2021. doi: 10.1128/AEM.72.3.2014-2021.2006.

Rinke, Christian, Raymond Lee, Sigrid Katz, and Monika Bright (2007). "The effects of sulphide on growth and behaviour of the thiotrophic *Zoothamnium niveum* symbiosis'. Proceedings - Royal Society of London Biological sciences 274: 2259–2269. doi:10.1098/rspb.2007.0631.

Roberts, Gilbert, and Thomas N. Sherratt (1998). "Development of cooperative relationships through increasing investment". Nature 394:175–179. doi: 10.1038/28160.

Sachs, Joel L., Ulrich G. Mueller, Thomas P. Wilcox, and James J. Bull (2004). "The evolution of cooperation". Quarterly Review of Biology 79(2):135–160. doi: 10.1086/383541.

Sachs, Joel L., et al. (2013). "The legume-rhizobium symbiosis". Global Biogeochem. Cycles 13:623–645.

Sapp, Jan (2004). "The dynamics of symbiosis: an historical overview". Canadian Journal of Botany 82(8):1046–1056. doi:10.1139/b04-055.

Seah, Brandon, Chakkiath Paul Antony, Bruno Huettel, Jan Zarzycki, Lennart Schada von Borzyskowski, Tobias Erb, Angela Kouris, et al. (2019). "Sulfur-oxidizing symbionts without canonical genes for autotrophic CO_2 fixation". mBio 10(3):e01112-19. doi:10.1101/540435.

Semmann, Dirk, Hans-Jürgen Krambeck, and Manfred Milinski (2003). "Volunteering leads to rock–paper–scissors dynamics in a public goods game". Nature 425(6956):390–393. doi:10.1038/nature01986.

Slobodkina, Galina, Alexander Merkel, Nataliya Ratnikova, Alexandra Kuchierskaya, and Alexander Slobodkin (2023). "*Sedimenticola hydrogenitrophicus* sp. nov. a chemolithoautotrophic bacterium isolated from a terrestrial mud volcano, and proposal of Sedimenticolaceae fam. nov. in the order Chromatiales". Systematic and Applied Microbiology 46(5):126451. doi:10.1016/j.syapm.2023.126451.

Sigmund, Karl, Christoph Hauert, and Martin A. Nowak (2001). "Reward and punishment". Proceedings of the National Academy of Sciences of USA 98(19):10757–10762. doi:10.1073/pnas.161155698.

Sogin, E. Maggie, Manuel Kleiner, Christian Borowski, Harald R. Gruber-Vodicka, and Nicole Dubilier (2021). "Life in the dark: phylogenetic and physiological diversity of chemosynthetic symbioses". Annual Review of Microbiology 75(1):695–718. doi:10.1146/annurev-micro-051021-123130.

Stelzer, Claus-Peter (2001). "Resource limitation and reproductive effort in a planktonic rotifer". Ecology 82(9):2521–2533. doi: 10.1890/0012-9658(2001)082[2521:RLAREI]2.0.CO;2.

Trivers, Robert L. (1971). "The evolution of reciprocal altruism". The Quarterly Review of Biology 46:35–57. doi: 10.1086/406755.

Van Beneden, Pierre-Joseph (1876). "Animal Parasites and Messmates". Henry S. King, London.

Volland, Jean-Marie, Arno Schintlmeister, Helena Zambalos, Siegfried Reipert, Patricija Mozetič, Salvador Espada-Hinojosa, Valentina Turk, Michael Wagner, and Monika Bright (2018). "NanoSIMS and tissue autoradiography reveal symbiont carbon fixation and organic carbon transfer to giant ciliate host'. The ISME Journal 12(3):714–727. doi:10.1038/s41396-018-0069-1.

Werner, Gijsbert D. A., Joan E. Strassmann, Aniek B. F. Ivens, Daniel J. P. Engelmoer, Erik Verbruggen, David C. Queller, Ronald Noë, Nancy Collins Johnson, Peter Hammerstein, and E. Toby Kiers (2014). "Evolution of microbial markets". Proceedings of the National Academy of Sciences of USA 111(4):1237–1244. doi:10.1073/pnas.1315980111.

Werner, Gijsbert DA, et al. (2015). "Evolutionary signals of symbiotic persistence in the legume–rhizobia mutualism". Proceedings of the National Academy of Sciences of USA 112(33):10262-10269. doi:10.1073/pnas.1424030112.

West, Stuart A., Ashleigh S. Griffin, and Andy Gardner (2007). "Evolutionary explanations for cooperation". Current Biology 17:R661–672. doi:10.1016/j.cub.2007.06.004.

West, Stuart A., Roberta M. Fisher, Andy Gardner, and E. Toby Kiers (2015). "Major evolutionary transitions in individuality". Proceedings of the National Academy of Sciences of USA 112(33):10112–10119. doi:10.1073/pnas.1421402112.

West-Eberhard, Mary Jane (1975). "The evolution of social behavior by kin selection". The Quarterly Review of Biology 50(1):1–33. doi:10.2307/2821184.

Yamagishi, T. (1986). "The provision of a sanctioning system as a public good". Journal of Personality and Social Psychology 51(1):110–116. doi:10.1037/0022-3514.51.1.110.

Chapter 1

The giant ciliate *Zoothamnium niveum* and its thiotrophic epibiont *Candidatus Thiobius zoothamnicola**: a model system to study interspecies cooperation

(*) The original title of the published paper uses the old denomination *Candidatus* Thiobius zoothamnicoli, superseded after Oren (2017)
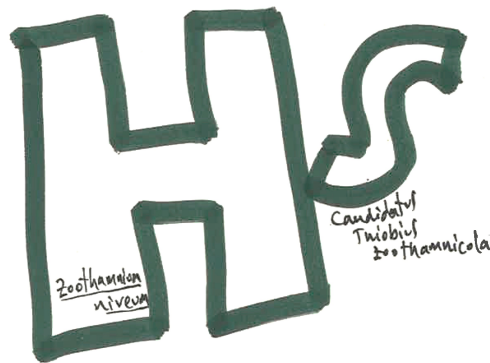
Coauthor paper

The giant ciliate *Zoothamnium niveum* and its thiotrophic epibiont *Candidatus* Thiobios zoothamnicoli: a model system to study interspecies cooperation

Monika Bright[1] *, Salvador Espada-Hinojosa[1], Ilias Lagkouvardos[2] and Jean-Marie Volland[1]

[1] Department of Limnology and Oceanography, University of Vienna, Vienna, Austria
[2] Department of Microbiology and Ecosystem Science, University of Vienna, Vienna, Austria

Symbioses between chemoautotrophic sulfur-oxidizing (thiotrophic) bacteria and protists or animals are among the most diverse and prevalent in the ocean. They are extremely difficult to maintain in aquaria and no thiotrophic symbiosis involving an animal host has ever been successfully cultivated. In contrast, we have cultivated the giant ciliate *Zoothamnium niveum* and its obligate ectosymbiont *Candidatus* Thiobios zoothamnicoli in small flow-through aquaria. This review provides an overview of the host and the symbiont and their phylogenetic relationships. We summarize our knowledge on the ecology, geographic distribution and life cycle of the host, on the vertical transmission of the symbiont, and on the cultivation of this symbiosis. We then discuss the benefits and costs involved in this cooperation compared with other thiotrophic symbioses and outline our view on the evolution and persistence of this byproduct mutualism.

Keywords: thiotrophic, sulfur-oxidizing, ciliate, symbiosis, mutualism, cooperation, wood fall

INTRODUCTION

The first illustration of a colonial ciliate from the Red Sea was published more than 180 years ago (Hemprich and Ehrenberg, 1829). Two years later, based on the small drawing of a single specimen, *Zoocladium niveum* was formally described and was named "small Abyssinian double bell" (Hemprich and Ehrenberg, 1831; translated by the first author; **Figure 1**). It was found on a rock at the coast of the Red Sea, probably close to the former kingdom of Abyssinia. Shortly thereafter, this species was placed in the earlier described genus *Zoothamnium* (Bory de Saint-Vincent, 1824). Ehrenberg (1838) observed in this specimen that "the whole stem suddenly contracted to a white knot" (p. 290; translated by the first author). Over the following decades, *Z. niveum* was discovered in other localities and with similar or slightly different morphology (see Bauer-Nebelsick et al., 1996a for further literature). Nonetheless, the typical white color, for which the species was named "niveum," was not mentioned again until it was discovered by Jörg Ott in mangrove islands of Belize. Only then was it redescribed and its association with white, sulfide-oxidizing bacteria characterized (Bauer-Nebelsick et al., 1996a,b).

The white color in many sulfur-oxidizing (thiotrophic) bacteria is due to elemental sulfur inclusions, which are an intermediate product in the oxidation process of reduced sulfur species (Pflugfelder et al., 2005; Himmel et al., 2009; Maurin et al., 2010; Gruber-Vodicka et al., 2011). When involving animal or protist hosts, this type of association is termed thiotrophic symbiosis. Thiotrophic bacteria use hydrogen sulfide or other reduced sulfur species (see Childress and Girguis, 2011), which are typically produced biologically by anaerobic sulfate-reducing bacteria or geothermally at hydrothermal vents, to gain energy for carbon fixation (see Dubilier et al., 2008). Such bacteria, both free-living and host-associated, are extremely widespread at marine

oxic–anoxic interfaces from shallow waters to the deep sea, including suboxic sediment layers, decaying plant matter, such as in sea grass meadows, mangrove peat, and wood, in whale bones, hydrocarbon seeps, and hydrothermal vents (Dubilier et al., 2008). Most symbioses are marine, but recently the first thiotrophic symbiosis was described from a freshwater limestone cave (Dattagupta et al., 2009). Thiotrophic symbionts belong to various clades of Gamma-, Epsilon- and, as recently discovered, also Alphaproteobacteria (Dubilier et al., 2008; Gruber-Vodicka et al., 2011).

The host taxa are even more diverse, although hydrogen sulfide is highly toxic (National Research Council, 1979) and eukaryotic hosts need to somehow cope with this poison. Extra- and intracellular endosymbioses as well as ectosymbioses are reported within six animal phyla (Nematoda, Platyhelminthes, Annelida, Arthropoda, Mollusca, Echinodermata) and one protist phylum (Ciliophora; see Ott et al., 2004; Stewart et al., 2005; Cavanaugh et al., 2006; Dubilier et al., 2008). All types of transmission modes – vertical from parents to offspring, horizontal from the environment, or mixed modes – are known within these prevalent bacterial symbioses in the sea (see Bright and Bulgheresi, 2010; Vrijenhoek, 2010).

Despite this dominance, research has been somewhat limited because many thiotrophic symbioses occur in poorly accessible, deep-sea environments. They are extremely difficult to maintain in the laboratory or even to culture. To our knowledge, only a few bivalves (for example, the lucinid *Codakia orbicularis*; Gros et al., 1997) were reared to maturity. This colonial ciliate, however, was successfully cultivated including the entire life cycle with the production of offsprings (Rinke et al., 2007). While bivalves exhibit intrinsically slower growth, and reproduction, the colonial ciliate has a much faster growth and reproduction, and a short
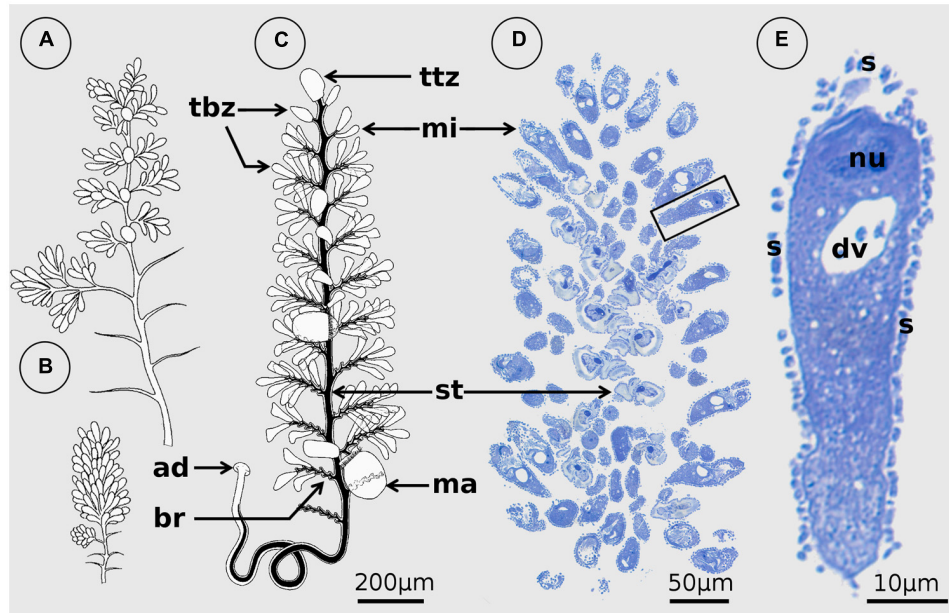
FIGURE 1 | *Zoothamnium niveum*. (A,B) Original illustrations modified from Hemprich and Ehrenberg (1829) showing the same colony expanded **(A)** and contracted **(B)**. **(C)** Drawing of a colony from the redescription of *Z. niveum* showing the different cell types: the macrozooid (ma), the microzooid (mi), the terminal branch zooids (tbz), and the terminal top zooid (ttz; modified from Bauer-Nebelsick et al., 1996a). **(D)** Microscopic observation of a longitudinal section of a *Z. niveum* colony. The stalk (st) of the contracted colony is visible as well as the numerous microzooids. **(E)** Detail of a single microzooid with macronucleus (nu) and digestive vacuole (dv), covered by its ectosymbionts (s).

life span. These characteristics along with easy access in shallow waters make this thiotrophic symbiosis of *Z. niveum* and its single bacterial partner, *Candidatus* Thiobios zoothamnicoli, a promising candidate for future studies. The present review summarizes our knowledge on this symbiosis and outlines our view on its evolution.

THE HOST *Zoothamnium niveum*

Zoothamnium niveum belongs to a morphologically well-defined colonial ciliate genus of Peritrichida (Oligohymenophora) characterized by zooids that are connected by a common stalk. The contractile spasmoneme runs uninterrupted through the whole colony and bends in a "zigzag" pattern upon contraction (see Clamp and Williams, 2006). *Z. niveum* shares an alternate branching pattern with several other species such as *Z. alternans* Claparède and Lachmann 1858, but is much larger and has typical bell-shaped microzooids (Bauer-Nebelsick et al., 1996a; **Figure 1**). With a length of up to 1.5 cm it is by far the largest representative of this genus (Vopel et al., 2005).

The 18S rRNA sequence from a population found on decaying mangrove leaves close to Fort Pierce, FL, USA and from a population collected from a whale bone in Tokyo Bay was almost identical, indicating an extremely wide geographic distribution (Clamp and Williams, 2006; Kawato et al., 2010). A sister taxa relationship of *Z. niveum* with *Z. alternans* + *Z. pelagicum* Du Plessis, 1891 was reported (Clamp and Williams, 2006; **Figure 2**). Both closely related species have been described with epibiotic bacteria (Dragesco, 1948; Fauré-Fremiet et al., 1963; Laval, 1968, 1970; Laval-Peuto and Rassoulzadegan, 1988). Epibionts of one morphotype consistently cover the pelagic *Z. pelagicum*. They were suggested to be cyanobacteria (Laval-Peuto and Rassoulzadegan, 1988). In *Z. alternans* it remains unclear whether the association is obligate for the host and involves a specific symbiont or merely represents unspecific microbial fouling.

The colonial host exhibits a central stalk with alternate branches and three cell morphotypes: terminal zooids on the tip of the stalk and each branch, feeding microzooids, and macrozooids (**Figure 1**). The latter develop on the base of the branches and leave the colony as swarmers to disperse and found new colonies (Bauer-Nebelsick et al., 1996a,b; **Figure 3**). Microzooids exhibit typical digestive structures with an oral ciliature and a cytopharynx (Bauer-Nebelsick et al., 1996b). Food vacuoles containing bacteria of similar size and microanatomical features as the symbionts are frequently found. The macrozooids, however, lack a cytopharynx, but their oral ciliature is fully developed. No food vacuoles were observed in macrozooids, leading to the conclusion that they are nourished by the microzooids (Bauer-Nebelsick et al., 1996b).

Sexual reproduction through conjugation has been described in some representatives of *Zoothamnium* (Furssenko, 1929; Summers, 1938), but never in *Z. niveum* (Bright M., personal observation). Asexual reproduction is through swarmers (Bauer-Nebelsick et al., 1996a,b). Macrozooid size varies considerably (20–150 μm). As soon as the somatic girdle (circular rows of cilia) is developed, macrozooids can leave the mother colony as swarmers. Somatic girdle development, however, is not correlated with macrozooid size (Bauer-Nebelsick et al., 1996a). The circumstances under which the somatic girdle develops prior to dispersal in the water column have not been studied.
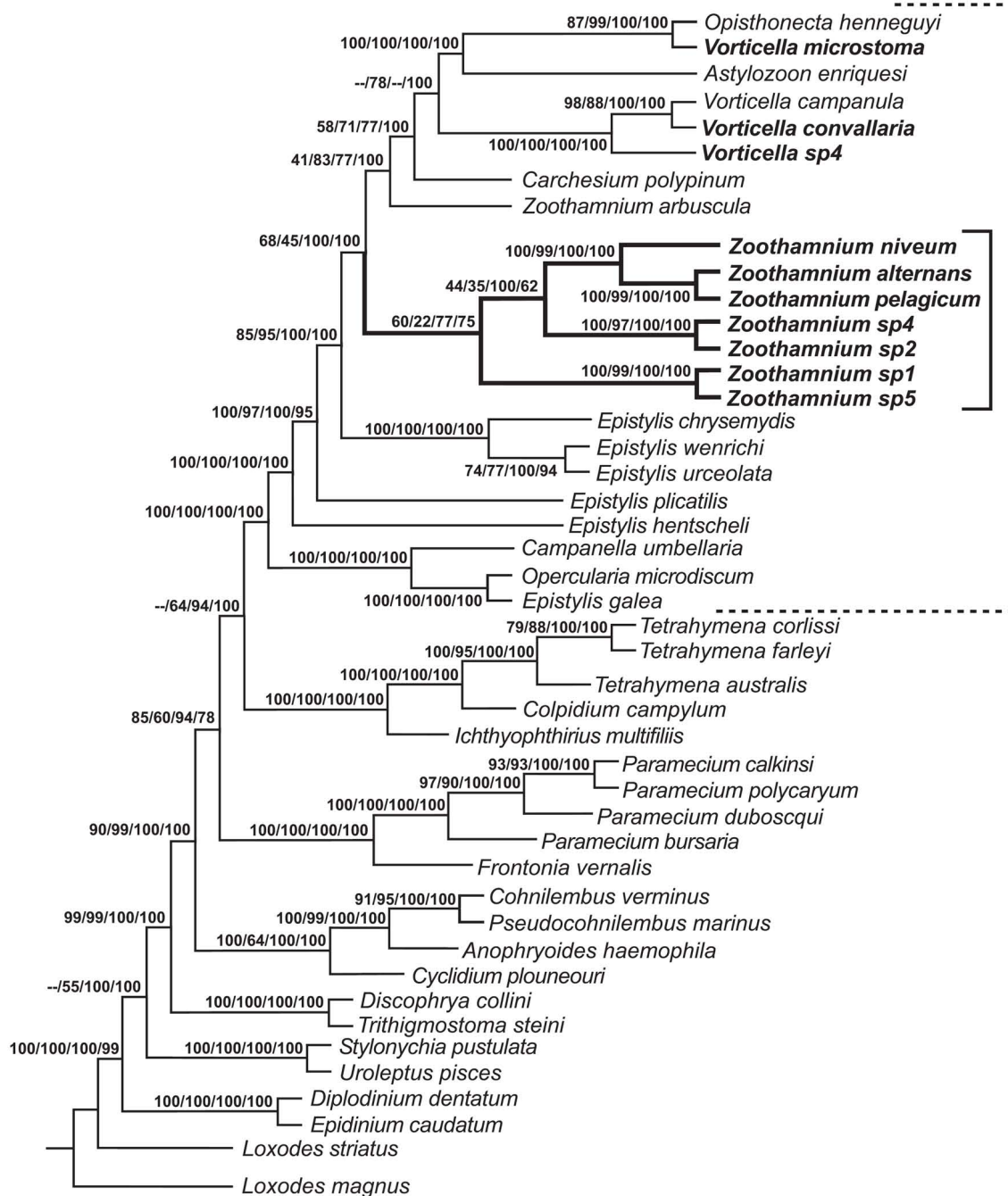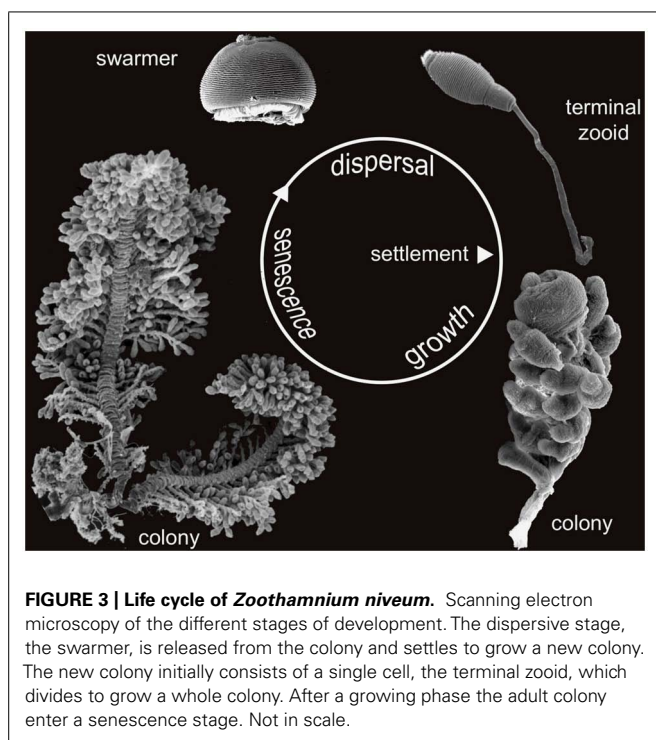
FIGURE 2 | Consensus tree formed from the four trees generated by phylogenetic analyses (Clamp and Williams, 2006). Neighbor-joining (NJ) bootstrap value, maximum parsimony (MP) bootstrap value, maximum likelihood (ML) consensus value, and Bayesian consensus value are given as numbers on branches; missing values reflect minor differences in topology that could not be represented on the consensus tree. Solid bracket indicates species of *Zoothamnium*; dashed bracket indicates species of peritrichs. Species sequenced in Clamp and Williams (2006) are shown in bold type.

Using bromodeoxyuridine, a thymidine analog, and immunocytochemistry to study proliferation kinetics, Kloiber et al. (2009) corroborated that DNA synthesis is restricted to terminal zooids and macrozooids (**Figure 4**). The terminal zooid on the tip of the stalk produced the terminal zooids of each branch. Thus the number of branches is equivalent to the divisions of this top terminal zooid, and the youngest parts are on the tip of the colony, the oldest on the bottom. The division rate of the top terminal zooid decreased as the colony grew, but never ceased (Kloiber et al., 2009). The terminal zooids of the branches produced the microzooids. They had limited proliferation capacity, increasing the branch length with maximally 20 microzooids. At

FIGURE 3 | Life cycle of *Zoothamnium niveum*. Scanning electron microscopy of the different stages of development. The dispersive stage, the swarmer, is released from the colony and settles to grow a new colony. The new colony initially consists of a single cell, the terminal zooid, which divides to grow a whole colony. After a growing phase the adult colony enter a senescence stage. Not in scale.

FIGURE 4 | General view of a *Zoothamnium niveum* colony showing the immunolocalization of BrdU incorporated into proliferating cells. Labeled nucleus are observed in the terminal top zooid, some of the terminal branch zooids and in the macrozooids located along the stalk. Modified from Kloiber et al. (2009).
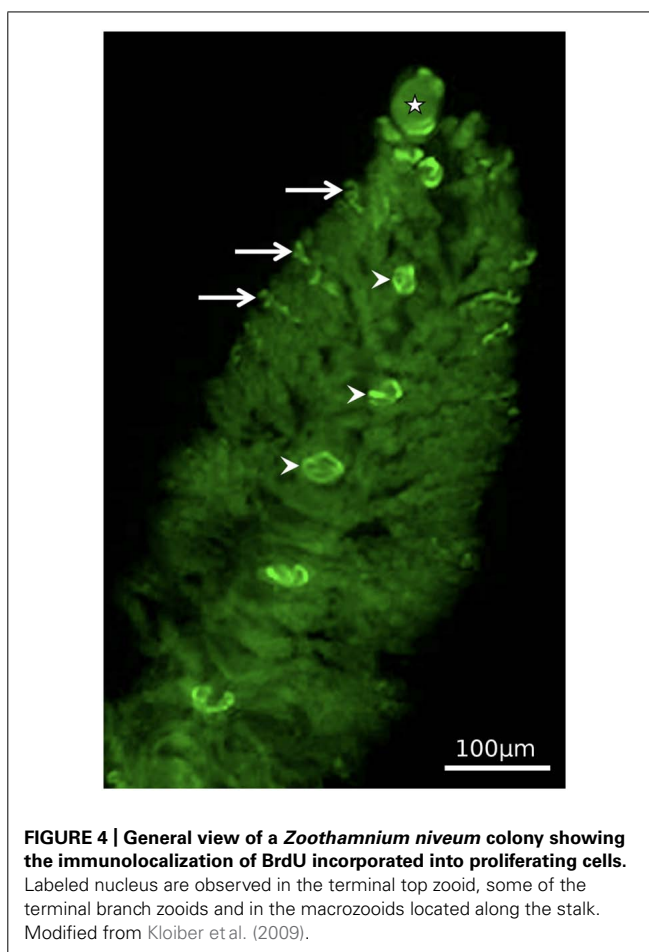
the base of the branches, macrozooids are produced. The number of macrozooids in large colonies with more than 50 branches was greater (about 15) than in small colonies with less then 50 branches (about 6). In macrozooids, DNA synthesis occurred on branches, but the cell cycle was arrested until swarmers left the colony. They probably resume mitosis and cell division upon settlement, when they in fact become the top terminal zooid (Kloiber et al., 2009).

THE SYMBIONT *Candidatus* Thiobios zoothamnicoli

A single 16S rRNA phylotype covers the host in a strict monolayer, except for the most basal part of the colony (Rinke et al., 2006; **Figure 5**). Depending on the location of the host, this phylotype grows either as rod or as cocci. They are rods on the stalk, branches, terminal zooids, macrozooids, and on the aboral parts of microzooids. The oral part of the microzooids, is covered with cocci, with a gradual change from cocci to rods from the oral to aboral side. The most basal, senescent parts of the colony are overgrown with all kinds of microbes and the symbiont is partly lost (Bauer-Nebelsick et al., 1996a,b; Rinke et al., 2006).

The symbionts have a cytoplasmic and an outer cell membrane, typical of Gram-negative bacteria (Bauer-Nebelsick et al., 1996b). Raman microspectroscopy revealed vesicles filled with S_8 sulfur (Maurin et al., 2010). Experiments in Cartesian divers showed a rapid decrease of oxygen consumption within 4 h, which remained at a low level for 24 h under normoxic conditions. This suggests that elemental sulfur is used with oxygen as an electron acceptor for about 4 h, during which the colonies are depleted of this intermediate storage product and turn pale. The baseline of oxygen consumption represents the respiration of host and symbiont. After injecting $100\ \mu mol\ L^{-1}\Sigma H_2S$ (sum of H_2S, HS^-, S^{2-}), oxygen consumption was increased and rapidly decreased again. This suggests that the sulfide pulse enables the symbionts to briefly resume their chemoautotrophic activity (Ott et al., 1998).

Each host population associates with a single specific symbiont (based on 16S rRNA). The symbiont from Twin Cays, Belize, was tentatively named *Cand.* Thiobios zoothamnicoli (Rinke et al., 2006). The similarity between this and another population from Calvi, Corsica, was 99.7% (Rinke et al., 2009) and 99.2% to a Pacific population, termed "ectosymbiont of *Zoothamnium niveum*" (Kawato et al., 2010). The internal transcribed spacer (ITS) was also highly similar between the Twin Cays and Calvi population (Rinke et al., 2009). Genes for the key enzyme in the Calvin Benson cycle for carbon fixation (ribulose 1,5-bisphosphate carboxylase/oxygenase) and for sulfur metabolism (APS reductase, dissimilatory sulfite reductase) were discovered (Rinke et al., 2009).

Besides other strains of *Cand.* Thiobios zoothamnicoli recovered from different *Z. niveum* isolates, the closest relatives, as revealed by 16S rRNA gene phylogenetic analysis, of *Cand.* Thiobios zoothamnicoli all belong to a well separated group of uncultivated sulfur oxidizing bacteria related to gamma proteobacteria (Rinke et al., 2006, 2009; Kawato et al., 2010).
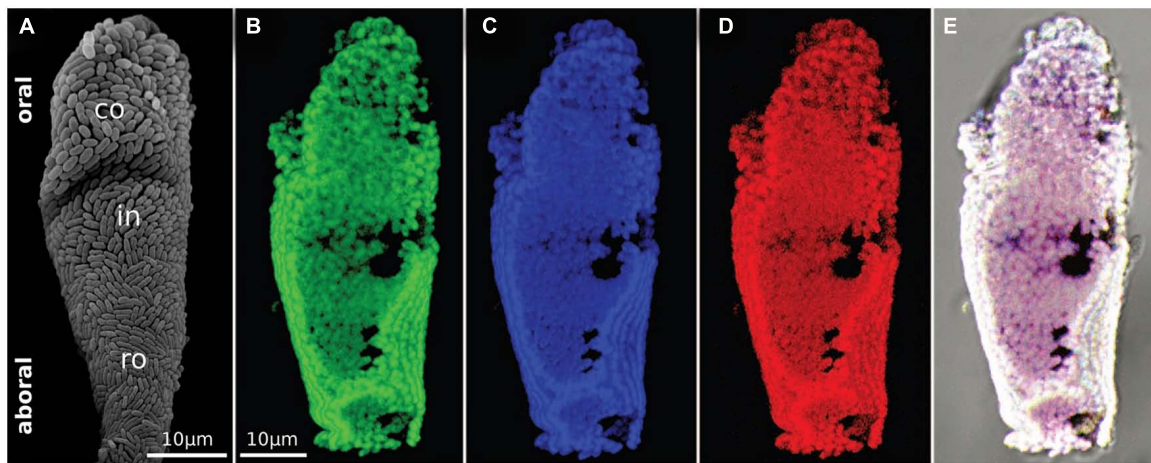
FIGURE 5 | The monospecific ectosymbiont monolayer. (A) SEM observation of a microzooid showing the monolayer of bacteria covering the host cell. The two morphotypes are visible, rod-shaped symbionts at the aboral part and coccioid symbionts at the oral part. **(B–D)** FISH micrographs of a single microzooid after hybridization with a general bacterial probe in green **(B)**, a gammaproteobacteria specific probe in blue **(C)**, and a *Cand.* Thiobios zoothamnicoli specific probe in red **(D)**. **(E)** Overlay of the three previous micrographs (Rinke et al., 2006).

The updated phylogenetic analysis reveals a group currently 19 16S rRNA sequences (all current close relatives in public databases; **Figure 6**). Overall this Thiobios group is dominated by free-living bacteria of shallow-water environments of all temperate to tropical oceans. Analyses restricted to the 16S rRNA gene provides insufficient resolution to fully clarify the evolutionary relations among the available representatives populating this branch of the tree, a problem that can only be resolved with genomic sequencing of targeted members. Nevertheless, symbiosis apparently evolved twice in the shallow waters as ectosymbioses in the Thiobios group: in *Z. niveum* and in the archaea *Giganthauma karukerense* (Muller et al., 2010). The available fragment of 16S rRNA from this archaea has a similarity of 93% to *Cand.* Thiobios zoothamnicoli (note that this sequence fragment is not included in **Figure 6**). In addition another clade of the Thiobios group colonized shallow-water and deep-sea vents, whereby endosymbiosis with two different gastropod hosts evolved.

HABITAT AND ECOLOGY

The data increasingly point to a widespread occurrence of the giant ciliate symbiosis on or near decaying organic material in shallow tropical to temperate waters. So far, this symbiosis has been detected in the biogeographic provinces of the Caribbean Sea (Bauer-Nebelsick et al., 1996a; Clamp and Williams, 2006; Laurent et al., 2009), the Atlantic Ocean (Clamp and Williams, 2006; Wirtz, 2008), the Mediterranean Sea (Rinke et al., 2007; Wirtz, 2008), the Red Sea (Ehrenberg, 1838), and the Pacific Ocean (Kawato et al., 2010; **Figure 7**).

In tropical and subtropical regions, the giant ciliate colonizes mangrove peat (mainly composed of wood; Lovelock et al., 2011) and sunken wood and leaves of the mangrove Rhizophora mangle (Bauer-Nebelsick et al., 1996a; Clamp and Williams, 2006; Laurent et al., 2009). In temperate waters, this ciliate inhabits whale falls (Kawato et al., 2010), wood (Bright M., personal observation), and

sea grass debris of *Posidonia oceanica* (Rinke et al., 2007; Wirtz, 2008; **Figure 8**).

The current findings are all restricted to shallow subtidal waters, but the depth limits remain to be investigated. Mangrove trees occur in the intertidal, and sea grasses are limited to the euphotic zone. Wood may be transported into the deep sea and potentially could be colonized by this symbiosis. A sperm whale bone, recovered from about 1000 m depth in Sagami Bay without this symbiosis, was colonized by *Z. niveum* after the bone was deployed in 5 m depth in Tokyo Bay for 1 year (Kawato et al., 2010).

Detailed studies on colony distribution on peat walls were conducted at the mangrove island Twin Cays, Belize (Ott et al., 1998). On average, 1200 giant ciliate colonies m^{-2} were found between 30 cm below low water level down to the lower end of the peat wall at about 2 m depth. They were patchily distributed in groups of 26 ± 17 colonies, with maxima of more than 100 colonies per patch. Interestingly, many colonies thrive in areas where the microbial mat of the peat surface was disturbed, e.g., after decomposed rootlets fall out. Such conduits were suggested to be analogous to hydrothermal vents, where vent fluid emerges from the basalt and mixes with the oxygenated overlain seawater (Ott et al., 1998).

Colonization and succession of artificially disturbed surfaces on mangrove peat led to the distinction of initial patches with small colonies, followed by mature patches with colonies of all sizes, and senescent patches with large colonies. The latter were characterized by loss of zooids on the lower branches and were often overgrown by other microbes on the lower colony. A life expectancy of about 3 weeks was estimated based on the disappearance of such colony groups (Ott et al., 1998; **Figure 9**).

The microhabitat of *Z. niveum* is temporally highly dynamic in terms of sulfide and oxygen concentrations. Measurements of oxygen and sulfide on peat surfaces from Twin Cays (Belize) were conducted in the lab (Ott et al., 1998; Vopel et al., 2001, 2002) and *in situ* (Vopel et al., 2005). Further *in situ* measurements
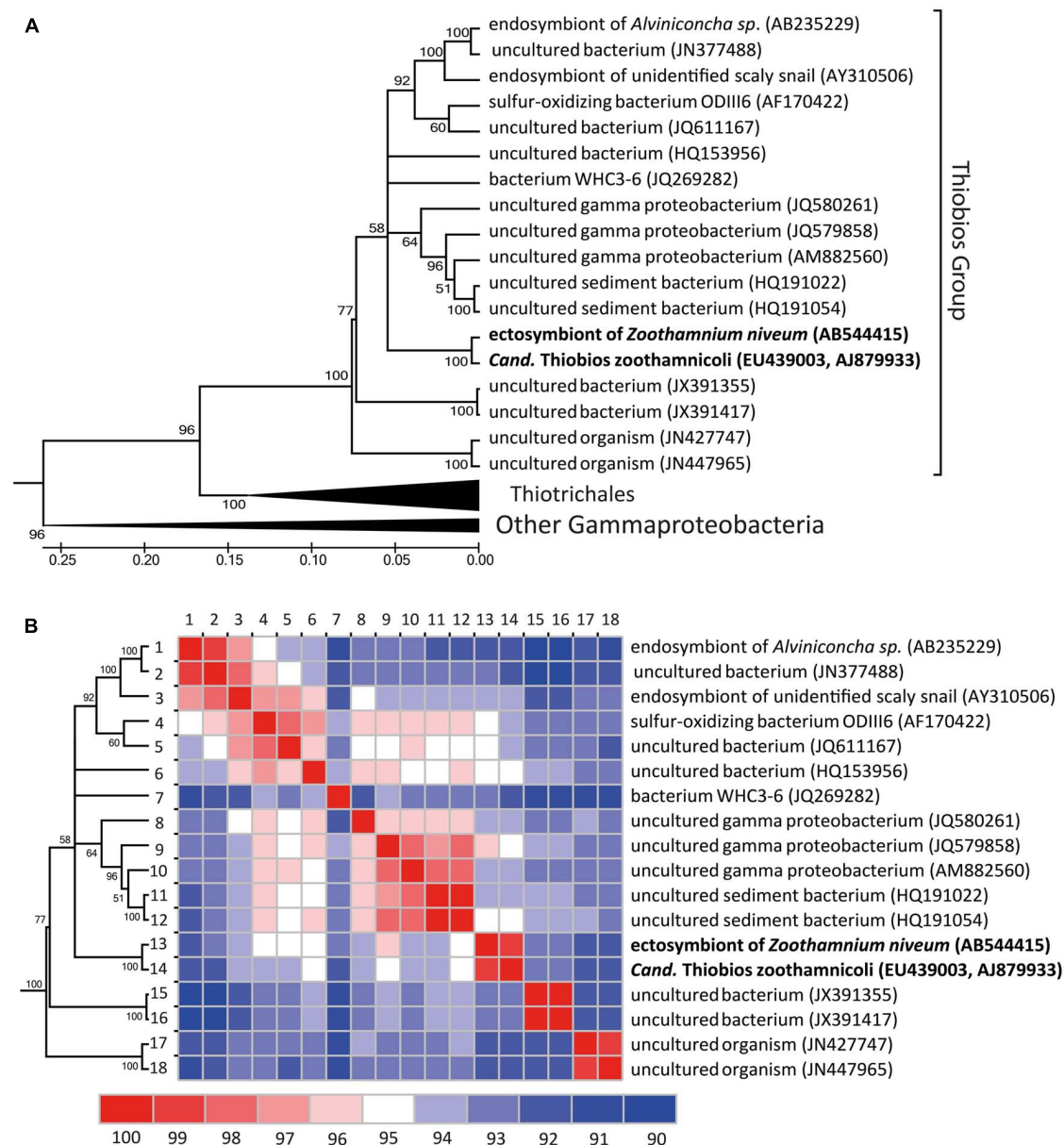
FIGURE 6 | Phylogenetic diversification of the *Cand.* Thiobios zoothamnicoli neighborhood. (A) Maximum likelihood phylogenetic tree (GTR model, 1000 bootstraps) of all long (>1300 nt), with good pintail value (>60) and non-redundant 16 rRNA sequences similar to *Cand.* Thiobios zoothamnicoli available in the SILVA database (Quast et al., 2013). The tree with the highest log likelihood is shown and is drawn to scale, with branch lengths measured in number of substitutions per site. Evolutionary analyses were conducted in MEGA5 (Tamura et al., 2011). **(B)** Similarity matrix of the 16S rRNA sequences belonging to the *Cand.* Thiobios zoothamnicoli group. The similarity was calculated as the percentage of identical positions over all shared positions (not considering gaps) for each pair of sequences in the multiple sequence alignment and visualized using JColorGrid (Joachimiak et al., 2006).

of wood surfaces colonized by ciliates from Guadeloupe were carried out (Laurent et al., 2009). Adjoining areas of peat or wood devoid of ciliates always exhibited different oxygen and sulfide concentrations (Ott et al., 1998; Vopel et al., 2001, 2002; Maurin et al., 2010), suggesting a highly specific chemical environment *Z. niveum* inhabits.

Large-scale sulfide fluctuations were associated with the tidal cycle. The highest maxima were recorded at high tide, the lowest at low tide (Laurent et al., 2009). Small-scale fluctuations of sulfide and oxygen at the opening of conduits on peat walls were caused by pulse exchange between deoxygenated, sulfidic seawater in conduits and oxygenated seawater adjacent to peat surface (Vopel et al., 2005). Peak values occurred in periods of 10–100 s. Depending on flow speed, sulfide was high or low (Vopel et al., 2005). Ciliates preferentially settled in areas of about 250–300 μmol L^{-1} ΣH$_2$S and oxygen values of about 20 μmol L^{-1} (Ott et al., 1998; Vopel
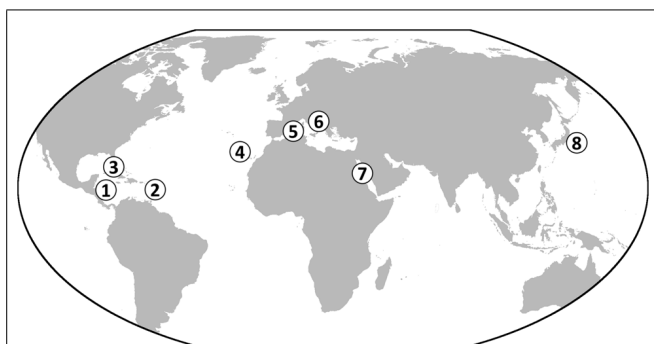
FIGURE 7 | World map showing the known occurrences of
Zoothamnium niveum. So far, colonies of the ciliate have been found in
the Caribbean on mangrove peat wall, sunken wood and leaf debris (**1**, Twin
Cays Island, Belize; **2**, Guadeloupe, French West Indies; Rinke et al., 2006;
Laurent et al., 2009, 2013). In the Gulf of Mexico, the symbiosis was found
in the Florida Keys (**3**) (Bauer-Nebelsick et al., 1996a). In the Atlantic Ocean,
it was found in Lanzarote in the Canary Islands (**4**) (Wirtz and Debelius,
2003). It was also collected from rocks near sea grass debris accumulation
in the Mediterranean Sea (**5**, Corsica, France) and in the Adriatic Sea from
sunken wood (**6**) (Bright M., personal observation). The original description
reported _Z. niveum_ from the Red Sea (**7**), and recently it has been
described growing on bones of a whale fall deployed in the Tokyo Bay,
Japan (**8**) (Kawato et al., 2010).

In addition, the host's peculiar behavior of contracting and
expanding, along with currents generated by the feeding micro-
zooids, change the chemical environment (**Figure 10**). Colony
contractions are extremely fast (520 mm s^{-1}) and occur on aver-
age every 1.7 min. The zooids bunch together and the colony
whips downward toward the peat surface followed by slow expan-
sions, which are about 700–1000 times slower than contraction
(Vopel et al., 2002). During slow expansion, sulfidic water sticks
to the colony and is dragged along upward (Vopel et al., 2001).
After fully expanded, the microzooids resume filter feeding by
beating their oral cilia (Vopel et al., 2002). The Reynolds numbers
change from about 102 during contraction to 10^{-1} during expan-
sion (Vopel et al., 2002), and the symbionts may overcome the
diffusion-limited substrate supply by beating of host cilia (Vopel
et al., 2005).

TRANSMISSION

Transmission is vertical: the macrozooids that leave the mother
colony to build new colonies are also covered with the symbionts
(Bauer-Nebelsick et al., 1996a,b). This has been confirmed with
two symbiont-specific 16S rRNA probes (ZNS 196, ZNS 1439;
Rinke et al., 2006) for both the population in Twin Cays (Belize)
and in Calvi (Mediterranean Sea; Rinke et al., 2006, 2009). For the
whale fall populations, one of the specific probes (ZNS 196) was
tested and proved positive (Kawato et al., 2010).

This model system might be especially interesting from an
evolutionary point of view. In general, horizontal transmission,
in which the symbiont is picked up from the environment each

et al., 2005). In contrast, the wood surface colonized by the ciliates
had only about 100 μmol L^{-1} ΣH$_2$S. Fluctuations between these
maxima and almost fully oxygenated seawater occurred in less than
one hour (Laurent et al., 2009).
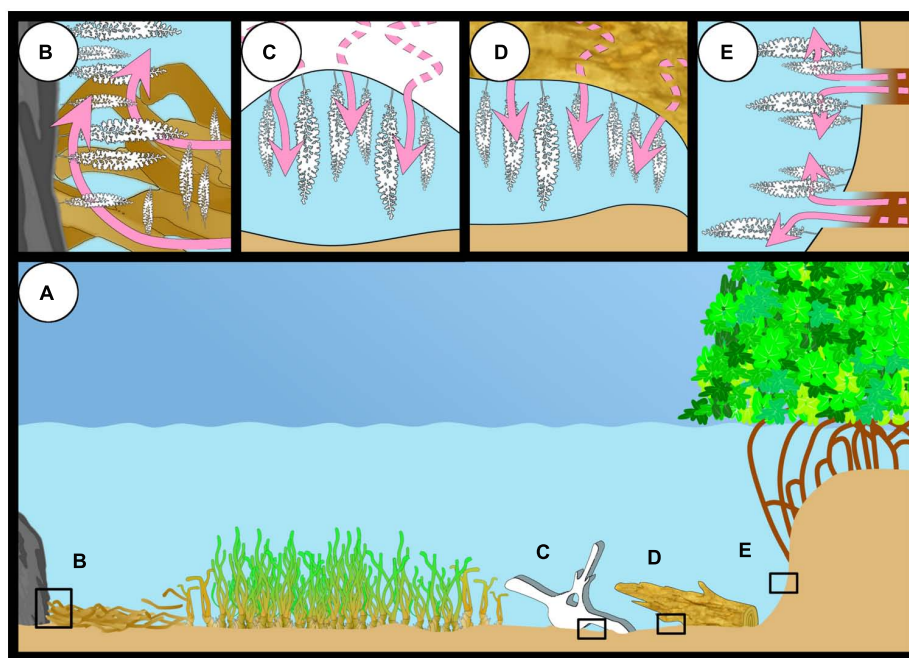
FIGURE 8 | The different habitats of _Zoothamnium niveum_ (A).
The giant ciliate can colonize hard substrate close to sea grass
debris accumulation where sulfide (pink arrows) is produced or grow
directly on the sea grass debris itself (**B**). They have also been

reported from a whale bone recovered from the deep sea and
experimentally deployed in shallow waters (**C**), from sunken wood
(**D**), and mangrove peat walls where degrading vegetal debris
including rootlets (**E**).

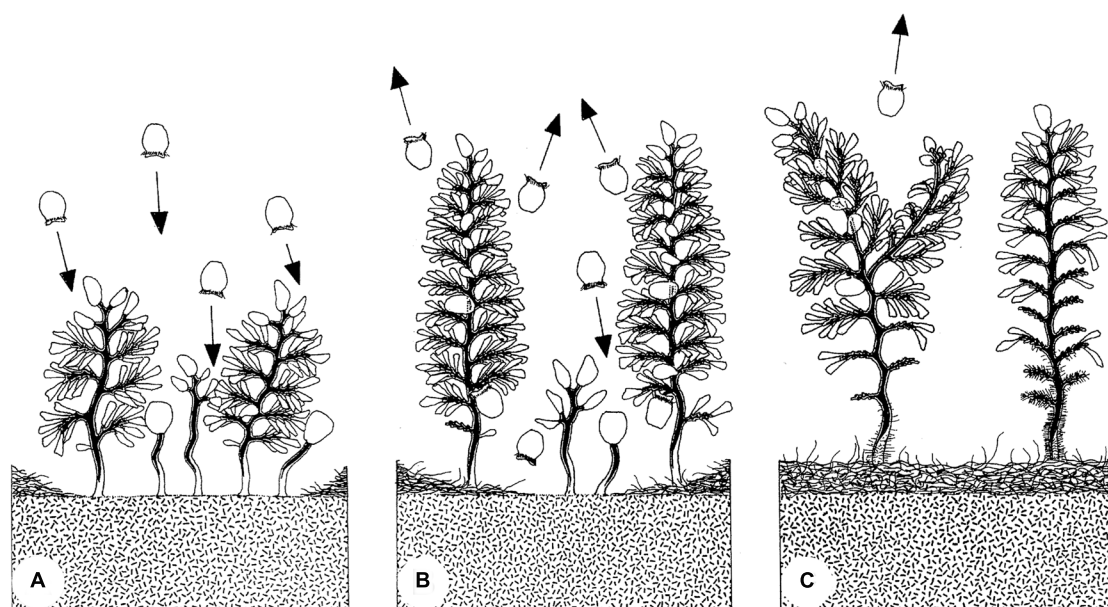**FIGURE 9 | Evolution of a patch of *Zoothamnium niveum* colony.** The swarmers colonize a disturbed area **(A)**. The settled colonies grow and start releasing new swarmers during a maturation phase **(B)**. Finally, the colonies enter a senescent phase **(C)**. Mature colonies are losing microzooids at the bottom part of the stalk, which starts to be overgrown by a variety of bacteria (Ott et al., 1998).

generation anew, is considered to be the ancestral mode of symbiont transfer between generations. Mixed modes or strict vertical transmissions are assumed to have evolved later (Bright and Bulgheresi, 2010). In contrast, in the *Z. niveum* symbiosis, we suggest that vertical transmission is the ancestral mode of transmission. This interpretation is based on the simple design of an ectosymbiotic partner covering also the asexually produced propagules.

Vertical transmission, however, may not be the only option. The symbiont's location on the host surface potentially allows for symbiont replacement by other bacteria from the surrounding environment. Moreover, release of symbionts due to sloppy feeding by the host and/or upon host death may support a free-living population from which the symbiont population could be re-inoculated. In contrast, strictly vertically transmitted symbionts no longer occur in the free-living environment and have co-evolved with their hosts (Bright and Bulgheresi, 2010). Thus, the potential of additional horizontal transmission in this model system should be explored in the future: it would influence the dynamics and demography of the symbiont population dramatically (see Vrijenhoek, 2010).

CULTIVATION OF SYMBIOSIS
Instead of experimentally creating a sulfide and oxygen gradient as found in nature, the symbiosis was successfully cultivated with populations from Calvi in a flow-through respirometer system with stable conditions (Rinke et al., 2007). The continuous flow of all chemicals enables breaking the host's control over the access to these chemicals and therefore also manipulating the environmental conditions for both partners. Optimal conditions (24–25°C, salinity 40, pH 8.2, $\sim$ 200 μmol L^{-1} O$_2$, 3–33 μmol L^{-1} ΣH$_2$S,
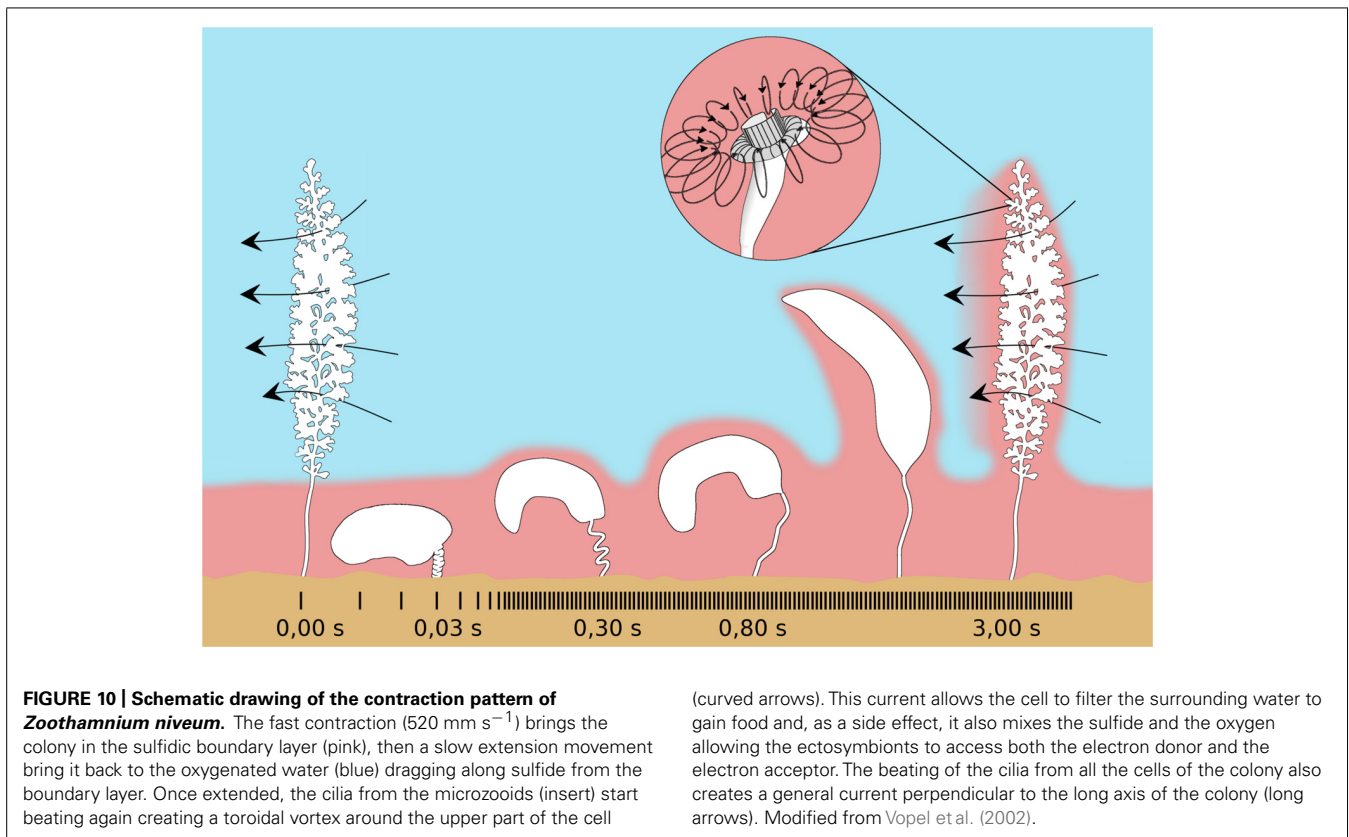
flow rate 100 ml h^{-1}) yielded a 10-fold increase in host colonies in 1 week. The mean life span of each colony was 11 days and host division rates of the top terminal zooid ranged from 4.1 to 8.2 day^{-1} during the first 8 days of growth phase; this was followed by a senescence phase during which more microzooids on branches were dying than being produced (**Figure 3**). In contrast, with no external sulfide source under normoxic conditions, growth was slower and the life span was considerably reduced to about 4 days (Rinke et al., 2007).

As expected due to uniform environmental conditions in this steady flow system, also uniform, rod-shaped symbionts covered the entire host. This finding supports the hypothesis that the ciliary beating in microzooids highly influences symbiont performance (Vopel et al., 2005). Furthermore, the frequency of dividing symbionts was taken as a measure of fitness. On the upper parts of microzooids, fitness was higher under optimal cultivation conditions compared to the *in situ* population. Fitness on the lower part of the microzooids was similar between the two populations.

Comparing the cultures of the Mediterranean and Caribbean populations, the latter reached maximal size within 4 days and had a mean life span of 7 days (Ott and Bright, 2004; Ott et al., 2004). The average water temperature of the former culture was 24–25°C, of the latter about 28°C (Vopel et al., 2001). The observed differences might reflect elevated metabolic rates under warmer conditions, leading to faster growth and shorter life span compared to colder conditions (Rinke et al., 2007).

BENEFITS AND COSTS
The question of benefits for both partners, which should exceed the costs in mutualism, is difficult to answer. It requires comparisons between host and symbiont fitness of free-living cultures as

FIGURE 10 | Schematic drawing of the contraction pattern of *Zoothamnium niveum*. The fast contraction (520 mm s^{-1}) brings the colony in the sulfidic boundary layer (pink), then a slow extension movement bring it back to the oxygenated water (blue) dragging along sulfide from the boundary layer. Once extended, the cilia from the microzooids (insert) start beating again creating a toroidal vortex around the upper part of the cell (curved arrows). This current allows the cell to filter the surrounding water to gain food and, as a side effect, it also mixes the sulfide and the oxygen allowing the ectosymbionts to access both the electron donor and the electron acceptor. The beating of the cilia from all the cells of the colony also creates a general current perpendicular to the long axis of the colony (long arrows). Modified from Vopel et al. (2002).

well as of cultures in which the partners cooperate or defect (Buston and Balshine, 2007). Appropriate experiments have proven extremely difficult to carry out. In thiotrophic symbioses, several lines of thought have been pursued, but direct evidence is scarce. Several potential benefits have been investigated for the host, including direct nourishment by the symbiont as well as detoxification of sulfide, and for the symbiont, including the provision of substrates for sulfur oxidation and carbon fixation and a competition-free habitat (see Fisher and Childress, 1992; Ott et al., 2004; Stewart et al., 2005; Cavanaugh et al., 2006; Dubilier et al., 2008).

In several systems, nourishment of the host at some costs to the symbiont has been shown. Fast release of fixed organic carbon and digestion of symbionts are the two means of translocation from the symbiont to the host, for example, in the vestimentiferan tubeworm *Riftia pachyptila* (Felbeck, 1985; Felbeck and Jarchow, 1998; Bright et al., 2000) and the bivalves *Loripes lucinalis*, *Lucinoma aequizonata*, and *Solemya reidi* (Felbeck, 1983; Fisher and Childress, 1986; Distel and Felbeck, 1988; Herry et al., 1989). Also, preliminary studies on *Z. niveum* and *Cand.* Thiobios zoothamnicoli point to both translocation processes using ^{14}C bicarbonate pulse chase incubations and tissue autoradiography (Rinke, 2002). After short pulses of 15 min label was present over host tissue indicating release, and after long pulses of 3 h and chases of 12 and 24 h, respectively, this label increased indicating digestion (Rinke, 2002). In addition, food vacuoles contained bacteria with the same size and shape as the symbiont with its typical sulfur vesicles (Bauer-Nebelsick et al., 1996b).

In some thiotrophic symbioses the digestive system is completely reduced, for example, in siboglinid tubeworms and gutless oligochaetes (see Dubilier et al., 2008). Here, the entire food should come from the symbiont. In other systems the digestive system still functions, additionally allowing for "normal" feeding. The microzooids in *Z. niveum* also have a functioning digestive system (Bauer-Nebelsick et al., 1996a,b). The degree to which host nourishment depends on symbionts or ingested prey has not been studied in any system yet. However, cultivation experiments in *Z. niveum* show that host fitness (measured as host growth and life span) was considerably decreased when symbionts were forced to defect. *Cand.* Thiobios zoothamnicoli could not fix carbon under normoxic culture conditions without sulfide (Rinke et al., 2007). The only means of nourishment left for the host were symbiont digestion and food uptake from the surrounding seawater. This indicates that a considerable portion of food comes from the symbionts.

Sulfide is highly toxic to aerobic eukaryotes (National Research Council, 1979). It inhibits cytochrome *c* oxidase, the eukaryote terminal enzyme of the mitochondrial electron transport chain (Dorman et al., 2002). Accordingly, the hosts of thiotrophic symbionts are challenged in providing their symbionts with sulfide while at the same time avoiding poisoning. Detoxification of sulfide through uptake and oxidation by symbionts has been proposed several times (Somero et al., 1989). Short incubations with Na$_2$^{35}S and autoradiographic analysis in the stilbonematid *Eubostrichus dianae* showed that most uptake

was in the thiotrophic ectosymbionts (Powell et al., 1979). Future studies are urgently needed using aposymbiotic hosts exposed to sulfide in order to determine whether symbiont presence (with their sulfide oxidation capabilities) affects host fitness.

Access to oxygen and sulfide for thiotrophic ectosymbionts is generally facilitated by the host's behavior (Ott et al., 2004). Migrations through the chemocline in sediments have been reported in the ciliate *Kentrophoros* ssp. (Fenchel and Finlay, 1989), the stilbonematin nematodes (Ott et al., 1991) and the gutless oligochaetes (Giere, 1992). Polz et al. (1999, 2000) observed the shrimp *Rimicaris exoculata* swimming in and out of hydrothermal vent fluid as well as ventilation of the chamber in which its symbionts reside. In *Z. niveum*, the host contracts and expands continuously, facilitating switches between sulfidic and oxygenated seawater (Ott et al., 1998). The symbionts on the host's surface were suggested to overcome the diffusion limitations of their substrate supply by two processes: feeding currents generated by the host, and the pulsed advection of sulfidic seawater from the peat caused by interactions of the boundary layer flow with groups of ciliates (Vopel et al., 2005). Interestingly, all the symbionts exposed to the feeding currents are larger and coccoid in shape, while the symbionts on the other host part are less favored and thus remain smaller and rod-shaped (Rinke et al., 2007). This emphasizes the importance of host-generated ciliary currents.

Although *Cand.* Thiobios zoothamnicoli is tightly associated with its ciliate host, the ectosymbiotic location does not provide shelter from competing microbes. Nevertheless, most parts of the host are exclusively covered by the symbiont, pointing to mechanisms developed against unspecific colonization. Microbial fouling on more basal, older host parts suggests that the host controls colonizers until it become senescent. Only then do other microbes appear on top of the symbionts, sometimes replacing them (Bauer-Nebelsick et al., 1996b).

Detailed analyses elucidated the importance of the host surface for colonization and of host behavior for the symbiont population density (Røy et al., 2009). Sulfide transport and estimated oxygen consumption were incorporated in a model of sulfide requirements sustaining chemoautotrophic growth by analyzing the flow field around individual zooids. Fluxes of 6.61 μmol O_2 m^{-2} s^{-1} and 3.19 μmol $\Sigma H_2 S$ m^{-2} s^{-1} were calculated. This model suggests that sulfide uptake rates are 100 times larger for host-associated symbionts than for free-living bacteria on flat surfaces (Røy et al., 2009).

Some evidence points to mutualism in this ciliate symbiosis. While the host benefits from the symbiont's organic carbon, translocated to the host (Rinke, 2002), the host's costs to carry an ectosymbiotic coat during all life stages have not been explored. Especially the costs involved in transporting the symbiont during dispersal in the water column are unknown (Genkai-Kato and Yamamura, 1999). Swarmers might move in the boundary layer close to the peat surface, enabling uninterrupted thiotrophic symbiont functioning. Alternatively, they might migrate through the oxygenated water column and, depending on dispersal time, must deal with a non-functioning symbiont; this would potentially incur some costs to the host. Overall, the host is by far the largest representative in the genus *Zoothamnium* (see Bauer-Nebelsick et al., 1996a), indicating that benefits exceed costs.

The symbiont benefits from the host, which provides large surfaces or colonization and therefore supports enhanced symbiont population density with optimal conditions for sulfide oxidation and carbon fixation compared to flat surfaces (Røy et al., 2009). This colonization appears to be host controlled: space is allocated exclusively to the symbiont, enhancing symbiont fitness. The symbiont's costs involve population reduction through digestion and possible host controlled enhanced leaking of fixed carbon to the host as has been shown for the photoautotrophic *Symbiodinium* in corals (see Trench, 1979). Such leaking processes occur to a certain degree in free-living microalgae and autotrophic bacteria, but are enhanced when the microalgae are host associated (see Trench, 1979). Also the thiotrophic endosymbiont of the giant tubeworm *Riftia pachyptila* leaks organic carbon when artificially separated from its host (Felbeck and Jarchow, 1998). Whether the ciliate host enhances this naturally occurring leaking process remains to be studied.

EVOLUTION AND PERSISTENCE

A longstanding paradigm in cooperation theory depicts the evolution of mutualism from parasitism (Roughgarden, 1975; Ewald, 1987; Lipsitch et al., 1996; Yamamura, 1996). It has been argued that through vertical transmission lower virulence is selected and thus shifts the relationship toward a beneficial one. More recently, this general hypothesis has been rejected because in many systems phylogenetic information suggests mutualism can also evolve *de novo* from previously free-living partners or from previous mutualistic associations (Douglas, 2010; Sachs et al., 2011). *De novo* evolution of the *Cand.* Thiobios zoothamnicoli – *Z. niveum* mutualism is also the most likely scenario. Based on 16S rRNA, *Cand.* Thiobios zoothamnicoli is most closely related to a variety of free-living bacteria (**Figure 6**). Furthermore, no pathogens or parasites are known with sulfur-oxidizing, autotrophic metabolism (Dubilier et al., 2008).

A mathematical model predicts that vertical transmission can evolve when the costs for vertical transmission are low, the availability of free-living symbiont is poor, and byproduct usage is high on both sides (Yamamura, 1993, 1996; Genkai-Kato and Yamamura, 1999). While we cannot comment on the first two parameters in the giant ciliate symbiosis, there are some indications that byproduct usage is present and played an important role for the evolution of this vertically transmitted symbiosis.

Byproduct benefits involve one partner providing goods to the other at no costs, but rather as an automatic, coincident consequence of selfish traits (West-Eberhard, 1975; Connor, 1986, 1995; Hauert et al., 2006). Such byproduct benefits are considered to be important in the initiation of mutualism (Sachs et al., 2011). This self-interest action benefits both the actor and the associated recipient. Byproduct benefits, however, do not challenge evolutionary theory because both partners cooperating is favored over one partner cooperating and the other one defecting (Hauert et al., 2006) and have been largely neglected (Douglas, 2010).

Several characteristics of the present symbiosis may point to byproduct benefits, one provided by the symbiont to the host, the
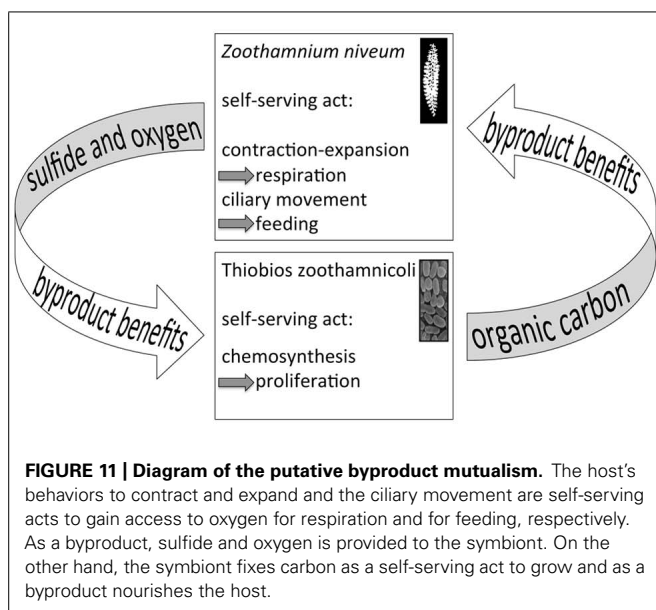
FIGURE 11 | Diagram of the putative byproduct mutualism. The host's behaviors to contract and expand and the ciliary movement are self-serving acts to gain access to oxygen for respiration and for feeding, respectively. As a byproduct, sulfide and oxygen is provided to the symbiont. On the other hand, the symbiont fixes carbon as a self-serving act to grow and as a byproduct nourishes the host.

other provided by the host to the symbiont – at no costs. The leaking of fixed carbon from the symbiont cell initially appears costly. Nonetheless, these costs are not associated with symbiosis per se but with the inability of autotrophs to keep all the fixed carbon inside the cell, independent of a free-living or host-associated life style. Such costs can be allocated to the symbiosis only if they are enhanced and controlled by the host. Finally, we consider the provision of sulfide and oxygen for chemosynthesis as a byproduct benefit provided by the host through its contracting and expanding behavior as well as by its ciliary movement (**Figure 11**).

Several mechanisms identified in evolutionary theory are crucial for the maintenance of mutualism: (1) partner choice, (2) partner sanctions, (3) and partner fidelity feedback (Bull and Rice, 1991; Noë and Hammerstein, 1994; Johnstone and Bshary, 2002; West et al., 2002a,b; Sachs et al., 2004; Weyl et al., 2010; Archetti et al., 2011). Their importance differs according to the mode of transmission (Ewald, 1987; Douglas, 2010; Sachs et al., 2011). In horizontal transmission, partner choice is crucial for the establishment, during which a cooperative symbiont is selected from the environment in advance of any possible exploitation (Bull and Rice, 1991). In contrast, during vertical transmission, the partner has already been chosen and is transferred to the next generation with high fidelity. Based on our current state of knowledge, this appears to be the case in the *Z. niveum* symbiosis.

Consensus exists on the crucial role of partner fidelity feedback in mutualism with vertical transmission that ensures maintenance after establishment (Douglas, 2010; Sachs et al., 2011). In the *Z. niveum* symbiosis, some of the interactions might be based on partner fidelity feedback (**Figure 11**). The host's behavior, which supplies the symbionts with chemicals for chemosynthesis (a byproduct benefit), boosts symbiont fitness while increasing host fitness through nourishment. Cessation or decrease of host contraction-expansion behavior and ciliary movement directly

negatively affect host fitness. This would also decrease the oxygen supply for the host's respiration and restrict food uptake by impacting the ciliary movement of microzooids. In addition, the oxygen and sulfide supply fueling chemosynthesis by the symbiont would be diminished, impeding the translocation of organic carbon from the symbiont to the host.

If the symbiont defects by reducing the amount of fixed carbon translocated to the host, then host growth would be reduced, decreasing the host surface available for symbiont colonization. Host growth and symbiont population density are finely tuned, sustaining a monolayer. Accordingly, a defecting and therefore fitter symbiont would overgrow the host unless the latter can sanction the cheater. If, however, the provision of goods to the host is a byproduct of carbon fixation, then the symbiont cannot defect, and partner fidelity feedback would regulate the provision (see Weyl et al., 2010; Archetti et al., 2011).

CONCLUSION

This review illustrates our current state of knowledge on the *Z. niveum* – *Cand.* Thiobios zoothamnicoli symbiosis. Its extremely wide geographical distribution points to a cosmopolitan symbiosis in tropical to temperate shallow-water environments in which oxic–anoxic interfaces develop on decaying plants or animals. This association is specific for both partners, and the symbiont is permanently associated with the host and transferred vertically to the next host generation. It is obligate for the host, but whether or not it is obligate for the symbiont remains to be determined. Of all thiotrophic symbiosis, this mutualistic association has the highest potential of becoming a model system to study interspecies cooperation and the molecular mechanisms by which host and symbiont initiate the association and interact to persist. It can be cultivated and manipulated, and we recently successfully separated the partners and cultivated the aposymbiotic host (Bright M., Espada-Hinojosa S., Volland J. -M., personal observations). This opens the door to experimentally study the pre- and postinfection mechanisms.

REFERENCES

Archetti, M., Scheuring, I., Hoffman, M., Frederickson, M. E., Pierce, N. E., and Yu, D. W. (2011). Economic game theory for mutualisms and cooperation. *Ecol. Lett.* 14, 1300–1312. doi: 10.1111/j.1461-0248.2011.01697.x

Bauer-Nebelsick, M., Bardele, C. F., and Ott, J. (1996a). Redescription of *Zoothamnium niveum* (Hemprich & Ehrenberg, 1831) Ehrenberg, 1838 (Oligohymenophora, Peritrichida), a ciliate with ectosymbiotic, chemoautotrophic bacteria. *Eur. J. Protistol.* 32, 18–30. doi: 10.1016/S0932-4739(96)80036-8

Bauer-Nebelsick, M., Bardele, C. F., and Ott, J. A. (1996b). Electron microscopic studies on *Zoothamnium niveum* (Hemprich & Ehrenberg, 1831) Ehrenberg, 1838 (Oligohymenophora, Peritrichida), a ciliate with ectosymbiotic, chemoautotrophic bacteria. *Eur. J. Protistol.* 32, 202–215. doi: 10.1016/S0932-4739(96)80020-4

Bory de Saint-Vincent, J.-B.-G.-M. (1824). Zoothamnie; Zoothamnia. *Encyl. Mèth. (Zooph.)* 138, 816–817.

Bright, M., and Bulgheresi, S. (2010). A complex journey: transmission of microbial symbionts. *Nat. Rev. Microbiol.* 8, 218–230. doi: 10.1038/nrmicro2262

Bright, M., Keckeis, H., and Fisher, C. R. (2000). An autoradiographic examination of carbon fixation, transfer and utilization in the *Riftia pachyptila* symbiosis. *Mar. Biol.* 136, 621–632. doi: 10.1007/s002270050722

Bull, J. J., and Rice, W. R. (1991). Distinguishing mechanisms for the evolution of cooperation. *J. Theor. Biol.* 149, 63–74. doi: 10.1016/S0022-5193(05)80072-4

Buston, P. M., and Balshine, S. (2007). Cooperating in the face of uncertainty: a consistent framework for understanding the evolution of cooperation. *Behav. Process.* 76, 152–159. doi: 10.1016/j.beproc.2007.01.020

Cavanaugh, C., Mckiness, Z., Newton, I. G., and Stewart, F. (2006). "Marine chemosynthetic symbioses," in *The Prokaryotes*, eds M. Dworkin, S. Falkow, E. Rosenberg, K.-H. Schleifer, and E. Stackebrandt (New York: Springer), 475–507.

Childress, J. J., and Girguis, P. R. (2011). The metabolic demands of endosymbiotic chemoautotrophic metabolism on host physiological capacities. *J. Exp. Biol.* 214, 312–325. doi: 10.1242/jeb.049023

Clamp, J. C., and Williams, D. (2006). A molecular phylogenetic investigation of *Zoothamnium* (Ciliophora, Peritrichia, Sessilida). *J. Eukaryot. Microbiol.* 53, 494–498. doi: 10.1111/j.1550-7408.2006.00132.x

Connor, R. C. (1986). Pseudo-reciprocity: investing in mutualism. *Anim. Behav.* 34, 1562–1584. doi: 10.1016/S0003-3472(86)80225-1

Connor, R. C. (1995). The benefits of mutualism: a conceptual framework. *Biol. Rev.* 70, 427–457. doi: 10.1111/j.1469-185X.1995.tb01196.x

Dattagupta, S., Schaperdoth, I., Montanari, A., Mariani, S., Kita, N., Valley, J. W., et al. (2009). A novel symbiosis between chemoautotrophic bacteria and a freshwater cave amphipod. *ISME J.* 3, 935–943. doi: 10.1038/ismej.2009.34

Distel, D. L., and Felbeck, H. (1988). Pathways of inorganic carbon fixation in the endosymbiont-bearing lucinid clam *Lucinoma aequizonata* Part 2. Analysis of the individual contributions of host and symbiont cells to inorganic carbon assimilation. *J. Exp. Zool.* 247, 11–22. doi: 10.1002/jez.1402470103

Dorman, D. C., Moulin, F. J.-M., Mcmanus, B. E., Mahle, K. C., James, R. A., and Struve, M. F. (2002). Cytochrome oxidase inhibition induced by acute hydrogen sulfide inhalation: correlation with tissue sulfide concentrations in the rat brain, liver, lung, and nasal epithelium. *Toxicol. Sci.* 65, 18–25. doi: 10.1093/toxsci/65.1.18

Douglas, A. E. (2010). *The Symbiotic Habit.* Princeton: Princeton University Press.

Dragesco, J. (1948). Sur la biologie du Zoothamnium pelagicum (du Plessis). *Bull. Soc. Zool. Fr.* 73, 130–134.

Dubilier, N., Bergin, C., and Lott, C. (2008). Symbiotic diversity in marine animals: the art of harnessing chemosynthesis. *Nat. Rev. Microbiol.* 6, 725–740. doi: 10.1038/nrmicro1992

Ehrenberg, C. G. (1838). *Die Infusionsthierchen als vollkommene Organismen. Ein Blick in das tiefere organische Leben der Natur.* Leipzig: Leopold Voss Verlag. doi: 10.5962/bhl.title.58475

Ewald, P. W. (1987). Transmission modes and evolution of the parasitism–mutualism continuum. *Ann. N. Y. Acad. Sci.* 503, 295–306. doi: 10.1111/j.1749-6632.1987.tb40616.x

Fauré-Fremiet, E., Favard, P., and Carasso, N. (1963). Images électroniques d'une microbiocénose marine. *Cah. Biol. Mar.* 4, 61–64.

Felbeck, H. (1983). Sulfide oxidation and carbon fixation by the gutless clam *Solemya reidi*: an animal–bacteria symbiosis. *J. Comp. Physiol. B* 152, 3–11. doi: 10.1007/BF00689721

Felbeck, H. (1985). CO_2 fixation in the hydrothermal vent tube worm *Riftia pachyptila* (Jones). *Physiol. Zool.* 58, 272–281.

Felbeck, H., and Jarchow, J. (1998). Carbon release from purified chemoautotrophic bacterial symbionts of the hydrothermal vent tubeworm *Riftia pachyptila. Physiol. Zool.* 71, 294–302.

Fenchel, T., and Finlay, B. J. (1989). Kentrophoros: a mouthless ciliate with a symbiotic kitchen garden. *Ophelia* 30, 75–93.

Fisher, C. R., and Childress, J. J. (1986). Translocation of fixed carbon from symbiotic bacteria to host tissues in the gutless bivalve *Solemya reidi. Mar. Biol.* 93, 59–68. doi: 10.1007/BF00428655

Fisher, C. R., and Childress, J. J. (1992). Organic carbon transfer from methanotrophic symbionts to the host hydrocarbon-seep mussel. *Symbiosis* 12, 221–235.

Furssenko, A. (1929). Lebenscyclus und Morphologie von *Zoothamnium arbuscula* Ehrenberg (infusoria Peritricha). *Arch. Protistenkunde* 67, 376–500.

Genkai-Kato, M., and Yamamura, N. (1999). Evolution of mutualistic symbiosis without vertical transmission. *Theor. Popul. Biol.* 55, 309–323. doi: 10.1006/tpbi.1998.1407

Giere, O. (1992). Benthic life in sulfidic zones of the sea-ecological and structural adaptations to a toxic environment. *Verh. Dtsch. Zool. Ges.* 85, 77–93.

Gros, O., Frenkiel, L., and Moueza, M. (1997). Embryonic, larval, and post-larval development in the symbiotic clam *Codakia orbicularis* (Bivalvia: Lucinidae). *Invertebr. Biol.* 116, 86–101. doi: 10.2307/3226973

Gruber-Vodicka, H. R., Dirks, U., Leisch, N., Baranyi, C., Stoecker, K., Bulgheresi, S., et al. (2011). Paracatenula, an ancient symbiosis between thiotrophic Alphaproteobacteria and catenulid flatworms. *Proc. Natl. Acad. Sci. U.S.A.* 108, 12078–12083. doi: 10.1073/pnas.1105347108

Hauert, C., Michor, F., Nowak, M. A., and Doebeli, M. (2006). Synergy and discounting of cooperation in social dilemmas. *J. Theor. Biol.* 239, 195–202. doi: 10.1016/j.jtbi.2005.08.040

Hemprich, F. W., and Ehrenberg, C. G. (1829). Symbolae Physicae. Evertebrata. I. Protozoa. Abhandlungen der Akademie der Wissenchaften zu Berlin.

Hemprich, F. W., and Ehrenberg, C. G. (1831). Symbolae Physicae. Evertebrata. I. Protozoa. Abhandlungen der Akademie der Wissenchaften zu Berlin.

Herry, A., Diouris, M., and Le Pennec, M. (1989). Chemoautotrophic symbionts and translocation of fixed carbon from bacteria to host tissues in the littoral bivalve *Loripes lucinalis* (Lucinidae). *Mar. Biol.* 101, 305–312. doi: 10.1007/BF00428126

Himmel, D., Maurin, L. C., Gros, O., and Mansot, J.-L. (2009). Raman microspectrometry sulfur detection and characterization in the marine ectosymbiotic nematode Eubostrichus dianae (Desmodoridae, Stilbonematinae). *Biol. Cell* 101, 43–54. doi: 10.1042/BC20080051

Joachimiak, M. P., Weisman, J. L., and May, B. C. H. (2006). JColorGrid: software for the visualization of biological measurements. *BMC Bioinformatics* 7:225. doi: 10.1186/1471-2105-7-225

Johnstone, R. A., and Bshary, R. (2002). From parasitic to mutualism: partner control in asymmetric interactions. *Ecol. Lett.* 5, 634–639. doi: 10.1046/j.1461-0248.2002.00358.x

Kawato, M., Uematsu, K., Kaya, T., Pradillon, F., and Fujiwara, Y. (2010). First report of the chemosymbiotic ciliate *Zoothamnium niveum* from a whale fall in Japanese waters. *Cah. Biol. Mar.* 51, 413–421.

Kloiber, U., Pflugfelder, B., Rinke, C., and Bright, M. (2009). Cell proliferation and growth in *Zoothamnium niveum* (Oligohymenophora, Peritrichia) – thiotrophic bacteria symbiosis. *Symbiosis* 47, 43–50. doi: 10.1007/BF03179969

Laurent, M. C. Z., Gros, O., Brulport, J.-P, Gaill, F., and Le Bris, N. (2009). Sunken wood habitat for thiotrophic symbiosis in mangrove swamps. *Mar. Environ. Res.* 67, 83–88. doi: 10.1016/j.marenvres.2008.11.006

Laurent, M. C. Z., Le Bris, N., Gaill, F., and Gros, O. (2013). Dynamics of wood fall colonization in relation to sulfide concentration in a mangrove swamp. *Mar. Environ. Res.* 87–88, 85–95. doi: 10.1016/j.marenvres.2013.03.007

Laval, M. (1968). Zoothamnium pelagicum du Plessis. Cilié péritricheplanctonique: morphologie, croissance et comportament. *Protistologica* 4, 333–363.

Laval, M. (1970). "Presence de bacteries intranucleaires chez Zoothamnium pelagicum (Cilié Peritriche) leur rôle dans la formation des pigments intracytoplasmatiques des zoides," in *Septième Congrès International de Microscopie Électronique* (Grenoble: Société Française de Microscopie Électronique), 403–404.

Laval-Peuto, M., and Rassoulzadegan, F. (1988). Autofluorescence of marine planktonic Oligotrichina and other ciliates. *Hydrobiologia* 159, 99–110. doi: 10.1007/BF00007371

Lipsitch, M., Siller, S., and Nowak, M. A. (1996). The evolution of virulence in pathogens with vertical and horizontal transmission. *Evolution* 50, 1729–1741. doi: 10.2307/2410731

Lovelock, C. E., Ruess, R. W., and Feller, I. C. (2011). CO2 efflux from cleared mangrove peat. *PLoS ONE* 6:e21279. doi: 10.1371/journal.pone.0021279

Maurin, L. C., Himmel, D., Mansot, J.-L., and Gros, O. (2010). Raman microspectrometry as a powerful tool for a quick screening of thiotrophy: an application on mangrove swamp meiofauna of Guadeloupe (F.W.I.). *Mar. Environ. Res.* 69, 382–389. doi: 10.1016/j.marenvres.2010.02.001

Muller, F., Brissac, T., Le Bris, N., Felbeck, H., and Gros, O. (2010). First description of giant Archaea (Thaumarchaeota) associated with putative bacterial ectosymbionts in a sulfidic marine habitat. *Environ. Microbiol.* 12, 2371–2383. doi: 10.1111/j.1462-2920.2010.02309.x

National Research Council. (1979). *Hydrogen Sulfide.* Baltimore: University Park Press.

Noë, R., and Hammerstein, P. (1994). Biological markets: supply and demand determine the effect of partner choice in cooperation, mutualism and mating. *Behav. Ecol. Sociobiol.* 35, 1–11. doi: 10.1007/BF00167053

Ott, J., and Bright, M. (2004). Sessile ciliates with bacterial ectosymbionts from Twin Cays, Belize. *Atoll Res. Bull.* 516, 1–7. doi: 10.5479/si.00775630.516.1

Ott, J., Bright, M., and Bulgheresi, S. (2004). Marine microbial thiotrophic ectosymbioses. *Oceanogr. Mar. Biol. Annu. Rev.* 42, 95–118. doi: 10.1201/9780203507810.ch4

Ott, J. A., Bright, M., and Schiemer, F. (1998). The ecology of a novel symbiosis between a marine peritrich ciliate and chemoautotrophic bacteria. *Mar. Ecol.* 19, 229–243. doi: 10.1111/j.1439-0485.1998.tb00464.x

Ott, J. A., Novak, R., Schiemer, F., Hentschel, U., Nebelsick, M., and Polz, M. (1991). Tackling the sulfide gradient: a novel strategy involving marine nematodes and chemoautotrophic ectosymbionts. *Mar. Ecol.* 12, 261–279. doi: 10.1111/j.1439-0485.1991.tb00258.x

Pflugfelder, B., Fisher, C. R., and Bright, M. (2005). The color of the trophosome: elemental sulfur distribution in the endosymbionts of *Riftia pachyptila* (Vestimentifera; Siboglinidae). *Mar. Biol.* 146, 895–901. doi: 10.1007/s00227-004-1500-x

Polz, M. F., Ott, J. A., Bright, M., and Cavanaugh, C. M. (2000). When bacteria hitch a ride. Ectosymbiotic associations between sulfur-oxidizing bacteria and eukaryotes represent a spectacular adaptation to environmental gradients. *ASM News* 66, 531–539.

Polz, M. F., Robinson, J. J., Cavanaugh, C. M., and Van Dover, C. L. (1999). Trophic ecology of massive shrimp aggregations at a Mid-Atlantic Ridge hydrothermal vent site. *Limnol. Oceanogr.* 43, 1631–1638. doi: 10.4319/lo.1998.43.7.1631

Powell, E. N., Crenshaw, M. A., and Rieger, R. M. (1979). Adaptations to sulfide in the meiofauna of the sulfide system. I. ^{35}S-sulfide accumulation and the presence of a sulfide detoxification system. *J. exp. mar. Biol. Ecol.* 37, 57–76. doi: 10.1016/0022-0981(79)90026-1

Quast, C., Pruesse, E., Yilmaz, P., Gerken, J., Schweer, T., Yarza, P., et al. (2013). The SILVA ribosomal RNA gene database project: improved data processing and web-based tools. *Nucleic Acids Res.* 41, D590–D596. doi: 10.1093/nar/gks1219

Rinke, C. (2002). *Nutritional Processes in the Chemoautotrophic Zoothamnium niveum Symbioses.* Diploma thesis, University of Vienna, Austria. Available at: http://othes.univie.ac.at/cgi/search/advanced

Rinke, C., Lee, R., Katz, S., and Bright, M. (2007). The effects of sulphide on growth and behavior of the thiotrophic *Zoothamnium niveum* symbiosis. *Proc. R. Soc. Lond. B Biol. Sci.* 274, 2259–2269. doi: 10.1098/rspb.2007.0631

Rinke, C., Schmitz-Esser, S., Loy, A., Horn, M., Wagner, M., and Bright, M. (2009). High genetic similarity between two geographically distinct strains of the sulfur-oxidizing symbiont "Candidatus Thiobios zoothamnicoli." *FEMS Microbiol. Ecol.* 67, 229–241. doi: 10.1111/j.1574-6941.2008.00628.x

Rinke, C., Schmitz-Esser, S., Stoecker, K., Nussbaumer, A. D., Molnár, D. A., Vanura, K., et al. (2006). "Candidatus Thiobios zoothamnicoli," an ectosymbiotic bacterium covering the giant marine ciliate *Zoothamnium niveum*. *Appl. Environ. Microbiol.* 72, 2014–2021. doi: 10.1128/AEM.72.3.2014-2021.2006

Roughgarden, J. (1975). Evolution of marine symbiosis – a simple cost-benefit model. *Ecology* 56, 1201–1208. doi: 10.2307/1936160

Røy, H., Vopel, K., Huettel, M., and Jørgensen, B. B. (2009). Sulfide assimilation by ectosymbionts of the sessile ciliate, *Zoothamnium niveum*. *Mar. Biol.* 156, 669–677. doi: 10.1007/s00227-008-1117-6

Sachs, J. L., Mueller, U. G., Wilcox, T. P., and Bull, J. J. (2004). The evolution of cooperation. *Q. Rev. Biol.* 79, 135–160. doi: 10.1086/383541

Sachs, J. L., Skophammer, R. G., and Regus, J. U. (2011). Evolutionary transitions in bacterial symbiosis. *Proc. Natl. Acad. Sci. U.S.A.* 108, 10800–10807. doi: 10.1073/pnas.1100304108

Somero, G. N., Childress, J. J., and Anderson, A. E. (1989). Transport, metabolism and detoxification of hydrogen sulfide in animals from sulfide rich marine environments. *Rev. Aquat. Sci.* 1, 591–614.

Stewart, F. J., Newton, I. L. G., and Cavanaugh, C. M. (2005). Chemosynthetic endosymbioses: adaptations to oxic–anoxic interfaces. *Trends Microbiol.* 13, 439–448. doi: 10.1016/j.tim.2005.07.007

Summers, F. M. (1938). Some aspects of normal development in the colonial ciliate *Zoothamnium alternans*. *Biol. Bull.* 74, 117–129. doi: 10.2307/1537891

Tamura, K., Peterson, D., Peterson, N., Stecher, G., Nei, M., and Kumar, S. (2011). MEGA5: molecular evolutionary genetics analysis using maximum likelihood, evolutionary distance, and maximum parsimony methods. *Mol. Biol. Evol.* 28, 2731–2739. doi: 10.1093/molbev/msr121

Trench, R. K. (1979). The cell biology of plant-animal symbiosis. *Annu. Rev. Plant. Physiol.* 30, 485–531. doi: 10.1146/annurev.pp.30.060179.002413

Vopel, K., Pöhn, M., Sorgo, A., and Ott, J. (2001). Ciliate-generated advective seawater transport supplies chemoautotrophic ectosymbionts. *Mar. Ecol. Prog. Ser.* 210, 93–99. doi: 10.3354/meps210093

Vopel, K., Reick, C. H., Arlt, G., Pöhn, M., and Ott, J. A. (2002). Flow microenvironment of two marine peritrich ciliates with ectobiotic chemoautotrophic bacteria. *Aquat. Microb. Ecol.* 29, 19–28. doi: 10.3354/ame029019

Vopel, K., Thistle, D., Ott, J., Bright, M., and Røy, H. (2005). Wave-induced H2S flux sustains a chemoautotrophic symbiosis. *Limnol. Oceanogr.* 50, 128–133. doi: 10.4319/lo.2005.50.1.0128

Vrijenhoek, R. C. (2010). Genetics and evolution of deep-sea chemosynthetic bacteria and their invertebrate hosts. *Top. Geobiol.* 33, 15–49. doi: 10.1007/978-90-481-9572-5_2

West, S. A., Kiers, E. T., and Denison, R. F. (2002a). Sanctions and mutualism stability: when should less beneficial mutualists be tolerated? *J. Evol. Biol.* 15, 830–837. doi: 10.1046/j.1420-9101.2002.00441.x

West, S. A., Kiers, E. T., Simms, E. L., and Denison, R. F. (2002b). Sanctions and mutualism stability: why do rhizobia fix nitrogen? *Proc. R. Soc. Lond. B Biol. Sci.* 269, 685–694. doi: 10.1098/rspb.2001.1878

West-Eberhard, M. J. (1975). The evolution of social behavior by kin selection. *Q. Rev. Biol.* 50, 1–33. doi: 10.2307/2821184

Weyl, E. G., Frederickson, M. E., Yu, D. W., and Pierce, N. E. (2010). Economic contract theory tests models of mutualism. *Proc. Natl. Acad. Sci. U.S.A.* 107, 15712–15716. doi: 10.1073/pnas.1005294107

Wirtz, P. (2008). New records of the giant ciliate *Zoothamnium niveum* (Protozoa, Peritricha). *Arquipélago* 25, 89–91.

Wirtz, P., and Debelius, H. (2003). *Niedere Tiere. Mittelmeer und Atlantik*. Hamburg: Jahr Top Special Verlag.

Yamamura, N. (1993). Vertical transmission and evolution of mutualism from parasitism. *Theor. Popul. Biol.* 44, 95–109. doi: 10.1006/tpbi.1993.1020

Yamamura, N. (1996). Evolution of mutualistic symbiosis: a differential equation model. *Res. Popul. Ecol.* 38, 211–218. doi: 10.1007/BF02515729

Chapter 2

NanoSIMS and tissue autoradiography reveal symbiont carbon fixation and organic carbon transfer to giant ciliate host

Coauthor paper

isme

ARTICLE
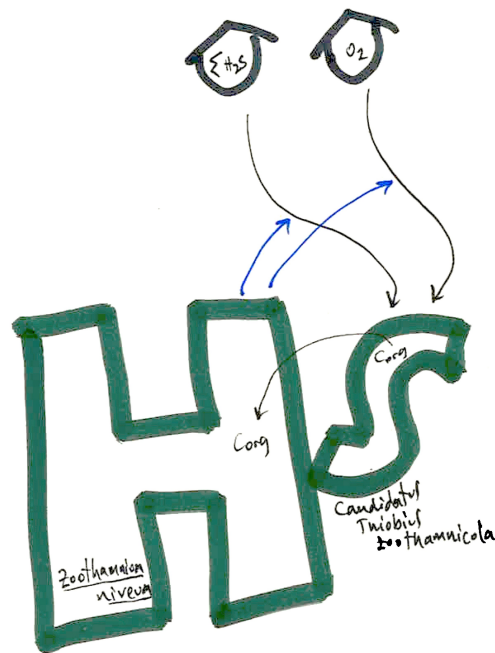
NanoSIMS and tissue autoradiography reveal symbiont carbon fixation and organic carbon transfer to giant ciliate host

Jean-Marie Volland[1] · Arno Schintlmeister[2] · Helena Zambalos[1] · Siegfried Reipert[3] · Patricija Mozetič[4] · Salvador Espada-Hinojosa[1] · Valentina Turk[4] · Michael Wagner [2] · Monika Bright [1]

Abstract

The giant colonial ciliate *Zoothamnium niveum* harbors a monolayer of the gammaproteobacteria *Cand*. Thiobios zoothamnicoli on its outer surface. Cultivation experiments revealed maximal growth and survival under steady flow of high oxygen and low sulfide concentrations. We aimed at directly demonstrating the sulfur-oxidizing, chemoautotrophic nature of the symbionts and at investigating putative carbon transfer from the symbiont to the ciliate host. We performed pulse-chase incubations with ^{14}C- and ^{13}C-labeled bicarbonate under varying environmental conditions. A combination of tissue autoradiography and nanoscale secondary ion mass spectrometry coupled with transmission electron microscopy was used to follow the fate of the radioactive and stable isotopes of carbon, respectively. We show that symbiont cells fix substantial amounts of inorganic carbon in the presence of sulfide, but also (to a lesser degree) in the absence of sulfide by utilizing internally stored sulfur. Isotope labeling patterns point to translocation of organic carbon to the host through both release of these compounds and digestion of symbiont cells. The latter mechanism is also supported by ultracytochemical detection of acid phosphatase in lysosomes and in food vacuoles of ciliate cells. Fluorescence in situ hybridization of freshly collected ciliates revealed that the vast majority of ingested microbial cells were ectosymbionts.

Introduction

In many symbiotic mutualisms, microbial symbionts provide benefits to their eukaryote host through nourishment [1, 2]. Two principal modes of organic carbon translocation from the symbiont to the host—host digestion of symbionts

✉ Jean-Marie Volland
volland_jeanmarie@hotmail.com

1 Department of Limnology and Bio-Oceanography, University of Vienna, Vienna, Austria

2 Department of Microbiology and Ecosystem Science, Research Network "Chemistry meets Microbiology" and Large-Instrument Facility for Advanced Isotope Research, University of Vienna, Vienna, Austria

3 Cell Imaging and Ultrastructure Research (CIUS), University of Vienna, Vienna, Austria

4 National Institute of Biology, Marine Biology Station, Piran, Slovenia

and direct release of soluble organic molecules and uptake into host tissue—are well characterized in photo-autotrophic [3–9] and in chemoautotrophic symbioses (see Nelson and Fisher [10]). Although all studied hosts actively digest symbionts, translocation of fixed carbon to the host through release from the symbiont has up to now been reported only for *Symbiodinium* in corals [7]; upside-down jellyfish [11]; sulfur-oxidizing, chemoautotrophic (thio-trophic) endosymbionts in solemyid and lucinid bivalves [12, 13]; and in vestimentiferans [14–16]. Much less attention has been paid to thiotrophic ectosymbiosis with the exception of the shrimp *Rimicaris*, for which transfer of fixed organic carbon from the ectosymbionts to the host was shown [17].

In mutualism, trait loss in the receiving partner may be the result of compensation of trait function by the providing partner [18, 19]. Nourished by their chemoautotrophic symbionts, compensatory trait loss is evident in some hosts that either have partly reduced (e.g., solemyid bivalves [20], stilbonematid nematodes [21]) or even entirely lost their digestive system (e.g., oligochaetes [22, 23]; vestimenti-ferans [24]; *Kentrophoros* ciliate [25]). Other hosts retain a fully functioning digestive system (e.g., bathymodiolin

bivalves) and apparently supplement their symbiotic diet with feeding on other food sources [22].

Protists frequently form associations with bacteria [26–28], but associations with thiotrophic bacteria are known only in two protist taxa, the euglenozoans and ciliates ([25, 29–32]). In contrast to the high diversity of thiotrophic symbiont location on (ectosymbionts) or in (extracellular and intracellular endosymbionts) animal hosts, the thiotrophic symbionts of protists exclusively colonize the host extracellularly.

The giant colonial ciliate *Zoothamnium niveum* thrives in marine shallow waters on sulfide-emitting decaying plants and animal bones. The host forms a feather-shaped, sessile colony up to 1.5 cm in length. Ciliates are mostly unicellular, but the giant ciliate is a physiologically and functionally integrated, multicellular unit [33]. It is composed of a stalk and alternate branches with hundreds to thousands of individual cells with different function: the feeding microzooids, the dividing terminal zooids, and the macrozooids, which detach from the mother colony and disperse as swarmers to found new asexually produced colonies (Supplementary Figure 1, [34, 35]). Conjugation, the sexual process in ciliates, is through microgamonts that also leave the mother colony, but then fuse with a terminal zooid of another colony so that the multicellular unit is not genetically homogeneous [36, 37].

Except for the lower part of the stalk, all other host parts are covered exclusively by the gammaproteobacterial, thiotrophic ectosymbiont *Cand.* Thiobios zoothamnicoli [34, 35, 38, 39]. The ciliate colony contracts into the sulfidic layer and expands into the oxic seawater, repeatedly exposing the symbionts to fluctuating environmental conditions between fully oxic without sulfide (access to electron acceptor) and anoxic conditions with up to $300 \, \mu mol \, L^{-1}$ of sulfide (access to electron donor) [31, 40]. Symbiont cells are coccoid shaped on the upper parts of microzooids, but rod shaped on all other parts of the colony (Supplementary Figure 1C, [34]). This suggests that the coccoid-shaped symbiont on microzooids benefits from more favorable host-regulated sulfide and oxygen conditions [41]. Potential benefits of this behavior and symbiont colonization for the host are sulfide detoxification and nourishment [31].

Although this is the only reported thiotrophic symbiosis that can be cultivated over generations [41], direct evidence of the symbionts' involvement in host nutrition has been lacking so far. Nutritional transfer through digestion of symbiont cells was hypothesized based on transmission electron microscopy (TEM) observations of symbiont-like bacteria in the cytopharynx and in digestive vacuoles of microzooids [35]. Because ciliates can directly uptake dissolved substances through active transport or pinocytosis

[27], we hypothesized that the host also directly takes up organic compounds released by symbiont cells.

We used a combination of tissue autoradiography (TA) and a newly developed cryo-preparation technique [42] coupled with resin embedding and nanoscale secondary ion mass spectrometry (NanoSIMS) correlated with TEM to investigate the autotrophic behavior of the bacterial symbiont cells and the translocation of organic carbon to the ciliate host from populations collected from wood in the Adriatic Sea. In addition, we studied the in situ host diet using fluorescence in situ hybridization (FISH), and ultra-cytochemistry. We provide evidence for chemoautotrophy of the ectosymbiont using sulfide in the seawater, as well as internally stored sulfur as electron donor. We show that using bicarbonate in the seawater as a source of inorganic carbon, fixed organic carbon is rapidly released from the ectosymbiont cells to the host. Moreover, we demonstrate that the food vacuoles of the host are mainly filled by symbionts that are phagocytosed.

Materials and methods

A detailed version of the materials and methods including the description of the sampling site is provided as supplementary material.

^{14}C and ^{13}C-bicarbonate incubations

Five colonies were incubated in normoxic seawater containing $2.5 \, \mu Ci \, mL^{-1}$ $NaH^{14}CO_3$ (DHI®). The following incubations were carried out: (1) $12.2 \, \mu mol \, L^{-1}$ ΣH_2S (^{14}C sulfidic pulse) and (2) no sulfide (^{14}C oxic pulse) for 25 min each. Aiming at depleting internal sulfur storage compounds in the symbiont cells, five additional colonies were kept in oxic conditions for 24 h prior to incubation in ^{14}C-bicarbonate at oxic conditions for 25 min (24-h oxic + ^{14}C oxic pulse). Two negative controls were performed: (i) colonies were killed with absolute ethanol prior to the sulfidic pulse incubation for 25 min (dead control) and (ii) colonies were incubated in $12.2 \, \mu mol \, L^{-1}$ ΣH_2S but without adding ^{14}C-bicarbonate for 25 min (natural carbon control). To follow the fate of labeled organic carbon, we performed the same sulfidic pulse incubation followed by a chase without ^{14}C-bicarbonate in $12.4 \, \mu mol \, L^{-1}$ sulfide for 6 h (^{14}C sulfidic pulse chase) (see Supplementary Methods and Supplementary Table 1).

We localized labeled carbon with high spatial resolution NanoSIMS analyses. Five colonies were incubated in seawater supplemented with $100 \, mmol \, L^{-1}$ of $NaH^{13}CO_3$ (Sigma-Aldrich®) and $27.1 \, \mu mol \, L^{-1}$ ΣH_2S for 3 h and two colonies were analyzed in detail (^{13}C sulfidic pulse). Another batch of five colonies was maintained in oxic

seawater for 24 h prior to incubation in ^{13}C-bicarbonate under oxic conditions for 3 h each (24-h oxic + ^{13}C oxic pulse). As described above, a dead control and a natural carbon control were prepared (see also Supplementary Methods and Supplementary Table 1).

Tissue autoradiography

Fixed specimens were embedded in resin and sections were processed for TA (see supplementary material). Briefly, sections were dipped in an emulsion, stored for 3 months, developed, fixed, and stained prior to light microscopic observation. The microzooids and the stalk, as well as the symbionts covering these host parts were chosen for quantitative analyses of the silver grain density (actual grain density: AGD; Supplementary Figure 2). For statistical comparisons between treatments and between cell types and stalk within the same treatment, we expressed the grain density of each area relative to a reference. As a reference, we took the average symbiont AGD. The resulting relative grain densities (RGDs) are expressed as a percentage of the reference and can be compared with each other [43].

Correlative NanoSIMS and TEM

One colony per treatment was analyzed with NanoSIMS except for the sulfidic pulse incubation where two replicate colonies were analyzed separately (for details, see supplementary material). Briefly, specimens were cryo-fixed after chemical fixation and rapidly cryo-substituted prior to resin embedding. For correlative imaging, consecutive TEM sections were cut, placed onto slot grids, and contrasted prior to imaging with a Zeiss® Libra 120 TEM. NanoSIMS sections placed onto silicon wafer platelets were analyzed with a Cameca NS50L utilizing C$^-$, CN$^-$, P$^-$ and S$^-$ secondary ions for elemental imaging as well as C$_2^-$ secondary ions for inference of the ^{13}C tracer content (displayed as ^{13}C/(^{12}C + ^{13}C) isotope fraction, given in at%). NanoSIMS and TEM images obtained from similar analysis areas were superimposed using the GIMP® software package.

Acid phosphatase ultracytochemistry

Three freshly collected colonies were fixed and processed for the ultracytochemical detection of acid phosphatase following Gomori's methods ([44], for details, see supplementary material).

16S rRNA gene sequencing and FISH

To confirm the identity of the symbiont, 16S rRNA gene clone libraries were obtained for three colonies (see supplementary material for details). For FISH, four colonies were fixed immediately after collection in the natural environment. Colonies were embedded in LR White resin and FISH was applied on sections of entire colonies using a mix consisting of probes EUB338-I, EUB338-II, EUB338-III [45] and Arch915 [46], all labeled with Cy5 to target most bacteria and archaea. A symbiont-specific probe labeled with Cy3 was used to target the ectosymbiont *Cand.* Thiobios zoothamnicoli (ZNS196_mod, Supplementary Figure 3). We counted the symbiont-specific FISH signals in all detected digestive vacuoles and compared their numbers to those labeled only with the EUB$_{mix}$ and Archaea probe mix to estimate the composition of the host diet (see supplementary material for detailed FISH procedure).

Results and Discussion

Carbon fixation and incorporation of organic carbon in the thiotrophic symbiont

Key genes for autotrophic carbon fixation and sulfur metabolism found in the symbiont suggested a thiotrophic metabolism [38, 47]. Consistently, previous cultivation experiments revealed highest host and symbiont fitness under low sulfide/high oxygen conditions [41], but direct proof of a thiotrophic symbiont lifestyle was lacking. To investigate the autotrophic behavior of the symbiont under these optimal conditions, we performed short labeling experiments with ^{14}C- and ^{13}C-bicarbonate in the presence of H$_2$S for 25 min and 3 h, respectively, and followed carbon incorporation with TA and NanoSIMS. Autoradiographs revealed high numbers of silver grains over symbiont cells ($N = 5$, AGD 23.06, interquartile range (IQR) 15.79–25.67; Fig. 1a and Table 1). Similarly, NanoSIMS isotope analysis and correlative TEM micrographs at higher resolution clearly showed that the symbiont was the site of incorporation ($N = 291$ symbiont cells, ^{13}C isotope fraction 2.68 at%, IQR 2.45–3.04; Figs. 2, 3a). In contrast, dead colonies incubated under identical conditions showed no incorporation ($N = 3$ colonies, AGD 0.00, IQR 0.00–0.00; $N = 50$ symbiont cells, ^{13}C isotope fraction 1.07 at%, IQR 1.06–1.07) and the same results were obtained for living colonies incubated without added bicarbonate ($N = 3$ colonies, AGD 0.02, IQR 0.01–0.03; $N = 50$ symbiont cells, ^{13}C isotope fraction 1.06 at%, IQR 1.06–1.06; Fig. 3 and Tables 1 and 2). This strongly suggests that the symbiont cells rapidly fix inorganic carbon in the presence of sulfide, similar to certain other thiotrophic symbionts [48–53].

Because the symbiont cells store elemental sulfur in membrane-bound vesicles [54] and oxygen consumption measurements suggested that the symbionts completely utilize intracellularly stored sulfur in the absence of sulfide
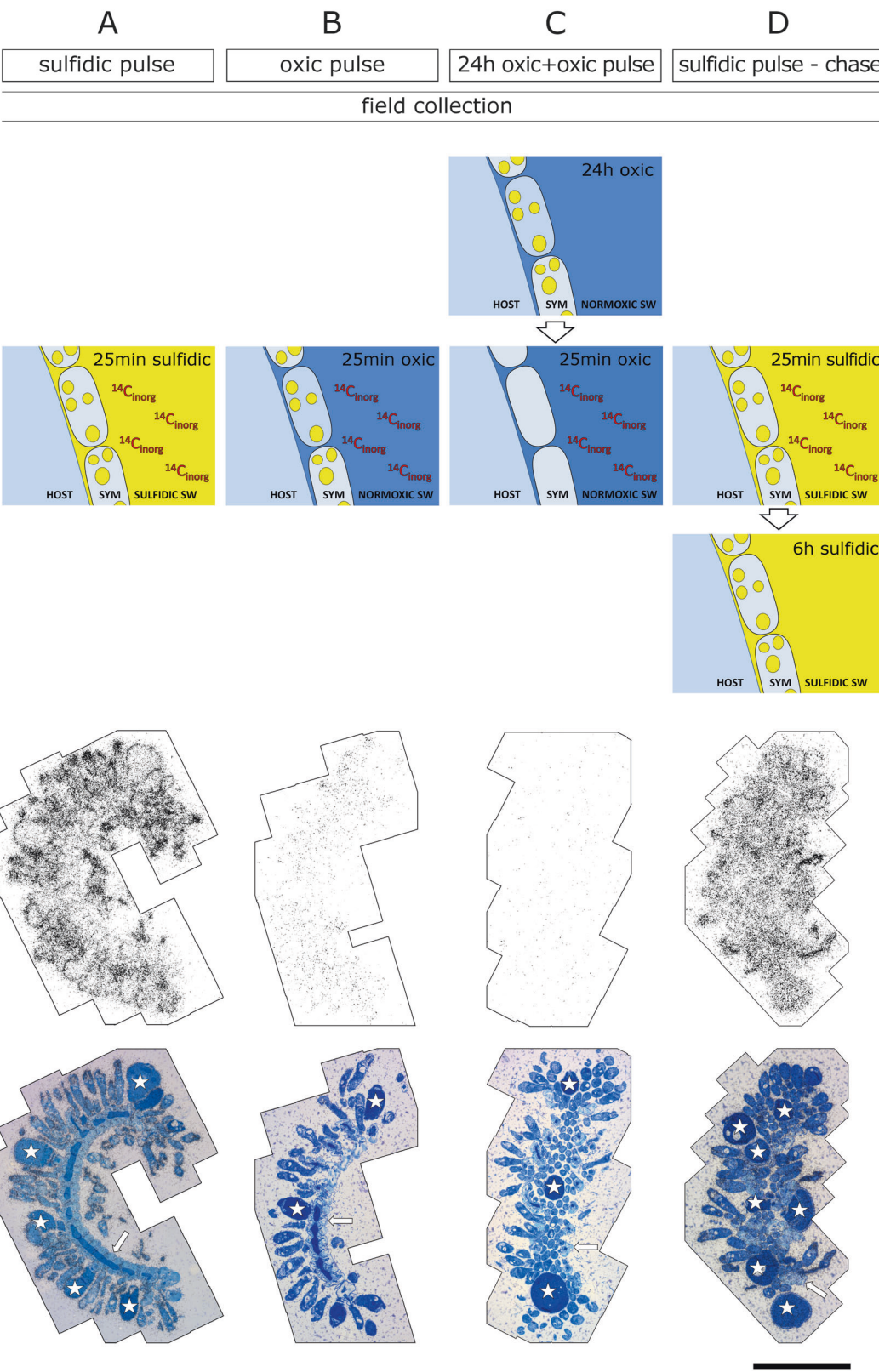
within 4 h [40], we hypothesized that the internal sulfur acts as electron donor for the thiotrophic metabolism, providing the energy needed for carbon fixation under oxic conditions.

Therefore, we performed a short ^{14}C-bicarbonate-labeling experiment under oxic conditions in the absence of H_2S and found an approximately eightfold lower median AGD over

◀ **Fig. 1** Four different ^{14}C-bicarbonate incubations with the inferred cell and environmental states (top half) with corresponding autoradiographs and colony sections (bottom half). **a** Directly after collecting ciliate colonies from the environment, we conducted a pulse labeling experiment with ^{14}C-bicarbonate in the presence of H$_2$S. After fixation and autoradiography, colony sections were covered with silver grains, showing that ^{14}C was incorporated into cellular biomass. Grains are denser in the periphery of host cells where symbionts are located. **b** After a labeling experiment with ^{14}C-bicarbonate under oxic (non-sulfidic) conditions, colony autoradiographs were also covered with grains but to a lesser extent, showing that less labeled carbon was incorporated during the pulse. **c** Colonies pre-treated 24 h under oxic conditions prior to labeling with ^{14}C-bicarbonate at oxic conditions did not incorporate [14]C: no silver grains are observed on the autoradiographs except for some background signals. **d** After a pulse labeling experiment with ^{14}C-bicarbonate in the presence of H$_2$S as in **a**, colonies were transferred into sulfidic seawater without the radiotracer for 6 h (chase). After autoradiography, incorporated labeled carbon is detected throughout the entire colony. A detail overview on these four incubation experiments together with a description of the control incubations is given in Supplementary Table 1. Each selected autoradiograph is representative of five colonies analyzed for each treatment. Yellow color represent available reduced sulfur species (elemental S in symbionts and ΣH$_2$S in the incubation media). Stars label macrozooids and arrows point to the stalk; all other cells are microzooids. Scale bar: 200 μm

symbiont cells (N = 5; AGD 2.97, IQR 2.91–3.63), than after the sulfidic pulse (Fig. 1b and Table 1), but significantly higher than the AGD of the controls. This points to the symbionts using elemental sulfur as an electron donor, gaining energy through sulfur oxidation and fixing carbon under oxic conditions, but to a lesser degree than when external sulfide was provided via the seawater.

To confirm that the internal sulfur storage indeed lasts only briefly [40], we kept colonies for 24 h in oxic seawater prior to labeling with [14]C- and ^{13}C-bicarbonate under oxic conditions for 25 min and 3 h, respectively. We hypothesized that after prolonged oxic conditions, sulfur was depleted and therefore carbon fixation ceased. Indeed, after this treatment the median AGD over symbiont cells (N = 5; AGD 0.09, IQR 0.08–0.11; Fig. 1c and Table 1), as well as the ^{13}C content in symbiont cells (N = 50, ^{13}C isotope fraction 1.07 at%, IQR 1.07–1.07%; Fig. 3 and Table 2) were in the range of the negative controls. These results indicate that chemoautotrophy has ceased within 24 h, most likely due to the lack of an electron donor (absence of an external sulfide source in oxic seawater and the depletion of sulfur stored in the symbionts).

NanoSIMS imaging revealed sulfur-rich areas in the cytoplasm of microzooids. The correlative TEM images showed that these areas corresponded to mitochondria (Fig. 2), known to have abundant disulfide bonds located in the inter-membrane space and membrane proteins [55]. Correlative TEM imaging of symbiont cells showed membrane-bound vesicles, which in successive sections analyzed by NanoSIMS exhibited high sulfur signals in

restricted, roundish areas of the symbiont cells (Fig. 4). Thus, NanoSIMS imaging confirmed the presence of sulfur in the symbiont cells after incubations in sulfidic seawater ([32]S$^-$/C$^-$ signal intensity ratio in symbiont cells 0.028, IQR 0.025–0.031, for details, see supplementary material). In contrast, after 24 h in oxic seawater, only a few and very small sulfur vesicles were observed in TEM and the relative amount of sulfur in the symbiont cells was significantly reduced ([32]S$^-$/C$^-$ signal intensity ratio 0.016, IQR 0.012–0.020; Fig. 4). These results corroborate the depletion of most of the internally stored sulfur within 24 h under oxic conditions.

The ^{13}C contents measured within individual symbionts on two separate colonies kept at sulfidic conditions for 3 h were significantly different (Wilcoxon–Mann–Whitney test, p-value 4×10^{-18}) and ^{13}C isotope fractions varied between 2.42 and 4.54 at% (N = 50) and 1.22 and 3.84 at% (N = 241), respectively (Fig. 3). The sulfur-related signal intensities in these cells were [32]S$^-$/C$^-$ 0.031, IQR 0.027–0.035 and [32]S$^-$/C$^-$ 0.028, IQR 0.020–0.031, respectively. This demonstrates that overall oxic seawater supplemented by 27.1 μmol L^{-1} sulfide (and even 12.2 μmol L^{-1} sulfide when taking ^{14}C experiments into account) is sufficient to fuel an active thiotrophic metabolism maintaining sulfur storage. This is consistent with the experimental optimal conditions in oxic seawater supplemented with 3–33 μmol L^{-1} sulfide [41]. Note that sulfide concentrations from 0.1 to 100 μmol L^{-1} were recorded from the sunken wood surface colonized by Z. niveum [56]. Nonetheless, the variability in metabolism was apparently high among colonies. Metabolic activity was variable among colonies and among the 141 investigated individual symbiont cells located on microzooids next to each other. A positive correlation of ^{13}C content and sulfur suggests that under sulfidic conditions the more carbon is fixed the more sulfur is also stored (Supplementary Figure 4).

Symbiont phenotypic plasticity and carbon incorporation

To investigate whether symbionts located on different parts of the colony incorporate carbon to different degrees, we compared the RGDs of symbiont populations covering the microzooids and the stalk. The RGDs of the mixed symbiont populations on the microzooids (with the upper part covered with cocci and the lower part covered with rods; [34]) were significantly higher than the values of the rods on stalks [34] after both the oxic and the sulfidic pulses (Table 1, Wilcoxon–Mann–Whitney test, p-value 0.008). Indeed, precise analyses of individual symbiont cells with NanoSIMS confirmed that ^{13}C enrichment in symbiont cells covering microzooids (N = 141 symbiont cells; 3.05 at%, IQR 2.69–3.28) was significantly higher than that of cells

Table 1 Summary of the analyses of the autoradiographs

	Sulfidic pulse		Oxic pulse		24-h oxic + oxic pulse		Sulfidic pulse-chase		Wilcoxon–Mann–Whitney test	
	AGD	RGD	AGD	RGD	AGD	RGD	AGD	RGD	sp vs op	sp vs spc
Microzooid symbiont	27.66	107.78 **	3.63	112.88 **	0.12	–	21.39	103.36	nd	nd
	(16.97–28.93)	(107.53–110.50)	(3.29–3.67)	(102.94–117.83)	(0.12–0.13)	–	(16.06–27.34)	(101.36–103.83)		
Stalk symbiont	9.20	51.75	2.03	68.30	0.02	–	16.63	80.97	nd	nd
	(8.17–10.65)	(31.61–69.82)	(2.00–3.58)	(61.81–68.76)	(0.01–0.08)	–	(14.22–21.32)	(79.31–90.69)		
Total symbiont	**23.06**	**100.00**	**2.97**	**100.00**	**0.09**	**–**	**19.79**	**100.00**	**nd**	**nd**
	(15.79–25.67)	(100–100)	(2.91–3.63)	(100–100)	(0.08–0.11)	-	(15.96–26.33)	(100–100)		
Microzooid host	10.44	44.36	1.05	32.65	0.07	–	12.65	63.89	nd	*
	(4.69–11.39)	(35.62–45.25)	(0.71–1.18)	(32.53–35.56)	(0.06–0.10)	–	(9.36–21.37)	(63.12–69.60)		
Stalk host	4.17	19.38	0.63	21.61	0.03	–	9.13	50.53	nd	**
	(0.46–5.60)	(2.89–21.81)	(0.43–1.25)	(14.51–24.57)	(0.03–0.03)	–	(8.79–11.56)	(44.40–67.85)		
Total host	**4.56**	**24.90**	**0.68**	**20.00**	**0.09**	**–**	**12.92**	**65.26**	**nd**	*******
	(2.31–6.39)	(9.99–33.75)	(0.59–1.10)	(19.04–30.29)	(0.04–0.11)	–	(10.73–18.38)	(61.59–69.8)		

For each incubation, the medians of the actual grain density (AGD) and relative grain density (RGD) of five replicates are shown together with the interquartile range of the data (Q25–Q75). The RGDs are the grain counts, which are set as a proportion of the overall symbiont grain count. All comparisons were then performed on the RGDs. Within a particular treatment, comparisons of the symbionts covering the microzooid and stalk areas as well as the respective host areas were performed using Wilcoxon–Mann–Whitney significance testing. This test was also performed to compare the sulfidic pulse and the oxic pulse (sp vs op), as well as the sulfidic pulse and the sulfidic pulse chase incubations (sp vs spc). Bonferroni correction was then applied

nd not different

*$p < 0.05$; **$p < 0.01$; ***$p < 0.001$
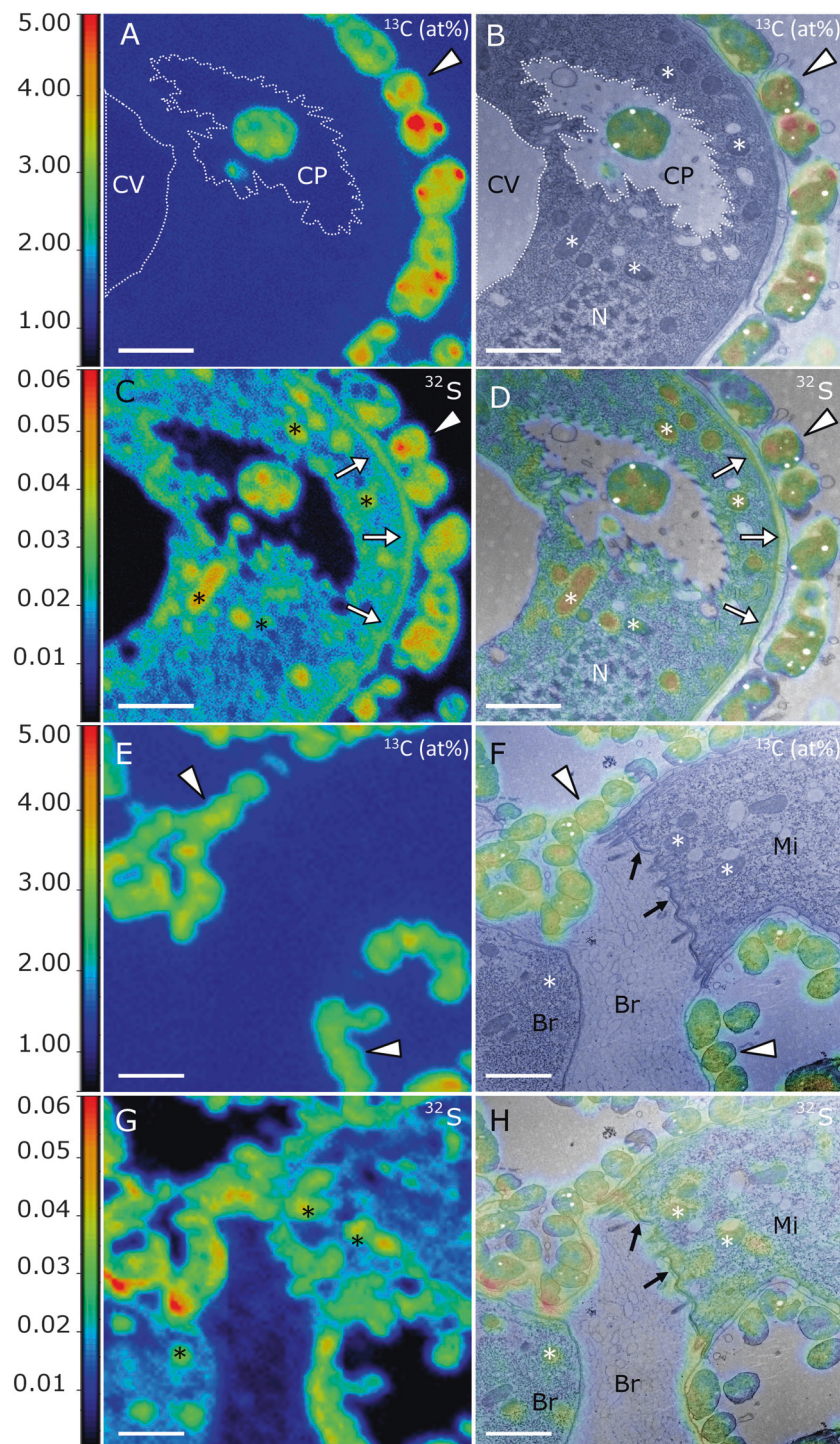
on stalks ($N = 150$ symbiont cells; median 2.51 at%, IQR 2.36–2.68) (Table 2) although they were not significantly different in size in the analyzed sections (Wilcoxon–Mann–Whitney test, p-value 0.385).

Overall, the symbiont cells on microzooids incorporated more labeled carbon than the rods on other colony parts. These results are in agreement with the ciliate behavior creating fine-scale differences in oxygen and sulfide concentrations along the microzooids [41]. The oral cilia of the microzooids resume beating as soon as the colony expands into the oxic seawater after dipping into the sulfidic layer through contraction of the spasmoneme, a special protein located throughout the stalk and the branches [57, 58]. The larger coccoid-shaped symbiont cells therefore were

◀ **Fig. 2** NanoSIMS/TEM correlative images after ^{13}C-bicarbonate labeling in the presence of H$_2$S. **a-d** Analysis of a part of a microzooid. **a** NanoSIMS visualization of the ^{13}C label distribution (^{13}C/(^{12}C + ^{13}C) isotope fraction, given in at%). The isotopically labeled carbon is mostly incorporated into symbionts (arrowhead points to one symbiont cell) but also visible within the host (c.f. data from region of interest (ROI) analysis in Fig. 3). The empty vacuole and cytopharynx (dotted line) do not show ^{13}C enrichment, whereas the cytoplasm does (Fig. 3). **b** Overlay of the NanoSIMS image with the corresponding TEM micrograph showing a partial view of a microzooid surrounded by symbionts. Inside the host cell, part of the contractile vacuole (CV) is visible, and a ^{13}C-rich symbiont-like bacterium is recognizable in the cytopharynx (CP). Many mitochondria are visible, some are labeled with asterisks (*). Region "N" refers to a macronucleus. **c** NanoSIMS visualization of the relative sulfur content as inferred from the C$^-$ normalized ^{32}S$^-$ secondary ion signal intensity (see section Materials and methods in the supplemental material for details). **d** TEM/NanoSIMS overlay showing sulfur being more concentrated in symbionts, mitochondria, and cortex of host (white arrows). **e-h** Detail of the basal part of a microzooid connected to a branch. **e** NanoSIMS visualization of the ^{13}C label distribution (^{13}C/(^{12}C + ^{13}C) isotope fraction, given in at%). **f** Overlay of the NanoSIMS image with the corresponding TEM micrograph showing the connection (black arrows) between the microzooid (Mi) and the branch (Br). Enriched symbionts (arrowheads) cover both structures. Mitochondria (*) are visible in both the microzooid and the branch. **g** NanoSIMS visualization of the relative sulfur content. **h** Overlay of the NanoSIMS inferred sulfur distribution with the corresponding TEM micrograph. Asterisks label mitochondria. Scale bars: **a-h** 2 μm

proposed to receive a mix of chemicals more favorable for chemoautotrophy than the smaller rods on all other parts of the colony [41]. When colonies were cultivated under steady oxygen and sulfide concentrations, the entire symbiont population grew as rods [41]. These results suggest that differences in previously described morphotypes are due to differences in chemoautotrophic rates leading to higher carbon incorporation in coccoid versus rod-shaped cells.

Organic carbon translocation through release and uptake

Carbon fixation and release of organic carbon into the surrounding host tissue is virtually concomitant in endosymbionts of *Riftia pachyptila* [16]. We therefore asked whether potential release from the ectosymbionts, which are attached to the ciliate host on one side only, occurs and leads to uptake by the host. Ciliates can directly take up dissolved organic carbon [59–63]. Some can even grow in axenic, nutrient-rich media without added prey [64, 65]. Our experiments enable differentiating between both nutrient translocation modes. Release of nutrients by the symbiont and subsequent uptake by the host should occur much faster than nutrient transfer via symbiont digestion by the host. This should enable the detection of the isotope label in the host after an incubation with ^{14}C-bicarbonate that is short enough to exclude digestion. Minimal time for
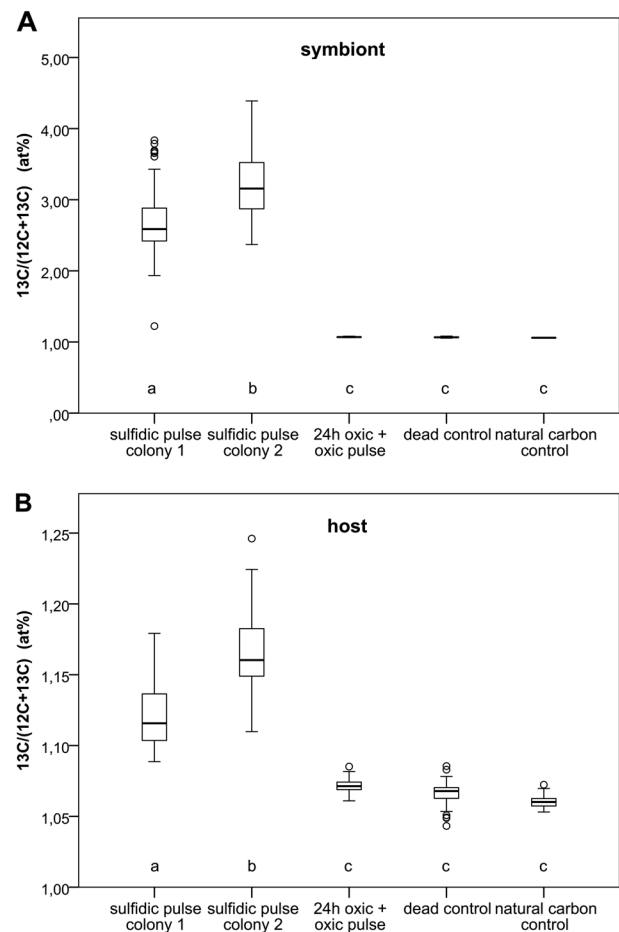

Fig. 3 NanoSIMS ROI analysis of the ^{13}C label content in symbionts and host after the different ^{13}C-bicarbonate incubations. **a** ^{13}C isotope fraction within the symbiont after the sulfidic incubation, the 24-h oxic + oxic incubation and the two control incubations. Symbionts significantly incorporated ^{13}C when incubated in the presence of sulfide (result of Scheffe test is shown with letters a, b, and c, alpha = 0.001). Colonies first treated 24 h in oxic conditions and then incubated in oxic conditions did not incorporate labeled carbon and resemble the natural abundance of ^{13}C (c.f. values from the two controls). **b** ^{13}C isotope fraction within the host after the same incubations. Significant host ^{13}C enrichment is detected after the sulfidic pulse (result of Scheffe test is shown with letters a, b, and c, alpha = 0.001). The 24-h oxic + oxic incubation did not lead to significant ^{13}C enrichment. Letters shared in common between groups indicate no significant difference

digestion in ciliates is 30 min, with maxima of up to 5 h [66, 67].

^{14}C-bicarbonate labeling for 25 min resulted in labeled carbon in host tissue after sulfidic (N = 5 colonies; AGD 4.56, IQR 2.31–6.39) and oxic incubations (N = 5 colonies; AGD 0.68, IQR 0.59–1.10; Figs. 1a, b, Table 1). We found no significant differences between stalk and microzooids (Table 1). Rather than symbionts fixing and incorporating inorganic carbon followed by host feeding and digestion of labeled symbiont cells within 25 min, we suggest that labeled organic carbon compounds produced by the

Table 2 Summary of the ROI analysis of NanoSIMS ^{13}C label distribution images

	Sulfidic pulse	24-h oxic + oxic pulse	Dead control	Natural carbon control
Microzooid symbiont	3.05 ***	1.07	1.07	1.06
	(2.69–3.28)	(1.07–1.07)	(1.06–1.07)	(1.06–1.06)
	$n = 141$	$n = 50$	$n = 50$	$n = 50$
Stalk symbiont	2.51	–	–	–
	(2.36–2.68)	–	–	–
	$n = 150$	–	–	–
Total symbiont	**2.68 a**	**1.07 b**	**1.07 b**	**1.06 b**
	(2.45–3.04)	(1.07–1.07)	(1.06–1.07)	(1.06–1.06)
	$n = 291$	$n = 50$	$n = 50$	$n = 50$
Microzooid host	1.15 ***	1.07	1.07	1.06
	(1.13–1.16)	(1.07–1.07)	(1.06–1.07)	(1.06–1.06)
	$n = 100$	$n = 50$	$n = 50$	$n = 50$
Stalk host	1.10	–	–	–
	(1.10–1.11)	–	–	–
	$n = 50$	–	–	–
Total host	**1.13 a**	**1.07 b**	**1.07 b**	**1.06 b**
	(1.11–1.15)	(1.07–1.07)	(1.06–1.07)	(1.06–1.06)
	$n = 150$	$n = 50$	$n = 50$	$n = 50$

For the sulfidic pulse and the 24-h oxic + oxic pulse, as well as for the two control experiments, the median of the ^{13}C isotope fraction (^{13}C/(^{12}C + ^{13}C), given in at%) is shown together with the interquartile range of the individual data points (Q25-Q75). (n) refers to the number of replicates analyzed within each treatment. For the symbiont, one replicate is one ROI drawn around one individual symbiont. For the host, the replicates are randomly selected ROIs within host cytoplasm. The Scheffe test (alpha = 0.05) was used to compare the ^{13}C label content in the symbiont and host after the different treatments. The result of the Scheffe test is given with lowercase letters "a" and "b", letters shared in common between groups indicate no significant difference. The Wilcoxon–Mann–Whitney test was performed to compare the microzooid and stalk area after the sulfidic pulse for both symbiont and host ^{13}C enrichment. The results of this test is shown with asterisks.

***$p < 0.001$

symbiont cells are released, directly taken up by the host and incorporated into its tissue. Note that these experiments revealed some labeled microbial cells in food vacuoles, but we excluded them from statistical analyses because they were clearly not yet digested and incorporated into host tissue. Moreover, in the colonial ciliate, phagocytosis is restricted to microzooids [35], but RGDs over the non-feeding stalk was not significantly different to that over feeding microzooids. Therefore, our results are consistent with the host taking up released carbon from the ecto-symbionts. Direct release of nutrients by the symbiont and host uptake was also demonstrated in *Solemya reidi* (with >45% of the fixed carbon being translocated to the bivalve; [12]) and in *Riftia pachyptila* (with $15.3 \pm 4.5\%$ RGD in tubeworm tissue after ^{14}C-bicarbonate 15-min pulse incubation; [16]). The RGDs in the ciliate host represent the host label as a percentage of the symbiont label. Microzooids, which represent most of the host biomass, have RGDs of 44.36% (IQR 35.62–45.25) after the sulfidic pulse and 32.65% (IQR 32.53–35.56) after the oxic pulse (Table 1). The ciliate uptake of released organic compounds is in the same order of magnitude as reported for the bivalve and vestimentiferan hosts.

In some symbioses, the host enhances the release of organic compounds from its symbiont. Evidence of the host influencing the rate of release was found in corals by comparing the amount of released compounds in host-associated and free-living *Symbiodinum* cells [68–70]. Because we have not detected a free-living symbiont population, such a comparison of release between host-associated and free-living symbiont populations is not possible in our system. Therefore, we compared the relative amount of label in hosts after oxic and sulfidic pulse incubations with labeled bicarbonate. The hypothesis is that, under host control, uptake of leaked organic carbon should be higher when symbionts fix less carbon under oxic conditions compared with higher fixation rates under sulfidic conditions. Alternatively, under symbiont control, a lower release should be found under oxic versus sulfidic conditions. The RGDs represent the host label expressed as a percentage of the average symbiont label in the colony, therefore showing the proportion of symbiont-fixed carbon transferred to the host through release during the pulse. Remarkably, no significant differences were observed in RGDs of host tissue between sulfidic ($N = 5$ colonies; RGD 24.90%, IQR 9.99–33.75) and oxic ($N = 5$ colonies; RGD
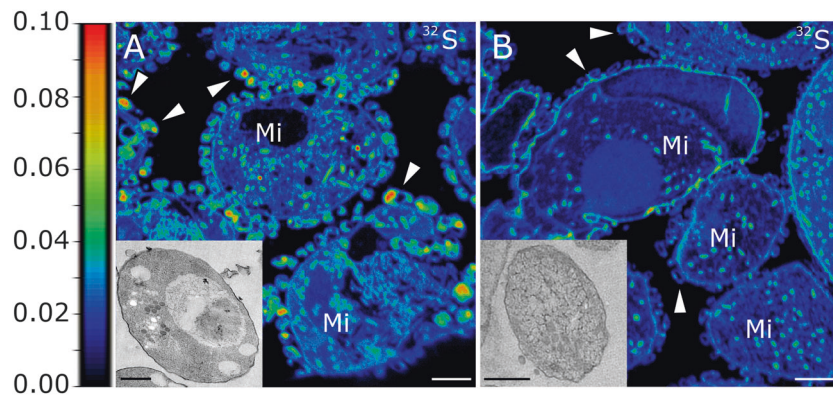
Fig. 4 Effect of the 24-h oxic treatment on the symbiont internal sulfur storage. The color scale indicates the C^- normalized $^{32}S^-$ secondary ion signal intensity. **a** NanoSIMS visualization of the relative sulfur content in a colony from the sulfidic pulse. Internal sulfur storage appears as sulfur hot spots in the symbionts (arrowheads) surrounding the microzooids (Mi) host cells. **b** NanoSIMS visualization of the relative sulfur content in the colony treated 24 h in oxic conditions before the oxic labeling experiment. The symbionts no longer show sulfur-rich regions. Representative TEM images of symbiont cells of corresponding treatments are given in the respective inserts. Symbionts show various electron-lucent vesicles identified by NanoSIMS as sulfur vesicles **a**, which are lacking after the 24-h incubation in oxic conditions **b**. NanoSIMS scale bars: 4 µm; TEM scale bars: 500 nm

20.00%, IQR 19.04–30.29) incubations. These results indicate a stable amount of released carbon correlated to the amount of fixed carbon governed by environmental conditions (which may be more or less favorable for chemosynthesis). Therefore, in contrast to corals, the ciliate host is apparently unable to enhance the release of fixed carbon from the symbiont under less favorable oxic conditions. Similarly, the symbiont apparently is also unable to actively reduce the release. About one order of magnitude lower AGDs in symbionts and host under less favorable oxic conditions compared with more favorable sulfidic conditions are consistent with this interpretation (Table 1).

Organic carbon translocation by symbiont cells digestion

The symbiont cells were highly labeled with ^{14}C at the end of the sulfidic pulse, therefore we transferred some colonies to sulfidic seawater without ^{14}C-bicarbonate for 6 h of chase in order to follow the fate of labeled carbon incorporated in the symbiont. To investigate whether symbiont cells labeled during the 25-min pulse continued to release labeled carbon in the 6-h chase with no ^{14}C-bicarbonate available, we compared the AGDs of symbionts between the sulfidic pulse and the sulfidic pulse-chase and found no significant differences (Table 1, Wilcoxon–Mann–Whitney test, p-value 0.841). We conclude that no further major leakage of labeled organic compounds occurred during the chase time. At the same time, however, the host RGD significantly increased 2.6-fold after the 6-h chase (Table 1). As the only source of labeled carbon for the ciliate cells was labeled symbiont cells, this observation is consistent with digestion of the symbiont, similar to pulse chase experiments in bathymodiolin mussels and vestimentiferans [16, 71].

Phagotrophy in microzooids was already hypothesized based on ultrastructural observations of a fully developed digestive system and symbiont-like bacteria in the cytopharynx and inside digestive vacuoles [35]. In ciliates, ingested organisms observed in digestion vacuoles are not necessarily digested [72]. We therefore sought to detect acid phosphatase, an intracellular digestion marker, ultracytochemically [73]. Acid phosphate is present in ciliate lysosomes and food vacuoles, and in situ detection of this enzyme has been commonly used to highlight digestion of food [72, 74, 75]. Enzymatic activity resulting in electron-dense precipitates was detected in microzooids in small vesicles, identified as lysosomes, and in large digestive vacuoles frequently containing symbiont-like bacterial cells in various stages of degradation (Fig. 5). The cytochemical detection of this enzyme allowed unequivocal identification of the digestive process in the ciliate microzooids (Fig. 5). Based on the distribution of signal, we propose that the enzyme is produced by the ciliate cells in lysosomes and secreted into the food vacuoles for digestion (rather than ingested bacteria actively secreting acid phosphatase and undergoing autolysis) [76]. Similar ultrastructural observations and/or cytoenzymatic investigations pointed to digestion of endosymbionts in the gills of bathymodiolin mussels [71, 77, 78] and lucinid clams [79, 80], as well as in the trophosome of vestimentiferans [16].

To unambiguously identify the ectosymbiont within the digestive vacuoles, we sequenced the 16S rRNA gene of the symbiont population from Slovenia. Interestingly, the obtained 16S rRNA gene had a single mismatch in the target region of the FISH probe ZNS196 [39] that was used

Fig. 5 Cytochemical detection of the digestive enzyme acid phosphatase in microzooids. **a** Survey over one entire microzooid after immersion in the reactive medium to detect acid phosphatase activity. Two digestive vacuoles (arrows) are surrounded by electron-dense precipitates resulting from acid phosphatase activity. **b** Survey over one entire microzooid from the negative control in which the analogous compound of the enzyme's substrate was omitted. No electron-dense precipitates are visible around digestive vacuoles (arrows). **c** Detail image of one digestive vacuole from the reactive medium. The borders of the vacuole are shown by white arrows. Electron-dense precipitates mostly located in small vacuoles identified as lysosomes indicate enzyme activity. The lysosomes surround the digestive vacuoles, where symbiont-like bacteria in various states of digestion are observed. One of the symbiont-like bacteria is shown by red arrowheads. **d** Detail image of two digestive vacuoles from the negative control. Triangles point to symbionts. C cilia, CV contractile vacuoles, St stalk. Scale bars: **a**, **b** 10 µm; **c**, **d** 2 µm
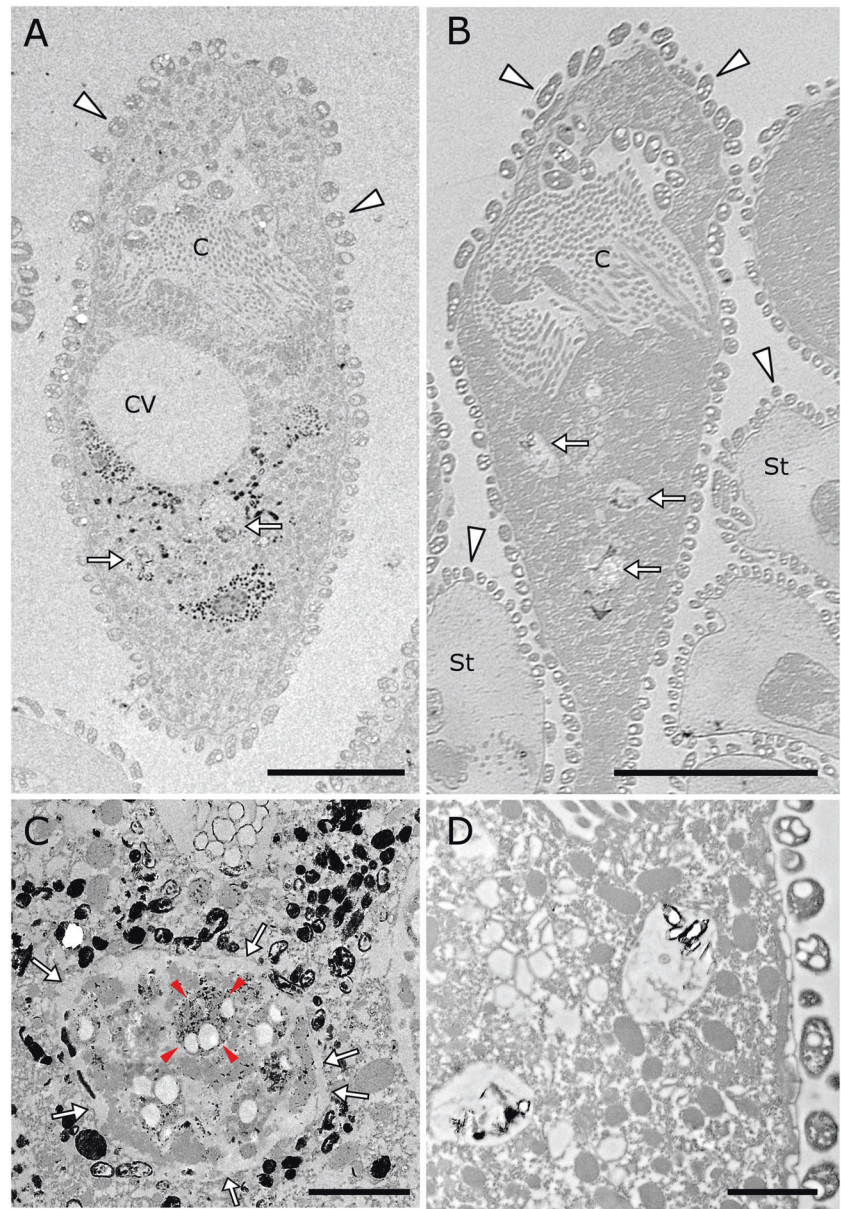
for identify populations from Corsica, Belize [38], and Japan [47]. We therefore modified the probe sequence in order to obtain a fully complementary FISH probe for this symbiont population. Epifluorescence microscopy revealed no difference in signal brightness between the symbiont specific and the bacterial/archaeal probe mix. Subsequently, we counted the symbiont-specific FISH signals and compared their numbers to those labeled only with the bacterial/archaeal probe mix to estimate the composition of the ciliate cells diet in four freshly collected colonies from the environment. In all, 53 digestive vacuoles were detected in 491 microzooids and analyzed. The symbiont cells highly dominated the food vacuole population (83.3–97.2% of total microbes) (Fig. 6, Supplementary Table 2). Our results indicate that mainly the ectosymbionts, and to a lesser

degree other microbes from the surrounding seawater, are ingested and ultimately digested. Considering that the ciliate is also capable of filter feeding on the free-living, non-symbiotic microbes in the seawater, our results emphasize the important role of the symbiont for the host's diet. In this context, the rapid colony contraction could play a role in the detachment of the symbiont cells from the plasma membrane of the outer host cell surface, a hypothesis that remains to be tested in the future [41, 58].

Conclusion

Recently we proposed that the *Zoothamnium niveum—Cand*. Thiobios zoothamnicoli association is a byproduct
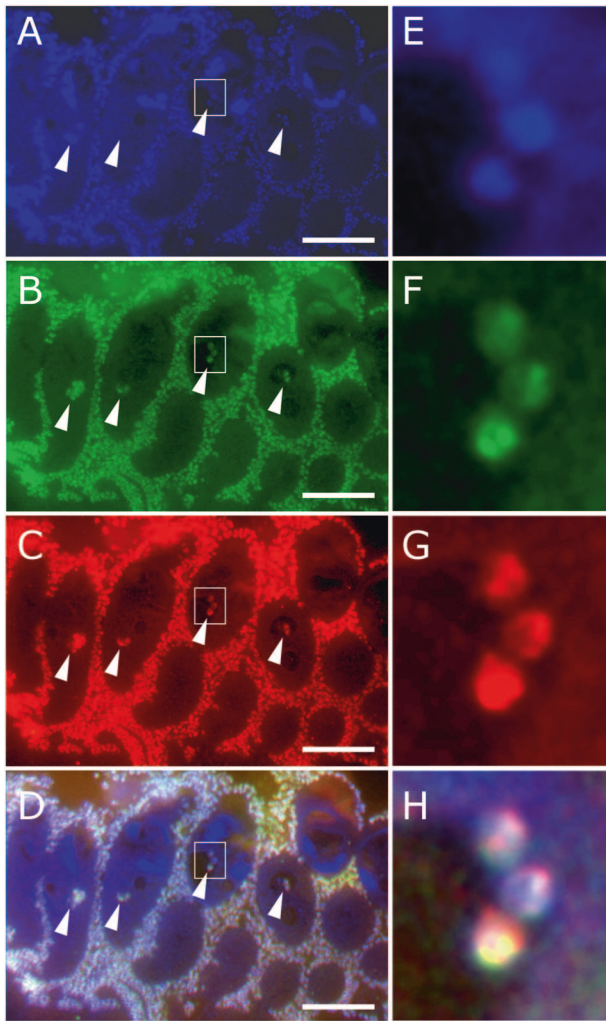
Fig. 6 FISH micrographs of a colony semi-thin section. **a** DAPI staining. **b** Cy5 probe mix of EUB I-III and Arch915. **c** Cy3 *Cand. Thiobios zoothamnicoli* Piran-population-specific probe. **d** Overlay. All ectosymbionts surrounding the host cells are labeled with both the bacterial and the symbiont-specific probe. Four microzooids are present with digestive vacuoles (arrowheads) containing ingested symbionts. Detail of one of the digestive vacuoles is given on the right of each micrograph **e-h**. Scale bars: **a-d** 20 μm

mutualism in which the symbiont cells benefit from the host behavior by gaining access to electron donors and acceptors for chemosynthesis and the host benefits from released organic carbon that the symbiont cells produce [31]. Here we provide experimental evidence of symbiont carbon fixation under various environmental conditions and suggest that the release of fixed carbon to the host is indeed a byproduct benefit, controlled neither by the symbiont nor by the host. In addition, active host cells' digestion of mainly symbiont cells contributes considerably to the host's diet and may also help control the population density on the host. Such control might be important for the host to avoid being overgrown by its symbiont and suffocate. The presence of a perfect symbiont monolayer on the ciliate surface

indicates a tight coupling of host and symbiont growth [31] fueled by the autotrophic behavior of the symbiont. How this mutualism is maintained over a wide range of environmental conditions in situ and how the shared fixed carbon and host digestion are finely tuned remain to be studied.

Compliance with ethical standards

Conflict of interest The authors declare that they have no conflict of interest.

References

1. Douglas AE. The symbiotic habit. Princeton: Princeton University Press; 2010.
2. Bronstein JL. Mutualism. Oxford: Oxford University Press; 2015.
3. Ceh J, Kilburn MR, Cliff JB, Raina J-B, Van Keulen M, Bourne DG. Nutrient cycling in early coral life stages: *Pocillopora damicornis* larvae provide their algal symbiont (*Symbiodinium*) with nitrogen acquired from bacterial associates. Ecol Evol. 2013;3:2393–400.
4. Clode PL, Stern RA, Marshall AT. Subcellular imaging of isotopically labeled carbon compounds in a biological sample by ion microprobe (NanoSIMS). Microsc Res Tech. 2007;70:220–9.
5. Kopp C, Domart-Coulon I, Escrig S, Humbel BM, Hignette M, Meibom A. Subcellular investigation of photosynthesis-driven carbon assimilation in the symbiotic reef coral *Pocillopora damicornis*. mBio. 2015;6:1–9.
6. Kopp C, Pernice M, Domart-Coulon I, Djediat C, Spangenberg JE, Alexander DTL, et al. Highly dynamic cellular-level response of symbiotic coral to a sudden increase in environmental nitrogen. mBio. 2013;4:e00052–13.
7. Muscatine L, Falkowski PG, Porter JW, Dubinsky Z. Fate of photosynthetic fixed carbon in light- and shade-adapted colonies of the symbiotic coral *Stylophora pistillata*. Proc R Soc Lond B Biol Sci. 1984;222:181–202.

8. Pernice M, Meibom A, Van Den Heuvel A, Kopp C, Domart-Coulon I, Hoegh-Guldberg O, et al. A single-cell view of ammonium assimilation in coral-dinoflagellate symbiosis. ISME J. 2012;6:1314–24.

9. Wangpraseurt D, Pernice M, Guagliardo P, Kilburn MR, Clode PL, Polerecky L, et al. Light microenvironment and single-cell gradients of carbon fixation in tissues of symbiont-bearing corals. ISME J. 2015;10:788–92.

10. Nelson DC, Fisher CR. Chemoautotrophic and methanotrophic endosymbiotic bacteria at deep-sea vents and seeps. In: Karl DM, editor). The microbiology of deep-sea hydrothermal vents. Boca Raton, New York, London, Tokyo: CRC Press; 1995. p. 125–67.

11. Freeman CJ, Stoner EW, Easson CG, Matterson KO, Baker DM. Symbiont carbon and nitrogen assimilation in the *Cassiopea-Symbiodinium* mutualism. Mar Ecol Prog Ser. 2016;544:281–6.

12. Fisher CR, Childress JJ. Translocation of fixed carbon from symbiotic bacteria to host tissues in the gutless bivalve *Solemya reidi*. Mar Biol. 1986;93:59–68.

13. Herry A, Diouris M, Pennec M. Chemoautotrophic symbionts and translocation of fixed carbon from bacteria to host tissues in the littoral bivalve *Loripes lucinalis* (Lucinidae). Mar Biol. 1989;101:305–12.

14. Felbeck H, Jarchow J. Carbon release from purified chemoautotrophic bacterial symbionts of the hydrothermal vent tubeworm *Riftia pachyptila*. Physiol Zool. 1998a;71:294–302.

15. Felbeck H, Jarchow J. The influence of different incubation media on the carbon transfer from the bacterial symbionts to the hydrothermal vent tube-worm *Riftia pachyptila*. Cah Biol Mar. 1998b;39:279–82.

16. Bright M, Keckeis H, Fisher CR. An autoradiographic examination of carbon fixation, transfer and utilization in the *Riftia pachyptila* symbiosis. Mar Biol. 2000;136:621–32.

17. Ponsard J, Cambon-Bonavita MA, Zbinden M, Lepoint G, Joassin A, Corbari L, et al. Inorganic carbon fixation by chemosynthetic ectosymbionts and nutritional transfers to the hydrothermal vent host-shrimp *Rimicaris exoculata*. ISME J. 2013;7:96–109.

18. Connor RC. The benefits of mutualism: a conceptual framework. Biol Rev Camb Philos Soc. 1995;70:427–57.

19. Ellers J, Toby Kiers E, Currie CR, Mcdonald BR, Visser B. Ecological interactions drive evolutionary loss of traits. Ecol Lett. 2012;15:1071–82.

20. Cavanaugh CM, McKiness ZP, Newton IL, Stewart FJ. Marine chemosynthetic symbioses. In: Dworkin M, editor. The prokaryotes. Singapore: Springer; 2006. p. 475–507.

21. Hoschitz M, Bright M, Ott JA. Ultrastructure and reconstruction of the pharynx of *Leptonemella juliae* (Nematoda, Adenophorea). Zoomorphology. 2001;121:95–107.

22. Dubilier N, Bergin C, Lott C. Symbiotic diversity in marine animals: the art of harnessing chemosynthesis. Nat Rev Microbiol. 2008;6:725–40.

23. Dubilier N, Blazejak A, Rühland C. Symbioses between bacteria and gutless marine oligochaetes. Prog Mol Subcell Biol. 2006;41:251–75.

24. Bright M, Lallier FH. The biology of vestimentiferan tubeworms. In: Barnes H, editor. Oceanography and marine biology: an annual review, Vol 48. Boca Raton: CRC Press; 2010. p. 213–65.

25. Seah BKB, Schwaha T, Volland J-M, Huettel B, Dubilier N, Gruber-Vodicka HR. Specificity in diversity: single origin of a widespread ciliate-bacteria symbiosis. Proc R Soc Lond B Biol Sci. 2017;20170764. https://doi.org/10.1098/rspb.2017.0764

26. Dziallas D, Allgaier M, Monaghan MT, Grossart H-P. Act together − implications of symbioses in aquatic ciliates. Front Microbiol. 2012;3:288.

27. Lynn DH, Corliss JO. Ciliophora. In: Harrison FW, etCorliss JO, editors. Microscopic anatomy of invertebrate, Protozoa. New York: WileyLiss; 1991. p. 333–467.

28. Schweikert M, Fujishima M, Görtz HD. Symbiotic associations between ciliates and prokaryotes. In: Rosenberg E, DeLong EF, Lory S, Stackebrandt E, Thompson F, editors. The prokaryotes-prokaryotic biology and symbiotic associations. Berlin, Heidelberg: Springer-Verlag; 2013. p. 427–63.

29. Fenchel T, Finlay BJ. *Kentrophoros*: a mouthless ciliate with a symbiotic kitchen garden. Ophelia. 1989;30:75–93.

30. Raikov IB. Bactéries épizoiques et mode de nutrition du cilié psammophile *Kentrophoros fistulosum* Fauré-Fremiet (étude au microscope électronique). Protistologica. 1971;7:365–78.

31. Bright M, Espada-Hinojosa S, Lagkouvardos I, Volland J-M. The giant ciliate *Zoothamnium niveum* and its thiotrophic epibiont *Candidatus* Thiobios zoothamnicoli: a model system to study interspecies cooperation. Front Microbiol. 2014;5:145.

32. Edgcomb VP, Breglia SA, Yubuki N, Beaudoin D, Patterson DJ, Leander BS, Bernhard JM. Identity of epibiotic bacteria on symbiontid euglenozoans in O2-depleted marine sediments: evidence for symbiont and host co-evolution. ISME J. 2011;5:231–43.

33. Herron MD, Rashidi A, Shelton DE, Driscoll WW. Cellular differentiation and individuality in the 'minor' multicellular taxa. Biol Rev. 2013;88:844–61.

34. Bauer-Nebelsick M, Bardele CF, Ott J. Redescription of *Zoothamnium niveum* (Hemprich & Ehrenberg, 1831) Ehrenberg, 1838 (Oligohymenophora, Peritrichida), a ciliate with ecto-symbiotic, chemoautotrophic bacteria. Eur J Protistol. 1996a;32:18–30.

35. Bauer-Nebelsick M, Bardele CF, Ott JA. Electron microscopic studies on *Zoothamnium niveum* (Hemprich & Ehrenberg, 1831) Ehrenberg 1838 (Oligohymenophora, Peritrichida), a ciliate with ectosymbiotic, chemoautotrophic bacteria. Eur J Protistol. 1996b;32:202–15.

36. Summers FM. Form regulation in *Zoothamnium alternans*. Biol Bull. 1938a;74:130–54.

37. Summers FM. Some aspects of normal development in the colonial ciliate *Zoothamnium alternans*. Biol Bull. 1938b;74:117–29.

38. Rinke C, Schmitz-Esser S, Loy A, Horn M, Wagner M, Bright M. High genetic similarity between two geographically distinct strains of the sulfur-oxidizing symbiont '*Candidatus* Thiobios zoothamnicoli'. FEMS Microbiol Ecol. 2009;67:229–41.

39. Rinke C, Schmitz-Esser S, Stoecker K, Nussbaumer AD, Molnár DA, Vanura K, et al. "*Candidatus* thiobios zoothamnicoli," an ectosymbiotic bacterium covering the giant marine ciliate *Zoothamnium niveum*. Appl Environ Microbiol. 2006;72:2014–21.

40. Ott JA, Bright M, Schiemer F. The ecology of a novel symbiosis between a marine peritrich ciliate and chemoautotrophic bacteria. Mar Ecol. 1998;19:229–43.

41. Rinke C, Lee R, Katz S, Bright M. The effects of sulphide on growth and behaviour of the thiotrophic *Zoothamnium niveum* symbiosis. Proc R Soc Lond B Biol Sci. 2007;274:2259–69.

42. Goldammer H, Hollergschwandtner E, Elisabeth NH, Frade PR, Reipert S. Automatized freeze substitution of algae accelerated by a novel agitation module. Protist. 2016;167:369–76.

43. Roger AW. Techniques of autoradiography. 3rd ed. Amsterdam: Elsvier North-Holland Biomedical Press; 1979.

44. Gomori G. Microscopic histochemistry: principles and practice. Chicago: University of Chicago Press; 1952.

45. Daims H, Brühl A, Amann R, Schleifer K-H, Wagner M. The domain-specific probe EUB338 is insufficient for the detection of all bacteria: development and evaluation of a more comprehensive probe set. Syst Appl Microbiol. 1999;22:434–44.

46. Stahl DA, Amann R. Development and application of nucleic acid probes in bacterial systematics. In: Stackebrandt E, Goodfellow M, editors. Nucleic acid techniques in bacterial systematics. Chichester, England: Wiley & Sons Ltd; 1991. p. 205–48.

47. Kawato M, Uematsu K, Kaya T, Pradillon F, Fujiwara Y. First report of the chemosymbiotic ciliate *Zoothamnium niveum* from a whale fall in Japanese waters. Cah Biol Mar. 2010;51:413–21.

48. Childress JJ, Fisher CR, Favuzzi JA, Sanders N. Sulfide and carbon dioxide uptake by the hydrothermal vent clam, *Calyptogena magnifica*, and its chemoautotrophic symbionts. Physiol Zool. 1991a;64:1444–70.

49. Childress JJ, Fischer CR, Favuzzi JA, Kochevar RE, Sanders NK, Alayse AM. Sulfide-driven autotrophic balance in the bacterial symbiont-containing hydrothermal vent tubeworm, *Riftia pachyptila* Jones. Biol Bull. 1991b;180:135–53.

50. Dando PR, Southward AJ, Southward EC, Terwilliger NB, Terwilliger RC. Sulfur-oxidising bacteria and haemoglobin in gills of the bivalve mollusc *Myrtea spinifera*. Mar Ecol Prog Ser. 1985;23:85–98.

51. Nelson DC, Hagen KD, Edwards DB. The gill symbiont of the hydrothermal vent mussel *Bathymodiolus thermophilus* is a psychrophilic, chemoautotrophic, sulfur bacterium. Mar Biol. 1995;121:487–95.

52. Schiemer F, Novak R, Ott J. Metabolic studies on thiobiotic free-living nematodes and their symbiotic microorganisms. Mar Biol. 1990;106:129–37.

53. Scott KM, Cavanaugh CM. CO2 uptake and fixation by endo-symbiotic chemoautotrophs from the bivalve *Solemya velum*. Appl Environ Microbiol. 2007;73:1174–9.

54. Maurin LC, Himmel D, Mansot J, Gros O. Raman microspectrometry as a powerful tool for a quick screening of thiotrophy: an application on mangrove swamp meiofauna of Guadeloupe (F.W.I.). Mar Environ Res. 2010;69:382–9.

55. Riemer J, Bulleid N, Herrmann JM. Disulfide formation in the ER and mitochondria: two solutions to a common process. Science. 2009;324:1284–7.

56. Laurent MCZ, Gros O, Brulport J-P, Gaill F, Le Bris N. Sunken wood habitat for thiotrophic symbiosis in mangrove swamps. Mar Environ Res. 2009;67:83–88.

57. Røy H, Vopel K, Huettel M, Jørgensen BB. Sulfide assimilation by ectosymbionts of the sessile ciliate. Zoothamnium niveum Mar Biol. 2009;156:669–77.

58. Vopel K, Reick CH, Arlt G, Pohn M, Ott JA. Flow microenvironment of two marine peritrich ciliates with ectobiotic chemoautotrophic bacteria. Aquat Microb Ecol. 2002;29:19–28.

59. Aomine M. The mechanism of sugar uptake in *tetrahymena pyriformzs*-iii general characterization. Comp Biochem Physiol A. 1978;60:41–56.

60. Aomine M. The amino acid absorption and transport in Protozoa. Comp Biochem Physiol A. 1981;68:531–40.

61. First MR, Hollibaugh JT. The model high molecular weight DOC compound, dextran, is ingested by the benthic ciliate *Uronema marinum* but does not supplement ciliate growth. Aquat Microb Ecol. 2009;57:79–87.

62. Rasmussen L, Orias E. Tetrahymena: growth without phagocytosis. Science. 1975;190:464–5.

63. Rasmussen L, Zdanowski MK. Evidence for di-peptide uptake in Tetrahymena. Experientia. 1980;36:1044–5.

64. Hanna BA, Lilly DM. Growth of *Uronema marinum* in chemically defined medium. Mar Biol. 1974;26:153–60.

65. Soldo AT, Van Wagtendonk WJ. The nutrition of *Paramecium aurelia*, stock 299. J Protozool. 1969;16:500–6.

66. Gonzalez JM, Iriberri J, Egea L, Barcina I. Differential rates of digestion of bacteria by freshwater and marine phagotrophic protozoa. Appl Environ Microbiol. 1990;56:1851–7.

67. Sherr BF, Sherr EB, Rassoulzadegan F. Rates of digestion of bacteria by marine phagotrophic protozoa: temperature dependence. Appl Environ Microbiol. 1988;54:1091–5.

68. Muscatine L. Glycerol excretion by symbiotic algae from corals and *Tridacna* and its control by the host. Science. 1967;156:516–9.

69. Sutton D, Hoegh-Guldberg O. Host-zooxanthella interactions in four temperate marine invertebrate symbioses: assessment of effect of host extracts on symbionts. Biol Bull. 1990;178:175–86.

70. Trench RK. The cell biology of plant-animal symbiosis. Annu Rev Plant Physiol. 1979;30:485–531.

71. Streams ME, Fischer CR, Fiala-Médioni A. Methanotrophic symbiont location and fate of carbon incorporated form methane in a hydrocarbon seep mussel. Mar Biol. 1997;129:465–76.

72. Vannini C, Schena A, Verni F, Rosati G. *Euplotes magnicirratus* (Ciliophora, Hypotrichia) depends on its bacterial endosymbiont 'Candidatus Devosia euplotis' for food digestion. Aquat Microb Ecol. 2004;36:19–28.

73. Holtzman E. Lysosomes. New York: Plenum Press; 1989.

74. Seaman GR. Acid phosphatase activity associated with phagotrophy in the ciliate, *Tetrahymena*. J Biophys Biochem Cytol. 1961;9:243–5.

75. Williams AG, Ellis AB, Coleman GS. Subcellular distribution of polysaccharide depolymerase and glycoside hydrolase enzymes in rumen ciliate protozoa. Curr Microbiol. 1986;13:139–47.

76. Ishikawa K, Mihara Y, Gondoh K, Suzuki E-I, Asano Y. X-ray structures of a novel acid phosphatase from *Escherichia blattae* and its complex with the transition-state analog molybdate. EMBO J. 2000;19:2412–23.

77. Fiala-Médioni A, McKiness ZP, Dando P, Boulegue J, Mariotti A, Alayse-Danet AM, et al. Ultrastructural, biochemical, and immunological characterization of two populations of the mytilid mussel *Bathymodiolus azoricus* from the Mid-Atlantic Ridge: evidence for a dual symbiosis. Mar Biol. 2002;141:1035–43.

78. Kádár E, Davis SA, Lobo-Da-Cunha A. Cytoenzymatic investigation of intracellular digestion in the symbiont-bearing hydrothermal bivalve *Bathymodiolus azoricus*. Mar Biol. 2008;153:995–1004.

79. König S, Le Guyader H, Gros O. Thioautotrophic bacterial endosymbionts are degraded by enzymatic digestion during starvation: case study of two lucinids *Codakia orbicularis* and *C. orbiculata*. Microsc Res Tech. 2015;78:173–9.

80. Liberge M, Gros O, Frenkiel L. Lysosomes and sulfide-oxidizing bodies in the bacteriocytes of *Lucina pectinata*, a cytochemical and microanalysis approach. Mar Biol. 2001;139:401–9.

Chapter 3

Host-symbiont stress response to lack-of-sulfide in the giant ciliate mutualism

PLOS ONE
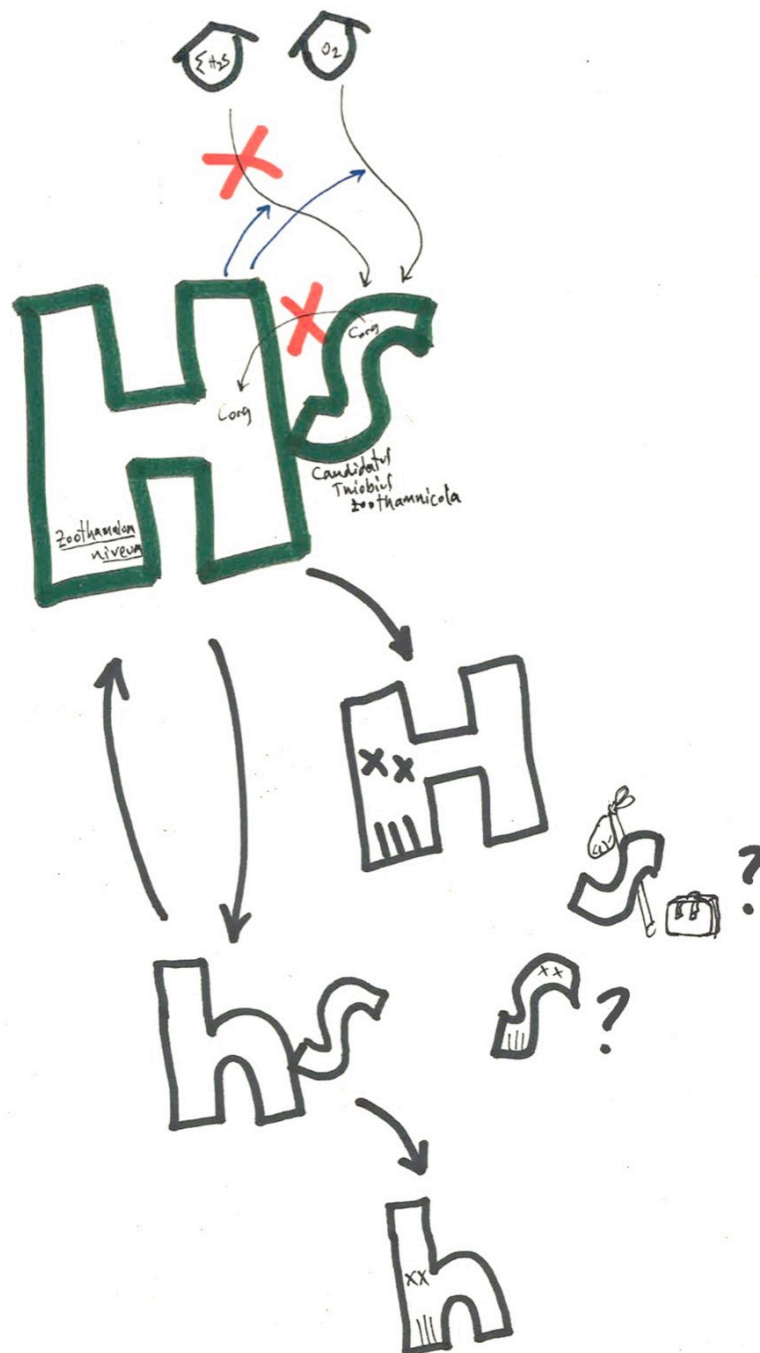
RESEARCH ARTICLE

Host-symbiont stress response to lack-of-sulfide in the giant ciliate mutualism

Salvador Espada-Hinojosa[ORCID]*, **Judith Drexel, Julia Kesting, Edwin Kniha**[¤a]**, Iason Pifeas, Lukas Schuster**[¤b]**, Jean-Marie Volland**[ORCID][¤c]**, Helena C. Zambalos, Monika Bright**

Department of Functional and Evolutionary Ecology, University of Vienna, Vienna, Austria

¤a Current address: Institute of Specific Prophylaxis and Tropical Medicine, Center for Pathophysiology, Infectiology and Immunology, Medical University of Vienna, Vienna, Austria
¤b Current address: Centre for Geometric Biology, School of Biological Sciences, Monash University, Melbourne, Victoria, Australia
¤c Current address: DOE JGI/LRC Systems, Menlo Park, California, United States of America
* salvador.espada@univie.ac.at
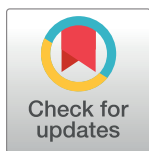
Abstract

The mutualism between the thioautotrophic bacterial ectosymbiont *Candidatus* Thiobius zoothamnicola and the giant ciliate *Zoothamnium niveum* thrives in a variety of shallow-water marine environments with highly fluctuating sulfide emissions. To persist over time, both partners must reproduce and ensure the transmission of symbionts before the sulfide stops, which enables carbon fixation of the symbiont and nourishment of the host. We experimentally investigated the response of this mutualism to depletion of sulfide. We found that colonies released some initially present but also newly produced macrozooids until death, but in fewer numbers than when exposed to sulfide. The symbionts on the colonies proliferated less without sulfide, and became larger and more rod-shaped than symbionts from freshly collected colonies that were exposed to sulfide and oxygen. The symbiotic monolayer was severely disturbed by growth of other microbes and loss of symbionts. We conclude that the response of both partners to the termination of sulfide emission was remarkably quick. The development and the release of swarmers continued until host died and thus this behavior contributed to the continuation of the association.

Introduction

While aerobic eukaryotes die after prolonged exposure to one of the most dangerous poisons, hydrogen sulfide ([1]; ΣH_2S i.e. sum of all forms of dissolved sulfide [2], hereafter called sulfide) most mutualistic associations between protist or animal hosts and thioautotrophic bacterial symbionts depend on the presence of sulfide (see [3]). These symbionts share the need for reduced sulfur species (e.g. exclusively sulfide or additionally thiosulfate) and oxygen or alternative electron acceptors to gain energy for carbon fixation [3, 4]. The hosts provide sulfide and oxygen through uptake and transport to the symbionts or through specific behavior such as swimming in and out of vent fluid in shrimps, contraction/expansion behavior in colonial

53

ciliates, or digging with the foot in some bivalves (see [3, 5, 6]). As far as is known, the hosts are also able of detoxify sulfide (see [1]). In return, the symbionts nourish their hosts (see [3]).

Many habitats of these symbioses are relatively short-lived, such as fast-spreading deep-sea hydrothermal vents, whale and wood falls depending on substrate size, and decaying seagrass debris (see [3]). In contrast to geothermally generated hydrogen sulfide as in vents (see [7]), the biological sulfide production by sulfate-reducing bacteria ceases when organic material is depleted (see [8]). Upon changes in chemical conditions, mobile animal hosts e.g. stilbonematine nematodes, gutless oligochaetes, snails and bathymodiolin mussels, can migrate to more suitable habitats (see [3]). However, sessile hosts like siboglinid tubeworms [9] or peritrich ciliates [10–13] do not have this option.

To persist over generations, hosts reproduce primarily by releasing motile larvae into the pelagial. Regardless of their mobility as adults, larvae of bathymodiolin mussels, lucinid clams, and tubeworms spread without their symbionts [14]. In these systems host reproduction and symbiont transmission are decoupled and the uptake of symbionts from a free-living population takes place after the larvae have settled. Experiments with some of these symbioses in oxic, non-sulfidic seawater showed that bathymodiolins and lucinids either lost their symbionts or greatly reduced their density. Nevertheless, hosts were able to survive between one and five months until the end of experiments [15–18]. In contrast, experiments with tubeworms showed that their symbionts escaped after the host died [19]. The larvae of other hosts like vesicomyid and solemyid clams carry their symbionts (see [14]). Whether such hosts with vertically transmitted symbionts react to sulfide deficiency with loss of symbionts has not been investigated. Furthermore, it is not known whether sessile hosts of thioautotrophic symbionts continue to reproduce under stress.

The symbiotic mutualism of the giant colonial ciliate *Zoothamnium niveum* (short *Zoothamnium*) and its thioautotrophic gammaproteobacterial ectosymbiont, originally described as *Cand.* Thiobios zoothamnicoli but due to nomenclature regulations corrected to *Cand.* Thiobius zoothamnicola, ([20], short Thiobius) is a suitable model to study host-symbiont response to environmental stress and disturbance when sulfide ceases. In contrast to slow-growing and reproducing animal hosts, this is a fast-growing and fast reproducing, sessile ciliate [21] which thrives on ephemeral sulfide-emitting surfaces in shallow, tropical to temperate environments such as wood, mangrove peat, decaying seagrass, and whale bones [22].

Zoothamnium colonies consist of a stalk and alternating branches on which individual cells grow: feeding cells called microzooids, dividing cells called terminal zooids, and macrozooids, cells responsible for asexual reproduction ([11], Fig 1). The vertical transmission of the ecto-symbiont is through macrozooids. These host propagules are released as swarmers into the pelagial for dispersal. Once settled, the swarmer transforms into the terminal zooid and begins to produce the stalk and to divide, producing the terminal zooid of each branch. Nourishing microzooids are produced through division of the terminal zooid on each branch, increasing the length of the branch. Macrozooids develop at the base of the branch. These macrozooids leave the colony as soon as a ciliary band has formed.

The dual partnership involves a single bacterial phylotype covering the host surface in a monolayer with the exception of the lowest, senescent parts of the colonies. There the symbionts become overgrown or replaced by other microbes [12, 23, 24]. The symbiont is rod-shaped on the aboral part of the microzooid and more coccoid-shaped on the oral part [12]. This phenotypic difference was explained by the movement of cilia around the oral ciliature in microzooids, which provides the symbionts with more balanced inorganic compounds for growth compared to all other cilia-free host parts [21].

In nature, host colonies are found at the interface between sulfidic and oxic layers of seawater [25, 26]. The ciliate is capable of rapid contractions of the stalk and branches [11, 12]. With
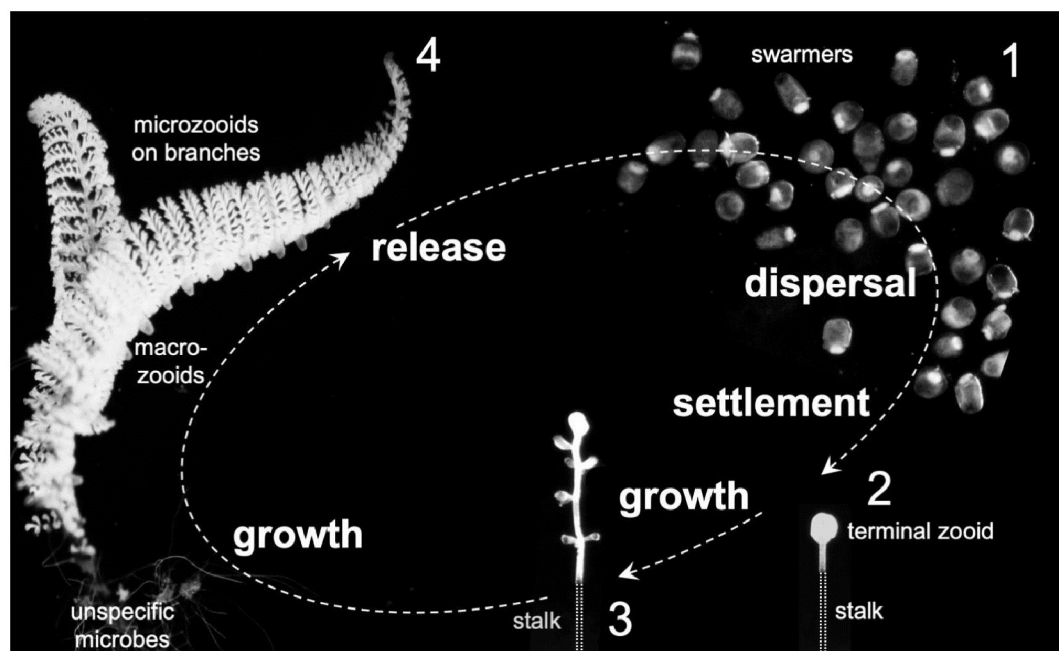
54

Fig 1. Life cycle of *Zoothamnium niveum*. The swarmers are the dispersal stage (1), and look for a sulfide source to settle. Once settled, the swarmer transforms into the terminal zooid at the top of the new colony and grows a stalk. Note that the white part of the stalk is overgrown by the symbiont, but the lower black part is aposymbiotic (2). The terminal zooid divides and produces the terminal zooids for each branch (3). The branch grows by divisions of the terminal zooid on the tip of the branch, creating microzooids and macrozooids, that eventually detach as swarmers (4). Light micrographs not to scale. Note that the lower part of the stalk, lacking white symbionts, is outlined.

https://doi.org/10.1371/journal.pone.0254910.g001

this repetitive movement they create a mixture of these chemicals [25, 27–29], which are necessary for host respiration as well as symbiont carbon fixation and translocation of fixed carbon to the host [30]. Carbon fixation in symbionts and direct nutritional transfer to the host has been demonstrated under oxic, sulfide supplemented conditions but ceased under oxic conditions without sulfide [30].

The host colonies are sessile and can only 'escape' sulfide starvation through producing macrozooids and releasing them as swarmers [11, 12]. How quickly colonies die in nature when sulfide stops is unknown. Experiments in the lab showed that all swarmers lost their symbionts in two days and thus became aposymbiotic. Regardless of presence or absence of symbionts, the vast majority only settled in the presence of sulfide [31]. Once they have settled, they can grow aposymbiotically into small colonies with or without sulfide in custom-designed flow-through chambers with a steady flow of oxic seawater. Symbiotic colony growth only happened in symbiotic swarmers exposed to sulfide and oxygen [31]. Fastest colony growth and a life span of 11 days was at low sulfide concentrations [21]. Colonies grew more slowly without sulfide and had a 4.5 days life span [21]. However, we do not know how long large colonies can survive under oxic conditions when sulfide stops and what happens to their symbionts. Furthermore, it is unknown whether the host releases swarmers that carry the symbionts as a response to sulfide starvation and how long these swarmers survive in order to find a suitable habitat for settlement.

Here, we followed the fate of large colonies and their propagules experimentally mimicking the waning of sulfide. We specifically asked how long freshly collected colonies and their swarmers survive under experimental oxic, non-sulfidic conditions (in short sulfide starvation). We also investigated whether the release of macrozooids comes only from those that

were already present on the colony at the beginning of the experiment, or whether the production of new macrozooids and their release as swarmers under sulfide deficiency was continued. For comparison we also performed a sulfidic control experiment. Further we studied the symbiont morphology, their frequency of dividing cells (FDC), as well as their density and coverage on the host surface, and the colonization of other microbes under oxic conditions using scanning electron microscopy (SEM) and fluorescence *in situ* hybridization (FISH). For comparison we used freshly collected colonies from the field. Given the lack of sulfide fueling symbiont carbon fixation [30], we hypothesized that the symbiont division should cease and consequently the monolayer on the host feeding on symbionts [30] should be disrupted. Since the symbiont is known to nourish the host [30] we hypothesized that the presence or absence of sulfide indirectly affects the host's longevity and its macrozooid production and release, which are taken as proxy for reproductive effort.

Material and methods

Ethic statement

No specific permissions were required for the listed locations as they are publicly accessible. Furthermore, we confirm that our field studies did not involve endangered or protected species.

Sampling

Zoothamnium niveum colonies were collected from shallow, subtidal submerged woods at two locations in the Northern Adriatic Sea close to Piran, Slovenia: the estuarine canal Sv. Jernej (45˚29'48.6"N, 13˚35'57.0"E) and the mudflat in Strunjan (45˚31'44.0"N, 13˚36'13.2"E). Simultaneously, water samples were taken adjacent to the wood pieces and *in situ* temperature, salinity, and pH were measured using a Multi 340i sensor WTW (S1 Table). Wood pieces were transported in buckets filled with on-site seawater to the laboratory and maintained in flow-through aquaria until colonies were used for the experiments, from immediately after collection up to five days later for the sulfide starvation experiment and 23 days for the sulfidic control experiment. During maintenance about 250 mL of 1 mmol L^{-1} sulfide solution was added to each 50 L liter aquarium daily during which fresh seawater flow was stopped for a few hours. Each colony was cut off the wood with a MicroPoint™ Scissor and cleaned from debris by rinsing it in filtered seawater prior the experimental procedure. All seawater used for this and further procedures was filtered through a 0.2 µm Acrodisc$^{\circledR}$ syringe filter.

Host response to sulfide starvation compared to sulfidic conditions

We used 60 colonies from each of the two collection sites Sv. Jernej and Strunjan for the sulfide starvation experiment in 2015. For comparison, 60 colonies were sampled for the sulfidic control experiment at Strunjan in 2021. Each colony was placed in a well of a multiwell plate. Each well was filled with 1 mL oxic, filtered seawater (sulfide starvation experiment). For the sulfidic control we added sodium sulfide to the filtered seawater at an average final concentration of 448 µmol L^{-1}.

The number of macrozooids present on each colony was counted at the start of the experiment (S1 Fig). Every 12 h, viability of colonies was assessed by their contraction/expansion behavior. Colonies that did not contract when being touched with a dissecting needle were considered dead. All swarmers released from each colony within 12 h time intervals were transferred into individual wells.

56

Every 12 h about two-thirds of the water from each well was replaced by new filtered oxic seawater (sulfide starvation experiment) or filtered sulfidic seawater (sulfide control experiment). The removed water was pooled for measurements of temperature, salinity, pH, and oxygen concentration (S2 Table). Oxygen and temperature were measured with a PreSenS Flow-through Cell FTC-PSt3. Salinity and pH and were measured with a Multi 340i sensor WTW. Additionally, sulfide concentration was measured photometrically according to Cline [32] in a few randomly chosen wells in the sulfidic control experiment in the newly prepared and in the removed water.

To estimate colony size, the number of branches was counted either after host death or at the end of the experiment (sulfide starvation experiment: n = 85; sulfidic control experiment: n = 60). Swarmers from the sulfide starvation experiment were mounted on glass slides and their body size was estimated using Leica DM2000 light microscope equipped with a Leica DFC295 camera and the image analysis software Gimp (GNU Image Manipulation Program) for Mac 2.8.

For statistical comparisons of the colonies used for the sulfide starvation experiment sampled from two locations, 60 colonies from each location were divided into four batches (A-D), with 15 colonies each. The size of the swarmers was measured according to the timeframe of 12-h-interval observations they were released from the colony and the timeframe they were kept in the water swimming (batch A 0 h, B 24 h, C 48 h, D 72 h; S2 Fig). All time points were considered as the upper bound of the intervals. Statistical analyses were conducted in PAST 3.04 [33] and R [34]. Because Shapiro-Wilk tests showed deviations from normality for all parameters (counted branches taken as estimate of colony size, initial macrozooids per colony, total released swarmers per colony, and swarmer size) the Wilcoxon-Mann-Whitney test for equal medians was used for comparisons of the two locations.

In both, the sulfide starvation and sulfidic control experiments, the mortalities of colonies and swarmers were estimated as the proportion of dead colonies/swarmers to the total number of colonies/swarmers used in the experiment. LT_{50} and their standard error estimates for colonies and swarmers were obtained by curve fitting of a binomial Generalized Linear Model (bGLM) with mortality rate as response and time as predictor, and the use of the R package MASS version 7.3–51.4. Goodness of fit was characterized with the Deviance (D^2) = (Null Deviance-Residual Deviance)/(Null Deviance). Ordinary Least Squares (OLS) regression-models were used to depict the correlation between relevant magnitudes, e.g. colony size and released swarmers. The number of macrozooids produced during the experiment (Δ_M) was calculated by subtracting the initial number of macrozooids present on colonies at the beginning of the experiment from the sum of the released swarmers plus the macrozooids remaining on the colony at the end of the experiment (S1 Fig). Δ_S, the number of macrozooids produced and released as swarmers during the experiment, was calculated by the subtraction of the initial number of macrozooids from the number of released swarmers. A positive Δ_S value indicates additionally produced swarmers during the experimental time frame, whereas a negative Δ_S value indicates remaining macrozooids on the respective colony that were not released at the end of the experiment. Linear fit slope comparisons between both experiments were performed through analyses of covariance by obtaining the significance of the interaction with R [34].

Symbiont response to sulfide starvation

In 2012, 2013, and 2014, sets of 15 to 20 freshly collected colonies from Sv. Jernej were put into embryo dishes, each kept completely filled with filtered, oxic seawater and covered with glass plates to avoid evaporation for up to 72 h. At the time points 12, 24, 48, and 72 h viability of

colonies was assessed as described above, and at most 3 live colonies were removed and fixed for SEM or divided into live and dead colonies and fixed for FISH (S1 Table). At each time point water was replaced with filtered seawater (S2 Table).

Fluorescence *in situ* hybridization (FISH)

Colonies from the 2014 embryo dish experiments were fixed and stored in 100% ethanol at 4˚C for 3 months. Colonies were embedded in LR-White resin and polymerization was performed in absence of oxygen at 41˚C for three days. Semi-thin sections (1 μm) were cut on a Reichert Ultracut S microtome, placed in a drop of 20% acetone on chromium(III)potassium sulfate coated glass slides and were left to dry at 40˚C. A total of 16 sections were placed on one slide with four spots of four sections each. To have a representative area of the colony on each slide, two slides per sample were used.

Hybridization was carried out as described in [24]. On each slide the symbiont-specific oligonucleotide probe ZNS196_mod [30] labeled with Cy3 together with a mix of EUB I, II, III (targeting most bacteria [35, 36]), and Arc 915 (targeting most archaea, [37]), all labeled with Cy5 to distinguish the symbiont from any other microbe, were used on two spots. Negative controls with nonsense probes (NON-EUB) labeled in both colors [38] were run on each slide on two different spots. In brief, applied probes were hybridized at 46˚C for 3 hours in the dark, then rinsed in the washing buffer at 48˚C for 15 min, stained with DAPI, washed with Milli Q, and mounted with Citifluor antifading solution. Sections were observed on a Zeiss Axio Imager M2 epifluorescence microscope and images were taken at 100x magnification with an AxioCam MRm, Zeiss using AxioVision Rel. 4.8. software. Composite pictures of entire colony sections were done with ICE software (Image Composite Editor 2.0, Microsoft).

Scanning electron microscopy (SEM)

Colonies from the 2012 and 2013 embryo dish experiments were placed in a freezer at -20˚C in 2.5 mL of filtered, oxic seawater for 9.5 min prior to fixation to avoid contraction of the colonies [21]. Before the freezing point was reached, the embryo dish was taken out and 2.5 mL of modified Trump´s fixative (2.5% glutaraldehyde, 2% paraformaldehyde in 0.1 M sodium cacodylate buffer 1100 mOsm, pH 7.2, filtered with a 0.2 μm filter prior fixation) was added (modified from [39]). The samples were immediately rinsed with this solution and stored until further treatment.

After storage in fixative for a few months, colonies were rinsed in 0.1 M sodium cacodylate buffer (1100 mOsm, pH 7.2) three times for 3 min each, dehydrated in acetone and transferred to a mixture of acetone/hexamethyldisilazane (HDMS) (1:1) for 15 min, followed by two baths of pure HDMS for 15 min each. Subsequently, the samples were air dried for 3 h, placed on a stub and sputter coated with gold-palladium using an Agar Sputter Coater Agar 108 for 250 seconds.

For detailed SEM observations on a Philips XL 20 scanning electron microscope (acceleration voltage of 20kV) we used two sets of three colonies kept in oxic seawater for 48 h (the set from 2012 was used for statistical analyses, the other one from 2013 for additional SEM micrographs). We used three colonies freshly collected from the environment in 2012 as control. From each colony, images were taken from 15 microzooids (feeding cells) at a magnification of 2000x. The following symbiont parameters were analyzed for the oral and the aboral part of each microzooid separately: 1) number of symbiont cells in a 70 μm^2 rectangular frame; all cells crossing the edge of the frame were counted only along one length and width of the frame; cells crossing the whole frame either longitudinally or horizontally were also counted. 2) The percentage of symbionts covering host surface (host coverage) was measured with

58

Gimp 2.8 software after manual segmentation of the bacteria, whereby all partially and total cells in the 70 μm^2 frame were included in the analysis. All other parameters were analyzed with AnalySIS$^®$ program (Soft Imaging System GmbH, Münster, Germany), for each oral and aboral part of the microzooids up to 70 cells each, whereby cells were selected in a clockwise helical pattern: 3) length, 4) width, and 5) frequency of dividing cells (FDC). Dividing cells were defined as bacteria showing an invagination but not a clear intervening zone between cells [40]. 6) Cell volume was calculated from length and width data considering each cell as a cylinder plus two hemispheres [41]. 7) The cell elongation factor (EF), the ratio of length to width, was calculated for each cell [42]. The larger the EF the more rod-shaped the cells are, while cocci have an EF of approximately 1.

Statistical analyses were conducted with R [34] on data comparing three colonies kept at sulfide starvation for 48 h and three colonies collected *in situ* in 2012 (S2 Table). Because the Shapiro-Wilk tests performed for all parameters for each part of each microzooid showed deviations from normality, we used the Wilcoxon-Mann-Whitney test to evaluate differences within and between *in situ* and 48h oxic conditions.

Results

Host response to sulfide starvation compared to sulfidic conditions

In situ collections to investigate the host's reaction to experimental oxic conditions (so-called sulfide starvation) came from two nearby subtidal locations in the northern Adriatic Sea, the Strunjan mudflat and the Sv. Jernej estuary. No significant differences were found in colony size (Wilcoxon-Mann-Whitney test: p = 0.721, W = 941, S3A Fig) and in numbers of macrozooids between the locations (p = 0.487, W = 1931, S3B Fig). The number of swarmers released during sulfide starvation was highly variable, ranging from 0 to 21 swarmers per colony. However, the two populations did not differ significantly (p = 0.462, W = 1936, S3C Fig). The size of the swarmers also did not differ significantly between populations (p = 0.408, W = 1306, S3D Fig). We have, therefore, merged the data from both locations for further analyses and for comparisons with a population from Strunjan that we exposed to sulfidic conditions.

Monitoring the physicochemical parameters showed that the colonies were exposed to stable oxygen concentrations under sulfide starvation (97 ± 6% mean ± standard deviation in freshly supplied seawater, 99 ± 4% in the removed water 12 h later). In contrast, fluctuations alternated from almost anoxic (4 ± 4%), high sulfidic (448 ± 11 μmol L^{-1} sulfide) conditions to oxic (89 ± 10%) and low sulfidic (6 ± 5 μmol L^{-1} sulfide) conditions in 12 h intervals (S2 Table).

The mortality of the colonies under sulfide starvation showed a sigmoid pattern (bGLM: D^2 = 0.93), which increased sharply 24 h after the start of the experiment and increased less and less after 60 h (Fig 2A). All times are expressed as the upper bounds of the observation intervals. A similar mortality pattern (bGLM: D^2 = 0.97), but shifted to an increase about half a day later, was seen in colonies kept under sulfidic conditions. As a result, these colonies lived about half a day longer (LT$_{50}$ = 56 h, estimated standard error SE = 10 h) than those without sulfide (LT$_{50}$ = 44 h, SE = 11 h; Fig 2A).

In the sulfide starvation experiment significantly fewer swarmers were released per colony (median number per colony 1, IQR from 0 to 4, n = 120) compared to the sulfidic control (median number per colony 8, IQR from 6 to 11, n = 60; Wilcoxon-Mann-Whitney test comparing both experiments, p < 0.001, W = 6429). The mortality of swarmers from the sulfide starvation experiment also showed a sigmoid pattern similar to that of the colonies (bGLM: D^2 = 0.99). The calculated LT$_{50}$ was 39 h (SE = 9 h; Fig 2B). In contrast, the majority of swarmers (82%) who were kept in sulfidic seawater settled and grew into new colonies. Therefore,

59
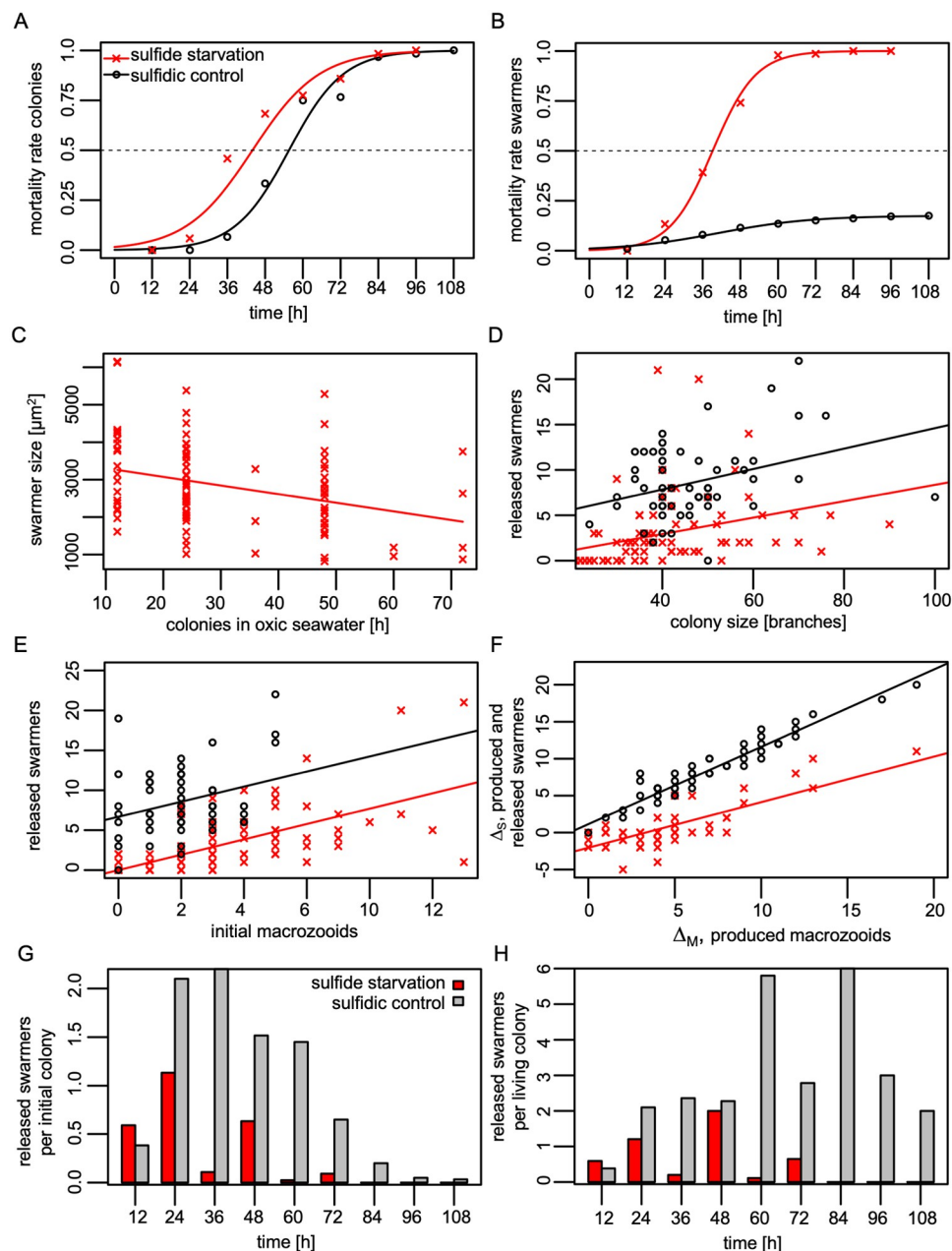
Fig 2. Host response to sulfide starvation in comparison with a sulfidic control. The sulfide starvation experiment is shown in red and the sulfidic control in black. (A) Binomial Generalized Linear Model of the mortality of the colonies given as the proportion of dead colonies in relation to the total number of colonies. LT_{50} is indicated as the point of intersection with the dashed line. (B) Binomial Generalized Linear Model of the mortality of swarmers given as the proportion of dead swarmers in relation to the total number of swarmers. The x-axis marks the upper bound of the swarmer survival time after release from the colony. (C) Ordinary least squares regression model showing a negative correlation between swarmer size and time colonies spent under sulfide starvation before swarmer release. (D) Positive correlation between colony size and the number of released swarmers, both in the sulfide starvation experiment and in the sulfidic control. The slopes of both experiments were not significantly different. (E) The number of swarmers (released macrozooids) was positively correlated with the initial number of macrozooids, both in the sulfide starvation experiment and in the sulfidic control. The slopes of both experiments were not significantly different. Δ_S is defined as the difference between the number of released swarmers and the initial number of macrozooids. Positive values of Δ_S indicate the net number of additionally released swarmers, whereas negative values display the net number of macrozooids remaining on the colony. (F) Δ_S, the net production and release of swarmers, is positively correlated with Δ_M the production of macrozooids in both sulfide starvation and sulfidic control experiments. The slopes of both experiments were significantly different. (G) At the population level, under sulfide

starvation less swarmers were released per initial colony than the sulfidic control in all time points except at 12h. They were also released in a shorter time period. (H) Each colony released less swarmers under sulfide starvation than in the sulfidic control also when only the colonies were considered which were still alive at each time-point.

the LT_{50} of swarmers could not be calculated, as death of half of the swarmers was not reached (Fig 2B).

Swarmer size varied greatly between individuals in the sulfide starvation experiment (median = 26601 μm^2, IQR from 20737 to 35947 μm^2, n = 99). Measurements of size in 12-h-intervals according to the time a swarmer spent in the oxic water, showed no significant decrease (OLS: p = 0.077, F = 3, n = 99). However, swarmer size decreased in relation to the time colonies spent in oxic seawater (OLS: r^2 = 0.11, p < 0.001, F = 12, n = 99, Fig 2C). Colonies that spent more time without sulfide released significantly smaller swarmers. Whether this is the case under sulfidic conditions has not been investigated.

Although we tried to sample similarly sized colonies for both experiments, the ones used for the sulfide starvation experiment were slightly smaller (median 43 branches, IQR from 38 to 53, n = 85) than those used for the sulfidic experiment (median 44, IQR from 40 to 50, n = 60; Wilcoxon-Mann-Whitney test, p < 0.001, W = 1641). Nevertheless, the number of initial macrozooids per colony was not significantly different (sulfide starvation: median 2, IQR from 0 to 4, n = 120; sulfidic control: median 2, IQR from 1 to 3, n = 60; Wilcoxon-Mann-Whitney test, p = 0.444, W = 3849). The colony size correlated positively with the number of released swarmers in both experiments (sulfide starvation: OLS: r^2 = 0.12, p = 0.001, F = 11, n = 85; sulfidic control: OLS: r^2 = 0.13, p = 0.006, F = 8, n = 59; Fig 2D). Their slopes did not differ (analysis of covariance, p = 0.643, F = 0; Fig 2D).

In both treatments, a positive correlation was found between the number of initial macrozooids and the number of swarmers released (sulfide starvation: OLS r^2 = 0.47, p < 0.001, F = 106, n = 120; sulfidic control: OLS r^2 = 0.09, p = 0.017, F = 6, n = 60; Fig 2E). Their slopes did not differ significantly (analysis of covariance, p = 0.960, F = 0; Fig 2E). The median number of unreleased macrozooids at the end of the sulfide starvation experiment was 3 (IQR from 1 to 5, n = 80), significantly higher than the sulfidic control (median 1, IQR from 1 to 2, n = 59; Wilcoxon-Mann-Whitney test, p < 0.001, W = 3539).

To investigate whether the released swarmers came from macrozooids that were present at the beginning of the experiment or from macrozooids that developed during the experiment we calculated the production of new macrozooids (Δ_M). In case of sulfide starvation, Δ_M showed a median of 3 (IQR from 1 to 5, n = 80). A significantly higher value was found in the sulfidic control experiment (median 6, IQR from 4 to 9, n = 60; Wilcoxon-Mann-Whitney test, p < 0.001, W = 1213). To investigate whether the colonies were able to release the additionally produced macrozooids (Δ_M), we calculated Δ_S, the number of macrozooids produced that were also released as swarmers during the experiment. In the sulfide starvation experiment Δ_S ranged from -5 to 11 with a median of 0 (IQR from -1 to 0, n = 71). This indicates high variability in colony performance: some colonies continued to produce and release these new swarmers (Δ_S > 0, n = 17), others produced no such swarmers (Δ_S = 0, n = 31), and others released only a few initial present macrozooids, while the remaining macrozooids died on the colony (Δ_S < 0, n = 23). In the sulfidic control experiment Δ_S ranged from 0 to 20 with a median of 8 (IQR from 5 to 10, n = 59; all $\Delta_S \geq 0$; Wilcoxon-Mann-Whitney test, p < 0.001, W = 317). In addition, both experiments showed a positive correlation between the macrozooids produced (Δ_M) and the produced and released swarmers (Δ_S) (Fig 2F). However, the slopes of both experiments were significantly different and indicate a different efficiency in production and release of swarmers from the colony (analysis of covariance, p < 0.001, F = 49;

). According to the sulfide starvation slope, the production of ten additional macrozooids was needed in order to effectively release six more swarmers (OLS: $\Delta_S = -2.0 + 0.6 * \Delta_M$, $r^2 = 0.63$, $p < 0.01$, F = 120, n = 71; Fig 2F). In contrast, the slope of the sulfidic control showed that every newly produced macrozooid was also released as swarmer (OLS: $\Delta_S = 1.1 + 1.0 * \Delta_M$, $r^2 = 0.93$, $p < 0.001$, F = 734, n = 59). This indicates an overall higher efficiency in reproductive effort under sulfidic condition than without sulfide.

On population level, swarmer release was overall much lower under sulfide starvation and ended earlier than in the sulfidic control with the exception of the first time point at 12 h (Fig 2G). A similar picture emerged at the level of individual colonies (Fig 2H).

Symbiont response to sulfide starvation

To study the change in symbiont coverage and colonization of other microbes in relation to host survival and time we repeated the sulfide starvation experiment with 10 to 20 colonies in different embryo dishes. We performed FISH with a symbiont-specific probe and a mixture of archaea and bacterial probes on semi-thin sections of some selected colonies, which were removed after each time point. All hosts survived for up to 24 h. At this point, the symbiont monolayer remained undisturbed in three of four colonies, similar in appearance to three colonies examined which were fixed immediately after collection from the field. The fourth colony suffered a small loss of symbionts.

After 48 h (n = 8; four live and four dead colonies) and after 72 h (n = 6; three live and three dead colonies) there was hardly any difference with regard to symbiont coverage on live and dead hosts. After 48 h, two out of the surviving four colonies showed little change in symbiont coverage (S4A–S4D Fig). One colony showed a large loss of symbionts, and one colony was aposymbiotic. Symbiont coverage on three out of four dead colonies was slightly disturbed, and the fourth dead colony suffered a great loss of symbionts. After 72 h two out of the three live colonies were aposymbiotic (S4E–S4H Fig), the third colony was severely disturbed and showed only very few symbionts. All three dead hosts were aposymbiotic.

The epigrowth of other microbes, including bacteria and archaea, began within the first 24 h. We found that microbial fouling originated mainly from the lower part of the colony (S4A–S4D Fig), sometimes overgrown by microbes in nature [11, 12]. Most of the time, other microbes colonized host surfaces after the symbiont was lost (Fig 3A–3D). In some cases, however, the symbiont monolayer was directly overgrown (Fig 3I–3L). Unspecific epigrowth was found in all colonies regardless of host viability.

In addition, unidentified microbes have been detected in a few microzooids. Some were limited to small spots and were most likely contained in food vacuoles (Fig 3A–3D). Others, however, filled the entire host cell, which we interpret as potential microbial infection (Fig 3E–3H). These individual host cell infections appeared to increase in number with time of incubation period and were randomly distributed within the colony. Since we did not find any branches, stalks, or clusters of infected microzooids, the infection did not appear to spread from one infected to neighboring microzooids.

In order to take into account the differences in symbiont morphology on the microzooids by means of SEM [12, 21], we differentiated between symbiont populations on the oral and aboral part of the microzooids freshly collected from the environment (Fig 4A) and compared them to those kept at oxic conditions for 48 h (Fig 4B–4G). Parts of the colony became covered with a mucus-like substance (Fig 4B) and/or other microbes (Fig 4F and 4G), which is in agreement with the FISH observations.

In freshly collected colonies (n = 3, Fig 4A), the microzooids were covered with a monolayer of symbionts, with similar symbiont coverage values in the oral and in the aboral part
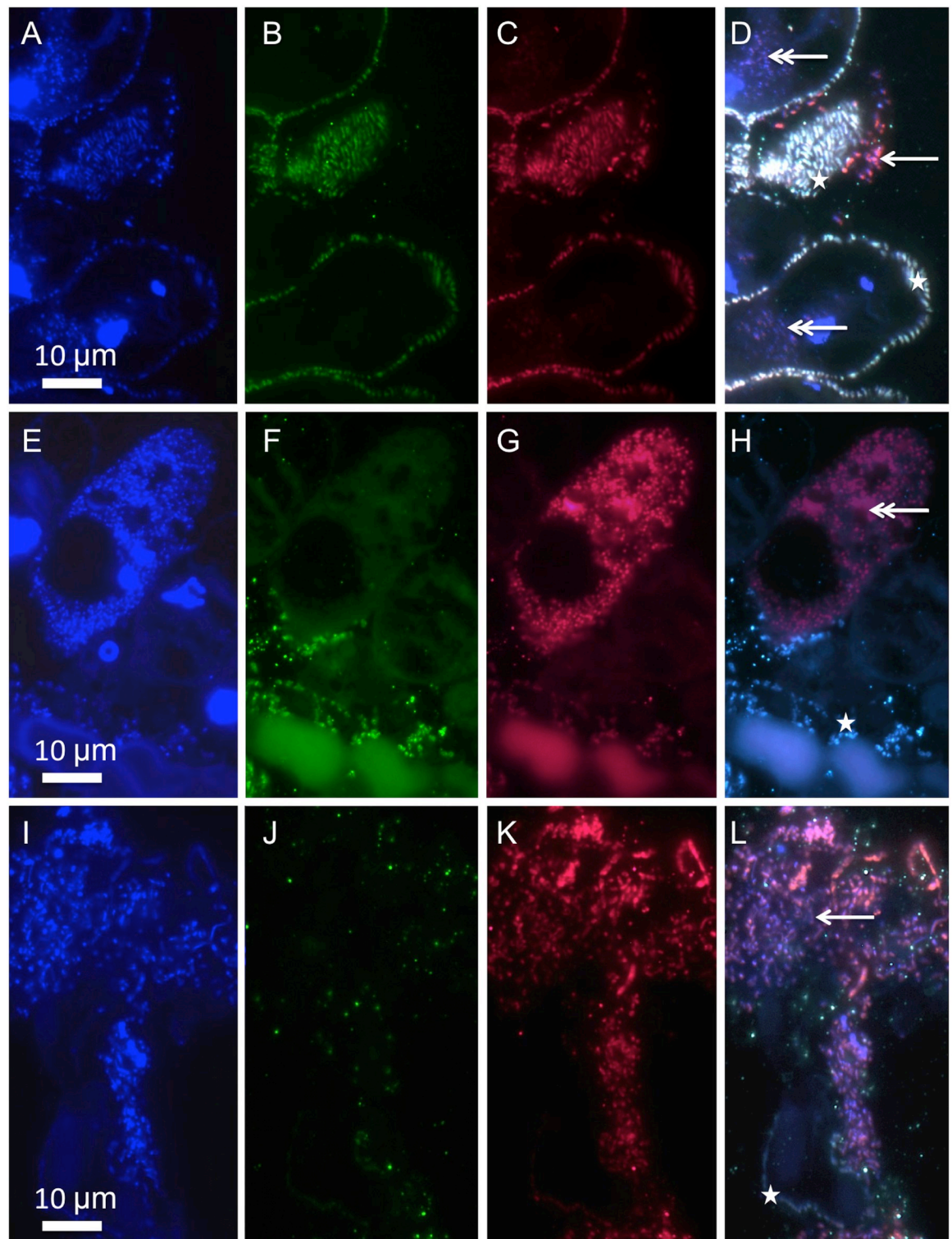
Fig 3. Symbiont response to sulfide starvation applying FISH. Symbionts (asterisk), other epibiotic microbes (arrow), and intracellular microbes in D confined to small areas most likely food vacuoles, in H filling the entire host cell most likely infection (double arrow); (A, E, I) DAPI staining (blue), (B, F, J) symbiont-specific probe (green); (C, G, K) EUB_{mix} and Archaea probes (red); (D, H, L) composite of DAPI, symbiont-specific and EUB_{mix}/Archaea probes. A-D and I-L from live colony after 48 h, E-H from dead colony after 48 h.

Fig 4. Symbiont response to sulfide starvation applying SEM. Microzooid from colony freshly collected from the environment (A), and several colonies after 48 h in oxic seawater (B-G); (B) overview of colony covered in part with mucus; (C-G) microzooids with symbionts fully covering the host, and with gradually less and less symbiont coverage; arrows point to very long rods most likely not symbionts.

Table 1. SEM analyses of symbiont traits.

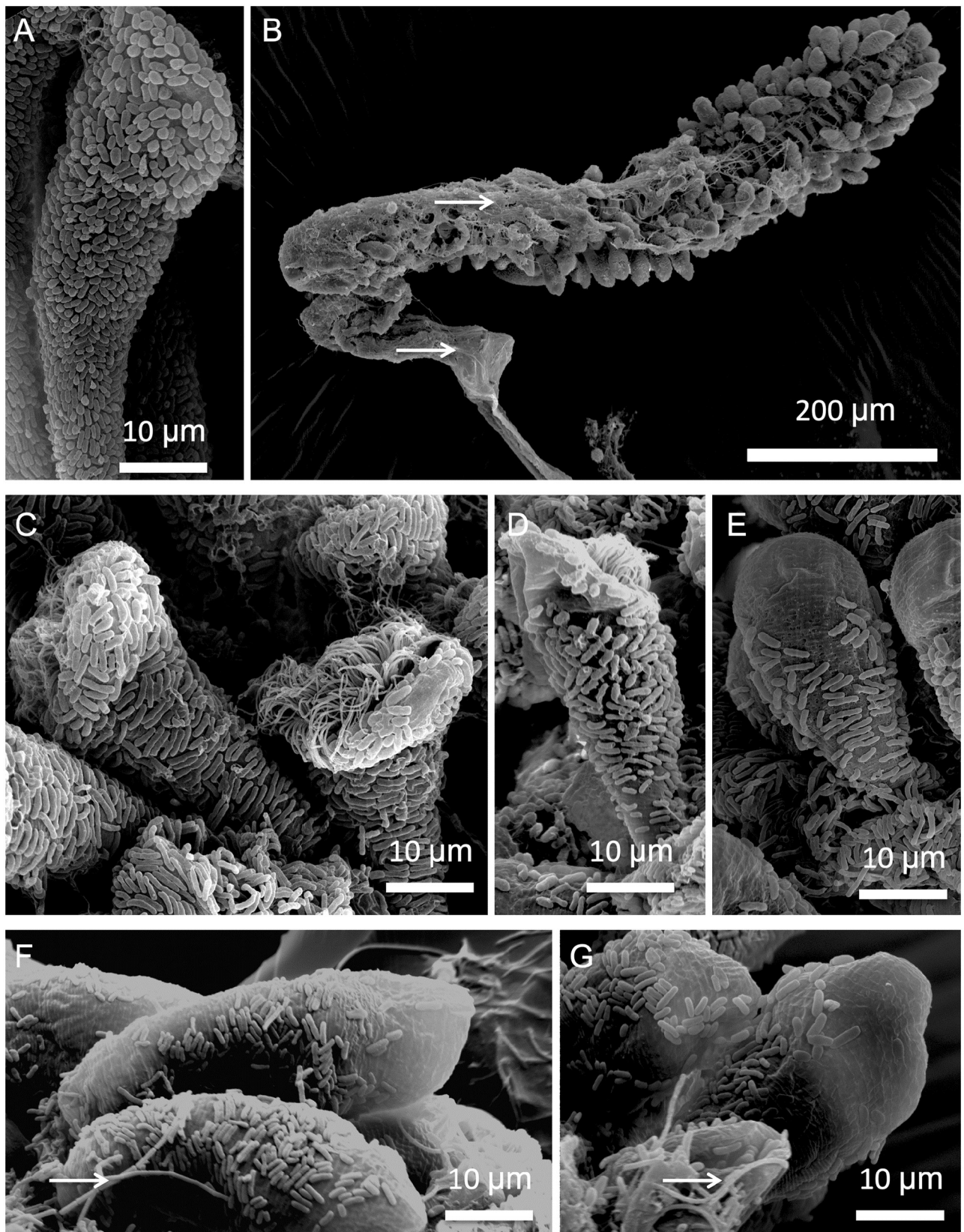| traits	*in situ* oral	*in situ* aboral	signinficance (W value)	48 h oxic oral	48 h oxic aboral	significance (W value)
coverage on host surface (%), n = 180	88.7 (85.9, 90.3)	90.1 (88.3, 91.3)	n.s. (1302)	10.4 (3.1, 36.2)	62.7 (53.6, 79.2)	* (1799)
number of cells per 70 μm², n = 180	51.1 (43.5, 60.9)	79.3 (68.5, 93.5)	* (1867)	3.3 (1.1, 10.9)	23.9 (16.3, 34,8)	* (1713)
frequency of dividing cells, FDC (%), n = 180	14.3 (12.9, 15.7)	11.4 (10.0, 12.9)	* (323)	7.7 (5.4, 9.1)	9.1 (7.4, 11.4)	n.s. (1318)
length (μm), n = 9271	1.81 (1.53, 2.18)	1.67 (1.39, 2.03)	* (3974591)	2.43 (2.04, 2.90)	2.56 (2.11, 3.06)	* (1256266)
width (μm), n = 9271	0.90 (0.78, 1.02)	0.60 (0.52, 0.68)	* (878280)	0.96 (0.76, 1.15)	0.75 (0.64, 0.91)	* (675978)
individual cell volume (μm³), n = 9271	0.87 (0.61, 1.22)	0.38 (0.27, 0.53)	* (1225584)	1.41 (0.85, 2.10)	0.96 (0.63, 1.45)	* (808464)
elongation factor, n = 9271	2.05 (1.65, 2.56)	2.84 (2.29, 3.47)	* (7333468)	2.56 (1.96, 3.35)	3.35 (2.61, 4.16)	* (1590929)

Values are shown as median and (Q_{25}, Q_{75}). Wilcoxon-Mann-Whitney test between oral and aboral parts: n.s. not significant, * 99% significance.

(Table 1). The host had significantly higher numbers of symbionts per unit of surface on the aboral part than on the oral part of microzooids (Table 1). Orally located symbionts were significantly longer and wider than on the aboral part; hence orally located symbionts had a larger volume than on the aboral part (Table 1). However, the cell elongation factor, calculated as length divided by width, showed that symbiont located aborally were more rod-shaped than those located orally (Table 1). The FDC of the symbiont population at the oral part was significantly higher than that at the aboral part (Table 1).

After 48 h in oxic seawater, the oral and the aboral symbiont populations differed significantly in all parameters at a 1% level of significance compared to freshly collected colonies (Table 1). Orally, symbiont coverage with a few symbionts was very low compared with a higher aboral coverage (Table 1). Orally localized symbionts were shorter and wider orally than aborally, had a higher cell volume and a lower elongation factor (Table 1).

The symbiont coverage on both parts of the microzooids changed dramatically within 48 h in oxic seawater. In comparison with freshly collected colonies, significantly lower symbiont coverage (Fig 5A and 5B) and symbiont number were observed on the oral and aboral parts of the microzooids (Fig 5C and 5D). Symbionts on both parts of the microzooids significantly increased in volume (Fig 5E and 5F) and became significantly more rod-shaped (Fig 5G and 5H). FDC was also significantly lower after 48 h (Table 1, Fig 5I and 5J) compared to freshly collected colonies.

Discussion

While maintenance of host-microbe mutualism over a host generation requires finely tuned exchange of goods and services between partners, persistence over ecological time scales requires reproduction prior host death and transmission of symbionts from one to next host generation [14, 43, 44]. In unstable environments like those inhabited by the giant ciliate mutualism, one of the greatest, naturally occurring threats is the cessation of sulfide flow. We have shown in a series of experiments that the association breaks down quickly when exposed to such sulfide deficiency conditions. Reproduction of the host colonies by swarmers was sustained until the host died in less than two days, albeit to a lesser extent than under sulfidic conditions, which resulted in many more swarmers released. Most notably, the mixture of supplied sulfide and oxygen in the control experiment resulted in the settlement of 82% of
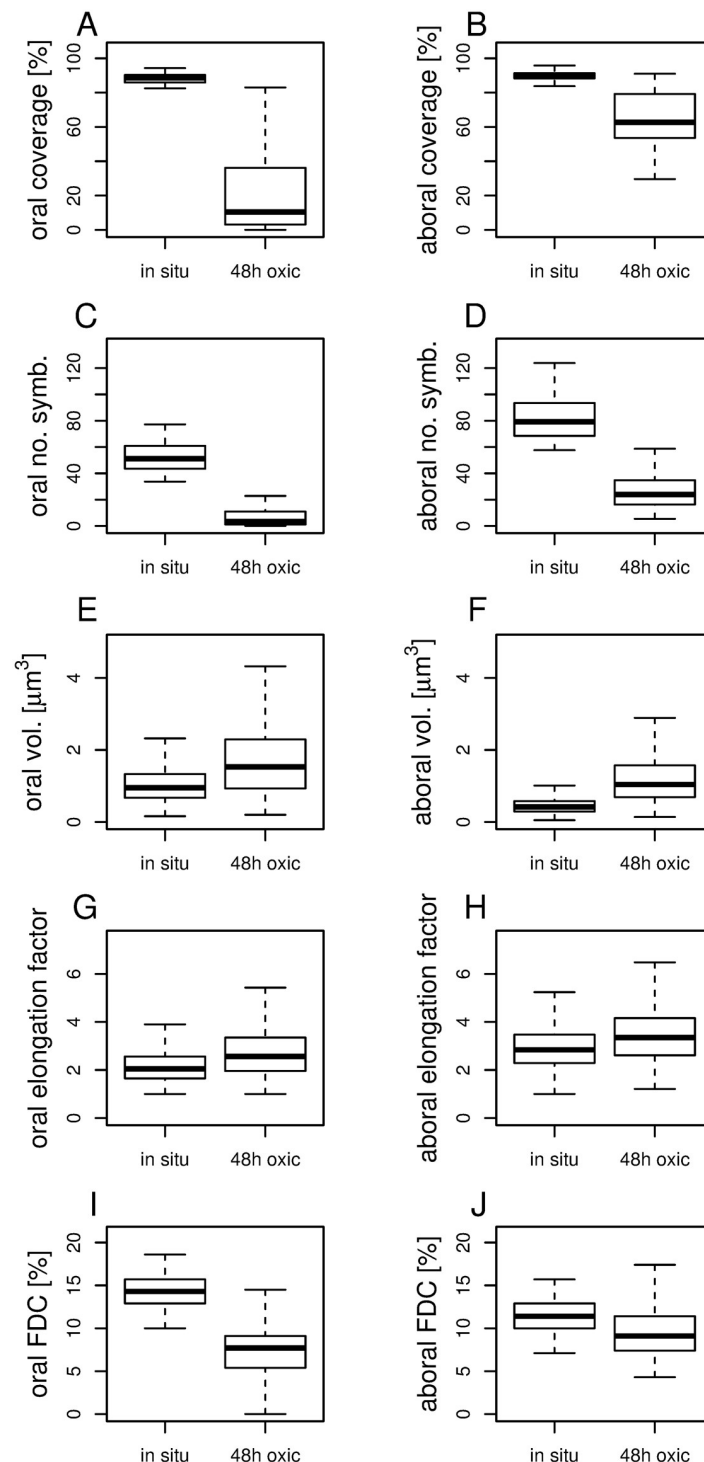
Fig 5. Symbiont response to sulfide starvation compared to freshly collected colonies. Box-and-whisker plots comparing orally (A, C, E, G, I) and aborally (B, D, F, H, J) located symbionts on microzooids of following parameters: percentage of symbiont coverage on host outer surface (A, B), number of symbionts per 70 μm² host surface area (C, D), volume of individual symbiont cells (E, F), cell elongation factor (ratio of symbiont length to width) (G, H), and frequency of dividing cells (FDC, ratio of dividing to total symbiont cells) (I, J). The box in the box-and-whisker plots shows the interquartile range with the median. The whiskers extend to the most extreme data points that are no more than 1.5 times the interquartile range from the box. All data were compared with the Wilcoxon-Mann-Whitney test and proved significantly different (99% significance) between *in situ* conditions and 48 h oxic experiments.

https://doi.org/10.1371/journal.pone.0254910.g005

swarmers and growth into viable colonies. Symbionts lacking sulfide showed changes in the morphology on the host and reduced division within two days compared to *in situ* values. Consequently, the loss of symbiont coverage resulted in more or less aposymbiotic hosts, which were often overgrown by unspecific microbes.

Our experiments show that the host's efforts to develop propagules under sulfide starvation continued until host death. This was shown by the fact that swarmers came not only from macrozooids that were already present on the colony at the beginning of the experiment, but also from macrozooids that had developed during the experiment. Since not all of the macrozooids that were initially present and not all of the newly developed macrozooids were released, the total number of swarmers released corresponds roughly to the number of macrozooids initially present in the sulfide starvation experiment. Although the number of propagules was much fewer than those that developed under sulfidic conditions and never developed into new colonies, these results clearly indicate the importance of macrozooid production until the host dies. The fact that these swarmers never settled was not unexpected, as previous studies in the field [27] and in the lab [31] showed that sulfide is the settlement signal.

A total of 310 swarmers from 120 colonies (a median of one swarmer per colony) were released under sulfide starvation, with more than half of all swarmers leaving the colonies on the first day. The release did not cease until the host died. The swarmer size decreased significantly with time the colony was sulfide deficient. This indicates a trade-off between quality and quantity of offspring. In comparison, in the sulfidic control experiment 60 initial colonies released 515 swarmers (with a median of eight swarmers per colony), showing much greater success in releasing the offspring. This is also reflected in the significantly higher slope of the linear fit between produced macrozooids (Δ_M) and produced and released swarmers (Δ_S) in the sulfidic control than under sulfide starvation ([Fig 2F](#)). Whether the swarmers change in size with the amount of time the colonies spend in sulfidic water remains to be investigated.

Following the fate of the swarmers kept under sulfidic conditions, we found that out of 515 swarmers released from 60 colonies 425 first generation colonies developed releasing 7 second generation swarmers in 4.5 days. Even one of these second generation swarmers settled. A previous study under steady flow conditions with fully oxygenated seawater supplemented with low sulfide concentrations resulted in about 80 new colonies from 13 initial colonies in five days [21]. Although these cultures differed in concentrations of chemicals and flow versus stagnant seawater conditions, in both each colony produced between six to seven offspring. We note, however, that under flow many swarmers may have been flushed out before they were able to settle. Comparing our sulfide starvation experiment under stagnant oxic conditions with a previous oxic flow-through experiment [21] shows remarkable differences. While no swarmers settled in the former, in the latter 13 colonies produced 15 first generation colonies [21]. The cut-off seagrass leaf on which the initial colonies grew was placed in the flow-through chamber. We suspect that it might have leaked sulfide due to degradation and triggered swarmer settlement. Therefore, direct comparisons of culture conditions are difficult to interpret.

We showed that colony death was accelerated under oxic conditions compared to sulfidic conditions. We hypothesize that the lack of sulfide resulted in reduced diet for the host, which resulted in a shorter lifespan. Earlier studies showed that with prolonged sulfide starvation the carbon fixation in the symbiont ceases and then the release and uptake of organic carbon also stops [30]. Symbionts on colonies that were kept under sulfide starvation for 24 h before incubations with ^{14}C or ^{13}C labeled bicarbonate showed no carbon fixation and incorporation and no uptake into the host tissue took place [30]. The host diet under such oxic conditions is then reduced to direct ingestion of free-living microbes and symbionts [30]. We do not know yet, whether the changes in host nutrition alone or other as-yet-unknown benefits that the

sulfide-deficient symbiont did not provide resulted in a stressed host and accelerated death compared to colonies kept under similar but sulfidic conditions.

A remarkable phenotypic change occurred in the symbionts under sulfide starvation in just two days. Differences in morphology between symbionts on oral and aboral microzooid parts known in freshly collected colonies from the environment [21], were retained, but symbionts on both parts became more rod-shaped and grew larger compared to freshly collected colonies.

Surprisingly, FDC values show that the proliferation did not stop completely as expected, but was greatly reduced. In view of the fact that internal sulfur storage in the symbionts can only support carbon fixation for a very short time [23], the symbiont may switch to heterotrophic metabolism and therefore maintain proliferation. A recent study showed an upregulation of transporter genes, indicating heterotrophy under oxic conditions in *Cand.* Thiosymbion oneisti, the thiotrophic ectosymbiont of the marine nematode *Laxus oneistus* [45]. Although genes that support this function are present in the metagenome assembled genome of Thiobius (Espada-Hinojosa pers. obs.), it remains to be investigated whether they are expressed under such conditions.

FDC values did not differ significantly (with a significance level of 1%) in orally and aborally located symbionts who were exposed to oxic seawater (Table 1). This indicates similar abiotic conditions for the symbionts regardless of their position on the microzooids. These results are consistent with previous cultivation experiments under a steady flow of oxic seawater, but supplemented with sulfide, where oral and aboral symbionts also had similar FDC values [21]. In contrast, the FDC values of orally located symbionts from our *in situ* colonies freshly collected from wood were higher than those located aborally, confirming the results from colonies collected from degrading seagrass leaves and from vertical, overhanging rocks over seagrass debris [21].

Host–symbiont maintenance was clearly disturbed under sulfide starvation. The symbiont coverage on the host was significantly reduced compared to freshly collected colonies with a monolayer on the host. This may be due to reduced symbiont proliferation under sulfide deficiency in combination with a loss of symbionts due to ingestion by the host. Whether loss of symbionts can also be traced back to death and/or to escape into the environment remains to be investigated.

The disturbance of host–symbiont maintenance was also visible through microbial fouling on symbiont-free host surfaces or even on top of the symbiont. In freshly collected colonies epigrowth occurs from the lower part of the colonies [11, 12] in a manner similar to what we observed in stressed hosts. As these are the oldest parts of the colony, this may suggest that the age of the host plays a role in warding off microbial fouling under natural sulfidic as well as experimental sulfide starvation conditions. Alternatively or additionally, symbionts may contribute to the antimicrobial defense.

Not only the numbers of swarmers produced per colony, but also the survival of the swarmer is important as it sets the limits of dispersal in order to find a patchy, sulfide-leaking habitat for settlement. In addition, symbionts are transmitted vertically on the swarmer [11, 12]. However, under oxic conditions, the swarmer gradually becomes aposymbiotic. Almost 40% of swarmers lost their symbionts within 24 h and 100% of swarmers within 48 h [31]. With a swarmer LT_{50} of 39 h and a considerable swimming speed of 5 mm s^{-1} [46] a spread of approximately 700 m can be achieved if the swarmer swims in a straight line. This estimate does not take into account that the spread is also strongly influenced by currents. Both, the life span of the swarmer and the period of time to keep at least some of the symbionts are critical to maintaining mutualism by dispersal in search for the right sulfidic site to settle and establish a new colony.

68

In summary, our experiments show that the beneficial interactions between *Zoothamnium niveum* and its only symbiont *Cand.* Thiobius zoothamnicola is quickly disturbed under stressful oxic conditions without sulfide. As expected, colonies die quickly in less than two days. Importantly, we observed that they continue to produce propagules until death. Symbionts are also quickly affected, changing their morphology and slowing down division. Now that the principal mode of stress response is known, we can begin to decipher the underlying mechanisms of changes in physiology and interactions at the molecular level.

Supporting information

S1 Fig. Scheme of colony. The colony is composed of a stalk with alternate branches and three different cell types–terminal zooids for division, microzooids for nutrition, and macrozooids for asexual reproduction. The size of the colony is counted in number of branches. A colony with initial macrozooids present at the start of the experiment and remaining macrozooids at the end of experiment is shown. During experimental time the release of swarmers was also counted.
(TIF)

S2 Fig. Time schedule of the sulfide starvation experiment. Colonies (n = 120) were monitored every 12 h (horizontal time line). Released swarmers from each of this time points were divided in 4 cohorts (A, B, C, D; vertical time line).
(TIF)

S3 Fig. Comparison of colonies from Sv. Jernej and Strunjan. All Wilcoxon-Mann-Whitney tests fail to reject the null hypothesis of equal medians: (A) colony size (p = 0.72), (B) number of initial macrozooids per colony (p = 0.49), (C) number of swarmers (released macrozooids) per colony (p = 0.46) and (D) size of swarmers (p = 0.41).
(TIF)

S4 Fig. FISH micrographs colonies. Colony alive after 48 h (A) DAPI staining (blue), (B) symbiont-specific probe (green), (C) EUB_{mix} and Archea probes (red) (D) composite of A, B, C; note the increase in microbial fouling from top to bottom. Colony alive after 72 h with very few symbionts left (E) DAPI staining (blue), (F) symbiont-specific probe (green), (G) EUB_{mix} and Archea probes (red), (H) composite of E, F and G.
(TIF)

S1 Table. Collections and abiotic parameters measured prior collection at wood surface. Samples listed according to type of experiment, applied technique, and time series of experiment, site, date of collection, number of wood, and abiotic parameters: depth, temperature, salinity, and pH. Abiotic parameters were measured using a Multi 340i sensor WTW.
(DOCX)

S2 Table. Abiotic parameters measured at the start (and at the end) of experiments. Abiotic parameters: temperature, salinity, pH, and oxygen and sulfide concentrations (mean ± standard deviation). Temperature, salinity, pH were measured using a Multi 340i sensor WTW. Oxygen concentration was measured using a PreSenS Flow-through Cell FTC-PSt3. Sulfide concentration was measured photometrically according to Cline (1969).
(DOCX)

Acknowledgments

69

University of Vienna. We would like to thank a reviewer for the highly valuable input and suggestions.

Author Contributions

References

1. Grieshaber MK, Völkel S. Animal adaptations for tolerance and exploitation of poisonous sulfide. Annu Rev Physiol. 1998; 60(1):33–53. https://doi.org/10.1146/annurev.physiol.60.1.33 PMID: 9558453

2. Millero FJ, Plese T, Fernandez M. The dissociation of hydrogen sulfide in seawater. Limnol Oceanogr. 1988; 33(2):269–74. https://doi.org/10.4319/lo.1988.33.2.0269

3. Dubilier N, Bergin C, Lott C. Symbiotic diversity in marine animals: the art of harnessing chemosynthesis. Nat Rev Microbiol. 2008; 6:725–40. https://doi.org/10.1038/nrmicro1992 PMID: 18794911

4. Stewart FJ, Newton ILG, Cavanaugh CM. Chemosynthetic endosymbioses: adaptations to oxic-anoxic interfaces. Trends Microbiol. 2005; 13(9):439–48. https://doi.org/10.1016/j.tim.2005.07.007 PMID: 16054816

5. Ott J, Bright M, Bulgheresi S. Marine microbial thiotrophic ectosymbioses. Oceanogr Mar Biol. 2004; 42:95–118.

6. Cavanaugh CM, McKiness ZP, Newton ILG, Stewart FJ. Marine chemosynthetic symbioses. Prokaryotes. 2006; 1:475–507.

7. Van Dover CL. Hydrothermal systems and the origin of life. The ecology of deep-sea hydrothermal vents. Princeton, New Jersey (USA): Princeton University Press; 2000. p. 397–411. https://doi.org/10.1038/35025044 PMID: 11001053

8. Jørgensen BB, Kasten S. Sulfur cycling and methane oxidation. In: Schulz HD, Zabel M, editors. Marine Geochemistry. Berlin, Heidelberg: Springer; 2006. p. 271–309.

9. Bright M, Lallier FH. The biology of vestimentiferan tubeworms. Oceanogr Mar Biol. 2010; 48:213–66. https://doi.org/10.1201/EBK1439821169-4

10. Grimonprez A, Molza A, Laurent M, Mansot J, Gros O. Thioautotrophic ectosymbiosis in Pseudovorticella sp., a peritrich ciliate species colonizing wood falls in marine mangrove. Eur J Protistol. 2018; 62:43–55. https://doi.org/10.1016/j.ejop.2017.11.002 PMID: 29202309

11. Bauer-Nebelsick M, Bardele CF, Ott JA. Redescription of *Zoothamnium niveum* (Hemprich & Ehrenberg, 1831) Ehrenberg, 1838 (Oligohymenophora, Peritrichida), a ciliate with ectosymbiotic, chemoautotrophic bacteria. Eur J Protistol. 1996; 32:18–30. https://doi.org/10.1016/S0932-4739(96)80036-8

12. Bauer-Nebelsick M, Bardele CF, Ott JA. Electron microscopic studies on *Zoothamnium niveum* (Hemprich & Ehrenberg, 1831) Ehrenberg 1838 (Oligohymenophora, Peritrichida), a ciliate with ectosymbiotic, chemoautotrophic bacteria. Eur J Protistol. 1996; 32:202–15. https://doi.org/10.1016/S0932-4739(96)80020-4

70

13. Schuster L, Bright M. A novel colonial ciliate *Zoothamnium ignavum* sp. nov. (Ciliophora, Oligohymenophorea) and its ectosymbiont *Candidatus* Navis piranensis gen. nov., sp. nov. from shallow-water wood falls. PLoS One. 2016; 11(9):e0162834. https://doi.org/10.1371/journal.pone.0162834 PMID: 27683199

14. Bright M, Bulgheresi S. A complex journey: transmission of microbial symbionts. Nat Rev Microbiol. 2010; 8:218–30. https://doi.org/10.1038/nrmicro2262 PMID: 20157340

15. Kádár E, Bettencourt R, Costa V, Santos RS, Lobo-da-Cunha A, Dando P. Experimentally induced endosymbiont loss and re-acquirement in the hydrothermal vent bivalve *Bathymodiolus azoricus*. J Exp Mar Biol Ecol. 2005; 318:99–110. https://doi.org/10.1016/j.jembe.2004.12.025

16. Brissac T, Gros O, Merçot H. Lack of endosymbiont release by two *Lucinidae* (Bivalvia) of the genus *Codakia*: consequences for symbiotic relationships. FEMS Microbiol Ecol. 2009; 67:261–7. https://doi.org/10.1111/j.1574-6941.2008.00626.x PMID: 19120467

17. Caro A, Got P, Bouvy M, Troussellier M, Gros O. Effects of long-term starvation on a host bivalve (*Codakia orbicularis*, Lucinidae) and its symbiont population. Appl Environ Microbiol. 2009; 75(10):3304–13. https://doi.org/10.1128/AEM.02659-08 PMID: 19346359

18. Elisabeth NH, Gustave SDD, Gros O. Cell proliferation and apoptosis in gill filaments of the lucinid *Codakia orbiculata* (Montagu, 1808) (Mollusca: Bivalvia) during bacterial decolonization and recolonization. Microsc Res Tech. 2012; 75(8):1136–46. https://doi.org/10.1002/jemt.22041 PMID: 22438018

19. Klose J, Polz MF, Wagner M, Schimak MP, Gollner S, Bright M. Endosymbionts escape dead hydrothermal vent tubeworms to enrich the free-living population. Proc Natl Acad Sci USA. 2015; 112 (36):11300–5. https://doi.org/10.1073/pnas.1501160112 PMID: 26283348

20. Oren A. A plea for linguistic accuracy—also for *Candidatus* taxa. Int J Syst Evol Microbiol. 2017; 67(4):1085–94. https://doi.org/10.1099/ijsem.0.001715 PMID: 27926819

21. Rinke C, Lee R, Katz S, Bright M. The effects of sulphide on growth and behaviour of the thiotrophic *Zoothamnium niveum* symbiosis. Proc R Soc Lond B Biol Sci. 2007; 274:2259–69. https://doi.org/10.1098/rspb.2007.0631 PMID: 17660153

22. Bright M, Espada-Hinojosa S, Lagkouvardos I, Volland J-M. The giant ciliate *Zoothamnium niveum* and its thiotrophic epibiont *Candidatus* Thiobios zoothamnicoli: a model system to study interspecies cooperation. Front microbiol. 2014; 5:145. https://doi.org/10.3389/fmicb.2014.00145 PMID: 24778630

23. Ott JA, Bright M, Schiemer F. The ecology of a novel symbiosis between a marine peritrich ciliate and chemoautotrophic bacteria. PSZN: Marine Ecology. 1998; 19(3):229–43. https://doi.org/10.1111/j.1439-0485.1998.tb00464.x

24. Rinke C, Schmitz-Esser S, Stoecker K, Nussbaumer AD, Molnár DA, Vanura K, et al. "*Candidatus* Thiobios zoothamnicoli", an ectosymbiotic bacterium covering the giant marine ciliate *Zoothamnium niveum*. Appl Environ Microbiol. 2006; 72(3):2014–21. https://doi.org/10.1128/AEM.72.3.2014-2021.2006 PMID: 16517650

25. Vopel K, Reick CH, Arlt G, Pöhn M, Ott JA. Flow microenvironment of two marine peritrich ciliates with ectobiotic chemoautotrophic bacteria. Aquat Microb Ecol. 2002; 29:19–28. https://doi.org/10.3354/ame029019

26. Laurent MCZ, Gros O, Brulport J-P, Gaill F, Le Bris N. Sunken wood habitat for thiotrophic symbiosis in mangrove swamps. Mar Environ Res. 2009; 67:83–8. https://doi.org/10.1016/j.marenvres.2008.11.006 PMID: 19131100

27. Vopel K, Pöhn M, Sorgo A, Ott J. Ciliate-generated advective seawater transport supplies chemoautotrophic ectosymbionts. Mar Ecol Prog Ser. 2001; 210:93–9. https://doi.org/10.3354/meps210093

28. Vopel K, Thistle D, Ott J, Bright M, Røy H. Wave-induced H_2S flux sustains a chemoautotrophic symbiosis. Limnol Oceanogr. 2005; 50(1):128–33. https://doi.org/10.4319/lo.2005.50.1.0128

29. Røy H, Vopel K, Huettel M, Jørgensen BB. Sulfide assimilation by ectosymbionts of the sessile ciliate, *Zoothamnium niveum*. Mar Biol. 2009; 156:669–77. https://doi.org/10.1007/s00227-008-1117-6 PMID: 32921817

30. Volland J-M, Schintlmeister A, Zambalos H, Reipert S, Mozetič P, Espada-Hinojosa S, et al. NanoSIMS and tissue autoradiography reveal symbiont carbon fixation and organic carbon transfer to giant ciliate host. ISME J. 2018; 12(3):714–27. https://doi.org/10.1038/s41396-018-0069-1 PMID: 29426952

31. Bright M, Espada-Hinojosa S, Volland J-M, Drexel J, Kesting J, Kolar I, et al. Thiotrophic bacterial symbiont induces polyphenism in giant ciliate host *Zoothamnium niveum*. Sci Rep. 2019; 9(1):15081. https://doi.org/10.1038/s41598-019-51511-3 PMID: 31636334

32. Cline JD. Spectrophotometric determination of hydrogen sulfide in natural waters. Limnol Oceanogr. 1969; 14:454–8. https://doi.org/10.4319/lo.1969.14.3.0454

33. Hammer Ø, Harper DAT, Ryan PD. PAST: Paleontological Statistics Software Package for Education and Data Analysis. Palaeontol Electron. 2001; 4(1).

71

34. Ihaka R, Gentleman R. R: a language for data analysis and graphics. J Comput Graph Stat. 1996; 5 (3):299–314. https://doi.org/10.2307/1390807

35. Amann RI, Krumholz L, Stahl DA. Fluorescent-oligonucleotide probing of whole cells for determinative, phylogenetic, and environmental studies in microbiology. J Bacteriol. 1990; 172(2):762–70. https://doi.org/10.1128/jb.172.2.762-770.1990 PMID: 1688842

36. Daims H, Brühl A, Amann R, Schleifer K-H, Wagner M. The domain-specific probe EUB338 is insufficient for the detection of all bacteria: development and evaluation of a more comprehensive probe set. Syst Appl Microbiol. 1999; 22(3):434–44. https://doi.org/10.1016/S0723-2020(99)80053-8 PMID: 10553296

37. Stahl DA, Amann R. Development and application of nucleic acid probes. In: Stackebrandt E, Goodfellow M, editors. Nucleic acid techniques in bacterial systematics: John Wiley & Sons; 1991. p. 205–48.

38. Wallner G, Amann R, Beisker W. Optimizing fluorescent in situ hybridization with rRNA-targeted oligonucleotide probes for flow cytometric identification of microorganisms. Cytometry. 1993; 14(2):136–43. https://doi.org/10.1002/cyto.990140205 PMID: 7679962

39. Trump BF, Bulger RE. New ultrastructural characteristics of cells fixed in a glutaraldehyde-osmium tetroxide mixture. Lab Invest. 1966; 15(1 Pt 2):368–79. PMID: 5326609

40. Hagström A, Larsson U, Hörstedt P, Normark S. Frequency of Dividing Cells, a new approach to the determination of bacterial growth rates in aquatic environments. Appl Environ Microbiol. 1979; 37 (5):805–12. https://doi.org/10.1128/aem.37.5.805-812.1979 PMID: 16345378

41. van Veen JA, Paul EA. Conversion of biovolume measurements of soil organisms, grown under various moisture tensions, to biomass and their nutrient content. Appl Environ Microbiol. 1979; 37(4):686–92. https://doi.org/10.1128/aem.37.4.686-692.1979 PMID: 16345366

42. Sunamura M, Higashi Y, Miyako C, Ishibashi J-i, Maruyama A. Two bacteria phylotypes are predominant in the Suiyo seamount hydrothermal plume. Appl Environ Microbiol. 2004; 70(2):1190–8. https://doi.org/10.1128/AEM.70.2.1190-1198.2004 PMID: 14766605

43. Douglas AE. The symbiotic habit. Princeton and Oxford: Princeton University Press; 2010.

44. Bronstein JL. Mutualism. New York: Oxford University Press; 2015.

45. Paredes GF, Viehboeck T, Lee R, Palatinszky M, Mausz MA, Reipert S, et al. Anaerobic sulfur oxidation underlies adaptation of a chemosynthetic symbiont to oxic-anoxic interfaces. mSystems. 2021; 6(3): e01186–20. https://doi.org/10.1128/mSystems.01186-20 PMID: 34058098

46. Ott J, Bright M. Sessile ciliates with bacterial ectosymbionts from Twin Cays, Belize. Atoll Research Bulletin. 2004; 516:1–7. https://doi.org/10.5479/si.00775630.516.1

Chapter 4

Thiotrophic bacterial symbiont induces polyphenism in giant ciliate host *Zoothamnium niveum*

Published in Scientific Reports, 2019
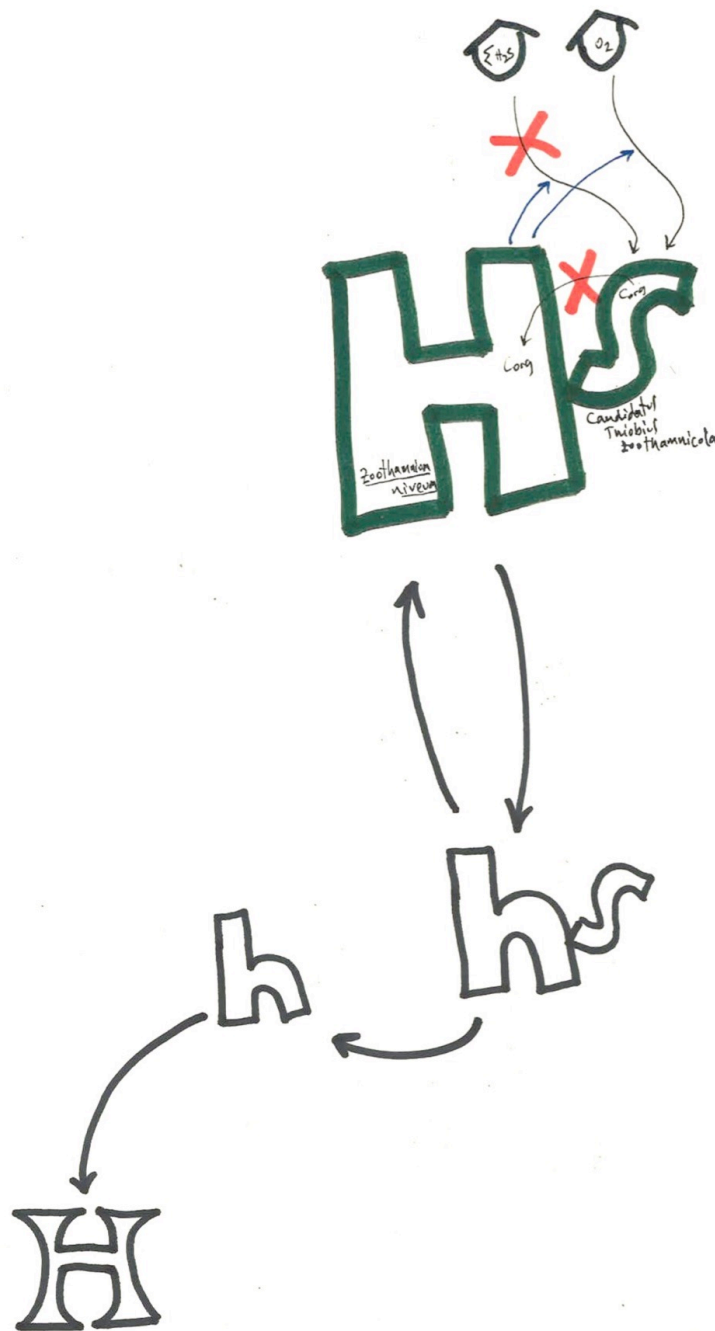
Coauthor paper

OPEN

Thiotrophic bacterial symbiont induces polyphenism in giant ciliate host *Zoothamnium niveum*

Monika Bright [ID][1]*, Salvador Espada-Hinojosa [ID][1], Jean-Marie Volland[1], Judith Drexel[1], Julia Kesting[1], Ingrid Kolar[1], Denny Morchner[1], Andrea Nussbaumer[1], Jörg Ott[1], Florian Scharhauser[1], Lukas Schuster[1], Helena Constance Zambalos[1] & Hans Leo Nemeschkal[2]

Evolutionary theory predicts potential shifts between cooperative and uncooperative behaviour under fluctuating environmental conditions. This leads to unstable benefits to the partners and restricts the evolution of dependence. High dependence is usually found in those hosts in which vertically transmitted symbionts provide nutrients reliably. Here we study host dependence in the marine, giant colonial ciliate *Zoothamnium niveum* and its vertically transmitted, nutritional, thiotrophic symbiont from an unstable environment of degrading wood. Previously, we have shown that sulphidic conditions lead to high host fitness and oxic conditions to low fitness, but the fate of the symbiont has not been studied. We combine several experimental approaches to provide evidence for a sulphide-tolerant host with striking polyphenism involving two discrete morphs, a symbiotic and an aposymbiotic one. The two differ significantly in colony growth form and fitness. This polyphenism is triggered by chemical conditions and elicited by the symbiont's presence on the dispersing swarmer. We provide evidence of a single aposymbiotic morph found in nature. We propose that despite a high fitness loss when aposymbiotic, the ciliate has retained a facultative life style and may use the option to live without its symbiont to overcome spatial and temporal shortage of sulphide in nature.

The notion that 'all development is co-development'[1] refers to the fact that hardly any animal or plant lives without microbial symbionts[2,3]. This entrenchment of environmental microbes[4] has served innumerable times as an integral element for phenotypic construction and phenotypic novelty in eukaryote hosts[5–9]. Symbiont-induced developmental change in host traits has yielded complex phenotypes with adapted physiology to interact with the symbionts[3,8,10–13].

The major transition from individuality of symbiotic partners in mutualistic relationships to a new integrated organism[14] requires mutual dependence and alignment of partner interests[15,16]. Some symbionts are considered as being strictly required for normal host development and reproduction[9,10], e.g. *Buchnera aphidicola* – aphids[3], 'Candidatus Endoriftia persephone' – giant tubeworm[17], 'Candidatus Kentron' – ciliate *Kentrophoros*[18,19], *Polynucleobacter* – ciliate *Euplotes*[20–26]. Such obligate hosts bearing symbionts can display phenotypic plasticity – the ability of an organism to express different phenotypes in response to the varying environmental conditions[4,27–29] - in various ways, but importantly, they do not retain the option to live aposymbiotically[30].

In some other associations, however, not becoming irreversibly dependent has major evolutionary advantages. As environmental conditions strongly impact the outcome of interactions[2,3], the elimination of aposymbiotic hosts is not selected for. Such facultative hosts have the option to interact with the partner as well as to live aposymbiotically[1,8]. For example, legumes develop root nodules in response to rhizobia infection only when fields are not fertilized with nitrogen[31]. The symbiotic and aposymbiotic anemone *Anthopleura elegantissima* occurs, according to light regime, either with *Symbiodinum* on sun-exposed or without these microalgae on shady substrates[32]. The endosymbiotic R-body producer *Caedibacter* transforms the host *Paramecium* into a killer of other paramecia including sometimes aposymbiotic individuals of the same species[33,34]. Most often *Paramecium bursaria* is found with photoautotrophic *Chlorella variabilis*[35] but also natural aposymbiotic hosts exist[36].

[1]University of Vienna, Department of Limnology and Bio-Oceanography, Vienna, Austria. [2]University of Vienna, Department of Theoretical Biology, Vienna, Austria. *email: monika.bright@univie.ac.at

Some hosts, however, are never found in nature without their symbionts although they can be experimentally purged from them and still grow and sometimes even reproduce, e.g. *Aliivibrio fischeri* and bobtail squids[37], methanogen bacteria and *Metopus contortus* ciliate[38]. To estimate host dependence over a range of animal and plant associations, the relative drop of host fitness between symbiotic and the experimentally purged or naturally occurring aposymbiotic hosts was calculated[39]. Overall hosts tend to be more dependent on vertically transmitted and nutritional symbionts than on horizontally transmitted and protective symbionts[39]. In ciliates fitness differences between symbiotic and aposymbiotic populations indicate the mutualistic advantage for the partners in nutritional[38] and defensive associations[34]. Fitness, however, was found to be highly context dependent[40]. Under a variety of abiotic and biotic conditions ciliate mutualism might shift to a host exploiting the symbiont[41] or a symbiont turning into a parasite[42].

The mutualism between the vertically transmitted and nutritional, sulphur-oxidizing, chemoautotrophic (thiotrophic) ectosymbiont 'Candidatus Thiobios zoothamnicoli' and its giant colonial ciliate host *Zoothamnium niveum*[43,44] is most suitable to test the hypothesis that symbiont function and transmission influence host dependence[39]. According to phylogenetic analyses based on the 18S rRNA gene sequence, *Z. niveum* belongs to the monophyletic clade 2[45] (termed clade 1[46]) within a non-monophyletic genus[45–51]. Morphologically clade 2 species exhibit a colony growth pattern of alternate branches[45]. They share with all *Zoothamnium* species a suite of morphological characters, e.g. a common stalk connecting all zooids and containing a continuous spasmoneme that facilitates contraction in a "zigzag" pattern[45,46,49]. Besides *Z. niveum*, most other clade 2 species are associated with ectosymbiotic bacteria: *Z. alternans*[52,53], *Z. ignavum*[51], *Z. pelagicum*[54–56]. Only in *Z. plumula* symbionts are not mentioned[57,58].

In contrast to other *Zoothamnium* species of clade 2, which occur in oxic environments[51,53–55,57,59], the *Z. niveum* partnership thrives in unstable and highly disturbed decaying plants and whale bones[60] in the presence of hydrogen sulphide ($\sum H_2S$, i.e. sum of all forms of dissolved sulphide[61], hereafter termed sulphide). The gammaproteobacterial symbiont has genes for sulphur oxidation and carbon fixation indicating a thiotrophic metabolism[62].

Individual cells (termed zooids) of the colony are differentiated with different functions for division (terminal zooids), feeding (microzooids), and asexual reproduction (macrozooids). The terminal zooid on the tip of the stalk produces the terminal zooids on each branch, which in turn produce feeding microzooids and the macrozooids on the branches[63]. Vertical transmission of the ectosymbiont is through macrozooids that leave the colony as swarmers[43,44], recruit to sulphide-emitting surfaces and grow into new colonies[64,65]. To date, the symbiont has neither been detected free-living in the environment nor has it been cultivated (MB unpublished data).

Through colony contraction and expansion, the colony dips into the sulphidic layer close to the substrate and extends into the oxic layer above, thereby alternately providing access to sulphide and oxygen as a byproduct benefit to the symbiont[60]. The symbiont fixes substantial amounts of inorganic carbon[66]. Host nourishment involves translocation of organic carbon to the host through both passive release, considered a byproduct benefit, and through digestion of symbionts[66]. Trading of goods in the mutualism, however, is interrupted when sulphide ceases during the cold season in temperate waters[67].

The *Z. niveum* mutualism is currently the only thiotrophic association that can be cultivated over several generations[68]. Experiments of the host under oxic, sulphide supplemented, flow-through conditions lead to fast growth, long life span, and high reproduction. The colonies are white because they are covered by symbionts that store elemental sulphur. Under oxic, flow-through conditions host reproduction was reduced and colonies were pale and short-lived[68]. At that time we did not investigate whether these small colonies still carried symbionts. We therefore hypothesized that swarmers lose their symbionts during dispersal, that settlement is preferentially on sulphide-emitting surfaces but may also be possible on oxic surfaces, and that aposymbiotic swarmers grow into aposymbiotic colonies.

To test these hypotheses, we designed laboratory experiments under oxic conditions that mimic cessation of sulphide flux in nature to explore the response of swarmers and colonies, and the fate of the symbiont on the host. Here, we report on experimental evidence for a striking polyphenism, i.e., the development of discrete alternative phenotypes[30]. We show that the environmental conditions encountered by the swarmer lead either to loss or maintenance of the symbiont. This triggers the developmental switch, expressed in two distinct colony growth forms. We developed a growth form index for statistical comparison. Our experiments show that each growth form performed better under the respective environmental conditions. The 18S rRNA gene sequences of two colonies collected in the field – one resembling the aposymbiotically grown morph, the other the symbiotic morph – were identical. This confirmed that both morphs occur in nature.

Results

Swarmers during dispersal.
All swarmers kept under oxic, stagnant conditions for 4 h were fully covered by the symbiont, (n = 11, Fig. 1a,b and Supplementary Table S1). After 24 h, swarmers (n = 16) were either still fully covered (31%, Fig. 1c,d), partially covered (31%, Fig. 1e,f), or aposymbiotic (38%, Fig. 1g,h). All swarmers were aposymbiotic after 48 h (n = 14, Fig. 1i,j).

Swarmer recruitment to sulphide-emitting surfaces.
In oxic, stagnant seawater only about 1% of the released swarmers settled within 72 h (n ≈ 3,000). These swarmers were pale. Because of the low swarmer recruitment, we used a preference experiment (n = 6) to test whether reduced sulphur species (sulphide, thiosulphate) or low oxygen concentrations act as a settlement cue. Settlement checked after 24 h revealed an overall median of 22.5% recruited swarmers (interquartile range IQR 6.6%) exclusively to sulphide-emitting surfaces. Settlement was not significantly different between high and low sulphide concentrations (Wilcoxon-Mann-Whitney test, p-value 0.85, Supplementary Table S2). No settlement occurred at the thiosulphate, the reduced oxygen membranes, or the walls of the experimental chamber exposed to oxic seawater.
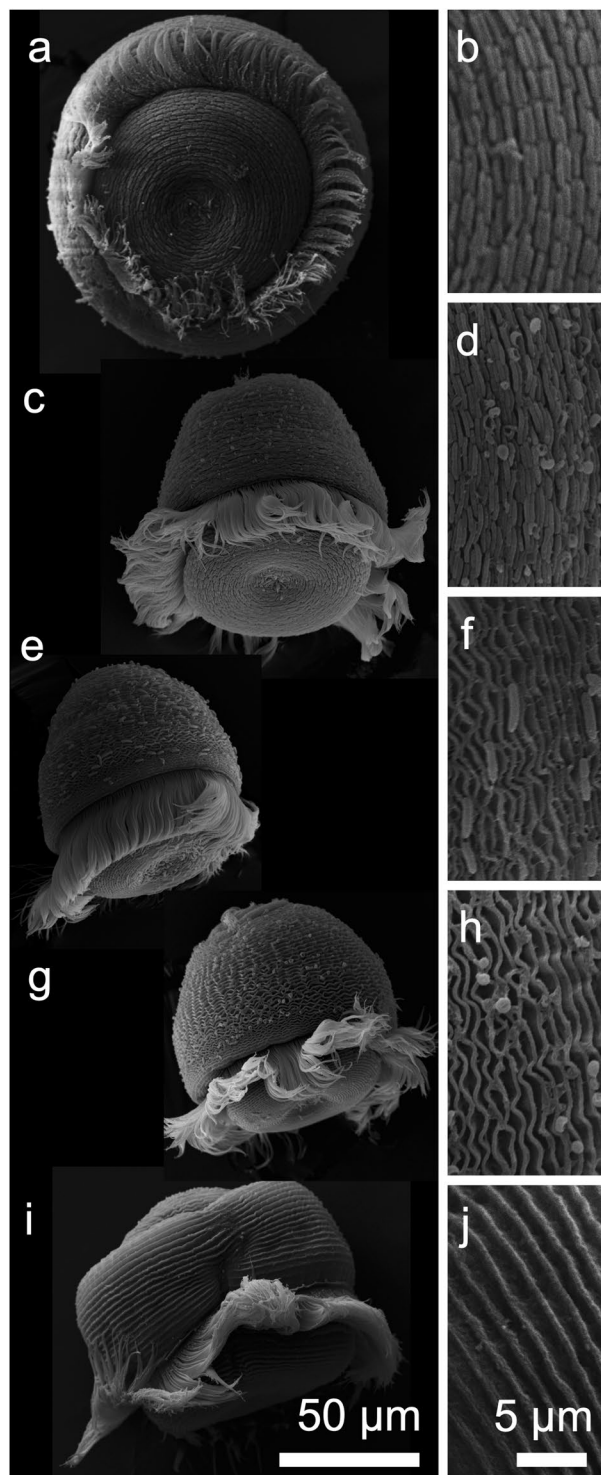
Figure 1. SEM micrographs of swarmers kept in oxic seawater for less than 4 h, and detail (**a,b**) between 4 h and 24 h old, fully covered with symbionts (**c,d**), partially covered with symbionts (**e,f**), with very few symbionts only, considered aposymbiotic (**g,h**) and between 24 h and 48 h old (**i,j**).

Because the swarmer recruitment experiment was carried out without chemical measurements, this experiment was repeated without swarmers to measure oxygen and sulphide concentration at the four membrane surfaces and revealed the presence of higher sulphide and lower oxygen at the high sulphide membrane and lower sulphide and higher oxygen at the low sulphide membrane until the end of the experiment. At the thiosulphate membrane, the oxygen concentration was similar to the concentration measured in the chamber, and sulphide was absent, whereas oxygen was very low and sulphide was absent at the membrane of the N_2-bubbled vial (Supplementary Table S2).
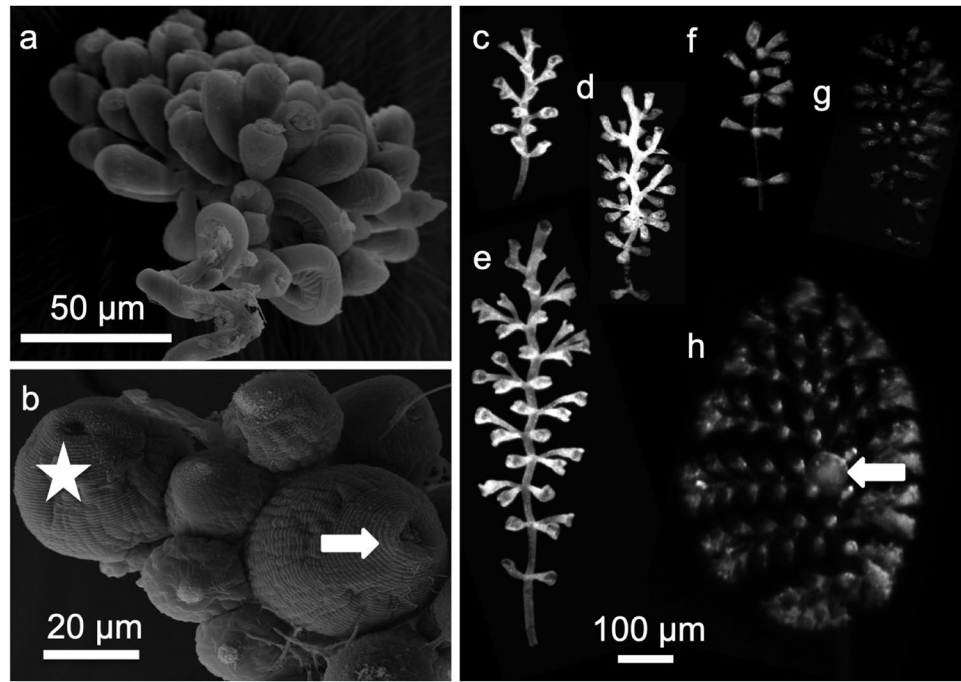
Figure 2. SEM micrographs of aposymbiotic colonies after seven days under sulphidic conditions (**a**), under oxic conditions with top terminal zooid (asterisk) and macrozooid (arrow) (**b**). Composite picture of light micrographs of symbiotic (**c**–**e**) and aposymbiotic morphs (**f**–**h**) macrozooid (arrow).

To investigate whether this selective host behaviour was influenced by the presence of the symbiont on the host over time, a mix of aposymbiotic and symbiotic swarmers was exposed to sulphide under stagnant conditions to avoid removal of swarmers from the chamber under flow-through conditions (n = 17). A median of 47.7% (IQR 20.4%) swarmers recruited to surfaces within 23 h. Distance covariance tests showed that the time of sulphide exposure – between 2 and 23 h – had no influence on the number of settled symbiotic (p-value 0.28), aposymbiotic (p-value 0.27) and total swarmers (p-value 0.21) (Supplementary Table S3).

Effects of sulphide and food supply on aposymbiotic host traits.

Settled pale swarmers grew into colonies both under oxic, flow-through and oxic, sulphide-supplemented, flow-through conditions. At the end of the experiment at day 7 scanning electron micrographs (SEM) confirmed that most colonies were without microbial overgrowth (Fig. 2). Because in a few colonies some patches of microbes were seen, we performed fluorescence *in situ* hybridisation (FISH) on semithin sections using the symbiont-specific and the EUB_{mix} and Arch915 probes to identify the microbes. Also FISH micrographs revealed that most colonies were aposymbiotic (Fig. 3a–d). In some cases, however, other microbes colonized the host surfaces in small patches, which were labelled with the EUB_{mix} and Arch915 probes but not with the symbiont-specific probe (Fig. 3e–h). In contrast, the symbiotic, white colonies were covered with a monolayer of symbionts with positive EUB_{mix} and Arch915 and symbiont-specific labels (Fig. 3i–l). During the 7-day experiments no colony switched from pale to white under either chemical conditions. Under either condition, a few macrozooids were produced (Fig. 2b,h). Release of macrozooids and settlement of swarmers could not be followed in this experiment.

At *in situ* microbial abundance (MA) aposymbiotic colonies had an estimated life span of 13.2 d (95% confidence interval 12.1, 15.3) under oxic, sulphide supplemented and 8.1 d (95% confidence interval 7.9, 8.2) under oxic conditions (Supplementary Table S4, Fig. 4a,d). The estimated maximal colony size reached a median of 7.2 branches (95% confidence interval 7.0, 7.4) in 4.0 d (95% confidence interval 4.0, 4.1) under oxic conditions and only 5.8 branches (95% confidence interval 5.2, 6.4) in 6.4 d (95% confidence interval 6.0, 7.3) in sulphidic conditions (Supplementary Table S4, Fig. 4a,d). Accordingly, colonies in oxic seawater grew faster with a relatively short, estimated life span, but to larger sizes, while oxic conditions supplemented with sulphide led to slow growth (hence longer life span) and smaller sizes.

Food density had no direct influence on the growth of aposymbiotic ciliates over a MA range of 2.0×10^5 to 1.6×10^6 mL^{-1}. Under oxic conditions, however, reduced MA restricted maximal colony sizes versus the larger sizes under *in situ* and enhanced MA (Fig. 4a–d). Survival of aposymbiotic colonies under oxic conditions ranged from 0% (enhanced MA), 25% (reduced MA) to 30% (*in situ* MA) (Supplementary Table S4). Under oxic, sulphide supplemented conditions, reduced and *in situ* MA led to similar estimated maximal colony sizes, whereas enhanced MA resulted in larger sizes (Fig. 4a–d). Survival of aposymbiotic colonies under oxic, sulphide supplemented conditions ranged from 28% (reduced MA), 64% (enhanced MA) to 100% (*in situ* MA).
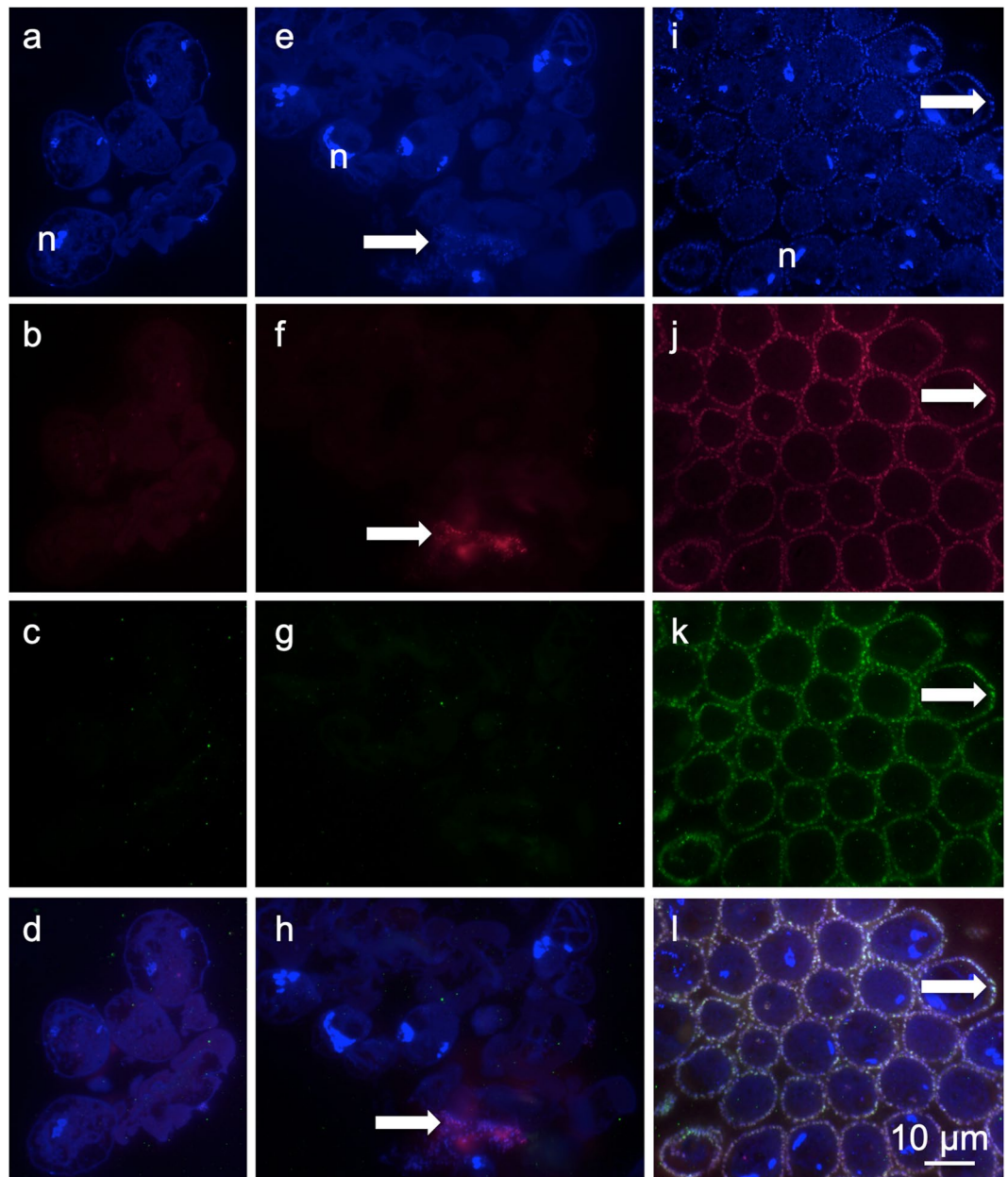
Figure 3. FISH micrographs of aposymbiotic morph grown under sulfidic conditions for seven days, stained with DAPI (**a**,**e**) (n macronuclei of host cells), labelled with EUB_{mix} and Arch915 probes (**b**,**f**), and symbiont-specific probe (**c**,**g**), and overlay (**d**,**h**) arrows points to microbes other than symbionts (**e**,**f**). Symbiotic morph grown under sulfidic conditions for seven days stained with DAPI (**i**)(n macronuclei of host cells), labelled with EUB_{mix} and Arch915 probes (**j**), and symbiont-specific probe (**k**) and overlay (**l**); arrows point to symbionts. Note that all micrographs are the same magnification.

Growth of symbiotic and aposymbiotic *Z. niveum* colonies.   The morphology differed remarkably between colonies grown from aposymbiotic and symbiotic swarmers under oxic, sulphide supplemented conditions (Supplementary Table S5). Survival was 100% in aposymbiotic morphs and 66% in symbiotic morphs (Supplementary Table S5). After settlement, the small colonies were morphologically similar (Fig. 2c,d,f,g). During further development, however, the colonies with 10 (Fig. 2e,h) or 11 branches (Supplementary Fig. S2) differed between aposymbiotic and symbiotic phenotypes. This indicates that the proliferation activity of the terminal zooid of each branch was comparatively higher in the aposymbiotic than in the symbiotic phenotype. In contrast, the proliferation activity of the top terminal zooid was comparatively higher in the symbiotic compared to the aposymbiotic phenotype (Fig. 4e, Supplementary Table S5) leading to a long but narrow symbiotic morph and a short but wide, aposymbiotic morph. Aposymbiotic colonies grown from aposymbiotic swarmers under oxic conditions were identical in morphology to those grown under oxic, sulphide supplemented conditions (Fig. 2).
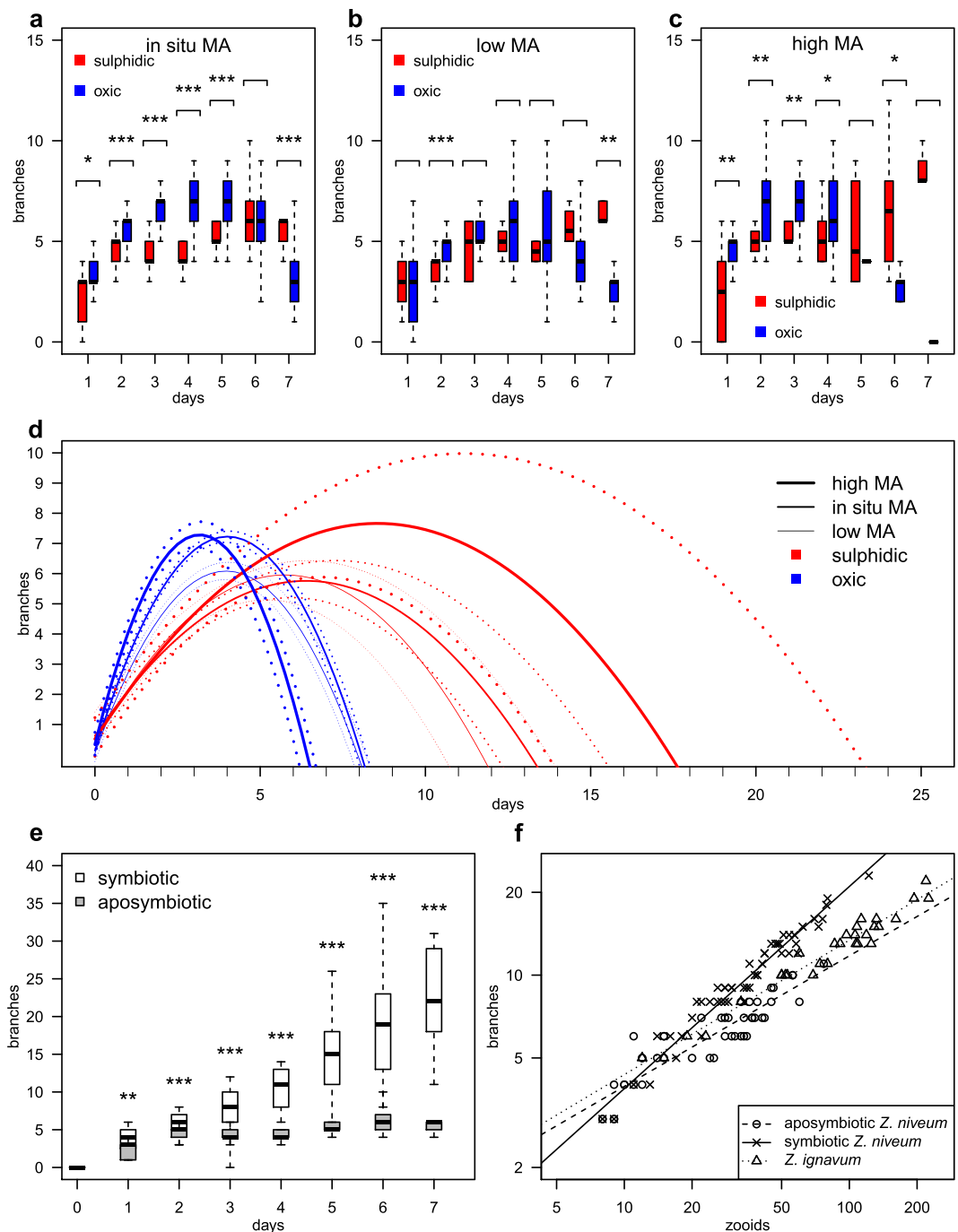
Figure 4. Box plots of growth (number of branches) of aposymbiotic colonies with *in situ* (**a**), low (**b**) and high (**c**) MA in sulphidic and oxic seawater (Wilcoxon-Mann-Whitney comparisons for each day; *p-value < 0.05, **p-value < 0.01, ***p-value < 0.001); (**d**) Estimated life span and maximal colony size of the aposymbiotic phenotype under sulphidic (red lines) and oxic (blue lines) conditions with reduced (thin line), *in situ* (medium line), and enhanced (thick line) MA, are inferred from the parabolas and 95% confidence intervals (dotted lines); (**e**) Box plots of growth of symbiotic and aposymbiotic colonies grown in the same chamber for seven days (Wilcoxon-Mann-Whitney comparisons for each day; **p-value < 0.01, ***p-value < 0.001); (**f**) Counted branches and total number of zooids in symbiotic and aposymbiotic colonies of *Z. niveum* and *Z. ignavum*, in double logarithmic scale of base 10 with power law fits.

Comparing both morphs under oxic, sulphide supplemented, *in situ* MA conditions, growth was significantly higher in the symbiotic phenotype from day 2 to day 7 (Fig. 4e, Supplementary Fig. S1, Wilcoxon-Mann-Whitney tests, p < 0.001). At the end of the experiment on day 7, symbiotic colonies exhibited a median of 22 branches bearing an estimated 107 zooids, while aposymbiotic colonies had 6 branches with an estimated 24 zooids only (Supplementary Table S5). The aposymbiotic life span was limited to an estimated 13.2 d, but the symbiotic growth

followed a monotonically increasing function (e.g. positive parabolic linear fit r² 0.70, p-value 2×10^{-44}, n = 169). The symbiotic morph therefore grew faster and to larger sizes. The estimated growth curve showed that the expected life span is much longer in the symbiotic than the aposymbiotic morph (Fig. 4e) confirming previous results[68].

Under oxic, *in situ* MA conditions, none of the symbiotic morphs were found after seven days. Survival of aposymbiotic morphs was 30% (Supplementary Table S4). Recruited white swarmers turned pale within the first 24 h and grew into aposymbiotic morphs, which was confirmed with SEM at the end of the experiment at day 7.

Growth form index (GFI). A colony GFI (exponent of the power law relating zooids and branches) was obtained from aposymbiotic and symbiotic *Z. niveum*. Because the aposymbiotic morph highly resembled the symbiotic *Z. ignavum* in morphology we also obtained a GFI for comparison from this closely related species collected in the field[51]. The aposymbiotic morph had a GFI of 0.47 (n = 45, 95% confidence interval 0.40, 0.54), significantly different (p-value 5×10^{-9}, analysis of covariance) from the symbiotic morph (GFI of 0.73, n = 51, 95% confidence interval 0.67, 0.78) (Fig. 4f, Supplementary Fig. S2). Symbiotic *Z. ignavum* showed a GFI of 0.49 (n = 30, 95% confidence interval 0.46, 0.52), non-significantly different to the aposymbiotic *Z. niveum* phenotype (p-value 0.73) but significantly different to the symbiotic *Z. niveum* phenotype (p-value 4×10^{-12}) (Fig. 4f, Supplementary Fig. S2).

Host 18S rRNA and symbiont 16S rRNA genes sequencing and phylogenetic analysis. Most of the colonies collected from minimally degraded wood and resembling the pale aposymbiotic phenotype were too low in DNA content to be sequenced (#4697/2-4,6,7). From one of these colonies (#4697/5, DNA content 3.6 ng/μL) 1,466 bp of the 18S rRNA gene could be retrieved. From a symbiotic, white colony collected from highly degraded wood (#4577, DNA content 32.4 ng/μL) 1,537 bp of the 18S rRNA gene were obtained. The sequence was identical to the pale colony (Supplementary Figs S3, S4) but differed to *Z. niveum* colony from USA[49] (Sequence similarity 99.5%) (Supplementary Fig. S4). All three *Z. niveum* colonies build a monophyletic subclade in clade 2 supported by 100% posterior probability (Bayesian inference, BI) and 100% bootstrap support (Maximum Likelihood, ML; Maximum Parsimony, MP; Fig. 5). The presence of the symbiont 16S rRNA gene using general primers could only be obtained from the symbiotic colony indicating that the aposymbiotic phenotype was containing microbes (including the symbiont) too low in abundance to be sequenced (Supplementary Fig. S3).

Discussion

The thiotrophic mutualism between *Zoothamnium niveum* and its symbiont faces the challenge of maintaining long-term stability in a notoriously unstable environment. Sulphide and oxygen are not always available, and unless the host provides access to these chemicals to the symbiont, the symbiont cannot provide organic carbon to the host[41]. This study reports the discovery of one aposymbiotic ciliate in nature and shows experimentally, how this ciliate loses its symbiont when trading of goods between partners is interrupted under oxic conditions (Fig. 6). Most interestingly this ciliate exhibits a polyphenism in colony growth form. Despite high dependency, indicated by a fitness drop of 73% growth reduction in the aposymbiotic phenotype (Supplementary Table S5) and consistent with other hosts of vertically transmitted and nutritional symbionts[39], this points to a facultative host. We propose that the aposymbiotic life style may ensure survival of the host at a temporal or spatial lack of sulphide in the environment.

New colonies can arise from swarmers under prolonged oxic conditions[68]. Here, we showed that swarmers easily lose the symbiont. Swarmers preferentially seek sulphidic surfaces for settlement to optimize symbiosis survival, but can also settle and grow aposymbiotically under unfavorable, oxic conditions, albeit to a very low percentage (Fig. 6). The time window for the swarmer to maintain its symbiont under oxic conditions is between 24 and 48 h. At a swarmer swim speed[69] of 5 mm s⁻¹, between 400 m and 800 m can be covered in one and two days, respectively. Accordingly, failing to find a sulphidic settlement near its release site leads to symbiont loss. The lack of a fully developed cytopharynx in swarmers suggests that symbionts cannot be digested[43]. It remains to be determined whether the host eliminates the symbiont because no benefits are provided and/or additional costs arise for the host to carry the symbiont during dispersal[70], or whether the symbiont dies or leaves the host due to adverse conditions.

Our experiments indicate that sulphide is the settlement cue. This is consistent with previous experiments in which swarmers settled at the edge of sulphide point sources on cut-out blocks of mangrove peat placed in aquaria[65]. Only 1% of swarmers settled within 72 h during dispersal in oxic seawater. Although the percentage of recruited aposymbiotic colonies is low, in nature the high density of symbiotic populations producing large numbers of swarmers might nevertheless allow survival of aposymbiotic host populations. Based on an average number of 15.5 ± 2.8 (mean ± standard error) macrozooids per colony[63] and 1,200 colonies m⁻² on mangrove peat[64] we estimate that well over 150 aposymbiotic colonies would be produced under oxic conditions from populations inhabiting a single square meter. Equally densely colonized wood (Supplementary Fig. S5), whale bones[71], and seagrass debris[68] have been documented elsewhere as well.

Most remarkably, this colonial ciliate exhibits a polyphenism in colony growth form, discernible as a long and narrow form in the symbiotic morph and a short and wide form in the aposymbiotic morph. The two morphs differ significantly in their growth form index. Polyphenism is well known from predator – prey, parasitic, and competitive interactions[72]. Other microbe – ciliate mutualisms are well known for their facultative host life style[73,74]. Often aposymbiotic and symbiotic morphs are quite similar in these unicellular hosts. *Metopus contortus* can be grown with its methanogen endosymbionts as well as aposymbiotically, revealing little morphological changes[38]. In the ciliate *Euplotidium itoi*, however, the presence of epixenosomes, unique ectosymbionts related to Verrucomicrobia[75] defending their host against predators[76], symbiotic morphs differ from artificially purged aposymbiotic morphs in the presence of a widened cortical region that the ectosymbionts are attached to[77].
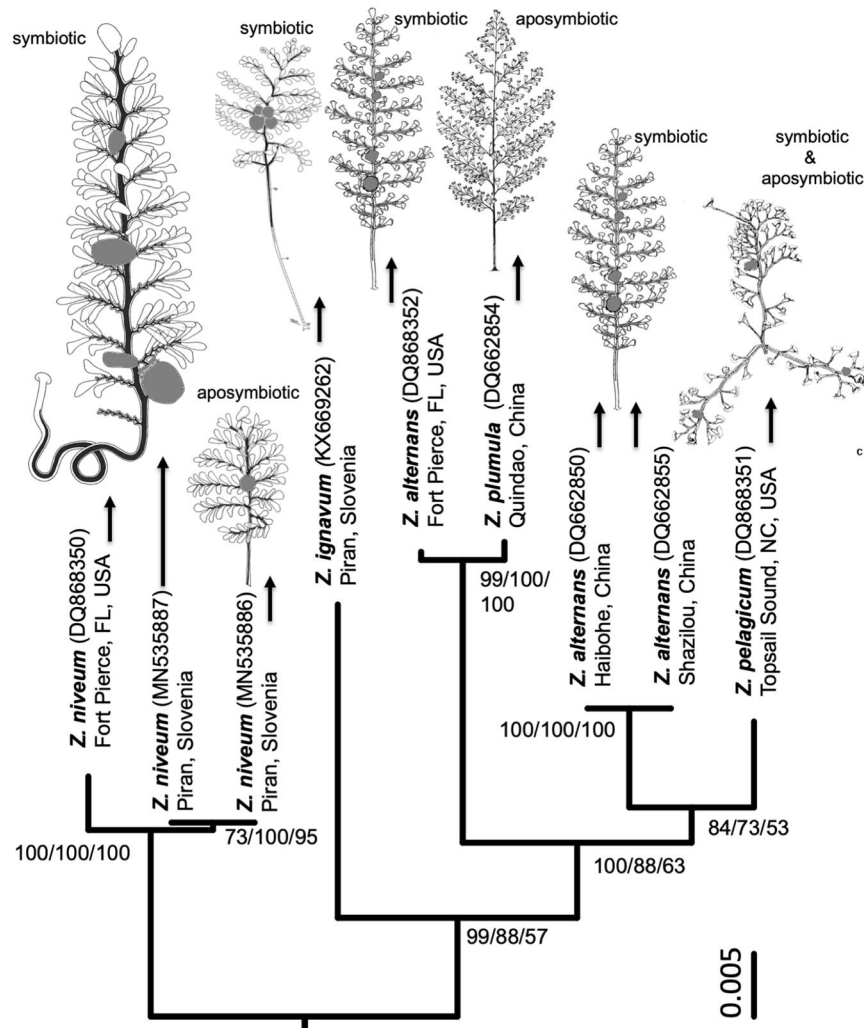
Figure 5. Bayesian tree inferred from the nucleotide sequences of the small subunit 18S rRNA gene of the monophyletic clade 2 of *Zoothamnium* and combined with colony drawings and life style. Support metrics are provided (BI/ML/MP). Scale bar corresponds to 1 substitution per 200 nt positions; numbers in parentheses are the NCBI accession numbers for each species. All colony drawings, including *Z. alternans*[53], *Z. pelagicum*[54], *Z. plumula*[57], *Z. ignavum*[51] and *Z. niveum* symbiotic[43] and aposymbiotic *Z. niveum* (drawing from a colony grown in a flow-through chamber) show macrozooids in grey. Colony drawing of *Z. plumula*[57] is under copyright and its use was granted by Magnolia Press www.mapress.com/j/zt. Colony drawings reproduction of *Z. alternans*[53] was granted by the Instytut Biologii Doświadczalnej im. M. Nenckiego, and of *Z. niveum*[43] by Elsevier. Colony drawing of *Z. pelagicum*[54] is under copyright and its use was granted by CNRS Éditions (M. Laval; Zoothamnium pelagicum du Plessis. Cilié Péritriche planctonique: morphologie, croissance et comportement *in Protistologica n°4* ©CNRS Éditions, 1968).

In the presence of sulphide in our experimental chamber, symbiotic and aposymbiotic swarmers gave rise to symbiotic and aposymbiotic morphs, respectively. In the absence of sulphide, only the aposymbiotic morph developed. In both cases the alternative phenotype exhibited significantly reduced growth indicating that each phenotype may be adaptive for the respective environment. The growth form expressed in oxic environments without symbionts experimentally would no doubt help the population to survive when swarmers fail to find a sulphidic substrate when such substrates are scarce or temporarily lacking at winter temperatures[67]. The finding of a single aposymbiotic morphotype of *Z. niveum* in nature may point to a much larger and more diverse habitat for this ciliate. Such aposymbiotic growth forms were not found on sulfide-emitting wood (MB pers. obs.). Whether host plasticity still retains the option to live aposymbiotically in nature or only in the lab by reverting to the growth form that they share with other species of clade 2 from oxic environments remains to be further investigated. The preferential recruitment behavior of the swarmer to abundant sulfide-emitting habitats and biological interactions such as competition and predation pressure may exclude the prevalence of aposymbiotic phenotypes when sulfide is produced during the warm seasons. They might be crucial, however, when temperature drops in late fall and ensure survival during the cold season.
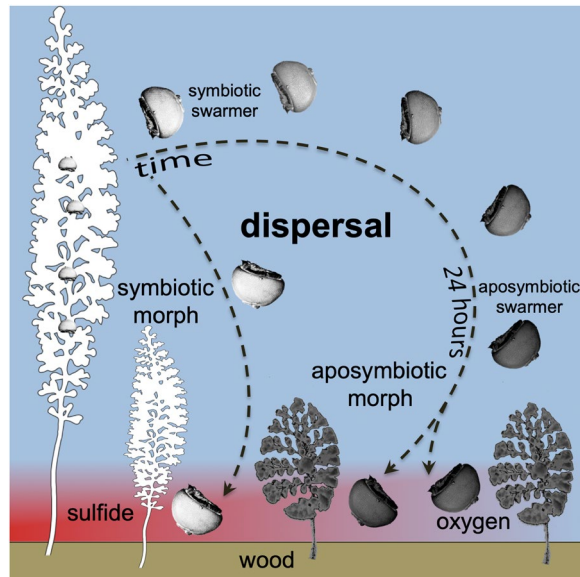
Figure 6. Proposed development of symbiotic morphs from symbiotic swarmers released from colony and short migration through oxic water prior to settlement on sulphide-emitting wood surface. In contrast, long migration of swarmers in oxic seawater leads to loss of symbionts and development of aposymbiotic morphs under both oxic and sulphidic conditions.

The different growth of aposymbiotic morphs grown under oxic versus oxic, sulphide supplemented conditions suggests that sulphide stresses the aposymbiotic host and impacts growth. The mitochondria of invertebrates and protists from sulphidic environments detoxify sulphide to thiosulphate in the presence of oxygen[78,79]. Our experiments point to a trade-off between growth and longevity. Growth was fast and led to larger sizes but shorter life spans under oxic conditions. Under oxic, sulphide supplemented conditions the energy-consuming processes of sulphide detoxification may slow growth and extend the life span.

The aposymbiotic and symbiotic morphs of *Zoothamnium niveum* grown in experimental chambers differ remarkably in morphological traits used in the classification of species in this genus. Without experimental proof these two highly different morphs would be classified as different species. The 18S rRNA gene sequences from one colony collected from the field and resembling the aposymbotically grown morph in the lab as well as the 18S rRNA gene sequence from the symbiotic colony from the field were identical and allowed us to identify them as *Z. niveum*. Both colonies from the Adriatic Sea have 99.5% similarity in their 18S rRNA gene sequence with the sequence from USA[49]. In contrast, *Z. alternans* also from geographically distant locations and considered morphologically identical[53] exhibit 96.7% sequence similarity[45]. This rather points to different species[51] when applying a threshold between 97 to 99%[51] or 99% sequence similarity[80]. Even more so, *Z. plumula* gene sequences from two relatively nearby locations in China[46,47] fall in different clades[46]. Overall, the presence of cryptic species in the genus *Zoothamnium* and the discovered polyphenism in *Z. niveum* warrants to call for the addition of possible symbiont descriptions on morphological and molecular level as well as host gene sequences applied when new species are described and when population from previously unknown locations are studied.

The closely related species[49] of *Zoothamnium niveum* in the clade 2 grow predominantly in oxic environments[51,53–55,57,59]. They show a wide range of either symbiotic or aposymbiotic life styles but share the diagnostic characteristic of a growth form with alternating branches[49]. They resemble, at first glance, the aposymbiotic morph with relatively long branches[51,53–55,57,59] (Fig. 5). We could confirm the similarity of GFIs of aposymbiotic *Z. niveum* (0.47) and symbiotic *Z. ignavum* (0.49), but for other species data are not yet available. Visually *Z. alternans*[53] highly resembles both aposymbiotic *Z. niveum* and *Z. ignavum*. Also relatively long branches are found in symbiotic *Z. pelagicum* that is in fact a "pseudo-colony", composed of several 'short and wide' colonies growing on each other[54–56] and in aposymbiotic *Z. plumula* with additional secondary branches[57]. Future research will help to determine whether specific growth forms can be related to specific environmental conditions.

Conclusion

Our study revealed a mechanism of mutualism breakdown. Host development with and without the symbiont led to a polyphenism i.e. to discrete alternative colony growth forms triggered by the chemical conditions in the environment that the swarmer encounters. Prolonged oxic conditions lead to symbiont loss inducing the development of an aposymbiotic morph with reduced fitness, whereas symbionts were maintained during sulphidic or brief oxic conditions leading to the development of the symbiotic morph with high fitness. Whether aposymbiotic host populations play indeed a role in nature and if so, how the aposymbiotic host regains its symbiont to guarantee connectivity from aposymbiotic to symbiotic host populations remains to be studied.

Methods

Swarmers during dispersal.   Colonies were collected from submerged wood at Sv. Jernej, Adriatic Sea, 2013 (replicate 1) and 2014 (replicate 2) (Supplementary Table S1). Colonies were cut from the substrate and transferred to embryo dishes filled with oxic seawater (24.5 °C ± 0.7 °C, salinity 33.3 ± 0.9, hereafter abiotic factors expressed as mean ± standard deviation). Release of swarmers was monitored after 4 h, 24 h, and 48 h (n = 2). Released swarmers were fixed for scanning electron microscopy (SEM) (Supplementary Table S1).

Swarmer recruitment in preference chambers.   Colonies were sampled from concrete blocks surrounded by seagrass debris in 2003 (Supplementary Table S2). For each experiment (n = 6), 30 to 50 released swarmers from about 50 colonies kept in oxic seawater (24 °C ± 1 °C, salinity 38 ± 1) were transferred into the central plastic cube (8 × 8 × 7 cm) of the preference chamber filled with oxic seawater. On each side of the cube, one vial was mounted and sealed with a dialysis polyethylene membrane (2.6 cm in diameter) permeable for small molecules to allow diffusion into the central chamber[81] (Supplementary Fig. S1). The vials were filled with 30 mL seawater containing 1) ~1.5 mmol L^{-1} sulphide, 2) ~2.5 mmol L^{-1} sulphide, 3) 10 mmol L^{-1} thiosulphate, and 4) continuously N$_2$-bubbled, anoxic seawater. After 24 h, the settlement of swarmers on the four membranes and on the inner cube's surface was counted using a dissection microscope. Medians and quartiles were calculated and the nonparametric Wilcoxon-Mann-Whitney test was performed to assess differences between swarmer recruitment to high and low sulphide (R[82] version 3.5.1, package *Coin*, v1.2-2).

Because abiotic parameters were not measured during this experiment in 2003, we repeated the experiment without swarmers to measure temperature, pH, salinity, oxygen, and sulphide in the chamber and oxygen and sulphide at all four membranes in October 2018 using a Fibox 4 (PreSenS, Germany) for oxygen and temperature, Multi 340i (WTW, Germany) for salinity and pH, and the Cline assay for ΣH_2S[83] (Supplementary Table S2).

Swarmer recruitment in flow-through chambers.   Colonies were collected from diverse submerged wood in the Adriatic Sea in 2013 and 2014 (Supplementary Table S3). Flow-through chambers[68] (n = 17; Supplementary Fig. S1) were filled with 17 mL of oxic seawater containing sulphide (147 ± 35 µmol L^{-1}). Between 90 and 227 pale, aposymbiotic and white, symbiotic swarmers were added to each chamber. The time for settlement was kept between 2 and 23 h during which the pumps were switched off to avoid swarmers being flushed out of the chamber. Afterwards, settled pale and white swarmers were counted, sulphide was measured, and flow through the chambers was established to follow colony growth (Supplementary Table S3). The covariance test (R package *Energy* v1.7-5) was used to show independence of time of sulphide exposure and number of settled swarmers.

Effects of sulphide and food supply on aposymbiotic host traits.   Colonies were collected from wood in Sv. Jernej in 2014 (Supplementary Table S4). For continuous flow through the chambers, we used an 8-channel peristaltic pump (Minipuls 3, Gilson International, Austria) set at 80 mL h^{-1} flow for oxic seawater and a syringe pump (KD Scientific, Inc., USA) set between 1.0 and 1.5 mL h^{-1} for sulphide supplementation in 50 mL syringes (between 1.5 and 1.8 mmol L^{-1} sulphide in Milli-Q water) (Supplementary Fig. S1). Three chambers were kept at oxic conditions, three others supplemented with sulphide. Two of these chambers (oxic and sulphidic) were fed with 32 µm filtered seawater to exclude eukaryote predation but to simulate the *in situ* microbial abundances (MA) commonly found in the northern Adriatic Sea during July[84]. To reduce the MA, we filtered the 32 µm pre-filtered seawater using the filter cartridge systems Polygard and Express SHC (Millipore, USA), with a final filtration of 0.2 µm pore size. To enhance the prokaryote density, we quadruple-concentrated 32 µm pre-filtered seawater using a Vivaflow 200 tangential flow module (Vivascience, Germany). Water and syringes were changed daily.

Abiotic parameters (flow, temperature, salinity, pH, oxygen, sulphide) and MA in the outflow water were monitored daily. Outflow water was filtered through polycarbonate filter membranes (Millipore GTBP02500 Isopore). Filters were fixed in 2% formalin for 24 h, air dried, and stored at −20 °C until staining with DAPI (4′,6-diamidino-2-phenylindole). MA was estimated by counting on an Axio Imager A1 epifluorescence microscope (Zeiss, Germany).

We followed survival as well as colony growth by counting the number of colonies and their respective branches under a dissection microscope daily. After 7 d the chambers were opened and colonies were fixed for SEM and fluorescence *in situ* hybridisation (FISH) (Supplementary Table S4). Shapiro-Wilk tests indicated deviations from normality for several of the experiments. Wilcoxon-Mann-Whitney tests were performed to assess differences of colony size between oxic and sulphidic conditions at low MA, *in situ* MA, and high MA. Linear regressions to quadratic polynomial parabolas (least squares fit) with Pearson R-square coefficients, and p-values were applied using R, because parabolas best reflected the growth and degenerative phase described for this ciliate[68]. Confidence intervals for parabolas were approximated by 10,000 random bootstrap re-samplings using the program 'MUBOQB'.

Growth of symbiotic and aposymbiotic *Z. niveum* colonies.   Using colonies collected at Sv. Jernej in 2014, both white symbiotic and pale aposymbiotic settled swarmers (Supplementary Table S3, experiment 68) grew together into white symbiotic and pale aposymbiotic colonies, respectively, in one flow-through chamber under *in situ* MA and sulphidic conditions for seven days (Supplementary Table S4, experiment 68). Differences in colony size of aposymbiotic and symbiotic morphs after seven days were assessed using the Wilcoxon-Mann-Whitney test.

Growth form index (GFI).   To estimate the relationship between cell population size (number of zooids) and colony size (number of branches), we selected micrographs of 96 *Z. niveum* (51 symbiotic and 45 aposymbiotic) from the above-described experiments and collections of white colonies at Sv. Jernej in 2014. For comparison we took photographs of 30 *Z. ignavum* colonies sampled at Sv. Jernej in 2014. A colony growth form index (GFI,

10

exponent of the power law relating zooids and branches) was obtained from aposymbiotic and symbiotic *Z. niveum* and *Z. ignavum* as the slope of the log-log linear regression of the number of branches and zooids. This approach is similar to a study in which the topology of plant roots was characterized by comparing the 'altitude' (longest path length of root system, equivalent to number of branches) and the 'magnitude' (the number of root tips, equivalent to the number of zooids)[85]. The GFI describes the (log-transformed) number of branches that will develop from the addition of one (log-transformed) new zooid. The significance of the difference between the GFIs was assessed with a covariance analysis[86] using R and by calculating of confidence intervals approximated by 10,000 random bootstrap re-samplings per analysis using 'MUBOQB'.

Scanning electron microscopy (SEM). Colonies sampled at Sv. Jernej in 2014 (Supplementary Table S4) and swarmers collected in 2013 and 2014 (Supplementary Table S1) were fixed in Trump's fixative (2.5% glutaraldehyde, 2% paraformaldehyde in $0.1\,mol\,L^{-1}$ sodium cacodylate buffer $1100\,mOsm\,L^{-1}$, pH 7.2) for up to 12 h, rinsed in $0.1\,mol\,L^{-1}$ sodium cacodylate buffer, dehydrated in an ethanol series, transferred to 100% acetone, chemically dried with hexamethyldisilazane (EMS), coated with gold using a Sputter Coater 108 (Agar, United Kingdom), and observed on a IT 300 scanning electron microscope (JEOL, Tokyo, Japan). We distinguished symbiotic hosts with full coverage and partial coverage, and aposymbiotic hosts with less than 10 symbionts in $1,000\,\mu m^2$.

Fluorescence *in situ* hybridisation (FISH). Colonies sampled at Sv. Jernej in 2014 (Supplementary Table S4) were fixed in 100% ethanol, embedded in the medium grade LR White resin, polymerized under nitrogen atmosphere at 40 °C for three days, and several semi-thin (0.5 μm) sections were placed in four drops of MilliQ water on gelatin-coated slides and air dried. Hybridisation was carried out according to Volland *et al.*[66] using the symbiont-specific oligonucleotide probe ZNS196_mod labelled with Cy3 and the EUB$_{mix}$ probes EUB338-I, EUB338-II, EUB338-III[87] together with the Arch915 probe[88] labelled with Cy5 to target most bacteria and archaea on sections placed into two drops. The sections of the other two drops of each slide were used for the nonsense probes labelled in Cy3 and Cy5 to control for false positives and no signals were observed.

Host 18S rRNA and symbiont 16S rRNA genes sequencing and phylogenetic analysis. Colonies resembling the pale, aposymbiotic growth form of *Z. niveum* (#4697/2-7) were collected from minimally degraded, most likely oxic parts of wood in July 2018. For comparison, also white, symbiotic *Z. niveum* (#4577) was collected nearby but from highly degraded, most likely sulphide emitting parts of wood. Samples were fixed in 100% ethanol, and DNA was extracted with DNeasy blood tissue kit (Quiagen, Germany). DNA content was measured with a Nanodrop 2000 spectrophotometer. The primers 82F[89] and MedlinB[90] were used for PCR amplification of the 18S rRNA gene. Gel electrophoresis was performed on a 1% Agarose gel in TBE buffer for 50 minutes at 90 Volt. For the 16S rRNA gene the primers 27F[91] and 1492R[92] were used. Bidirectional Sanger sequencing was performed (Microsynth AG, Switzerland). Sequences were analyzed with Geneious v. 11.1. (Biomatters, New Zealand).

To test the close affiliation between *Z. niveum* from Fort Pierce, USA and *Z. niveum* from Piran, Slovenia the nucleotide sequences of the small subunit rRNA genes of all members of clade 2[46,51] were obtained from NCBI, aligned with MAFFT[93] v7.407 and trimmed to the shortest sequence length obtained from the collected pale phenotype (1,466 bp) using SeaView[94] version 4 and ape[95] v5.2 package of R: *Z. niveum* DQ868350, Fort Pierce, FL, USA[49]; *Z. alternans* DQ868352, Fort Pierce, FL USA[49]; *Z. alternans* DQ662855, Shazikou, China[47]; *Z. alternans* DQ662850, Haibohe, China[47]; *Z. pelagicum* DQ868351 Topsail Sound, NC, USA[49]; *Z. plumula* DQ662854, Quindao, China (published under the name *Z. pluma*)[47]; *Z. ignavum*. KX669262, Piran, Slovenia[51]. *Z. plumula* KY675162, Yantai, China[46] was used as outgroup. The 18S rRNA eukaryote gene sequences of both collected colonies were deposited in the GenBank database under accession number MN535886 (Aposymbiotic_*Zoothamnium_niveum*_str._Piran_4697/5) and MN535887 (Symbiotic_*Zoothamnium_niveum*_str._Piran_4577).

Maximum Likelihood and Maximum Parsimony phylogenies with bootstrap support were calculated with ape and phangorn[96] v2.4.0 packages in R, under a GTR + I nucleotide substitution model (with best corrected AIC value). Bayesesian inference phylogeny with posterior probability support was generated with MrBayes[97] v3.2.7a with 1,750,000 generations and a burn-in of 25% of the length. The obtained tree was combined with colony drawings of a symbiotic colony[43] and a aposymbiotically grown colony of *Z. niveum* (this publication), *Z. alternans*[53], *Z. pelagicum*[54], *Z. plumula*[57], and *Z. ignavum*[51] and data on life style[43,51,53–55,57,59]. Reproduction of *Z. plumula*[57] drawing was granted by Magnolia Press, of *Z. alternans*[53] by the Instytut Biologii Doświadczalnej im. M. Nenckiego, of *Z. niveum*[43] by Elsevier, and *Z. pelagicum*[54] by CNRS Éditions.

Data availability

The datasets generated during and/or analysed during the current study are included in this published article and its Supplementary Information Files and are available in the FigShare repository, https://figshare.com/s/98e63972a493c272930e.

References

1. Gilbert, S. F. & Epel, D. *Ecological developmental biology: integrating epigenetics, medicine, and evolution.* (Sinauer Associates Inc., 2009).
2. Bronstein, J. L. *Mutualism.* (Oxford University Press, 2015).
3. Douglas, A. E. *The symbiotic habit.* (Princeton University Press, 2010).
4. West-Eberhard, M. J. *Developmental plasticity and evolution.* (Oxford University Press, 2003).

5. Fraune, S. & Bosch, T. C. G. Why bacteria matter in animal development and evolution. *BioEssays* **32**, 571–580, https://doi.org/10.1002/bies.200900192 (2010).

6. Gilbert, S. F. Ecological developmental biology: environmental signals for normal animal development. *Evolution & Development* **14**, 20–28, https://doi.org/10.1111/j.1525-142X.2011.00519.x (2012).

7. Gilbert, S. F., Sapp, J. & Tauber, A. I. A symbiotic view of life: we have never been individuals. *The Quarterly Review of Biology* **87**, 325–341, https://doi.org/10.1086/668166 (2012).

8. McFall-Ngai, M. Unseen forces: the influence of bacteria on animal development. *Developmental Biology* **242**, 1–14, https://doi.org/10.1006/dbio.2001.0522 (2002).

9. McFall-Ngai, M. *et al.* Animals in a bacterial world, a new imperative for the life sciences. *Proceedings of the National Academy of Sciences* **110**, 3229–3236, https://doi.org/10.1073/pnas.1218525110 (2013).

10. Bennett, G. M. & Moran, N. A. Heritable symbiosis: The advantages and perils of an evolutionary rabbit hole. *Proceedings of the National Academy of Sciences* **112**, 10169–10176, https://doi.org/10.1073/pnas.1421388112 (2015).

11. Gilbert, S. F. *et al.* Symbiosis as a source of selectable epigenetic variation: taking the heat for the big guy. *Philosophical Transactions of the Royal Society B* **365**, 671–678 (2010).

12. Gilbert, S. F., Bosch, T. C. G. & Ledón-Rettig, C. Eco-Evo-Devo: developmental symbiosis and developmental plasticity as evolutionary agents. *Nature Reviews Genetics* **16**, 611, https://doi.org/10.1038/nrg3982 (2015).

13. Pradeu, T. A mixed self: the role of symbiosis in development. *Biological Theory* **6**, 80–88, https://doi.org/10.1007/s13752-011-0011-5 (2011).

14. Szathmáry, E. & Smith, J. M. The major evolutionary transitions. *Nature* **374**, 227–232, https://doi.org/10.1038/374227a0 (1995).

15. Kiers, E. T. & West, S. A. Evolving new organisms via symbiosis. *Science* **348**, 392–394, https://doi.org/10.1126/science.aaa9605 (2015).

16. West, S. A., Fisher, R. M., Gardner, A. & Kiers, E. T. Major evolutionary transitions in individuality. *Proceedings of the National Academy of Sciences* **112**, 10112–10119, https://doi.org/10.1073/pnas.1421402112 (2015).

17. Bright, M. & Lallier, F. H. The biology of vestimentiferan tubeworms. *Oceanography and Marine Biology: An Annual Review* **48**, 213–266, https://doi.org/10.1201/EBK1439821169-c4 (2010).

18. Raikov, I. Bactéries épizoiques et mode de nutrition du cilié psammophile *Kentrophoros fistulosum* Fauré-Fremiet (étude au microscope électronique). *Protistologica* **7**, 365–378 (1971).

19. Seah, B. K. B. *et al.* Specificity in diversity: single origin of a widespread ciliate-bacteria symbiosis. *Proceedings of the Royal Society B: Biological Sciences* **284**, 764, https://doi.org/10.1098/rspb.2017.0764 (2017).

20. Heckmann, K., Hagen, R. T. & Görtz, H.-D. Freshwater *Euplotes* species with a 9 type 1 cirrus pattern depend upon endosymbionts. *The Journal of Protozoology* **30**, 284–289, https://doi.org/10.1111/j.1550-7408.1983.tb02917.x (1983).

21. Heckmann, K. & Schmidt, H. J. *Polynucleobacter necessarius* gen. nov., sp. nov., an obligately endosymbiotic bacterium living in the cytoplasm of *Euplotes aediculatus*. *International Journal of Systematic and Evolutionary Microbiology* **37**, 456–457, https://doi.org/10.1099/00207713-37-4-456 (1987).

22. Vannini, C., Petroni, G., Verni, F. & Rosati, G. *Polynucleobacter* bacteria in the brackish-water species *Euplotes harpa* (Ciliata Hypotrichia). *Journal of Eukaryotic Microbiology* **52**, 116–122, https://doi.org/10.1111/j.1550-7408.2005.04-3319.x (2005).

23. Vannini, C. *et al.* Endosymbiosis in statu nascendi: close phylogenetic relationship between obligately endosymbiotic and obligately free-living *Polynucleobacter* strains (Betaproteobacteria). *Environmental Microbiology* **9**, 347–359, https://doi.org/10.1111/j.1462-2920.2006.01144.x (2007).

24. Vannini, C., Ferrantini, F., Ristori, A., Verni, F. & Petroni, G. Betaproteobacterial symbionts of the ciliate *Euplotes*: origin and tangled evolutionary path of an obligate microbial association. *Environmental Microbiology* **14**, 2553–2563, https://doi.org/10.1111/j.1462-2920.2012.02760.x (2012).

25. Hahn, M. W., Schmidt, J., Pitt, A., Taipale, S. J. & Lang, E. Reclassification of four *Polynucleobacter necessarius* strains as representatives of *Polynucleobacter asymbioticus* comb. nov., *Polynucleobacter duraquae* sp. nov., *Polynucleobacter yangtzensis* sp. nov. and *Polynucleobacter sinensis* sp. nov., and emended description of *Polynucleobacter necessarius*. *International Journal of Systematic and Evolutionary Microbiology* **66**, 2883–2892, https://doi.org/10.1099/ijsem.0.001073 (2016).

26. Boscaro, V. *et al.* Parallel genome reduction in symbionts descended from closely related free-living bacteria. *Nature Ecology & Evolution* **1**, 1160–1167, https://doi.org/10.1038/s41559-017-0237-0 (2017).

27. Mayr, E. *Animal species and evolution.* (Harvard University Press, 1963).

28. Pfennig, D. W. *et al.* Phenotypic plasticity's impacts on diversification and speciation. *Trends in Ecology & Evolution* **25**, 459–467, https://doi.org/10.1016/j.tree.2010.05.006 (2010).

29. Whitman, D. W. & Agrawal, A. A. In *Phenotypic plasticity of insects* (eds D. W. Whitman & T. N. Ananthakrishnan) Ch. 1, 1–63 (Science Publishers: Enfield, NH, 2009).

30. Nijhout, H. F. Development and evolution of adaptive polyphenisms. *Evolution & Development* **5**, 9–18, https://doi.org/10.1046/j.1525-142X.2003.03003.x (2003).

31. Sachs, J. L., Gano, K. A., Hollowell, A. C. & Regus, J. U. The legume-rhizobium symbiosis, http://www.oxfordbibliographies.com/view/document/obo-9780199830060/obo-9780199830060-0095.xml (2013).

32. Weis, V. M. & Levine, R. P. Differential protein profiles reflect the different lifestyles of symbiotic and aposymbiotic *Anthopleura elegantissima*, a sea anemone from temperate waters. *The Journal of Experimental Biology* **199**, 883 (1996).

33. Schrallhammer, M., Castelli, M. & Petroni, G. Phylogenetic relationships among endosymbiotic R-body producer: Bacteria providing their host the killer trait. *Systematic and Applied Microbiology* **41**, 213–220, https://doi.org/10.1016/j.syapm.2018.01.005 (2018).

34. Grosser, K. *et al.* More than the "killer trait": infection with the bacterial endosymbiont *Caedibacter taeniospiralis* causes transcriptomic modulation in *Paramecium* host. *Genome Biology and Evolution* **10**, 646–656, https://doi.org/10.1093/gbe/evy024 (2018).

35. Decelle, J., Colin, S. & Foster, R. A. In *Marine Protists: Diversity and Dynamics* (eds Susumu Ohtsuka *et al.*) Ch. 19, 465–500 (Springer Japan, 2015).

36. Tonooka, Y. & Watanabe, T. A natural strain of *Paramecium bursaria* lacking symbiotic algae. *European Journal of Protistology* **38**, 55–58, https://doi.org/10.1078/0932-4739-00846 (2002).

37. McFall-Ngai, M. J. The importance of microbes in animal development: lessons from the squid-Vibrio symbiosis. *Annual Review of Microbiology* **68**, 177–194, https://doi.org/10.1146/annurev-micro-091313-103654 (2014).

38. Fenchel, T. O. M. & Finlay, B. J. Endosymbiotic methanogenic bacteria in anaerobic ciliates: significance for the growth efficiency of the host. *The Journal of Protozoology* **38**, 18–22, https://doi.org/10.1111/j.1550-7408.1991.tb04788.x (1991).

39. Fisher, R. M., Henry, L. M., Cornwallis, C. K., Kiers, E. T. & West, S. A. The evolution of host-symbiont dependence. *Nature Communications* **8**, 15973, https://doi.org/10.1038/ncomms15973 (2017).

40. Keeling, P. J. & McCutcheon, J. P. Endosymbiosis: The feeling is not mutual. *Journal of Theoretical Biology* **434**, 75–79, https://doi.org/10.1016/j.jtbi.2017.06.008 (2017).

41. Lowe, C. D., Minter, E. J., Cameron, D. D. & Brockhurst, M. A. Shining a light on exploitative host control in a photosynthetic endosymbiosis. *Current Biology* **26**, 207–211, https://doi.org/10.1016/j.cub.2015.11.052 (2016).

42. Dusi, E. *et al.* Vertically transmitted symbiont reduces host fitness along temperature gradient. *Journal of Evolutionary Biology* **27**, 796–800, https://doi.org/10.1111/jeb.12336 (2014).

43. Bauer-Nebelsick, M., Bardele, C. F. & Ott, J. A. Redescription of *Zoothamnium niveum* (Hemprich & Ehrenberg, 1831) Ehrenberg, 1838 (Oligohymenophora, Peritrichida), a ciliate with ectosymbiotic, chemoautotrophic bacteria. *European Journal of Protistology* **32**, 18–30 (1996).
44. Bauer-Nebelsick, M., Bardele, C. F. & Ott, J. A. Electron microscopic studies on *Zoothamnium niveum* (Hemprich & Ehrenberg, 1831) Ehrenberg 1838 (Oligohymenophora, Peritrichida), a ciliate with ectosymbiotic, chemoautotrophic bacteria. *European Journal of Protistology* **32**, 202–215 (1996).
45. Li, L., Ma, H. & Al-Rasheid, K. A. S. Monophyly or polyphyly? Possible conflict between morphological and molecular interpretations of the well-known genus Zoothamnium (Ciliophora, Peritrichia). *Chinese Journal of Oceanology and Limnology* **33**, 490–499, https://doi.org/10.1007/s00343-015-4083-0 (2015).
46. Zhuang, Y., Clamp, J. C., Yi, Z. & Ji, D. Phylogeny of the families Zoothamniidae and Epistylididae (Protozoa: Ciliophora: Peritrichia) based on analyses of three rRNA-coding regions. *Molecular Phylogenetics and Evolution* **118**, 99–107, https://doi.org/10.1016/j.ympev.2017.09.023 (2018).
47. Li, L. *et al.* Reconsideration of the phylogenetic positions of five peritrich genera, *Vorticella*, *Pseudovorticella*, *Zoothamnopsis*, *Zoothamnium*, and *Epicarchesium* (Ciliophora, Peritrichia, Sessilida), based on small subunit rRNA gene sequences. *Journal of Eukaryotic Microbiology* **55**, 448–456 (2008).
48. Sun, P., Clamp, J., Xu, D., Huang, B. & Shin, M. K. An integrative approach to phylogeny reveals patterns of environmental distribution and novel evolutionary relationships in a major group of ciliates. *Scientific Reports* **6**, 21695, https://doi.org/10.1038/srep21695 (2016).
49. Clamp, J. C. & Williams, D. A molecular phylogenetic investigation of *Zoothamnium* (Ciliophora, Peritrichia, Sessilida). *Journal of Eukaryotic Microbiology* **53**, 494–498, https://doi.org/10.1111/j.1550-7408.2006.00132.x (2006).
50. Ji, D. *et al.* Two new species of *Zoothamnium* (Ciliophora, Peritrichia) from Korea, with new observations of *Z. parahentscheli* Sun *et al.* 2009. *Journal of Eukaryotic Microbiology* **62**, 505–518, https://doi.org/10.1111/jeu.12205 (2015).
51. Schuster, L. & Bright, M. A novel colonial ciliate *Zoothamnium ignavum* sp. nov. (Ciliophora, Oligohymenophorea) and its ectosymbiont *Candidatus* Navis piranensis gen. nov., sp. nov. from shallow-water wood falls. *PLoS One* **11**, e0162834, https://doi.org/10.1371/journal.pone.0162834 (2016).
52. Fauré-Fremiet, E. Images électroniques d'une mirobiocénose marine. *Cahiers de Biologie Marine* **4**, 61–64 (1963).
53. Ji, D., Song, W. & Warren, A. Redescriptions of three marine peritrichous ciliates, *Zoothamnium alternans* Claparède et Lachmann, 1859, *Z. sinense* Song, 1991 and *Z. commune* Kahl, 1933 (Ciliophora, Peritrichia), from North China. *Acta Protozoologica* **45**, 27–39 (2006).
54. Laval, M. *Zoothamnium pelagicum* du Plessis. Cilié péritriche planctonique: morphologie, croissance et comportement. *Protistologica* **4**, 333–363 (1968).
55. Gómez, F. Motile behaviour of the free-living planktonic ciliate *Zoothamnium pelagicum* (Ciliophora, Peritrichia). *European Journal of Protistology* **59**, 65–74, https://doi.org/10.1016/j.ejop.2017.03.004 (2017).
56. Dragesco, J. Sur la biologie du *Zoothamnium pelagicum* (du Plessis). *Bulletin de la Société Zoologique de France* **73**, 130–134 (1948).
57. Ji, D. *et al.* Redescriptions of five species of marine peritrichs, *Zoothamnium plumula*, *Zoothamnium nii*, *Zoothamnium wang*, *Pseudovorticella bidulphiae*, and *Pseudovorticella marina* (Protista, Ciliophora). *Zootaxa* **2930**, 47–59, https://doi.org/10.5281/zenodo.278023 (2011).
58. Song, W.-B., Al-Rasheid, K. A. S. & Hu, X.-Z. Notes on the poorly-known marine peritrichous ciliate, *Zoothamnium plumula* Kahl, 1933 (Protozoa: Ciliophora), an ectocommensal organism from cultured scallops in Qingdao, China. *Acta Protozoologica* **41**, 163–168 (2002).
59. Summers, F. M. Some aspects of normal development in the colonial ciliate *Zoöthamnium alternans*. *The Biological Bulletin* **74**, 117–129, https://doi.org/10.2307/1537891 (1938).
60. Bright, M., Espada-Hinojosa, S., Lagkouvardos, I. & Volland, J.-M. The giant ciliate *Zoothamnium niveum* and its thiotrophic epibiont *Candidatus* Thiobios zoothamnicoli: a model system to study interspecies cooperation. *Frontiers in Microbiology* **5**, 145, https://doi.org/10.3389/fmicb.2014.00145 (2014).
61. Millero, F. J. *Chemical Oceanography*. (CRC Press, 1996).
62. Rinke, C. *et al.* High genetic similarity between two geographically distinct strains of the sulfur-oxidizing symbiont '*Candidatus* Thiobios zoothamnicoli'. *FEMS Microbiology Ecology* **67**, 229–241, https://doi.org/10.1111/j.1574-6941.2008.00628.x (2009).
63. Kloiber, U., Pflugfelder, B., Rinke, C. & Bright, M. Cell proliferation and growth in *Zoothamnium niveum* (Oligohymenophora, Peritrichida) – thiotrophic bacteria symbiosis. *Symbiosis* **47**, 43–50, https://doi.org/10.1007/BF03179969 (2009).
64. Ott, J. A., Bright, M. & Schiemer, F. The ecology of a novel symbiosis between a marine peritrich ciliate and chemoautotrophic bacteria. *P.S.Z.N.: Marine Ecology* **19**, 229–243, https://doi.org/10.1111/j.1439-0485.1998.tb00464.x (1998).
65. Vopel, K., Pöhn, M., Sorgo, A. & Ott, J. Ciliate-generated advective seawater transport supplies chemoautotrophic ectosymbionts. *Marine Ecology Progress Series* **210**, 93–99, https://doi.org/10.3354/meps210093 (2001).
66. Volland, J.-M. *et al.* NanoSIMS and tissue autoradiography reveal symbiont carbon fixation and organic carbon transfer to giant ciliate host. *The ISME Journal*, https://doi.org/10.1038/s41396-018-0069-1 (2018).
67. Nedwell, D. B. & Floodgate, G. D. The effect of microbial activity upon the sedimentary sulphur cycle. *Marine Biology* **16**, 192–200, https://doi.org/10.1007/bf00346941 (1972).
68. Rinke, C., Lee, R., Katz, S. & Bright, M. The effects of sulphide on growth and behaviour of the thiotrophic *Zoothamnium niveum* symbiosis. *Proceedings - Royal Society of London. Biological sciences* **274**, 2259–2269, https://doi.org/10.1098/rspb.2007.0631 (2007).
69. Ott, J. & Bright, M. Sessile ciliates with bacterial ectosymbionts from Twin Cays, Belize. *Atoll Research Bulletin* **516**, 1–7 (2004).
70. Genkai-Kato, M. & Yamamura, N. Evolution of mutualistic symbiosis without vertical transmission. *Theoretical Population Biology* **55**, 309–323, https://doi.org/10.1006/tpbi.1998.1407 (1999).
71. Kawato, M., Uematsu, K., Kaya, T., Pradillon, F. & Fujiwara, Y. First report of the chemosymbiotic ciliate *Zoothamnium niveum* from a whale fall in Japanese waters. *Cahiers de Biologie Marine* **51**, 413–421 (2010).
72. Agrawal, A. A. Phenotypic plasticity in the interactions and evolution of species. *Science* **294**, 321–326, https://doi.org/10.1126/science.1060701 (2001).
73. Görtz, H.-D. Towards an understanding of the distribution, dynamics and ecological significance of bacterial symbioses in protists. *Denisia* **23**, 307–311 (2008).
74. Dziallas, C., Allgaier, M., Monaghan, M. & Grossart, H.-P. Act together—implications of symbioses in aquatic ciliates. *Frontiers in Microbiology* **3**, https://doi.org/10.3389/fmicb.2012.00288 (2012).
75. Petroni, G., Spring, S., Schleifer, K.-H., Verni, F. & Rosati, G. Defensive extrusive ectosymbionts of *Euplotidium* (Ciliophora) that contain microtubule-like structures are bacteria related to *Verrucomicrobia*. *Proceedings of the National Academy of Sciences* **97**, 1813, https://doi.org/10.1073/pnas.030438197 (2000).
76. Rosati, G., Petroni, G., Quochi, S., Modeo, L. & Verni, F. Epixenosomes: peculiar epibionts of the hypotrich ciliate *Euplotidium itoi* defend their host against predators. *Journal of Eukaryotic Microbiology* **46**, 278–282, https://doi.org/10.1111/j.1550-7408.1999.tb05125.x (1999).

77. Giambelluca, M. A. & Rosati, G. Behavior of epixenosomes and the epixenosomal band during divisional morphogenesis in *Euplotidium itoi* (Ciliata, Hypotrichida). *European Journal of Protistology* **32**, 77–80, https://doi.org/10.1016/S0932-4739(96)80041-1 (1996).

78. Powell, M. A. & Somero, G. N. Adaptations to sulfide by hydrothermal vent animals: sites and mechanisms of detoxification and metabolism. *The Biological Bulletin* **171**, 274–290, https://doi.org/10.2307/1541923 (1986).

79. Grieshaber, M. K. & Völkel, S. Animal adaptations for tolerance and exploitation of poisonous sulfide. *Annual Review of Physiology* **60**, 33–53, https://doi.org/10.1146/annurev.physiol.60.1.33 (1998).

80. Boscaro, V., Syberg-Olsen, M. J., Irwin, N. A. T., del Campo, J. & Keeling, P. J. What can environmental sequences tell us about the distribution of low-rank taxa? The case of *Euplotes* (Ciliophora, Spirotrichea), including a description of *Euplotes enigma* sp. nov. *Journal of Eukaryotic Microbiology* **66**, 281–293, https://doi.org/10.1111/jeu.12669 (2019).

81. Goodwin, L. R., Francom, D., Urso, A. & Dieken, F. P. Determination of trace sulfides in turbid waters by gas dialysis/ion chromatography. *Analytical Chemistry* **60**, 216–219, https://doi.org/10.1021/ac00154a006 (1988).

82. Ihaka, R. & Gentleman, R. R: a language for data analysis and graphics. *Journal of Computational and Graphical Statistics* **5**, 299–314, https://doi.org/10.2307/1390807 (1996).

83. Cline, J. D. Spectrophotometric determination of hydrogen sulfide in natural waters. *Limnology and Oceanography* **14**, 454–458 (1969).

84. Vojvoda, J. *et al*. Seasonal variation in marine-snow-associated and ambient-water prokaryotic communities in the northern Adriatic Sea. *Aquatic Microbial Ecology* **73**, 211–224, https://doi.org/10.3354/ame01718 (2014).

85. Fitter, A. H. An architectural approach to the comparative ecology of plant root systems. *New Phytologist* **106**(Suppl.), 61–77, https://doi.org/10.1111/j.1469-8137.1987.tb04683.x (1987).

86. Cochran, W. G. Analysis of Covariance: its nature and uses. *Biometrics* **13**, 261–281, https://doi.org/10.2307/2527916 (1957).

87. Daims, H., Brühl, A., Amann, R., Schleifer, K.-H. & Wagner, M. The domain-specific probe EUB338 is insufficient for the detection of all bacteria: development and evaluation of a more comprehensive probe set. *Systematic and Applied Microbiology* **22**, 434–444, https://doi.org/10.1016/S0723-2020(99)80053-8 (1999).

88. Stahl, D. A. & Amann, R. In *Nucleic acid techniques in bacterial systematics* (eds E. Stackebrandt & M. Goodfellow) 205–248 (Wiley & Sons Ltd., 1991).

89. Elwood, H. J., Olsen, G. J. & Sogin, M. L. The small-subunit ribosomal RNA gene sequences from the hypotrichous ciliates *Oxytricha nova* and *Stylonychia pustulata*. *Molecular Biology and Evolution* **2**, 399–410, https://doi.org/10.1093/oxfordjournals.molbev.a040362 (1985).

90. Medlin, L., Elwood, H. J., Stickel, S. & Sogin, M. L. The characterization of enzymatically amplified eukaryotic 16S-like rRNA-coding regions. *Gene* **71**, 491–499, https://doi.org/10.1016/0378-1119(88)90066-2 (1988).

91. Lane, D. J. In *Nucleic acid techniques in bacterial systematics* (eds E. Stackebrandt & M. Goodfellow) 115–175 (John Wiley & Sons Ltd, 1991).

92. Loy, A. *et al*. 16S rRNA gene-based oligonucleotide microarray for environmental monitoring of the betaproteobacterial order "Rhodocyclales". *Applied and Environmental Microbiology* **71**, 1373–1386, https://doi.org/10.1128/AEM.71.3.1373-1386.2005 (2005).

93. Katoh, K., Misawa, K., Kuma, K. I. & Miyata, T. MAFFT: a novel method for rapid multiple sequence alignment based on fast Fourier transform. *Nucleic Acids Research* **30**, 3059–3066, https://doi.org/10.1093/nar/gkf436 (2002).

94. Gouy, M., Guindon, S. & Gascuel, O. SeaView Version 4: A multiplatform graphical user interface for sequence alignment and phylogenetic tree building. *Molecular Biology and Evolution* **27**, 221–224, https://doi.org/10.1093/molbev/msp259 (2009).

95. Paradis, E., Claude, J. & Strimmer, K. APE: Analyses of Phylogenetics and Evolution in R language. *Bioinformatics* **20**, 289–290, https://doi.org/10.1093/bioinformatics/btg412 (2004).

96. Schliep, K. P. Phangorn: phylogenetic analysis in R. *Bioinformatics* **27**, 592–593, https://doi.org/10.1093/bioinformatics/btq706 (2011).

97. Ronquist, F. & Huelsenbeck, J. P. MrBayes 3: Bayesian phylogenetic inference under mixed models. *Bioinformatics* **19**, 1572–1574, https://doi.org/10.1093/bioinformatics/btg180 (2003).

Acknowledgements

Author contributions

M.B. designed the research, A.N. designed and J.O. participated in the preference experiment, J.-M.V. led the growth experiments together with M.B., S.E.H., I.K. and L.S., J.D. and J.K. performed SEM, H.C.Z. performed FISH, D.M. and F.S. performed sequencing, S.E.H. and H.L.N. analysed the data and performed the statistical analyses, M.B. wrote the paper.

Competing interests

The authors declare no competing interests.

Additional information

Supplementary information is available for this paper at https://doi.org/10.1038/s41598-019-51511-3.

Correspondence and requests for materials should be addressed to M.B.

Reprints and permissions information is available at www.nature.com/reprints.

Publisher's note Springer Nature remains neutral with regard to jurisdictional claims in published maps and institutional affiliations.
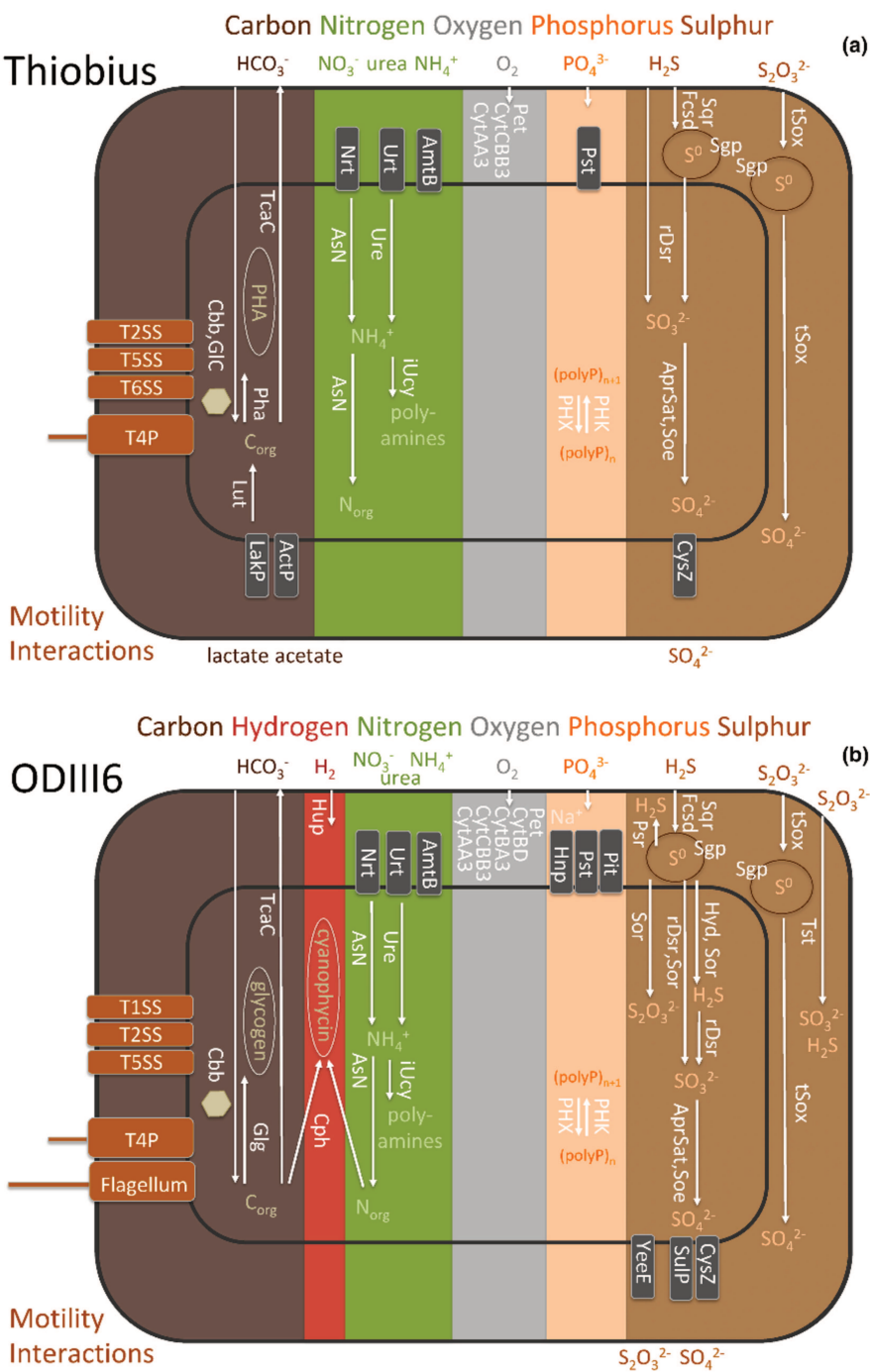
Chapter 5

Comparative genomics of a vertically transmitted thiotrophic bacterial ectosymbiont and its close free-living relative

First author paper

MOLECULAR ECOLOGY
RESOURCES **WILEY**

Comparative genomics of a vertically transmitted thiotrophic bacterial ectosymbiont and its close free-living relative

Salvador Espada-Hinojosa[1] | Clarissa Karthäuser[2] | Abhishek Srivastava[1] | Lukas Schuster[1] | Teresa Winter[1] | André Luiz de Oliveira[1] | Frederik Schulz[3] | Matthias Horn[3] | Stefan Sievert[2] | Monika Bright[1]

[1]Department of Functional and Evolutionary Ecology, University of Vienna, Vienna, Austria

[2]Biology Department, Woods Hole Oceanographic Institution, Woods Hole, Massachusetts, USA

[3]Center for Microbiology and Environmental Systems Science, University of Vienna, Vienna, Austria

Correspondence
Monika Bright, Department of Functional and Evolutionary Ecology, University of Vienna, Schlachthausgasse 43, Vienna, Austria.
Email: monika.bright@univie.ac.at

Present address
Lukas Schuster, Deakin University, Burwood, Australia
André Luiz de Oliveira, Max Planck Institute for Marine Microbiology, Bremen, Germany
Frederik Schulz, DOE Joint Genome Institute, Berkeley, California, USA

Abstract

Thiotrophic symbioses between sulphur-oxidizing bacteria and various unicellular and metazoan eukaryotes are widespread in reducing marine environments. The giant colonial ciliate *Zoothamnium niveum*, however, is the only host of thioautotrophic symbionts that has been cultivated along with its symbiont, the vertically transmitted ectosymbiont *Candidatus* Thiobius zoothamnicola (short Thiobius). Because theoretical predictions posit a smaller genome in vertically transmitted endosymbionts compared to free-living relatives, we investigated whether this is true also for an ectosymbiont. We used metagenomics to recover the high-quality draft genome of this bacterial symbiont. For comparison we have also sequenced a closely related free-living cultured but not formally described strain Milos ODIII6 (short ODIII6). We then performed comparative genomics to assess the functional capabilities at gene, metabolic pathway and trait level. 16S rRNA gene trees and average amino acid identity confirmed the close phylogenetic relationship of both bacteria. Indeed, Thiobius has about a third smaller genome than its free-living relative ODIII6, with reduced metabolic capabilities and fewer functional traits. The functional capabilities of Thiobius were a subset of those of the more versatile ODIII6, which possessed additional genes for oxygen, sulphur and hydrogen utilization and for the acquisition of phosphorus illustrating features that may be adaptive for the unstable environmental conditions at hydrothermal vents. In contrast, Thiobius possesses genes potentially enabling it to utilize lactate and acetate heterotrophically, compounds that may be provided as byproducts by the host. The present study illustrates the effect of strict host-dependence of a bacterial ectosymbiont on genome evolution and host adaptation.

KEYWORDS
ectosymbiosis, low-complexity metagenome, sulphur-oxidizing bacteria, thiotrophy, *Zoothamnium niveum*

---

1 | INTRODUCTION

The beneficial associations between sulphur-oxidizing bacteria (SOBs) and diverse protist and invertebrate hosts (Cavanaugh et al., 2006; Dubilier et al., 2008; Ott et al., 2004; Sogin et al., 2021; Stewart et al., 2005) span the entire range of ectosymbiotic mutualism, from the highly diverse microbiomes of alvinocarid shrimps and the low-diversity microbiomes of alvinellid polychaetes at deep-sea hydrothermal vents (Cambon-Bonavita et al., 2021; Grzymski et al., 2008) to strictly single symbiont species such as those on stilbonematine nematodes from marine shallow-water sediments (Ott et al., 1991; Paredes et al., 2021; Petersen et al., 2010; Polz et al., 1994), or on an amphipod in freshwater caves (Dattagupta et al., 2009). Among ciliates, monolayered coats of single ectosymbiotic SOB species are known from the karyorelictid *Kentrophoros* (Faure-Fremiet, 1951; Fauré-Fremiet, 1950; Fenchel & Finlay, 1989; Finlay & Fenchel, 1989; Raikov, 1971, 1974; Seah et al., 2019) and the peritrichs *Pseudovorticella* (Grimonprez et al., 2018; Laurent et al., 2009; Maurin et al., 2010) and *Zoothamnium* (Bauer-Nebelsick et al., 1996a, 1996b; Hemprich & Ehrenberg, 1829, 1831; Rinke et al., 2006, 2009; Schuster & Bright, 2016). Some symbiotic SOBs form phylogenetic clusters with free-living relatives (Figure 1; Dubilier et al., 2008). Here, we provide genomic information on two closely related SOBs with different lifestyles, that is, an obligate vertically transmitted ectosymbiont and a free-living chemolithoautotrophic bacterium.

Candidatus Thiobius zoothamnicola of the Chromatiaceae (Chromatiales, Gammaproteobacteria) (Oren, 2017, short Thiobius) – originally introduced as *Candidatus* Thiobios zoothamnicoli (Rinke et al., 2006) – covers the surface of the giant colonial ciliate *Zoothamnium niveum* (short *Zoothamnium*) that can typically be found in shallow-water environments from tropical to temperate waters with decaying organic material (Bauer-Nebelsick et al., 1996a, 1996b, Rinke et al., 2006, 2009, reviewed in Bright et al., 2014). Thiobius is transmitted vertically (Bauer-Nebelsick et al., 1996a, 1996b; Rinke et al., 2006) and has not been found free-living despite extensive searches using general bacterial primers as well as a symbiont-specific primer and direct Sanger sequencing (Monika Bright personal observation, 2022). To our best knowledge, the giant ciliate mutualism is the only thiotrophic symbiosis that has been cultivated in the laboratory over several host generations (Rinke et al., 2007). In contrast, the facultative endosymbiont *Thiosocius teredinicola* of the shipworm *Kuphus polithalamius* is the only thiotrophic symbiont that has been cultivated without its host (Distel et al., 2017).

The host *Zoothamnium niveum* grows fast and reproduces asexually developing specialized macrozooids that leave the colony as ectosymbionts-covered propagules called swarmers to found new colonies upon settlement (Bauer-Nebelsick et al., 1996a, 1996b). Thiobius thriving on the host surface fixes inorganic carbon using sulphide and provides organic carbon to the host (Volland et al., 2018). In return, benefits to the symbiont come through the host's peculiar contraction and expansion behaviour that ensures the supply of oxygen and sulphide (Rinke et al., 2007). The ciliate colonies can show

unspecific overgrowth on the stalk, which connects them to the substrate surface (Bauer-Nebelsick et al., 1996a).

Strain Milos ODIII6 (short ODIII6) is a cultured, but not yet formally described bacterium, that has been isolated from the shallow-water hydrothermal vents in Paliochori Bay (Milos, Greece; Kuever et al., 2002; Sievert, 1999). ODIII6 is mesophilic (optimal growth at 34°C) and oxidizes reduced sulphur compounds under aerobic conditions.

Evolutionary theory predicts that the genome of obligate microbial symbionts, transmitted vertically from one to the next host generation, will be reduced in size compared to free-living relatives and will contain a lower proportion of mobile elements than facultative symbionts (Newton & Bordenstein, 2011; Sachs et al., 2011). Being obligately host-associated, these bacteria experience bottlenecks in population size during each transmission event leading to genome reduction (Bobay & Ochman, 2017; McCutcheon & Moran, 2012; Moran, 1996; Moran et al., 2009; Toft et al., 2009; Toft & Andersson, 2010; Wernegreen, 2015). Trait function compensation by the host or other symbionts can lead to further gene loss and reduced genome size (Ellers et al., 2012). Since obligate symbiotic bacteria are often isolated in the host as endosymbionts, they experience limited possibilities for horizontal gene transfer and access to foreign DNA. Some even lack the machinery for uptake and incorporation of DNA (Medina & Sachs, 2010). In contrast, obligate ectosymbionts have access to novel gene pools (Newton & Bordenstein, 2011). Nevertheless, some thermophilic ectosymbiotic archaea undergo genome reduction. This so-called thermophilic streamlining was explained by having fewer and shorter genes in hot environments compared to archaea from other environments (Nicks & Rahn-Lee, 2017). Much less studied are vertically transmitted bacterial ectosymbionts located on the surface of eukaryotic hosts. Mostly, these ectosymbiotic microbiomes are composed of complex microbial communities. Only a few cases with a single microbial partner are known and even fewer genomic studies are available (Fokin & Serra, 2022; Husnik et al., 2021).

Here, we show that the ectosymbiont Thiobius has a smaller genome, fewer genes, reduced GC content, and a smaller mobilome than the free-living bacterium ODIII6, matching theoretical predictions. The analyses of metabolic capabilities revealed that the functional traits of Thiobius are largely a subset of the repertoire of ODIII6, which has a higher functional versatility to cope with broader environmental conditions as a free-living bacterium from a highly unstable, fluctuating hydrothermal vent environment. In contrast, Thiobius shows a potential genetic capability to grow heterotrophically as an adaptation to its host.

2 | MATERIALS AND METHODS

2.1 | Specimen collection and cultivation

Three *Zoothamnium niveum* colonies were collected from attached submerged mangrove roots and wood at 1 m depth in 2015 at Twin Cays (Belize, 6°50′3″ N, 88°6′14″ W; strains G42, G43 and G44), and one colony from a sunken wood at 70 cm depth in 2014

16S rRNA gene tree

FIGURE 1 Maximum likelihood (ML) tree based on the 16S rRNA gene. Bootstrap support of the internal nodes is indicated with the colour of the outgoing branches. Topology conflicts with two other techniques Maximum parsimony (MP, ⊕) and Bayesian inference (BI, ★) indicated with symbols in the affected internal nodes. The two microbes analysed in this study are highlighted in bold. The tree was generated with 306 sequences (Table S1), but only 40 organisms that have publicly released genomes are shown.

at Guadeloupe (16°16′38″ N, 61°33′27″ W; strain G4). The ODIII6 isolate was originally obtained from the 10^{-6} dilution of a sediment sample collected at a sediment depth of 8–13 mm and at 2 m distance from the centre of a gaseous hydrothermal vent at a water depth of 8 m in Paliochori Bay (Milos Island, Greece, 36°40′23″ N, 24°31′13″ E) (Kuever et al., 2002; Sievert, 1999; Sievert et al., 1999). A culture frozen at −80°C in dimethylsulphoxide was reactivated in 2015 and used to obtain DNA for genome sequencing.

2.2 | DNA preparation and sequencing

The lower parts of *Zoothamnium niveum* colonies are usually overgrown with diverse microbes (Bauer-Nebelsick et al., 1996a; Rinke et al., 2006), and were therefore cut off to minimize contamination using Schreiber micro scissors (Fridingen, Germany, European Union). The upper parts, covered by a monolayer of Thiobius, were homogenized with Tris-EDTA buffer by vortexing and DNA was extracted according to Zhou et al. (1996). The DNA extraction yielded up to 7 ng DNA per μL in ~30 μL of final volume for G43. Nextera XT (Illumina)

DNA library preparation was used for multiplexing the *Zoothamnium* samples, and they were sequenced in a paired-end mode with 125 nucleotides of read length using the Illumina HiSeqV4 platform at the Vienna Biocenter Core Facility (https://www.viennabiocenter.org/vbcf/). The low amount of DNA yielded by a single *Zoothamnium* ciliate colony precluded the use of long-read sequencing technologies. The ODIII6 isolate was regrown from a frozen stock culture in 2015 and DNA was extracted with an UltraClean® microbial DNA isolation kit (MoBio laboratories). The DNA was sequenced with a MiSeq (Illumina) sequencer by a commercial provider, MR DNA (Shallowater, TX, https://www.mrdnalab.com/), using the 600 Cycles v3 Reagent Kit (Illumina). At MR DNA, the library of the sample was prepared with a Nextera DNA Sample Preparation Kit (Illumina).

2.3 | Quality refinement, de novo assembly and binning

The sequenced reads of the four *Zoothamnium* samples were quality filtered with the *bbduk* command of the suite *bbmap* v35.92

(BBMap–Bushnell B.–sourceforge.net/projects/bbmap/) under a more stringent quality threshold of 25 (Phred units). The filtered paired-end reads were assembled with *SPAdes* v3.7.1 in the metagenomic mode (Nurk et al., 2016). *MetaBAT* v0.26.3 (Kang et al., 2015) was then used for binning with default parameters. A nucleotide sequence homology *BLAST* search (Altschul et al., 1990) of the published 16S rRNA gene sequence of Thiobius (Rinke et al., 2006) identified the targeted bin. The genome of ODIII6 was de novo assembled by MR DNA using *NGEN* (DNAstar, https://www.dnastar.com). Completeness, heterogeneity and contamination of the ODIII6 and Thiobius assemblies were assessed with *CheckM* v1.0.5 (Parks et al., 2015). Presence of rRNAs and tRNAs for each amino acid was checked with *tRNAscan-SE* (Lowe & Eddy, 1997). Average amino acid identity (AAI; Konstantinidis & Tiedje, 2005) was calculated with *CompareM* (https://github.com/dparks1134/CompareM). The assembly of ODIII6 with *SPAdes* was performed to exclude contamination, using the same set of reads as the MR DNA assembly. The alignment between both assemblies was generated and visualized with *Mauve* (Darling et al., 2010, version snapshot_2015-02-25), establishing the correspondence between the contigs. The fastg file containing paired-end linkage information of the de Bruijn graph was visually inspected with *Bandage* v0.8.0 (Wick et al., 2015), allowing the assessment of physical connectivity between contigs of the bacterial chromosome.

2.4 | Synteny analysis and localized gap filling

The four Thiobius draft genome assemblies were aligned with *Mauve* (Darling et al., 2010) and the ordering of the contigs was partly reconciled. A less stringent quality threshold of 20 (Phred units) was applied for the quality filtering and trimming of the G43 reads with *bbduk* resulting in the recovery of the full 16S rRNA gene.

2.5 | Phylogenetic analyses

A total of 306 16S rRNA gene sequences were chosen following the taxa selection of Petersen et al. (2016) and Distel et al. (2017). 16S rRNA gene sequences were directly obtained from GenBank and RefSeq when available or extracted from publicly available genomes using *Metaxa* v2.2 (Bengtsson-Palme et al., 2015). The alignment was done with *MAFFT* v7 (Katoh & Standley, 2013) and *TrimAl* v1.2 (Capella-Gutierrez et al., 2009) was employed for trimming and filtering the alignments with default parameters. The obtained sequences were allocated to 292 putative species according to a 98.65% identity threshold (Kim et al., 2014; Table S1). Four species were excluded due to multiple divergent 16S rRNA gene copies (*Hydrogenovibrio halophilus*, *Lamprocystis purpurea*, *Thiofilum flexile* and *Thiothrix lacustris*). Phylogenetic analyses were performed using three methodological frameworks in order to assess the robustness of the tree inference: maximum parsimony (MP; Farris, 1970), maximum likelihood (ML; Felsenstein, 1981) and Bayesian inference (BI; Hastings, 1970). Packages *ape* v5.2 (Paradis

et al., 2004) and *phangorn* v2.4.0 (Schliep, 2011) were used for MP and ML, and BI was computed with *MrBayes* v3.2.7a (Huelsenbeck & Ronquist, 2001). The substitution model choice followed a Bayesian information criterion (Schwarz, 1978) as implemented in *phangorn*. Bootstrap support (Felsenstein, 1985) in ML and MP trees was calculated with 100 trees in each, and in BI posterior probability was used as metric of support. To facilitate visualization, 16S rRNA gene trees were reduced by pruning most of the branches (Rodriguez-Puente & Lazo-Cortes, 2013) retaining only the 40 organisms with genomes available. By comparing the tree topologies, shared internal nodes and conflicting topologies were manually identified. We used ML tree as the base of the representation to show the support of the three approaches.

2.6 | Functional inference of predicted genes and metabolic pathways

To predict and annotate genes the web version of *RASTtk* (https://rast.nmpdr.org, Brettin et al., 2015) was employed with default settings. Functional categories were assigned to the predicted genes by the use of *eggNOG mapper* version 2 (Huerta-Cepas et al., 2017, 2019). Metabolic pathways were obtained using the predicted and annotated genes as an input by two independent methods, followed by a manual curation: (a) the online KEGG tool (www.kegg.jp, Kanehisa & Goto, 2000, Moriya et al., 2007) interrogating pathway complete modules; and (b) the *PathoLogic* module from *Pathway Tools* (v23.5, Karp et al., 2002, 2010) of *MetaCyc* (Caspi et al., 2008). To these two levels of granularity (the fine grain of the genes and the coarser grain of the metabolic pathways; Vogt, 2010) we added the overarching level of functional traits (De Oliveira et al., 2022), defined as microbial characteristics that can be observed and are linked to fitness (Green et al., 2008). Additionally, secretion, motility and defence potential capabilities encoded in the genomes were assessed with *MacSyFinder* (Abby et al., 2016). The potential presence of traits was determined by putting together constituent genes following *MetaCyc* and *KEGG* when available, or *MacSyFinder* for motility and interaction traits (Abby et al., 2016). Some traits were not detected by *MetaCyc* and *KEGG*, and therefore, were manually inferred based on scientific literature (Table S2). In the manual curation logical operators (AND, OR) were employed to combine the gene presence/absence evidence into traits, as outlined in Karaoz and Brodie (2022) (Table S2).

2.7 | Orthology analysis

A total of 30 bacterial genomes, closest to Thiobius and ODIII6 based on the 16S rRNA gene tree phylogeny (Table S3), were selected excluding the genome of *Bathymodiolus* sp. SMAR symbiont due to poor quality of the assembly (52 scaffolds comprising 339 contigs with N_{50} as low as 10,280 nt). Protein sequences were clustered into orthologous groups using *OrthoFinder* v2.5.4 (Emms & Kelly, 2019).

3 | RESULTS AND DISCUSSION

3.1 | Close phylogenetic relationship of Thiobius and ODIII6

In order to confirm the previously reported close phylogenetic placement of Thiobius and ODIII6 (Distel et al., 2017; Lenk et al., 2011; Nunoura et al., 2014; Rinke et al., 2006, 2009; Schuster & Bright, 2016), 16S rRNA gene ML, MP and BI phylogenies were constructed. A pruned visualization of the resulting ML tree with indication of the conflicts between the three approaches is shown in Figure 1 (full ML tree in Figure S1). While some of the shallower internal nodes (closer to the tips) showed good support (e.g. bootstrap values greater than 70%) and agreement between the three phylogenetic approaches, many of the deeper internal nodes were poorly supported and showed topology conflicts. While ODIII6 falls in a clade containing the endosymbionts of the hydrothermal vent snails *Chrysomallon squamiferum* and *Alviniconcha* sp. Lau Basin, and free-living bacteria, Thiobius can be assigned as sister taxon of this clade. The internal node connecting these clades obtained bootstrap supports of 70% (ML) and 63% (MP), while the posterior probability support of BI was 73%. The 16S rRNA gene sequences of Thiobius and ODIII6 were 95% identical (over 1396 aligned nucleotide positions). A relatively low average amino acid identity (AAI) of 67% was obtained for the whole genomes of Thiobius and ODIII6. Both 16S rRNA gene and AAI comparisons show that these two bacteria are related but ODIII6 is more closely related to both gastropod symbionts than to Thiobius (Distel et al., 2017, Lenk et al., 2011, Nunoura et al., 2014, Rinke et al., 2006, 2009, Schuster & Bright, 2016).

3.2 | High-quality draft genomes of Thiobius and ODIII6

The best Thiobius metagenome assembled genome (MAG) in terms of assembly completeness and contiguity was obtained from a single ciliate colony collected in Belize (labelled G43, Figure S2; Tables 1 and S4). A total of 8.8 million of the initial 13.5 million read pairs passed a more stringent quality threshold filtering (phred 25). *SPAdes* assembled these reads into 44,538 contigs. *MetaBAT* binning grouped these contigs into four bins, one of them containing two partial matches at contig ends to the published 16S rRNA gene of Thiobius according to a BLAST search (Rinke et al., 2006; Figure S3). A less stringent quality threshold filtering (phred 20) led to a very similar *SPAdes* assembly that recovered the full 16S rRNA gene. The corresponding long contig containing the full 16S rRNA gene was used to replace three contigs from the stringent filtering assembly that covered the same span (Figure S4, Table S5). Overall, Thiobius G43 assembly resulted in 46 contigs with a total length of 2.38 Mb, a N_{50} value of 98,217, a coverage of 216× and a GC content of 49.4% (Figure 2). *CheckM* estimated its completeness as 96.0% and its contamination as 0.1%, and found no heterogeneity (Table 1), meeting the MIMAG standard for high-quality MAGs (Bowers et al., 2017). Synteny analysis with *Mauve* between the four Thiobius MAGs led to the identification of 26 clusters of contiguity that were utilized in the final ordering of the contigs (Figures 2 and S2, Table S5).

ODIII6's genome MR DNA assembly consisted of 26 contigs, and had no paired-end linkage associated information available (fastg file). Because *RASTtk* annotation revealed one contig with only phage related genes, we re-assembled the genome using *SPAdes* and found through the paired-end linkage information that the corresponding contig was circular and was thereby excluded (Figure S5). Accordingly, the final ODIII6 assembly resulted in 25 contigs, with a total of 3.53 Mb, a N_{50} value of 245,984, a coverage of 103×, and a GC content of 61.9%. *CheckM* estimated its completeness as 99.6% and its contamination as 0.8%, and found no heterogeneity either (Table 1).

A comparison between the high-quality draft genomes of Thiobius and ODIII6 (both appropriate for general assessment of gene content, Chain et al., 2009), revealed a complete set of tRNAs for translation of all 20 amino acids in both bacteria. In agreement with theoretical

TABLE 1 Statistics of the genomes assembled in this study.

|	Thiobius str. BelizeG43	Thiobius str. BelizeG42	Thiobius str. BelizeG44	Thiobius str. GuadeloupeG4	ODIII6
Sequencing coverage	216×	296×	176×	131×	103×
Assembly size (bp)	2,381,364	2,379,254	2,311,386	2,369,374	3,528,654
GC content	49.4%	49.4%	49.6%	49.6%	61.9%
Number of contigs	46	47	57	46	25
N50 (bp)	98,217	98,217	66,776	73,149	245,984
Completeness	96.0%	96.0%	94.4%	96.0%	99.6%
Contamination	0.1%	0.1%	0.1%	0.4%	0.8%
Heterogeneity	0.0%	0.0%	0.0%	0.0%	0.0%
16S recovered	Yes	Partially	Partially	Yes	Yes
Number of extracted tRNAs	36	34	34	37	41
Amino acids with tRNA	20	19	19	20	20
Missing tRNA amino acid	–	Ile	Ile	–	–
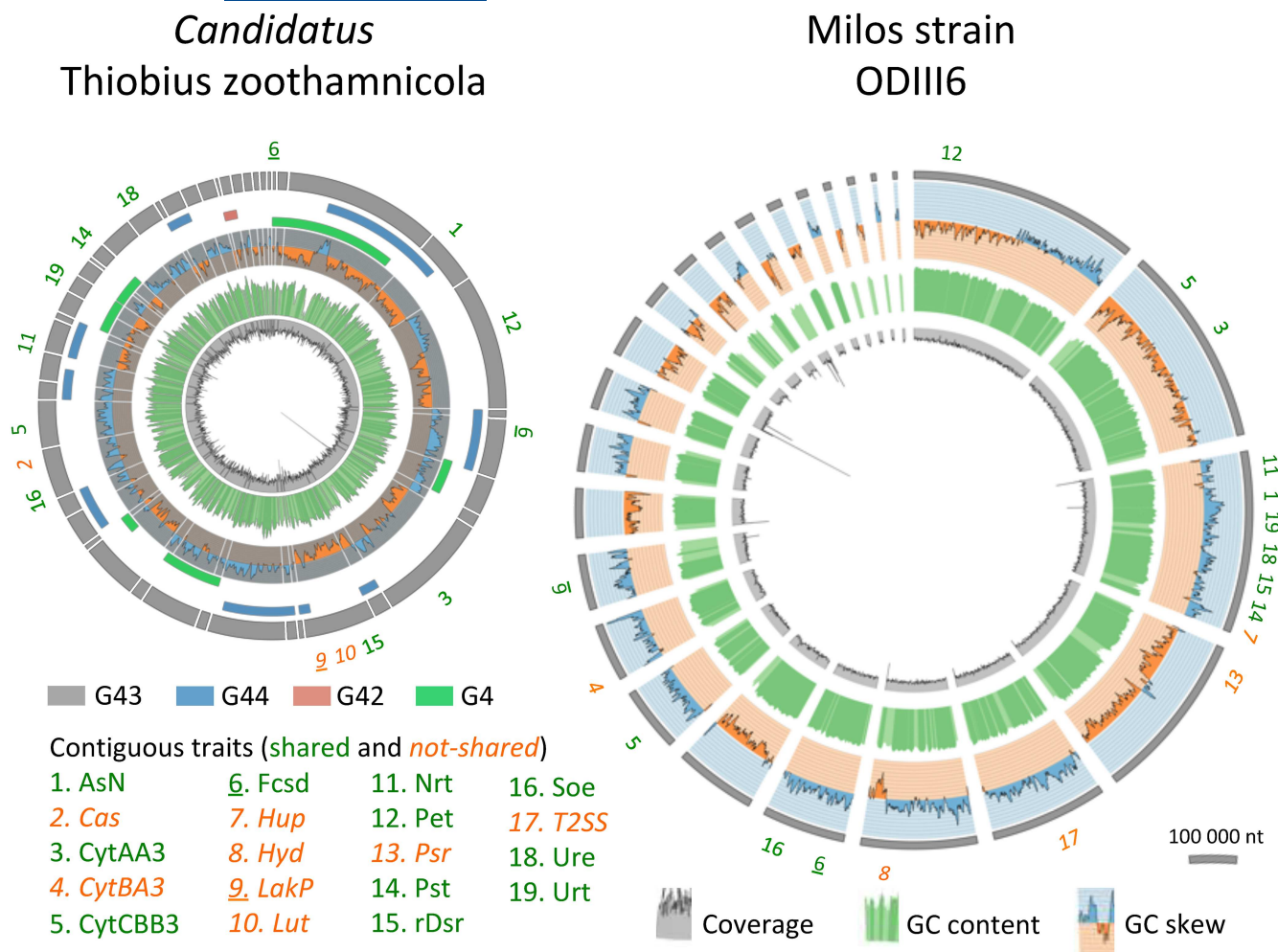
FIGURE 2 Representation of the draft genomes of Thiobius strain G43 (left) and ODIII6 (right). The most outer grey solid arcs represent the contigs. ODIII6 contigs are ordered by decreasing length. In Thiobius, information of three additional MAGs was employed to retrieve putative clusters of contiguity that are presented in decreasing length order. The bridging contigs are shown as solid arcs in colours, the rest of their contigs are omitted. GC skew typically reflects the attribution of the contig to the leading or to the lagging DNA strand. The correct ordering of the contigs has not been fully resolved, and this is reflected in the inconsistent GC skew pattern between neighbouring contigs. GC content and coverage are shown in the most inside rings. The location of relevant traits that show contiguity of their constitutive genes is also shown.

predictions (Sachs et al., 2011), the genome of the vertically transmitted ectosymbiont Thiobius was 33% smaller than the one of the free-living bacterium ODIII6, and showed a reduced relative GC content, consistent with the significant positive correlation between GC content and genome size in bacterial genomes (Almpanis et al., 2018). Whether the reduced genome size of the vertically transmitted ectosymbiont is due to any of the mechanisms that are known to affect vertically transmitted endosymbionts, such as those of thiotrophic vesicomyid clams (Kuwahara et al., 2007; Newton et al., 2007) and of marine flatworms *Paracatenula* (Jäckle et al., 2019), remains to be studied.

3.3 | Thiobius encodes fewer genes, pathways and functional traits compared to ODIII6

To characterize the potential functional capabilities of Thiobius and ODIII6, their gene complements were predicted with *RASTtk* (Brettin

et al., 2015). The annotation of Thiobius yielded 2486 predicted protein-coding sequences, of which 1494 (60%) received a meaningful automatic functional prediction. In the manual curation process 21 hypothetical genes (18 non-redundant) obtained a putative annotation. ODIII6 had 3452 predicted protein-coding sequences including 2063 (60%) with meaningful functional predictions, and in the manual curation 21 hypothetical genes (19 non-redundant) were functionally annotated. Thiobius contains about 28% less protein-coding sequences than ODIII6. Accordingly, the lower number of protein-coding sequences in Thiobius compared to ODIII6 is consistent with their genome sizes.

We manually selected 46 relevant functional traits involved in key metabolism and additional functions like storage or interactions, of these two SOBs. These traits can range from a single gene to the combination of several metabolic pathways (Tables 2 and S2). Less than half of the traits (19) showed a compact localization of their constitutive genes within contigs (Figure 2). *PathwayTools* inferred

203 *MetaCyc* metabolic pathways for Thiobius, while 39 complete *KEGG* modules were identified. The annotation of ODIII6 resulted in 233 *MetaCyc* pathways and 53 complete *KEGG* modules. Thiobius obtained 31 traits and ODIII6 yielded 39, of which 24 traits were shared (Table S6). Accordingly, Thiobius showed less pathways and relevant traits compared to ODIII6, particularly in those related with oxygen, phosphorus and sulphur.

In order to assess the functional commonalities between Thiobius and ODIII6 we performed an orthology analysis over a background set of 28 additional genomes of species included in the phylogenetic analysis (Table S3). Thiobius and ODIII6 shared 1409 orthogroups (Figure 3). A higher proportion of functional pathways were shared between the two organisms (Figure 3). Most of the genes of both organisms presented an orthologous one-to-one relationship (84% of genes in Thiobius and 90% of genes in ODIII6; Table S7). Overall, the relatively high percentage of shared orthogroups, pathways, modules and traits in Thiobius indicates that its functional capabilities are mainly a subset of those present in ODIII6 (Figure S6).

To further investigate the distribution of functional categories, *eggNOG* was applied to determine the attribution of COG categories (Tatusov et al., 2000). In general, the gene counts of the COG categories followed the genome sizes (Table S8), but there were some exceptions. ODIII6 and Thiobius COG categories yielded high count similarities in the categories 'lipid metabolism' and 'secondary structure'. Nevertheless, this did not imply a fully identical sets of genes, for example, of the orthogroups involved in the 'lipid metabolism' category only a 52% were shared, indicating that different 'non-orthologous' gene sets were recruited to perform same biological tasks in the two different bacteria. The least similar categories were 'cell motility' and 'signal transduction', for which the respective proportions were much lower in Thiobius in relation to its genome size (Table S8). Therefore, the COG functional categories composition reflects the free-living lifestyle of ODIII6, with increased motility representation and a more complex gene regulation that match the requirements of a free-living lifestyle.

3.4 | Potential for a mixotrophic lifestyle as an adaptation to the ciliate host

Both Thiobius and ODIII6 show the genomic potential to fix inorganic carbon through the Calvin-Benson-Bassham cycle (Cbb) with the capability to form carboxysomes to concentrate ribulose-1,5-bisphosphate carboxylase oxygenase (RuBisCO; Badger & Bek, 2008), the key enzyme of the Calvin–Benson cycle responsible for CO_2-assimilation. According to the neighbouring genes the RuBisCO type in both Thiobius and ODIII6 is form IAc with a potential functional niche of low CO_2 and low to high oxygen concentration (Badger & Bek, 2008). This is in line with previous studies in Thiobius, in which RuBisCO was histochemically detected, carboxysomes were identified by TEM (Bauer-Nebelsick et al., 1996b) and a type IA RuBisCO large subunit sequence was retrieved (Rinke et al., 2009). In addition, carbon fixation in Thiobius was confirmed through tissue

autoradiography and NanoSIMS (Volland et al., 2018). Further, the contraction and expansion behaviour of the host creates a continuously changing abiotic environment for Thiobius ranging from oxygen rich to sulphidic, anoxic conditions (Bright et al., 2014). ODIII6 shows two putative bicarbonate transporter-encoding genes downstream of the carboxysome structural genes operon, consistent with previous reports on other chemoautotrophs (Axen et al., 2014; Scott et al., 2020). ODIII6 further possesses a gene for a beta class carbonic anhydrase not integrated in the carboxysome operon but elsewhere in the genome, which converts bicarbonate to CO_2 for carbon fixation (Supuran & Capasso, 2017).

Organic carbon is stored differently in Thiobius compared to ODIII6. While Thiobius has the genetic potential for using polyhydroxyalkanoates (Pha), genes for glycogen (Glg) and cyanophycin synthesis (Cph; storing carbon and nitrogen) were found in ODIII6. In both organisms, the organic carbon is oxidized through the TCA cycle (TcaC), although. Thiobius encodes additionally genes for the glyoxylate cycle pathway (GlC; Cozzone & El-Mansi, 2005). Putative genes encoding for transporters to import acetate (ActP) and lactate (LakP) along with genes encoding for all three components of L-lactate dehydrogenase for lactate utilization (Lut) were also present. Both acetate and lactate could potentially be metabolized by the glyoxylate cycle (El-Mansi et al., 1986; Serafini et al., 2019). While in many organisms (including *Bacillus subtilis*) *lutABC* belongs to the same operon with a lactate permease (Chai et al., 2009), Thiobius possesses a different DctP–TRAP-like transporter (LakP), similar to the one described for *Thermus thermophilus* (Fischer et al., 2010). The presence of these transporters indicates a potential for heterotrophic metabolism in Thiobius. As the ciliate host may potentially be able to switch to an anaerobic metabolism under sulphidic conditions and produce lactate and acetate, similarly to the rumen ciliate *Entodinium caudatum* (Park et al., 2021), it is tempting to speculate that these fermentation products may then be released from the host and taken up by the symbiont, but these anaerobic processes have yet to be studied in this mutualism. No equivalent capabilities were found in the genome of ODIII6 in line with its obligate autotrophic metabolism.

3.5 | Oxygen is the only electron acceptor in both bacteria, but ODIII6 is more versatile than Thiobius

According to the genomic potential of their draft genomes, oxygen is the only electron acceptor that Thiobius and ODIII6 can utilize. Genes for nitrate respiration, known in many free-living and symbiotic thiotrophic bacteria living at oxic–anoxic interfaces (De Oliveira et al., 2022; Flood et al., 2015; König et al., 2016; Nunoura et al., 2014; Paredes et al., 2021), were not found. This indicates that both bacteria strongly rely on oxygen both for respiration and for the oxidation of reduced sulphur species to generate energy. Indeed, both genomes encode for a cytochrome bc_1 electron transport complex (Pet), and two cytochrome terminal oxidases, that is, cbb_3 (CytCBB3), which was shown to have a high affinity for oxygen

WILEY MOLECULAR ECOLOGY RESOURCES

TABLE 2 Selection of relevant functional traits.

Id	TraitGroup	TraitName	ShortTraitName	GeneTraitComposition	Thiobius	ODIII6
1	Carbon	Acetate transporter	ActP	+actP	Present	Absent
2	Carbon	Calvin-Benson-Bassham cycle	Cbb	+((+cbbS+cbbL),cbbL_formII)+pgk+gapA+tpiA+fbaA+fbp+tkt+rpe+prk+sir+rplA+PPi_PFK	Present	Present
3	Carbon	Glycogen biosynthesis	Glg	+glgC+glgA	Absent	Present
4	Carbon	Glyoxylate cycle	GlC	+mdh+CS+(acnA,acnB)+icl+aceB	Present	Absent
5	Carbon	Lactate transporter	LakP	+lakP+dctQ+dctM	Present	Absent
6	Carbon	Lactate utilization	Lut	+lutA+lutB+lutC	Present	Absent
7	Carbon	Polyhydroxyalkanoate synthesis	Pha	+pha	Present	Absent
8	Carbon	TCA cycle	TcaC	+CS+(acnA,acnB)+icd+((+sucA+sucB+lpd),(+korA+korB))+sucD+sucC+sdhA+sdhB+sdhC+sdhD+(fumA,fumC)+(mdh,mqo)	Present	Present
9	Carbon (and Nitrogen)	Cyanophycin synthesis	Cph	+cph	Absent	Present
10	Hydrogen	NiFe hydrogenase-based hydrogen oxidation	Hup	+hupS+hupL	Absent	Present
11	Nitrogen	Ammonium transporter	AmtB	+amtB	Present	Present
12	Nitrogen	Assimilatory nitrate reduction	AsN	+narB+nirB+nirD	Present	Present
13	Nitrogen	Incomplete urea cycle	iUcy	+carA+carB+argF+argG+argH	Present	Present
14	Nitrogen	Nitrate transporter	Nrt	+nrtA+nrtB+nrtC	Present	Present
15	Nitrogen	Urea transporter	Urt	+urtA+urtB+urtC+urtD+urtE	Present	Present
16	Nitrogen	Urease mediated urea degradation	Ure	+ureA+ureB+ureC	Present	Present
17	Oxygen	Cytochrome aa3 based oxygen respiration	CytAA3	+coxA+coxB+coxC	Present	Present
18	Oxygen	Cytochrome ba3 based oxygen respiration	CytBA3	+cbaA+cbaB	Absent	Present
19	Oxygen	Cytochrome bc1 complex mediated electron transport	Pet	+petA+petB+petC	Present	Present
20	Oxygen	Cytochrome bd based oxygen respiration	CytBD	+ndhA_to_ndhN+shdA+sdhB+sdhC+cydA+cydB	Absent	Present
21	Oxygen	Cytochrome cbb3 based oxygen respiration	CytCBB3	+ccoN+ccoO+ccoP+ccoQ	Present	Present
22	Phosphorous	High-affinity Na+/Pi symporter	Hnp	+hnp	Absent	Present
23	Phosphorous	High-affinity phosphate transporter	Pst	+pstA+pstB+pstC+pstS	Present	Present
24	Phosphorous	Low-affinity phosphate transporter	Pit	+pit	Absent	Present
25	Phosphorous	Polyphosphate usage	PHK and PHX	PHK, PHX	Present	Present
26	Sulphur	APR and SAT mediated sulphite oxidation	AprSat	+sat+aprB+aprA-aprM	Present	Present
27	Sulphur	Reverse dissimilatory sulphate reductase mediated thiosulphate oxidation to sulphite	rDsr	+dsrA+dsrB+dsrC+dsrE+dsrF+dsrK+dsrH+tusA+rhd	Present	Present

TABLE 2 (Continued)

Id	TraitGroup	TraitName	ShortTraitName	GeneTraitComposition	Thiobius	ODIII6
28	Sulphur	Rhodanese mediated thiosulphate disproportionation	Tst	+tst	Absent	Present
29	Sulphur	Sulphate permease	SulP	+sulP	Absent	Present
30	Sulphur	Sulphate transporter	CysZ	+cysZ	Present	Present
31	Sulphur	Sulphydrogenase mediated sulphur reduction	Hyd	+hydA+hydB+hydC+hydD	Absent	Present
32	Sulphur	Polysulphide reductase	Psr	+psrA+psrB+psrC	Absent	Present
33	Sulphur	Sulphide dehydrogenase (flavocytochrome C) mediated sulphur oxidation	Fcsd	+fccA+fccB	Present	Present
34	Sulphur	Sulphide:quinone oxidoreductase mediated sulphur oxidation	Sqr	+sqr	Present	Present
35	Sulphur	Sulphite-oxidizing enzyme mediated sulphite oxidation	Soe	+soeA+soeB+soeC	Present	Present
36	Sulphur	Sulphur globules proteins	Sgp	sgpCV1,sgpCV2,sgpA,sgpB,sgpC,sgpD	Present	Present
37	Sulphur	Sulphur oxygenase reductase mediated sulphur disproportionation	Sor	+sor	Absent	Present
38	Sulphur	Thiosulphate transporter	YeeE	+yeeE	Absent	Present
39	Sulphur	Truncated SOX mediated sulphur oxidation from thiosulphate to sulphate	tSox	+soxA+soxB+soxX+soxL	Present	Present
40	Interactions	CRISPR associated proteins	Cas	+cas1+cas2+((cas3,cas7),cas9,cas10)-cas4-cas5-cas6-cas8-cse1-cse2-csb1-csb2-cmr4-cmr5-cmr6-csy1-csy2-csy3	Present	Absent
41	Interactions	Type I secretion system	T1SS	+lapB+lapC+tolC	Absent	Present
42	Interactions	Type II secretion system	T2SS	-gspC+gspD+gspE+gspF+gspG-gspH+gspI+gspJ+gspK-gspL+gspM-gspN	Present	Present
43	Interactions	Type V secretion system	T5SS	apeE,fhaC,yadA	Present	Present
44	Interactions	Type VI secretion system	T6SS	-evpJ+tssA+tssB+tssC+tssD+tssE+tssF+tssG+tssH+tssI+tssJ+tssK+tssL+tssM	Present	Absent
45	Motility	Flagellum	Fla	+filF+filI+filN+filP+filQ+filR+flhB+flhA+flgB+flgC+filE	Absent	Present
46	Motility	Type IV pilus	T4P	+pilE+pilV+pilB+pilC+pilO+pilQ+pilM+pilN+pilP+pilT-pilD	Present	Present

98

Note: '+' indicates that the following gene is required, '-' indicates that the following gene is not required, ',' indicates interchangeability; brackets are used for grouping; 'ndhA_to_ndhN' stands for 14 genes.
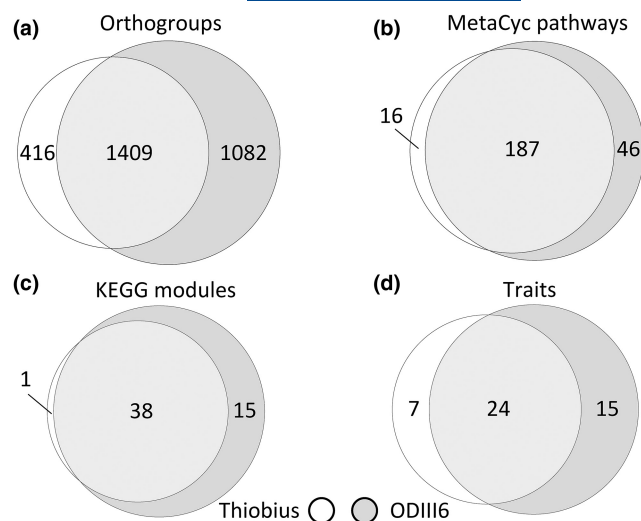
(a) Orthogroups
416 | 1409 | 1082

(b) MetaCyc pathways
16 | 187 | 46

(c) KEGG modules
1 | 38 | 15

(d) Traits
7 | 24 | 15

Thiobius ◯ ◯ ODIII6

FIGURE 3 Euler diagrams of different levels of granularity showing shared and unique genetic potential capabilities of Thiobius and ODIII6. The finer granularity level is the genes from the orthogroups (a). Two metabolic pathway databases were employed: MetaCyc (b), and KEGG modules (c). The coarser granularity level are the traits (d).

in *Bradyrhizobium japonicum* (Pitcher & Watmough, 2004), and aa$_3$ (CytAA3), which belongs to the Class A of oxidases with lower apparent oxygen affinities (Han et al., 2011). This indicates the ability to utilize oxygen at various concentrations. Interestingly, the genome of ODIII6 contains two copies of the genes encoding cbb$_3$, which is unusual and could be an additional adaptation to optimize oxygen utilization under varying concentrations, as was shown for *Pseudomonas aeruginosa* (Comolli & Donohue, 2004). Further, ODIII6 possesses two more high-affinity terminal oxidases, cytochrome bd (CytBD)- and ba$_3$ (CytBA3)-encoding genes, which points to a higher versatility under a broader range of oxygen regimes than Thiobius. In contrast, Thiobius lives on a ciliate host that can position itself

in microhabitats with optimal oxygen concentrations, which potentially renders the ability to express multiple terminal oxidases unnecessary.

3.6 | Both organisms use the oxidation of reduced sulphur compounds to generate energy

The energy fuelling processes for carbon fixation in Thiobius and ODIII6 comes from the oxidation of reduced sulphur species using oxygen as terminal electron acceptor. Sulphide oxidation to elemental sulphur occurs in both bacteria through two possible pathways, sulphide dehydrogenase (Fcsd; flavocytochrome C, Sorokin et al., 1998), and sulphide:quinone oxidoreductase (Sqr). ODIII6 has a type VI Sqr and Thiobius has type I and type VI Sqr (Dahl, 2017). The elemental sulphur formed by sulphide oxidation is stored in sulphur globules that are enveloped by proteins (Dahl, 2017) identified in both genomes (Sgp). Indeed, transmission electron micrographs (Bauer-Nebelsick et al., 1996b) and Raman microspectrometry previously revealed membrane bound elemental sulphur vesicles in Thiobius (Maurin et al., 2010) used to store sulphur under sulphidic conditions and oxidize it further during oxic conditions (Volland et al., 2018). In ODIII6 cultures, the formation of sulphur globules attached to the cell could also be observed if thiosulphate was provided (Stefan Sievert personal observation, 2022).

Thiosulphate is potentially oxidized in both organisms to sulphate and elemental sulphur through the truncated Sox pathway (tSox, Welte et al., 2009, Dahl, 2020), with the possible involvement of *SoxL* (Weissgerber et al., 2011). For both organisms, elemental sulphur is oxidized to sulphite in the cytoplasm by the reverse dissimilatory sulphate reductase pathway (rDsr; Dahl, 2015, Gregersen et al., 2011, Hensen et al., 2006), and sulphite is oxidized to sulphate either by the adenylylsulphate reductase and the sulphate adenylyltransferase (AprSat), or by the sulphite-oxidizing enzyme (Soe;

FIGURE 4 Major metabolic capabilities found in the draft genomes of (a) *Candidatus* Thiobius zoothamnicola strain BelizeG43, and (b) strain Milos ODIII6. Chosen relevant potential functional capabilities are shown (for simplicity not all transporters are depicted in the figure). Predicted and functionally annotated genes are grouped in metabolic pathways. Functional traits are features such as single metabolic pathways or composites of them that affect the organism fitness. Structural features such as transporters or secretion systems, and storage capabilities are also considered as traits. Trait labels are generally in white fonts and in vertical orientation, except for the motility and interactions on the left. Compound labels are horizontally oriented. Storage compartments are indicated with ellipses. ActP, acetate transporter; AmtB, ammonium transporter; AprSat, sulphate adenylyltransferase and adenylylsulphate reductase sulphite oxidation; AsN, assimilatory nitrate reduction; Cbb, Calvin-Benson-Basham cycle; Cph, cyanophycin biosynthesis; CysZ, sulphate transporter; CytAA3, cytochrome aa$_3$ based oxygen respiration; CytBA3, cytochrome ba$_3$ based oxygen respiration; CytBD, cytochrome bd based oxygen respiration; CytCBB3, cytochrome cbb$_3$ based oxygen respiration; Fcsd, flavocytochrome c sulphide dehydrogenase sulphide oxidation; GlC, glyoxylate cycle; Glg, glycogen biosynthesis; Hnp, high-affinity sodium-phosphate symporter; Hup, putative hydrogen oxidation; Hyd, sulphydrogenase elemental sulphur oxidation; iUcy, incomplete urea cycle lacking last step arginase gene; LakP, lactate transporter; Lut, lactate utilization; Nrt, nitrate transporter; Pet, cytochrome bc$_1$ complex mediated electron transport chain; Pha; polyhydroxyalkanoate synthesis; PHK, polyphosphate kinase; PHX, exopolyphosphatase; Pit, low-affinity phosphate transporter; Psr, polysulphide reductase; Pst, high-affinity phosphate transporter; rDsr, reverse dissimilatory sulphate reductase mediated sulphur oxidation; Sgp, sulphur globule proteins; Soe, sulphite-oxidation enzyme sulphite oxidation; Sor, Sulphur oxygenase reductase mediated sulphur oxidation; Sqr, sulphide:quinone oxydoreductase sulphide oxidation; SulP, sulphate permease; T1SS, type I secretion system; T2SS, type II secretion system; T5SS, type V secretion system; T6SS, type VI secretion system; T4P, type IV pilus; TcaC, TCA cycle; tSox, truncated Sox mediated sulphur oxidation; Tst, thiosulphate disproportionation; Ure, Urease mediated urea degradation; Urt, urea transporter; YeeE, thiosulphate transporter. The hexagon represents a carboxysome.
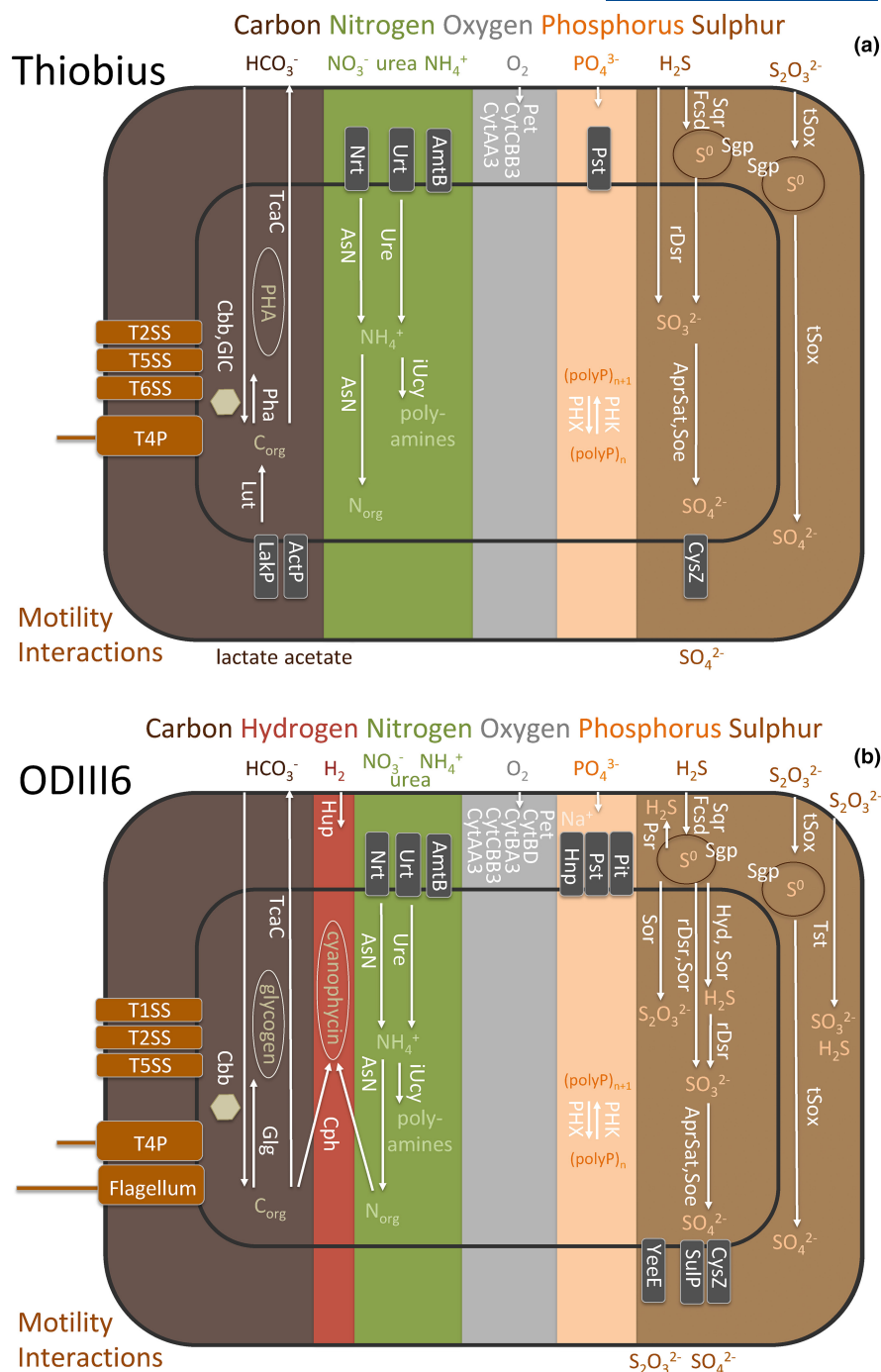
Dahl, 2017). Gene sequences for the alpha and beta subunits of the reverse-type dissimilatory sulphite reductase (*dsrAB*) and for the alpha subunit of the adenylylsulphate reductase (*aprA*) were previously reported in Thiobius (Rinke et al., 2009). Finally, the putative sulphate transporter CysZ exports the sulphate to the periplasm (Figure 4a; Hryniewicz et al., 1990).

In contrast to Thiobius, ODIII6 has additional sulphur-metabolizing capabilities: the periplasmic disproportionation of thiosulphate by a rhodanese-like sulphurtransferase to sulphide and sulphite (Tst; Deckert et al., 1998); elemental sulphur reduction to sulphide in the periplasm by a putative polysulphide reductase (Psr; De Oliveira et al., 2022), that might also be involved in oxidation as

suggested for *Allochromatium vinosum* (Weissgerber et al., 2013); cytoplasmic disproportionation of elemental sulphur to thiosulphate, sulphite and sulphide by the sulphur oxygenase reductase (Sor; Janosch et al., 2015), as suggested for *Thioalkalivibrio paradoxus* (Rühl et al., 2017); reduction of elemental sulphur to sulphide coupled to the oxidation of hydrogen by the sulphhydrogenase (Hyd; Ng et al., 2000); and sulphate exportation to the periplasm by the sulphate permease SulP (Figure 4b; Aguilar-Barajas et al., 2011). A thiosulphate transporter gene (YeeE; Tanaka et al., 2020) is also found in the genome of ODIII6.

Although many sulphur oxidation traits are shared, we observe a higher versatility in ODIII6 than in Thiobius. In addition, the presence

of [NiFe] hygrogenase Hup genes (Vignais et al., 2001) in ODIII6 may indicate the potential of hydrogen oxidation. However, it was recently found in *Candidatus* Endoriftia persephone that *hup* genes present in its genome were not involved in hydrogen oxidation but may instead facilitate intracellular redox homeostasis (Mitchell et al., 2019). The two subunits L and S in ODIII6 show 75% and 71% amino acid identity with their *Candidatus* Endoriftia persephone orthologues.

3.7 | Similarities in nitrogen and phosphorous metabolism

Both organisms show similar potential capabilities in nitrogen metabolism. Nitrate is imported into the cytoplasm through the nitrate transporter Nrt (Maeda et al., 2019), and is reduced to ammonium in the first step of assimilatory nitrate reduction, and from there assimilated as organic nitrogen in form of biomolecules (AsN; Takai, 2019). In addition, the ammonium can be imported into the cytoplasm by the ammonium transporter AmtB (Wang et al., 2012) further fuelling assimilation. Urea is acquired by the urea transporter Urt and oxidized to ammonium by the urease (Ure; Bossé et al., 2001). An incomplete urea cycle lacking arginase is also present (iUcy; De Oliveira et al., 2022). Overall, urea as well as ammonium are well-known nitrogen waste products of ciliates (Caron & Goldman, 1990), and may serve as byproducts the host provides to the symbiont. Urea was shown to be a source of incorporated nitrogen for bacteria in intertidal sediments (Veuger & Middelburg, 2007). Whether urea is utilized by ODIII6 in its natural environment remains to be studied.

Phosphorus is a limiting nutrient in many marine environments, present in its inorganic dissolved fraction generally as orthophosphate (Paytan & McLaughlin, 2007). Both organisms encode the genes for a high-affinity phosphate transporter (Pst), and additionally ODIII6 possesses genes for two other transporters: a high-affinity Na^+/P_i symporter (Hnp) and a low-affinity phosphate transporter (Pit). Once phosphate is incorporated into the cells, both organisms also show the potential for polymerizing it into polyphosphate and hydrolysing back to inorganic phosphates (PHKandPHX), using it as energy storage (Achbergerová & Nahálka, 2011).

3.8 | Interaction and motility in both organisms

Both Thiobius and ODIII6 have a repertoire of genes to interact with other organisms and with the environment. They share genes for the type II (T2SS) and type V (T5SS) secretion systems. Thiobius additionally has genes for the type VI secretion system (T6SS; Kapitein & Mogk, 2013) known to function in host interaction (Hachani et al., 2016) and CRISPR-Cas proteins (Cas), while ODIII6 has genes for the type I secretion system (T1SS). It remains to be studied how both bacteria use these traits in their natural environment and whether they may help Thiobius to interact with its host.

Both organisms further possess genes for type IV pilus potentially involved in twitching motility (T4P; Ayers et al., 2010), and

additionally ODIII6 genome contains several loci for the biosynthetic genes encoding for a flagellum (Fla). Indeed, ODIII6 was observed to be motile in cultures, however, loses its motility after a longer period of cultivation (Sievert pers. obs.). This suggests that the flagellum may no longer be expressed in ODIII6 if constant, favourable conditions render motility unnecessary. ODIII6 additionally shows genes for photolyase DNA protection against UV radiation, and repair (Sancar et al., 1987).

3.9 | Mobile genetic elements are less abundant in Thiobius than in ODIII6

Bacteria can experience horizontal gene transfer through mobile genetic elements such as phages, plasmids, transposons and insertion sequences, also referred to as the mobilome (Frost et al., 2005). Free-living bacteria like ODIII6 are more likely to be exposed to novel gene pools than symbionts (Newton & Bordenstein, 2011). In addition, vertically transmitted symbionts, such as Thiobius experience population bottlenecks as each swarmer is covered with relatively few symbionts that grow to cover the new colony (Bauer-Nebelsick et al., 1996a, 1996b). Accordingly, we hypothesized a smaller mobilome in the obligate symbiont Thiobius than in the free-living ODIII6. Indeed, *RASTtk* annotation of Thiobius revealed three genes attributed to phages and 18 genes attributed to other mobile genetic elements, while ODIII6 has two genes attributed to phages and 58 genes attributed to other mobile genetic elements (Table S9). Roughly 60% of these mobile elements were located at the extremes of the contigs, consistent with their disruptive effect on the assembly processes. These results point to a smaller mobilome in the host-associated Thiobius than in the free-living ODIII6.

4 | CONCLUSIONS

The phylogenetic relationship of the ectosymbiont Thiobius and the strain Milos ODIII6 is confirmed through 16S rRNA phylogeny and average amino acid identity and serves as baseline to compare the genomes of these two bacteria with very different lifestyles. In agreement with theoretical predictions, but hardly studied in ectosymbiotic bacteria, Thiobius' genome is smaller than that of its free-living relative ODIII6. The characterization at the levels of genes, metabolic pathways and traits reveals that Thiobius and ODIII6 share a large proportion of their genetic repertoire and metabolic capabilities. The lower number of lineage-specific metabolic pathways and relevant traits in Thiobius compared to ODIII6 may point to a more stable environment provided by the host, requiring less versatility. This may have led to a loss of genetic potential in Thiobius and/or gain in ODIII6. In comparison with Thiobius, ODIII6 shows a larger functional repertoire, in particular for its energy metabolism regarding the utilization of sulphur, oxygen and hydrogen, consistent with the requirements for a free-living bacterium to live under the fluctuating conditions of the hydrothermal vent environment. Thiobius, however, shows potential

for heterotrophic metabolism, which may be fuelled by byproducts from the host and thus might represent a remarkable adaptation to the life style of its protist host. In contrast to reduced genomes of vertically transmitted, thiotrophic endosymbionts like those of vesicomyid clams or catenulid plathylhelmints that experience no microbial competition and little potential for horizontal gene transfer inside host organs and cells, Thiobius, as an ectosymbiont, faces potential competitive interactions and viral attacks similar to free-living bacteria such as ODIII6, which is reflected in its capacity to interact with the environment. In the future, transcriptome evidence and other omics analyses in conjunction with physiological experiments can elaborate on the intricacy of these functional capabilities.

AUTHOR CONTRIBUTIONS

ACKNOWLEDGEMENTS

CONFLICT OF INTEREST STATEMENT

The authors declare no conflict of interest.

DATA AVAILABILITY STATEMENT

ORCID

Salvador Espada-Hinojosa https://orcid.org/0000-0001-9569-409X

Clarissa Karthäuser https://orcid.org/0000-0001-9239-1528

Abhishek Srivastava https://orcid.org/0000-0002-8459-471X

Teresa Winter https://orcid.org/0000-0002-3848-8342

André Luiz de Oliveira https://orcid.org/0000-0003-3542-4439

Frederik Schulz https://orcid.org/0000-0002-4932-4677

Matthias Horn https://orcid.org/0000-0002-8309-5855

Stefan Sievert https://orcid.org/0000-0002-9541-2707

Monika Bright https://orcid.org/0000-0001-7066-1363

REFERENCES

Abby, S. S., Cury, J., Guglielmini, J., Néron, B., Touchon, M., & Rocha, E. P. C. (2016). Identification of protein secretion systems in bacterial genomes. *Scientific Reports*, 6, 23080. https://doi.org/10.1038/srep23080

Achbergerová, L., & Nahálka, J. (2011). Polyphosphate–An ancient energy source and active metabolic regulator. *Microbial Cell Factories*, 10(1), 1–14. https://doi.org/10.1186/1475-2859-10-63

Aguilar-Barajas, E., Díaz-Pérez, C., Ramírez-Díaz, M. I., Riveros-Rosas, H., & Cervantes, C. (2011). Bacterial transport of sulfate, molybdate, and related oxyanions. *Biometals*, 24, 687–707. https://doi.org/10.1007/s10534-011-9421-x

Almpanis, A., Swain, M., Gatherer, D., & McEwan, N. (2018). Correlation between bacterial G+C content, genome size and the G+C content of associated plasmids and bacteriophages. *Microbial Genomics*, 4(4), e000168. https://doi.org/10.1099/mgen.0.000168

Altschul, S. F., Gish, W., Miller, W., Myers, E. W., & Lipman, D. J. (1990). Basic local alignment search tool. *Journal of Molecular Biology*, 215, 403–410. https://doi.org/10.1016/S0022-2836(05)80360-2

Axen, S. D., Erbilgin, O., & Kerfeld, C. A. (2014). A taxonomy of bacterial microcompartment loci constructed by a novel scoring method. *PLoS Computational Biology*, 10(10), e1003898. https://doi.org/10.1371/journal.pcbi.1003898

Ayers, M., Howell, P. L., & Burrows, L. L. (2010). Architecture of the type II secretion and type IV pilus machineries. *Future Microbiology*, 5(8), 1203–1218. https://doi.org/10.2217/fmb.10.76

Badger, M. R., & Bek, E. J. (2008). Multiple RuBisCO forms in proteobacteria: Their functional significance in relation to CO_2 acquisition by the CBB cycle. *Journal of Experimental Botany*, 59(7), 1525–1541. https://doi.org/10.1093/jxb/erm297

Bauer-Nebelsick, M., Bardele, C. F., & Ott, J. A. (1996a). Redescription of *Zoothamnium niveum* (Hemprich & Ehrenberg, 1831) Ehrenberg, 1838 (Oligohymenophora, Peritrichida), a ciliate with ectosymbiotic, chemoautotrophic bacteria. *European Journal of Protistology*, 32, 18–30. https://doi.org/10.1016/S0932-4739(96)80036-8

Bauer-Nebelsick, M., Bardele, C. F., & Ott, J. A. (1996b). Electron microscopic studies on *Zoothamnium niveum* (Hemprich & Ehrenberg, 1831) Ehrenberg 1838 (Oligohymenophora, Peritrichida), a ciliate with ectosymbiotic, chemoautotrophic bacteria. *European Journal of Protistology*, 32, 202–215. https://doi.org/10.1016/S0932-4739(96)80020-4

Bengtsson-Palme, J., Hartmann, M., Eriksson, K. M., Pal, C., Thorell, K., Larsson, S. G. J., & Nilsson, R. H. (2015). Metaxa2: Improved identification and taxonomic classification of small and large subunit

rRNA in metagenomic data. *Molecular Ecology Resources*, 15, 1403–1414. https://doi.org/10.1111/1755-0998.12399

Bobay, L. M., & Ochman, H. (2017). The evolution of bacterial genome architecture. *Frontiers in Genetics*, 8, 72. https://doi.org/10.3389/fgene.2017.00072

Bossé, J. T., Gilmour, H. D., & MacInnes, J. I. (2001). Novel genes affecting urease acivity in *Actinobacillus pleuropneumoniae*. *Journal of Bacteriology*, 183(4), 1242–1247. https://doi.org/10.1128/JB.183.4.1242-1247.2001

Bowers, R. M., Kyrpides, N. C., Stepanauskas, R., Harmon-Smith, M., Doud, D., Reddy, T. B. K., Schulz, F., Jarett, J., Rivers, A. R., Eloe-Fadrosh, E. A., Tringe, S. G., Ivanova, N. N., Copeland, A., Clum, A., Becraft, E. D., Malmstrom, R. R., Birren, B., Podar, M., Bork, P., … Woyke, T. (2017). Minimum information about a single amplified genome (MISAG) and a metagenome-assembled genome (MIMAG) of bacteria and archaea. *Nature Biotechnology*, 35(8), 725–731. https://doi.org/10.1038/nbt.3893

Brettin, T., Davis, J. J., Disz, T., Edwards, R. A., Gerdes, S., Olsen, G. J., Olson, R., Overbeek, R., Parrello, B., Pusch, G. D., Shukla, M., Thomason, I. I. I. J. A., Stevens, R., Vonstein, V., Wattam, A. R., & Xia, F. (2015). RASTtk: A modular and extensible implementation of the RAST algorithm for building custom annotation pipelines and annotating batches of genomes. *Scientific Reports*, 5, 8365. https://doi.org/10.1038/srep08365

Bright, M., Espada-Hinojosa, S., Lagkouvardos, I., & Volland, J.-M. (2014). The giant ciliate *Zoothamnium niveum* and its thiotrophic epibiont *Candidatus* Thiobios zoothamnicoli: A model system to study inter-species cooperation. *Frontiers in Microbiology*, 5, 1–13. https://doi.org/10.3389/fmicb.2014.00145

Cambon-Bonavita, M. A., Aubé, J., Cueff-Gauchard, V., & Reveillaud, J. (2021). Niche partitioning in the *Rimicaris exoculata* holobiont: The case of the first symbiotic Zetaproteobacteria. *Microbiome*, 9(1), 1–16. https://doi.org/10.1186/s40168-021-01045-6

Capella-Gutierrez, S., Silla-Martínez, J. M., & Gabaldón, T. (2009). trimAl: A tool for automated alignment trimming in large phylogenetic analyses. *Bioinformatics*, 25(15), 1972–1973. https://doi.org/10.1093/bioinformatics/btp348

Caron, D. A., & Goldman, J. C. (1990). Protozoan nutrient regeneration. In G. M. Capriulo (Ed.), *Ecology of marine protozoa* (pp. 283–306). Oxford University Press.

Caspi, R., Foerster, H., Fulcher, C. A., Kaipa, P., Krummenacker, M., Latendresse, M., Mueller, L. A., Ong, Q., Paley, S., Subhraveti, P., Weaver, D. S., & Karp, P. D. (2008). The MetaCyc database of metabolic pathways and enzymes and the BioCyc collection of pathway/genome databases. *Nucleic Acids Research*, 36(Database issue), D471–D480. https://doi.org/10.1093/nar/gkv1164

Cavanaugh, C. M., McKiness, Z. P., Newton, I. L. G., & Stewart, F. J. (2006). Marine chemosynthetic symbioses. In *The prokaryotes* (Vol. 1, pp. 475–507). Springer.

Chai, Y., Kolter, R., & Losick, R. (2009). A widely conserved gene cluster required for lactate utilization in *Bacillus subtilis* and its involvement in biofilm formation. *Journal of Bacteriology*, 191(8), 2423–2430. https://doi.org/10.1128/JB.01464-08

Chain, P. S. G., Grafham, D. V., Fulton, R. S., Fitzgerald, M. G., Hostetler, J., Muzny, D., Ali, J., Birren, B., Bruce, D. C., Buhay, C., Cole, J. R., Ding, Y., Dugan, S., Field, D., Garrity, G. M., Gibbs, R., Graves, T., Han, C. S., Harrison, S. H., … Detter, J. C. (2009). Genome project standards in a new era of sequencing. *Science*, 326, 236–237. https://doi.org/10.1126/science.1180614

Comolli, J. C., & Donohue, T. J. (2004). Differences in two *Pseudomonas aeruginosa* Cbb3 cytochrome oxidases: Two distinct *P. Aeruginosa* Cbb3 oxidases. *Molecular Microbiology*, 51(4), 1193–1203. https://doi.org/10.1046/j.1365-2958.2003.03904.x

Cozzone, A. J., & El-Mansi, M. (2005). Control of isocitrate dehydrogenase catalytic activity by protein phosphorylation in *Escherichia*

coli. *Journal of Molecular Microbiology and Biotechnology*, 9, 132–146. https://doi.org/10.1159/000089642

Dahl, C. (2015). Cytoplasmic sulfur trafficking in sulfur-oxidizing prokaryotes. *IUBMB Life*, 67, 268–274. https://doi.org/10.1002/iub.1371

Dahl, C. (2017). Sulfur metabolism in phototrophic bacteria. In P. C. Hallenbeck (Ed.), *Modern topics in the phototrophic prokaryotes: Metabolism, bioenergetics, and omics* (pp. 27–66). Springer International Publishing.

Dahl, C. (2020). A biochemical view on the biological sulfur cycle. In N. L. Piet (Ed.), *Environmental technologies to treat Sulphur pollution: Principles and engineering* (pp. 55–96). IWA Publishing. https://doi.org/10.2166/9781789060966_0055

Darling, A. E., Mau, B., & Perna, N. T. (2010). ProgressiveMauve: Multiple genome alignment with gene gain, loss and rearrangement. *PLoS One*, 5, e11147. https://doi.org/10.1371/journal.pone.0011147

Dattagupta, S., Schaperdoth, I., Montanari, A., Mariani, S., Kita, N., Valley, J. W., & Macalady, J. L. (2009). A novel symbiosis between chemoautotrophic bacteria and a freshwater cave amphipod. *The ISME Journal*, 3, 935–943. https://doi.org/10.1038/ismej.2009.34

De Oliveira, A.-L., Srivastava, A., Espada-Hinojosa, S., & Bright, M. (2022). The complete and closed genome of the facultative generalist *Candidatus* Endoriftia persephone from deep-sea hydrothermal vents. *Molecular Ecology Resources*, 22(8), 3106–3123. https://doi.org/10.1111/1755-0998.13668

Deckert, G., Warren, P. V., Gaasterland, T., Young, W. G., Lenox, A. L., Graham, D. E., Overbeek, R., Snead, M., Keller, M., Aujay, M., Huberk, R., Feldman, R., Short, J., Olsen, G., & Swanson, R. V. (1998). The complete genome of the hyperthermophilic bacterium *Aquifex aeolicus*. *Nature*, 392(6674), 353–358. https://doi.org/10.1038/32831

Distel, D., Altamia, M. A., Lin, Z., & Haygood, M. G. (2017). Discovery of chemoautotrophic symbiosis in the giant shipworm *Kuphus polythalamia* (Bivalvia: Teredinidae) extends wooden-steps theory. *Proceedings of the National Academy of Sciences*, 114, E3652–E3658. https://doi.org/10.1073/pnas.1620470114

Dubilier, N., Bergin, C., & Lott, C. (2008). Symbiotic diversity in marine animals: The art of harnessing chemosynthesis. *Nature Reviews Microbiology*, 6, 725–740. https://doi.org/10.1038/nrmicro1992

Ellers, J., Kiers, E. T., Currie, C. R., McDonald, B. R., & Visser, B. (2012). Ecological interactions drive evolutionary loss of traits. *Ecology Letters*, 15(10), 1071–1082. https://doi.org/10.1111/j.1461-0248.2012.01830.x

El-Mansi, E. M. T., Nimmo, H. G., & Holms, W. H. (1986). Pyruvate metabolism and the phosphorylation state of isocitrate dehydrogenase in *Escherichia coli*. *Journal of General Microbiology*, 132(3), 797–806. https://doi.org/10.1099/00221287-132-3-797

Emms, D. M., & Kelly, S. (2019). OrthoFinder: Phylogenetic orthology inference for comparative genomics. *Genome Biology*, 20, 238. https://doi.org/10.1186/s13059-019-1832-y

Farris, J. S. (1970). Methods for computing Wagner trees. *Systematic Biology*, 19(1), 83–92. https://doi.org/10.1093/sysbio/19.1.83

Fauré-Fremiet, E. (1950). Caulobactéries épizoïques associées aux Centrophorella (ciliés holotriches). *Bulletin de la Société Zoologique de France*, 75, 134–137.

Faure-Fremiet, E. (1951). The marine sand-dwelling ciliates of Cape Cod. *Biological Bulletin*, 100, 59–70. https://doi.org/10.2307/1538541

Felsenstein, J. (1981). Evolutionary trees from DNA sequences: A maximum likelihood approach. *Journal of Molecular Evolution*, 17, 368–376. https://doi.org/10.1007/bf01734359

Felsenstein, J. (1985). Confidence limits on phylogenies: An approach using the bootstrap. *Evolution*, 39, 783–791. https://doi.org/10.1111/j.1558-5646.1985.tb00420.x

Fenchel, T., & Finlay, B. J. (1989). Kentrophoros: A mouthless ciliate with a symbiotic kitchen garden. *Ophelia*, 30(2), 75–93.

Finlay, B., & Fenchel, T. (1989). Everlasting picnic for protozoa. *New Scientist*, 123(1671), 66–69.

Fischer, M., Zhang, Q. Y., Hubbard, R. E., & Thomas, G. H. (2010). Caught in a TRAP: Substrate-binding proteins in secondary transport. *Trends in Microbiology*, 18(10), 471–478. https://doi.org/10.1016/j.tim.2010.06.009

Flood, B. E., Jones, D. S., & Bailey, J. V. (2015). Complete genome sequence of *Sedimenticola thiotaurini* strain SIP-G1, a polyphosphate- and poly-hydroxyalkanoate-accumulating sulfur-oxidizing gammaproteobacterium isolated from salt marsh sediments. *Genome Announcements*, 3(3), e00671. https://doi.org/10.1128/genomeA.00671-15

Fokin, S. I., & Serra, V. (2022). Bacterial symbiosis in ciliates (Alveolata, Ciliophora): Roads traveled and those still to be taken. *Journal of Eukaryotic Microbiology*, 69(5), e12886. https://doi.org/10.1111/jeu.12886

Frost, L. S., Leplae, R., Summers, A. O., & Toussaint, A. (2005). Mobile genetic elements: The agents of open source evolution. *Nature Reviews Microbiology*, 3(9), 722–732. https://doi.org/10.1038/nrmicro1235

Green, J. L., Bohannan, B. J. M., & Whitaker, R. J. (2008). Microbial biogeography: From taxonomy to traits. *Science*, 320, 1039–1043. https://doi.org/10.1126/science.1153475

Gregersen, L. H., Bryant, D. A., & Frigaard, N.-U. (2011). Mechanisms and evolution of oxidative sulfur metabolism in green sulfur bacteria. *Frontiers in Microbiology*, 2, 116. https://doi.org/10.3389/fmicb.2011.00116

Grimonprez, A., Molza, A., Laurent, M. C., Mansot, J. L., & Gros, O. (2018). Thioautotrophic ectosymbiosis in Pseudovorticella sp., a peritrich ciliate species colonizing wood falls in marine mangrove. *European Journal of Protistology*, 62, 43–55. https://doi.org/10.1016/j.ejop.2017.11.002

Grzymski, J. J., Murray, A. E., Campbell, B. J., Kaplarevic, M., Gao, G. R., Lee, C., Daniel, R., Ghadiri, A., Feldman, R. A., & Cary, S. C. (2008). Metagenome analysis of an extreme microbial symbiosis reveals eurythermal adaptation and metabolic flexibility. *Proceedings of the National Academy of Sciences*, 105(45), 17516–17521. https://doi.org/10.1073/pnas.0802782105

Hachani, A., Wood, T. E., & Filloux, A. (2016). Type VI secretion and anti-host effectors. *Current Opinion in Microbiology*, 29, 81–93. https://doi.org/10.1016/j.mib.2015.11.006

Han, H., Hemp, J., Pace, L. A., Ouyang, H., Ganesan, K., Roh, J. H., Daldal, F., Blanke, S. R., & Gennis, R. B. (2011). Adaptation of aerobic respiration to low O_2 environments. *Proceedings of the National Academy of Sciences*, 108(34), 14109–14114. https://doi.org/10.1073/pnas.1018958108

Hastings, W. K. (1970). Monte Carlo sampling methods using Markov chains and their applications. *Biometrika*, 57(1), 97–109. https://doi.org/10.2307/2334940

Hemprich, F. W., & Ehrenberg, C. G. (1829). *Symbolae Physicae. Evertebrata. I. Protozoa*. Abhandlungen der Akademie der Wissenchaften zu Berlin.

Hemprich, F. W., & Ehrenberg, C. G. (1831). *Evertebrata I. Phytozoa. Simbolae physicae*. Abhandlungen der Akademie der Wissenchaften zu Berlin.

Hensen, D., Sperling, D., Trüper, H. G., Brune, D. C., & Dahl, C. (2006). Thiosulphate oxidation in the phototrophic Sulphur bacterium *Allochromatium vinosum*. *Molecular Microbiology*, 62, 794–810. https://doi.org/10.1111/j.1365-2958.2006.05408.x

Hryniewicz, M., Sirko, A., Pałucha, A., Böck, A., & Hulanicka, D. (1990). Sulfate and thiosulfate transport in *Escherichia coli* K-12: Identification of a gene encoding a novel protein involved in thiosulfate binding. *Journal of Bacteriology*, 172(6), 3358–3366. https://doi.org/10.1128/jb.172.6.3358-3366.1990

Huelsenbeck, J. P., & Ronquist, F. (2001). MRBAYES: Bayesian inference of phylogenetic trees. *Bioinformatics*, 17, 754–755. https://doi.org/10.1093/bioinformatics/17.8.754

Huerta-Cepas, J., Forslund, K., Coelho, L. P., Szklarczyk, D., Jensen, L. J., von Mering, C., & Bork, P. (2017). Fast genome-wide functional annotation through orthology assignment by eggNOG-mapper. *Molecular Biology and Evolution*, 34(8), 2115–2122. https://doi.org/10.1093/molbev/msx148

Huerta-Cepas, J., Szklarczyk, D., Heller, D., Hernández-Plaza, A., Forslund, S. K., Cook, H., Mende, D. R., Letunic, I., Rattei, T., Jensen, L. J., von Mering, C., & Bork, P. (2019). eggNOG 5.0: A hierarchical, functionally and phylogenetically annotated orthology resource based on 5090 organisms and 2502 viruses. *Nucleic Acids Research*, 47(D1), D309–D314. https://doi.org/10.1093/nar/gky1085

Husnik, F., Tashyreva, D., Boscaro, V., George, E. E., Lukeš, J., & Keeling, P. J. (2021). Bacterial and archaeal symbioses with protists. *Current Biology*, 31(13), R862–R877. https://doi.org/10.1016/j.cub.2021.05.049

Jäckle, O., Seah, B., Tietjen, M., Leisch, N., Liebeke, M., Kleiner, M., Berg, J. S., & Gruber-Vodicka, H. R. (2019). Chemosynthetic symbiont with a drastically reduced genome serves as primary energy storage in the marine flatworm Paracatenula. *Proceedings of the National Academy of Sciences*, 116, 8505–8514. https://doi.org/10.1073/pnas.1818995116

Janosch, C., Remonsellez, F., Sand, W., & Vera, M. (2015). Sulfur oxygenase reductase (sor) in the moderately thermoacidophilic leaching bacteria: Studies in *Sulfobacillus thermosulfidooxidans* and *Acidithiobacillus caldus*. *Microorganisms*, 3, 707–724. https://doi.org/10.3390/microorganisms3040707

Kanehisa, M., & Goto, S. (2000). KEGG: Kyoto encyclopedia of genes and genomes. *Nucleic Acids Research*, 28, 27–30. https://doi.org/10.1093/nar/28.1.27

Kang, D. D., Froula, J., Egan, R., & Wang, Z. (2015). MetaBAT, an efficient tool for accurately reconstructing single genomes from complex microbial communities. *PeerJ*, 3, e1165. https://doi.org/10.7717/peerj.1165

Kapitein, N., & Mogk, A. (2013). Deadly syringes: Type VI secretion system activities in pathogenicity and interbacterial competition. *Current Opinion in Microbiology*, 16, 52–58. https://doi.org/10.1016/j.mib.2012.11.009

Karaoz, U., & Brodie, E. L. (2022). MicroTrait: A toolset for a trait-based representation of microbial genomes. *Frontiers in Bioinformatics*, 2, 918853. https://doi.org/10.3389/fbinf.2022.918853

Karp, P. D., Paley, S., & Romero, P. (2002). The pathway tools software. *Bioinformatics*, 18(suppl 1), S225–S232. https://doi.org/10.1093/bioinformatics/18.suppl_1.s225

Karp, P. D., Paley, S. M., Krummenacker, M., Latendresse, M., Dale, J. M., Lee, T. J., Kaipa, P., Gilham, F., Spaulding, A., Popescu, L., Altman, T., Paulsen, I., Keseler, I. M., & Caspi, R. (2010). Pathway tools version 13.0: Integrated software for pathway/genome informatics and systems biology. *Briefings in Bioinformatics*, 11, 40–79. https://doi.org/10.1093/bib/bbp043

Katoh, K., & Standley, D. M. (2013). MAFFT multiple sequence alignment software version 7: Improvements in performance and usability. *Molecular Biology and Evolution*, 30(4), 772–780. https://doi.org/10.1093/molbev/mst010

Kim, M., Oh, H.-S., Park, S.-C., & Chun, J. (2014). Towards a taxonomic coherence between average nucleotide identity and 16S rRNA gene sequence similarity for species demarcation of prokaryotes. *International Journal of Systematic and Evolutionary Microbiology*, 64(2), 346–351. https://doi.org/10.1099/ijs.0.059774-0

König, S., Gros, O., Heiden, S. E., Hinzke, T., Thürmer, A., Poehlein, A., Meyer, S., Vatin, M., Mbéguié-A-Mbéguié, D., Tocny, J., Ponnudurai, R., Daniel, R., Becher, D., Schweder, T., & Markert, S. (2016). Nitrogen fixation in a chemoautotrophic lucinid symbiosis. *Nature Microbiology*, 2(1), 16193. https://doi.org/10.1038/nmicrobiol.2016.193

Konstantinidis, K. T., & Tiedje, J. M. (2005). Towards a genome-based taxonomy for prokaryotes. *Journal of Bacteriology*, 187(18), 6258–6264. https://doi.org/10.1128/jb.187.18.6258-6264.2005

Kuever, J., Sievert, S. M., Stevens, H., Brinkhoff, T., & Muyzer, G. (2002). Microorganisms of the oxidative and reductive part of the Sulphur cycle at a shallow-water hydrothermal vent in the Aegean Sea (Milos, Greece). *Cahiers de Biologie Marine*, 43, 413–416.

Kuwahara, H., Yoshida, T., Takaki, Y., Shimamura, S., Nishi, S., Harada, M., Matsuyama, K., Takishita, K., Kawato, M., Uematsu, K., Fujiwara, Y., Sato, T., Kato, C., Kitagawa, M., Kato, I., & Maruyama, T. (2007). Reduced genome of the thioautotrophic intracellular symbiont in a deep-sea clam, *Calyptogena okutanii*. *Current Biology*, 17(10), 881–886. https://doi.org/10.1016/j.cub.2007.04.039

Laurent, M. C. Z., Gros, O., Brulport, J. P., Gaill, F., & Bris, N. L. (2009). Sunken wood habitat for thiotrophic symbiosis in mangrove swamps. *Marine Environmental Research*, 67, 83–88. https://doi.org/10.1016/j.marenvres.2008.11.006

Lenk, S., Arnds, J., Zerjatke, K., Musat, N., Amann, R., & Mußmann, M. (2011). Novel groups of Gammaproteobacteria catalyse sulfur oxidation and carbon fixation in a coastal, intertidal sediment. *Environmental Microbiology*, 13(3), 758–774. https://doi.org/10.1111/j.1462-2920.2010.02380.x

Lowe, T. M., & Eddy, S. R. (1997). tRNAscan-SE: A program for improved detection of transfer RNA genes in genomic sequence. *Nucleic Acids Research*, 25(5), 955–964. https://doi.org/10.1093/nar/25.5.955

Maeda, S., Aoba, R., Nishino, Y., & Omata, T. (2019). A novel bacterial nitrate transporter composed of small transmembrane proteins. *Plant and Cell Physiology*, 60(10), 2180–2192. https://doi.org/10.1093/pcp/pcz112

Maurin, L. C., Himmel, D., Mansot, J., & Gros, O. (2010). Raman microspectrometry as a powerful tool for a quick screening of thio- trophy: An application on mangrove swamp meiofauna of Guadeloupe (F.W.I.). *Marine Environmental Research*, 69, 382–389. https://doi.org/10.1016/j.marenvres.2010.02.001

McCutcheon, J. P., & Moran, N. A. (2012). Extreme genome reduction in symbiotic bacteria. *Nature Reviews Microbiology*, 10, 13–26. https://doi.org/10.1038/nrmicro2670

Medina, M., & Sachs, J. L. (2010). Symbiont genomics, our new tangled bank. *Genomics*, 95(3), 129–137. https://doi.org/10.1016/j.ygeno.2009.12.004

Mitchell, J. H., Leonard, J. M., Delaney, J., Girguis, P. R., & Scott, K. M. (2019). Hydrogen does not appear to be a major electron donor for symbiosis with the deep-sea hydrothermal vent tubeworm *Riftia pachyptila*. *Applied and Environmental Microbiology*, 86(1), e01522-19. https://doi.org/10.1128/AEM.01522-19

Moran, N. A. (1996). Accelerated evolution and Muller's rachet in endosymbiotic bacteria. *Proceedings of the National Academy of Sciences*, 93(7), 2873–2878. https://doi.org/10.1073/pnas.93.7.2873

Moran, N. A., McLaughlin, H. J., & Sorek, R. (2009). The dynamics and time scale of ongoing genomic erosion in symbiotic bacteria. *Science*, 323, 379–382. https://doi.org/10.1126/science.1167140

Moriya, Y., Itoh, M., Okuda, S., Yoshizawa, A. C., & Kanehisa, M. (2007). KAAS: An automatic genome annotation and pathway reconstruction server. *Nucleic Acids Research*, 35(Web Server), W182–W185. https://doi.org/10.1093/nar/gkm321

Newton, I. L., & Bordenstein, S. R. (2011). Correlations between bacterial ecology and mobile DNA. *Current Microbiology*, 62(1), 198–208. https://doi.org/10.1007/s00284-010-9693-3

Newton, I. L. G., Woyke, T., Auchtung, T. A., Dilly, G. F., Dutton, R. J., Fisher, M. C., Fontanez, K. M., Lau, E., Stewart, F. J., Richardson, P. M., Barry, K. W., Saunders, E., Detter, J. C., Wu, D., Eisen, J. A., & Cavanaugh, C. M. (2007). The *Calyptogena magnifica* chemoautotrophic symbiont genome. *Science*, 315(5814), 998–1000. https://doi.org/10.1126/science.1138438

Ng, K. Y., Kamimura, K., & Sugio, T. (2000). Production of hydrogen sulfide from tetrathionate by the iron-oxidizing bacterium *Thiobacillus ferrooxidans* NASF-1. *Journal of Bioscience and Bioengineering*, 90(2), 193–198. https://doi.org/10.1016/s1389-1723(00)80109-7

Nicks, T., & Rahn-Lee, L. (2017). Inside out: Archaeal ectosymbionts suggest a second model of reduced-genome evolution. *Frontiers in Microbiology*, 8, 384. https://doi.org/10.3389/fmicb.2017.00384

Nunoura, T., Takaki, Y., Kazama, H., Kakuta, J., Shimamura, S., Makita, H., Hirai, M., Miyazaki, M., & Takai, K. (2014). Physiological and genomic features of a novel sulfur-oxidizing gammaproteobacterium belonging to a previously uncultivated symbiotic lineage isolated from a hydrothermal vent. *PLoS One*, 9(8), e104959. https://doi.org/10.1371/journal.pone.0104959

Nurk, S., Meleshko, D., Korobeynikov, A., & Pevzner, P. (2016). metaSPAdes: a new versatile de novo metagenomic assembler. *Genome Research*, 27, 824–834. https://doi.org/10.1101/gr.213959.116

Oren, A. (2017). A plea for linguistic accuracy–Also for Candidatus taxa. *International Journal of Systematic and Evolutionary Microbiology*, 67(4), 1085–1094. https://doi.org/10.1099/ijsem.0.001715

Ott, J., Bright, M., & Bulgheresi, S. (2004). Marine microbial thiotrophic ectosymbioses. *Oceanography and Marine Biology: An Annual Review*, 42, 95–118. https://doi.org/10.1201/9780203507810.ch4

Ott, J. A., Novak, R., Schiemer, F., Hentschel, U., Nebelsick, M., & Polz, M. (1991). Tackling the sulfide gradient: A novel strategy involving marine nematodes and chemoautotrophic ectosymbionts. *Marine Ecology*, 12, 261–279. https://doi.org/10.1111/j.1439-0485.1991.tb00258.x

Paradis, E., Claude, J., & Strimmer, K. (2004). APE: Analyses of phylogenetics and evolution in R language. *Bioinformatics*, 20, 289–290. https://doi.org/10.1093/bioinformatics/btg412

Paredes, G. F., Viehboeck, T., Lee, R., Palatinszky, M., Mausz, M. A., Reipert, S., Schintlmeister, A., Maier, A., Volland, J.-M., Hirschfeld, C., Wagner, M., Berry, D., Markert, S., Bulgheresi, S., & König, L. (2021). Anaerobic sulfur oxidation underlies adaptation of a chemosynthetic symbiont to oxic-anoxic interfaces. *mSystems*, 6(3), e01186-20. https://doi.org/10.1128/mSystems.01186-20

Park, T., Wijeratne, S., Meulia, T., Firkins, J. L., & Yu, Z. (2021). The macronuclear genome of anaerobic ciliate *Entodinium caudatum* reveals its biological features adapted to the distinct rumen environment. *Genomics*, 113(3), 1416–1427. https://doi.org/10.1016/j.ygeno.2021.03.014

Parks, D. H., Imelfort, M., Skennerton, C. T., Hugenholtz, P., & Tyson, G. W. (2015). CheckM: Assessing the quality of microbial genomes recovered from isolates, single cells, and metagenomes. *Genome Research*, 25, 1043–1055. https://doi.org/10.1101/gr.186072.114

Paytan, A., & McLaughlin, K. (2007). The oceanic phosphorus cycle. *Chemical Reviews*, 107(2), 563–576. https://doi.org/10.1021/cr0503613

Petersen, J. M., Kemper, A., Gruber-Vodicka, H., Cardini, U., van der Geest, M., Kleiner, M., Bulgheresi, S., Mußmann, M., Herbold, C., Seah, B. K., Antony, C. P., Liu, D., Belitz, A., & Weber, M. (2016). Chemosynthetic symbionts of marine invertebrate animals are capable of nitrogen fixation. *Nature Microbiology*, 2, 16195. https://doi.org/10.1038/nmicrobiol.2016.195

Petersen, J. M., Ramette, A., Lott, C., Cambon-Bonavita, M. A., Zbinden, M., & Dubilier, N. (2010). Dual symbiosis of the vent shrimp *Rimicaris exoculata* with filamentous gamma- and epsilonproteobacteria at four mid-Atlantic ridge hydrothermal vent fields. *Environmental Microbiology*, 12(8), 2204–2218. https://doi.org/10.1111/j.1462-2920.2009.02129.x

Pitcher, R. S., & Watmough, N. J. (2004). The bacterial cytochrome cbb3 oxidases. *Biochimica et Biophysica acta (BBA)–Bioenergetics*, 1655, 388–399. https://doi.org/10.1016/j.bbabio.2003.09.017

Polz, M. F., Distel, D. L., Zarda, B., Amann, R., Felbeck, H., Ott, J. A., & Cavanaugh, C. M. (1994). Phylogenetic analysis of a highly specific association between ectosymbiotic, sulfur-oxidizing bacteria and a marine nematode. *Applied and Environmental Microbiology*, 60(12), 4461–4467. https://doi.org/10.1128/aem.60.12.4461-4467.1994

Raikov, I. B. (1971). Bactéries épizoiques et mode de nutrition du cilié psammophile *Kentrophoros fistulosum* Fauré-Fremiet (étude au microscope électronique). *Protistologica*, 7, 365–378. https://doi.org/10.1016/S0074-7696(08)60584-7

Raikov, I. B. (1974). Étude ultrastructurale des bactéries épizoiques et endozoiques de *Kentrophoros latum* Raikov, cilié holotriche mésopsammique. *Cahiers de Biologie Marine*, 15, 379–393.

Rinke, C., Lee, R., Katz, S., & Bright, M. (2007). The effects of sulphide on growth and behaviour of the thiotrophic *Zoothamnium niveum* symbiosis. *Proceedings–Royal Society of London. Biological Sciences*, 274, 2259–2269. https://doi.org/10.1098/rspb.2007.0631

Rinke, C., Schmitz-Esser, S., Loy, A., Horn, M., Wagner, M., & Bright, M. (2009). High genetic similarity between two geographically distinct strains of the sulfur-oxidizing symbiont 'Candidatus Thiobios zoothamnicoli'. *FEMS Microbiology Ecology*, 67, 229–241. https://doi.org/10.1111/j.1574-6941.2008.00628.x

Rinke, C., Schmitz-Esser, S., Stoecker, K., Nussbaumer, A. D., Molnár, D. A., Vanura, K., Wagner, M., Horn, M., Ott, J. A., & Bright, M. (2006). "Candidatus Thiobios zoothamnicoli", an ectosymbiotic bacterium covering the giant marine ciliate *Zoothamnium niveum*. *Applied and Environmental Microbiology*, 72, 2014–2021. https://doi.org/10.1128/AEM.72.3.2014-2021.2006

Rodriguez-Puente, R., & Lazo-Cortes, M. S. (2013). Algorithm for shortest path search in geographic information systems by using reduced graphs. *Springerplus*, 2, 291. https://doi.org/10.1186/2193-1801-2-291

Rühl, P., Pöll, U., Braun, J., Klingl, A., & Kletzin, A. (2017). A sulfur oxygenase from the haloalkaliphilic bacterium *Thioalkalivibrio paradoxus* with atypically low reductase activity. *Journal of Bacteriology*, 199(4), e00675-16. https://doi.org/10.1128/JB.00675-16

Sachs, J. L., Essenberg, C. J., & Turcotte, M. M. (2011). New paradigms for the evolution of beneficial infections. *Trends in Ecology and Evolution*, 26(4), 202–209. https://doi.org/10.1016/j.tree.2011.01.010

Sancar, G. B., Smith, F. W., Reid, R., Payne, G., Levy, M., & Sancar, A. (1987). Action mechanism of *Escherichia coli* DNA photolyase. I. Formation of the enzyme-substrate complex. *Journal of Biological Chemistry*, 262(1), 478–485.

Schliep, K. P. (2011). Phangorn: Phylogenetic analysis in R. *Bioinformatics*, 27, 592–593. https://doi.org/10.1093/bioinformatics/btq706

Schuster, L., & Bright, M. (2016). A novel colonial ciliate *Zoothamnium ignavum* sp. nov.(Ciliophora, Oligohymenophorea) and its ectosymbiont *Candidatus* Navis piranensis gen. Nov., sp. nov. from shallow-water wood falls. *PLoS One*, 11(9), e0162834. https://doi.org/10.1371/journal.pone.0162834

Schwarz, G. (1978). Estimating the dimension of a model. *The Annals of Statistics*, 6(2), 461–464. https://doi.org/10.1214/aos/1176344136

Scott, K. M., Harmer, T. L., Gemmell, B. J., Kramer, A. M., Sutter, M., Kerfeld, C. A., Barber, K. S., Bari, S., Boling, J. W., Campbell, C. P., Gallard-Gongora, J. F., Jackson, J. K., Lobos, A., Mounger, J. M., Radulovic, P. W., Sanson, J. M., Schmid, S., Takieddine, C., Warlick, K. F., & Whittaker, R. (2020). Ubiquity and functional uniformity in CO_2 concentrating mechanisms in multiple phyla of bacteria is suggested by a diversity and prevalence of genes encoding candidate dissolved inorganic carbon transporters. *FEMS Microbiology Letters*, 367(13), fnaa106. https://doi.org/10.1093/femsle/fnaa106

Seah, B. K. B., Antony, C. P., Huettel, B., Zarzycki, J., Schada von Borzyskowski, L., Erb, T. J., Kouris, A., Kleiner, M., Liebeke, M., Dubilier, N., & Gruber-Vodicka, H. R. (2019). Sulfur-oxidizing symbionts without canonical genes for autotrophic CO_2 fixation. *mBio*, 10, e01112–e01119. https://doi.org/10.1128/mBio.01112-19

Serafini, A., Tan, L., Horswell, S., Howell, S., Greenwood, D. J., Hunt, D. M., Phan, M. D., Schembri, M., Monteleone, M., Montague, C. R., Britton, W., Garza-Garcia, A., Snijders, A. P., VanderVen, B., Gutierrez, M. G., West, N. P., & de Carvalho, L. P. S. (2019). *Mycobacterium tuberculosis* requires glyoxylate shunt and reverse methylcitrate cycle for lactate and pyruvate metabolism. *Molecular Microbiology*, 112(4), 1284–1307. https://doi.org/10.1111/mmi.14362

Sievert, S. M. (1999). *Microbial communities at a shallow submarine hydrothermal vent in the Aegean Sea (Milos, Greece)*. PhD Dissertation. Universität Bremen. Chapter 6. https://pure.mpg.de/rest/items/item_3254112/component/file_3254113/content

Sievert, S. M., Brinkhoff, T., Muyzer, G., Ziebis, W., & Kuever, J. (1999). Spatial heterogeneity of bacterial populations along an environmental gradient at a shallow submarine hydrothermal vent near Milos Island (Greece). *Applied and Environmental Microbiology*, 65, 3834–3842. https://doi.org/10.1128/AEM.65.9.3834-3842.1999

Sogin, E. M., Kleiner, M., Borowski, C., Gruber-Vodicka, H.-R., & Dubilier, N. (2021). Life in the dark: Phylogenetic and physiological diversity of chemosynthetic symbioses. *Annual Review of Microbiology*, 75(1), 695–718. https://doi.org/10.1146/annurev-micro-051021-123130

Sorokin, D. Y., de Jong, G. A., Robertson, L. A., & Kuenen, G. J. (1998). Purification and characterization of sulfide dehydrogenase from alkaliphilic chemolithoautotrophic sulfur-oxidizing bacteria. *FEBS Letters*, 427, 11–14. https://doi.org/10.1016/s0014-5793(98)00379-2

Stewart, F. J., Newton, I. L. G., & Cavanaugh, C. M. (2005). Chemosynthetic endosymbioses: Adaptations to oxic-anoxic interfaces. *Trends in Microbiology*, 13(9), 439–448. https://doi.org/10.1016/j.tim.2005.07.007

Supuran, C. T., & Capasso, C. (2017). An overview of the bacterial carbonic anhydrases. *Metabolites*, 7(4), 56. https://doi.org/10.3390/metabo7040056

Takai, K. (2019). The nitrogen cycle: A large, fast, and mystifying cycle. *Microbes and Environments*, 34(3), 223–225. https://doi.org/10.1264/jsme2.ME3403rh

Tanaka, Y., Yoshikaie, K., Takeuchi, A., Ichikawa, M., Mori, T., Uchino, S., Sugano, Y., Hakoshima, T., Takagi, H., Nonaka, G., & Tsukazaki, T. (2020). Crystal structure of a YeeE/YedE family protein engaged in thiosulfate uptake. *Science Advances*, 6(35), p.eaba7637. https://doi.org/10.1126/sciadv.aba7637

Tatusov, R. L., Galperin, M. Y., Natale, D. A., & Koonin, E. V. (2000). The COG database: A tool for genome-scale analysis of protein functions and evolution. *Nucleic Acids Research*, 28(1), 33–36. https://doi.org/10.1093/nar/28.1.33

Toft, C., & Andersson, S. G. (2010). Evolutionary microbial genomics: Insights into bacterial host adaptation. *Nature Reviews Genetics*, 11(7), 465–475. https://doi.org/10.1038/nrg2798

Toft, C., Williams, T. A., & Fares, M. A. (2009). Genome-wide functional divergence after the symbiosis of proteobacteria with insects unraveled through a novel computational approach. *PLoS Computational Biology*, 5, e1000344. https://doi.org/10.1371/journal.pcbi.1000344

Veuger, B., & Middelburg, J. J. (2007). Incorporation of nitrogen from amino acids and urea by benthic microbes: Role of bacteria versus algae and coupled incorporation of carbon. *Aquatic Microbial Ecology*, 48(1), 35–46.

Vignais, P., Billoud, B., & Meyer, J. (2001). Classification and phylogeny of hydrogenases. *FEMS Microbiology Reviews*, 25, 455–501. https://doi.org/10.1111/j.1574-6976.2001.tb00587.x

Vogt, L. (2010). Spatio-structural granularity of biological material entities. *BMC Bioinformatics*, 11(1), 289. https://doi.org/10.1186/1471-2105-11-289

Volland, J.-M., Schintlmeister, A., Zambalos, H., Reipert, S., Mozetič, P., Espada-Hinojosa, S., Turk, V., Wagner, M., & Bright, M. (2018). NanoSIMS and tissue autoradiography reveal symbiont carbon fixation and organic carbon transfer to giant ciliate host. *ISME Journal*, 12, 714–727. https://doi.org/10.1038/s41396-018-0069-1

Wang, S., Orabi, E. A., Baday, S., Bernèche, S., & Lamoureux, G. (2012). Ammonium transporters achieve charge transfer by fragmenting their substrate. *Journal of the American Chemical Society*, 134(25), 10419–10427. https://doi.org/10.1021/ja300129x

Weissgerber, T., Dobler, N., Polen, T., Latus, J., Stockdreher, Y., & Dahl, C. (2013). Genome-wide transcriptional profiling of the purple sulfur bacterium *Allochromatium vinosum* DSM 180^T during growth on different reduced sulfur compounds. *Journal of Bacteriology, 195*(18), 4231–4245. https://doi.org/10.1128/JB.00154-13

Weissgerber, T., Zigann, R., Bruce, D., Chang, Y. J., Detter, J. C., Han, C., Hauser, L., Jeffries, C. D., Land, M., Munk, A. C., Tapia, R., & Dahl, C. (2011). Complete genome sequence of *Allochromatium vinosum* DSM 180^T. *Standards in Genomic Sciences, 5*, 311–330. https://doi.org/10.4056/sigs.2334270

Welte, C., Hafner, S., Krätzer, C., Quentmeier, A., Friedrich, C. G., & Dahl, C. (2009). Interaction between sox proteins of two physiologically distinct bacteria and a new protein involved in thiosulfate oxidation. *FEBS Letters, 583*(8), 1281–1286. https://doi.org/10.1016/j.febslet.2009.03.020

Wernegreen, J. J. (2015). Endosymbiont evolution: Predictions from theory and surprises from genomes. *Annals of the new York Academy of Sciences, 1360*(1), 16–35. https://doi.org/10.1111/nyas.12740

Wick, R. R., Schultz, M. B., Zobel, J., & Holt, K. E. (2015). Bandage: Interactive visualisation of de novo genome assemblies. *Bioinformatics, 31*(20), 3350–3352. https://doi.org/10.1093/bioinformatics/btv383

Zhou, J., Bruns, M. A., & Tiedje, J. M. (1996). DNA recovery from soils of diverse composition. *Applied and Environmental Microbiology, 62*, 316–322. https://doi.org/10.1128/aem.62.2.316-322.1996

SUPPORTING INFORMATION

Additional supporting information can be found online in the Supporting Information section at the end of this article.

How to cite this article: Espada-Hinojosa, S., Karthäuser, C., Srivastava, A., Schuster, L., Winter, T., de Oliveira, A. L., Schulz, F., Horn, M., Sievert, S., & Bright, M. (2024). Comparative genomics of a vertically transmitted thiotrophic bacterial ectosymbiont and its close free-living relative. *Molecular Ecology Resources, 24*, e13889. https://doi.org/10.1111/1755-0998.13889

Chapter 6

The complete and closed genome of the facultative generalist *Candidatus Endoriftia persephone* from deep-sea hydrothermal vents

MOLECULAR ECOLOGY
RESOURCES **WILEY**

The complete and closed genome of the facultative generalist *Candidatus* Endoriftia persephone from deep-sea hydrothermal vents

André Luiz De Oliveira | Abhishek Srivastava | Salvador Espada-Hinojosa | Monika Bright

Department of Functional and Evolutionary Ecology, University of Vienna, Vienna, Austria

Correspondence
André Luiz de Oliveira and Monika Bright, Department of Functional and Evolutionary Ecology, University of Vienna, Djerassiplatz 1, Vienna, Austria.
Emails: andre.luiz.de.oliveira@univie.ac.at (A.L.O.), monika.bright@univie.ac.at (M.B.)

Funding information
Austrian Science Fund, Grant/Award Number: 31543-B29

Handling Editor: Kin-Ming (Clement) Tsui

Abstract

The mutualistic interactions between *Riftia pachyptila* and its endosymbiont *Candidatus* Endoriftia persephone (short Endoriftia) have been extensively researched. However, the closed Endoriftia genome is still lacking. Here, by employing single-molecule real-time sequencing we present the closed chromosomal sequence of Endoriftia. In contrast to theoretical predictions of enlarged and mobile genetic element-rich genomes related to facultative endosymbionts, the closed Endoriftia genome is streamlined with fewer than expected coding sequence regions, insertion-, prophage-sequences and transposase-coding sequences. Automated and manually curated functional analyses indicated that Endoriftia is more versatile regarding sulphur metabolism than previously reported. We identified the presence of two identical rRNA operons and two long CRISPR regions in the closed genome. Additionally, pangenome analyses revealed the presence of three types of secretion systems (II, IV and VI) in the different Endoriftia populations indicating lineage-specific adaptations. The *in depth* mobilome characterization identified the presence of shared genomic islands in the different Endoriftia drafts and in the closed genome, suggesting that the acquisition of foreign DNA predates the geographical dispersal of the different endosymbiont populations. Finally, we found no evidence of epigenetic regulation in Endoriftia, as revealed by gene screenings and absence of methylated modified base motifs in the genome. As a matter of fact, the restriction-modification system seems to be dysfunctional in Endoriftia, pointing to a higher importance of molecular memory-based immunity against phages via spacer incorporation into CRISPR system. The Endoriftia genome is the first closed tubeworm endosymbiont to date and will be valuable for future gene oriented and evolutionary comparative studies.

KEYWORDS
endosymbiont, evolutionary theory, genomics, long-read sequencing, molecular evolution, *Riftia pachyptila*

1 | INTRODUCTION

Many symbiotic mutualisms involve horizontally transmitted microbes that live solitary in the environment as well as sheltered in/on eukaryote hosts (Bright & Bulgheresi, 2010; Douglas, 2010). Often for both symbiont and host the mutualism is facultative. Mutualism for the giant tubeworm *Riftia pachyptila* (short *Riftia*), however, is strictly obligate (Bright & Lallier, 2010). High dependency on its sole partner *Candidatus* Endoriftia persephone (short Endoriftia) is apparent already in *Riftia*'s (and other vestimentiferan) aposymbiotic larvae that must pick up the suitable partner from the hydrothermal vent environment once they settle (Nussbaumer et al., 2006). Later, the gutless adult only survives if the provision of inorganic nutrients for the chemotrophic sulphur oxidizing Endoriftia is reciprocated with released organic carbon (Bright et al., 2000; Childress & Girguis, 2011; Felbeck & Jarchow, 1998). In addition, the host also digests the bacteria (Bosch & Grassé, 1984; Bright & Sorgo, 2003; de Oliveira et al., 2021; Hand, 1987; Hinzke et al., 2019, 2021). In contrast, apparently, life for host-associated Endoriftia is facultative as evidenced by the uptake of these bacteria during horizontal transmission (Nussbaumer et al., 2006) from a free-living environmental pool detected at East Pacific Rise hydrothermal vents and adjacent cold deep-sea basalts and sediments as well as at the pelagic zone (Harmer et al., 2008; Polzin et al., 2019). Further, release of symbionts upon host death was shown experimentally to lead to free-living dividing populations in high pressure vessels (Klose et al., 2015), indicative of proliferating free-living Endoriftia in the environment. Several ribosomal and nuclear marker studies showed that Endoriftia is present in different vestimentiferans other than *Riftia* (i.e., *Tevnia jerichonana*, *Ridgeia piscesae*, *Oasisia alvinae*, *Esparpia spicata* at vents only) ruling out the codiversification of this bacterium with their respective hosts (Di Meo et al., 2000; Feldman et al., 1997; Nelson & Fisher, 2000).

Theory establishes that partner choice is a mechanism for positive assortment between cooperating partners (Fletcher & Doebeli, 2009; Queller, 1985) that acts prior establishment of the association (Bull & Rice, 1991). In horizontally transmitted symbionts, partner choice is expected to ensure the selection of the cooperating partner. This mechanism is selective enough not to allow any other microbe to enter but is also permissive enough to allow polyclonal symbiont populations selected from the environment to establish in the host (Genkai-Kato & Yamamura, 1999; Heath & Stinchcombe, 2014; Vrijenhoek, 2010). Indeed, many different associations involving horizontal transmitted symbionts house polyclonal symbiont populations which are selected from the environment (Perez et al., 2021; Polzin et al., 2019; Sachs et al., 2009; Wollenberg & Ruby, 2009). Unique among horizontal transmitted symbionts, however, is that *Riftia* and other vestimentiferan hosts have a single symbiont-housing organ, the trophosome, in which a single strain of Endoriftia dominates over many others, as evidenced by multilocus gene sequencing (Perez et al., 2021; Polzin et al., 2019) and metagenomics (Polzin et al., 2019). This is in contrast to other horizontally transmitted symbioses as those involving the bobtail squid (Wollenberg & Ruby, 2009) or the legumes (Sachs et al., 2009) in which several symbiont-housing organ compartments are present with each harbouring usually one or two strains. In this respect, it is important to stress that studies on the genetic diversity of Endoriftia are focused on small discreet parts of the trophosome of single individual hosts, thus not providing a complete view of the genetic makeup of *Riftia*'s endosymbionts across the entirety of the large symbiont-housing organ nor across the *Riftia* population level.

The first draft genome of this facultative generalist bacterium was obtained from *Riftia* (Robidart et al., 2008), followed by further draft genomes from *Riftia* and the other vent host species *Tevnia jerichonana* and *Ridgeia piscesae* (Gardebrecht et al., 2012; Perez & Juniper, 2016). However, so far, despite extensive in silico and experimental investigations, a complete and closed Endoriftia genome is still lacking. The varying degrees of the Endoriftia genome fragmentation affect many "genome-centric" analyses (e.g. gene content investigations, synteny, pangenome analyses) and negatively impact gene prediction and annotation (e.g. false positive/negative annotation rates (Klassen & Currie, 2012)), thus hampering downstream analyses and the correct biological interpretation of the data. Here, by using accurate circular consensus long-read sequencing (Wenger et al., 2019), we closed the genome of the dominant strain of *Riftia*'s endosymbiont *Ca.* Endoriftia persephone. Moreover, we thoroughly characterized, in a broad comparative evolutionary genomics framework, the Endoriftia genome in relation to its metabolic capabilities, defence system mechanisms, genetic mobile elements, and epigenetic regulation. To date, the Endoriftia genome constitutes the first closed tubeworm endosymbiont's genome publicly available and will be an important resource to broaden our understanding not only about *Riftia*-Endoriftia symbiosis, but also for other chemosynthetic animal-microbe systems.

2 | MATERIALS AND METHODS

2.1 | Sample collection and sequencing

A sample of trophosome obtained from a female *Riftia pachyptila* collected at the Tica hydrothermal vent site (Alvin dive 4839, 9° 50.398 N, 104° 17.506 W, 2514 m depth, 2016) was separated from the host tissue as described in Polzin et al. (2019). The DNA of the enriched endosymbiont fraction was extracted using the Qiagen Blood & Cell Culture DNA Mini Kit (cat no./ID: 13323) following the manufacturer's instructions. The long-read metagenome library was prepared using the PacBio large-insert DNA protocol and the SMRTbell Express Kit. The sequencing was performed on a Sequel1. The library construction and sequencing were performed at the Vienna BioCenter Core Facilities (https://www.viennabiocenter.org/vbcf/). Highly accurate single-molecule consensus reads (HiFi reads) with a minimum of three passes were generated from the raw sequence data using the ccs tool present in the "PacBio Secondary Analysis Tools on Bioconda". The HiFi reads were assembled with Flye version 2.5 (Kolmogorov et al., 2019). The circularized contig containing the full

genome of Endoriftia was polished using the tool arrow available at the "PacBio Secondary Analysis Tools" on Bioconda package. Genome completeness was performed with the CheckM software using the "Gammaproteobacteria" lineage (Parks et al., 2015). We manually fixed the first codon of the gene *dnaA* as the chromosome origin in the closed, already circularized, and polished Endoriftia genome.

2.2 | Annotation and genotyping

To annotate the genome we employed a nested approach of integrative levels (Novikoff, 1945). The predicted genes were treated as a part of identifiable metabolic pathways and these were grouped as functional traits, which are understood as microbial characteristics linked to the microbe's fitness (Green et al., 2008). Other relevant structural features were also treated as traits (e.g. transporters, storage capabilities). Additionally, we further annotated the protein coding sequences predicted from the closed Endoriftia genome using automated tools such as Prokka version 1.14.0 (Seemann, 2014), eggNOG mapper version 2 (Huerta-Cepas et al., 2017, 2019), and KEGG through the web-based server KAAS (Moriya et al., 2007) followed by manual curation of the automatic results. The identification of the mobile genetic elements (i.e., mobilome) was performed with the online version of ISfinder (https://isfinder.biotoul.fr/) (Kichenaradja et al., 2010; Siguier et al., 2006), IslandViewer4 (https://pathogenomics.sfu.ca/islandviewer) (Bertelli et al., 2017), alien hunter (https://www.sanger.ac.uk/tool/alien-hunter/), PHASTER (https://phaster.ca/) (Arndt et al., 2016; Zhou et al., 2011), SpacePHARER (Zhang et al., 2021), and BacANT (Hua et al., 2021). CRISPR regions were further investigated and characterized with CRISPRCasFinder browser (https://crisprcas.i2bc.paris-saclay.fr/CrisprCasFinder/Index) (Couvin et al., 2018). To enrich the comparative genomic analyses we downloaded, filtered, and assembled the host-associated metagenome described in Polzin et al. (2019), using BBDuk version38.42 and metaSPAdes version 3.13.0 (Nurk et al., 2017), respectively. Genotyping was performed by comparing four housekeeping loci retrieved from the closed genome, (i.e., *atpA*, *gyrB*, *recA* and *uvrD*) against the sequence types generated by Polzin et al. (2019) through BLASTN similarity searches (Camacho et al., 2009).

2.3 | Methylome analyses

The base modification analysis was performed with SMRTLink version 9.0.0.92188, and the screening of important methyltransferase enzymes was executed with hmmsearch version 3.2.1 using MTases PFAM domains (PF00145, P02384, PF01555).

2.4 | Comparative genomic analyses

Average nucleotide identity index analysis was performed with OAU (OrthoANI) tool (Lee et al., 2016) and publicly available tubeworm

endosymbiont genomes. Three orthology analysis inferences (*phylogenomic set* (N = 13): all Endoriftia genomes, other available tubeworm endosymbionts and *Sedimenticola thiotaurini*; *pangenome set* (N = 7): solely Endoriftia genomes; and, *positive selection set* (N = 7): the complete closed Endoriftia genome, all available non-Endoriftia tubeworm endosymbionts, and *Sedimenticola thiotaurini*) were performed with Orthofinder version 2.3.8 (Emms & Kelly, 2019).

The phylogenomic analysis was performed with a super-matrix generated with FasConCAT version 1 (Kück & Meusemann, 2010) by concatenating the single copy orthologue sequences present in the *phylogenomic set*. The phylogenomic tree inference was performed on a partition model analysis using IQ-TREE version 1.6.11 combining ModelFinder, tree search, and 1000 ultra-fast bootstrap (Hoang et al., 2018; Kalyaanamoorthy et al., 2017; Nguyen et al., 2015). The Venn diagrams were obtained using the package venn available at R (https://CRAN.R-project.org/package=venn). Circular plots were generated using Circos (Krzywinski et al., 2009).

The pangenome (persistent, shell, cloud) was calculated with the tool PPanGGOLiN version 1.1.136 (Gautreau et al., 2020) using the six previously published Endoriftia draft genomes (Gardebrecht et al., 2012; Perez & Juniper, 2016; Polzin et al., 2019; Robidart et al., 2008) and the closed genome herein reported. The Orthofinder results obtained from the *pangenome set* were used as input in PPanGGOLiN version 1.1.136 under the "--clusters" parameter.

Nonsynonymous (dN) and synonymous (dS) substitution rates in the closed Endoriftia genome were calculated with PAML/CODEML version 4.8a package (Yang, 2007) using the Orthofinder version 2.3.8 *positive selection set* results. Briefly, the single copy protein orthologues identified in Orthofinder version 2.3.8 and the corresponding gene sequences were converted into a codon alignment using the software PAL2NAL (Suyama et al., 2006). Gene trees were inferred from codon alignments with IQ-TREE version 1.6.11 (Kalyaanamoorthy et al., 2017; Nguyen et al., 2015) and used in the subsequent analyses. Pairwise estimates of dN/dS ratio obtained from positive (model = 2, NSsites = 2, fix_omega = 0, omega = 1) and null (model = 2, NSsites = 2, fix_omega = 1, omega = 1) branch-site models (Zhang et al., 2005) specific to the Endoriftia closed genome lineage were calculated using PAML/CODEML version 4.8a package. The closed Endoriftia lineage was defined as "foreground branch" and assumed to contain different values of dN/dS, whereas the dN/dS of all other branches of the tree (i.e., "background" branches) contained a fixed distribution. The estimated log likelihoods of the positive and null models were then used to construct likelihood ratio tests and the *p*-values were obtained employing the following formula: $p\text{-value} = \chi^2 (2*\Delta\ln L, \text{degree of freedom})$; where the degree of freedom is 1. The aforementioned pipeline was performed one more time with the single copy orthologues obtained from the *phylogenomic set*. Since recombination events can falsely be interpreted as signs of molecular adaption (Anisimova et al., 2003), we identified positive selected genes which were located in inferred recombination hotspots in the closed Endoriftia genome. Recombination events were inferred using ClonalFrameML (Didelot & Wilson, 2015) by specifying a starting phylogenetic tree and the

core alignment blocks (>500 nt) extracted from the multiple sequence alignment generated with progressiveMauve version 2.4.0 (Darling et al., 2010), and the genomes present in the *positive selection set*. All previous bioinformatic tools were executed with the default parameters.

The positively selected genes present in the nonrecombinant regions of the closed Endoriftia genome were annotated with InterproScan version 5.39–77.0 (Jones et al., 2014) and the enrichment analysis for GO was performed with topGO version 2.36.0 (https://bioconductor.org/packages/release/bioc/html/topGO.html) using Fisher's exact test against the Endoriftia background (all genes identified in the closed Endoriftia genome) coupled with weight01 algorithm (Alexa et al., 2006).

3 | RESULTS AND DISCUSSION

3.1 | Overview of the closed genome of *Ca.* Endoriftia persephone

The draft (meta)genome of Endoriftia was first generated by Robidart et al. (2008) using Sanger sequencing. Further pyrosequencing, short-read sequencing and genome assemblies of Endoriftia greatly improved contiguity (Gardebrecht et al., 2012; Perez & Juniper, 2016), however, a closed genome was not obtained (Figure 1a). Using accurate

single-molecule consensus reads (PacBio HiFi reads) we sequenced and closed with ~2000 fold-coverage (~120× circular consensus sequencing with three passes) the Endoriftia genome (Figure 1b). The genome size is ~3.6 Mb and presents a completeness of 99.18%, as revealed by CheckM (Parks et al., 2015), rendering this genome the first closed and most complete Endoriftia genome (Figure 2) (Gardebrecht et al., 2012; Perez & Juniper, 2016; Polzin et al., 2019; Robidart et al., 2008) and of a vestimentiferan endosymbiont to date (Breusing et al., 2020; Gardebrecht et al., 2012; Li et al., 2018, 2019; Robidart et al., 2008). The extremely low strain homogeneity and contamination levels (0% and 1.05%, respectively; Supplementary Table S1) are a clear indicative that the complete closed Endoriftia genome are not composed of closely related strains (i.e., chimeric assembly). Furthermore, the sequences of the dominant strain of *Riftia*-associated Endoriftia present at the vent site Tica at the East Pacific Rise, generated by Polzin et al. (2019) and the respective orthologs in the complete closed genome (also sampled in Tica) were identical, showing that the genome herein described belongs to the dominant strain of Endoriftia.

The genome encodes 3217 coding sequences (CDS), from which 319 present a signal peptide sequence, 49 tRNAs coding for all 20 amino acids, 12 non-coding RNAs and six rRNA genes (two copies of 5S, 16S and 23S) (Table 1) located in two distinct and identical chromosomal clusters, contradicting previous studies (Perez & Juniper, 2016; Polzin et al., 2019) (Figure 3a).
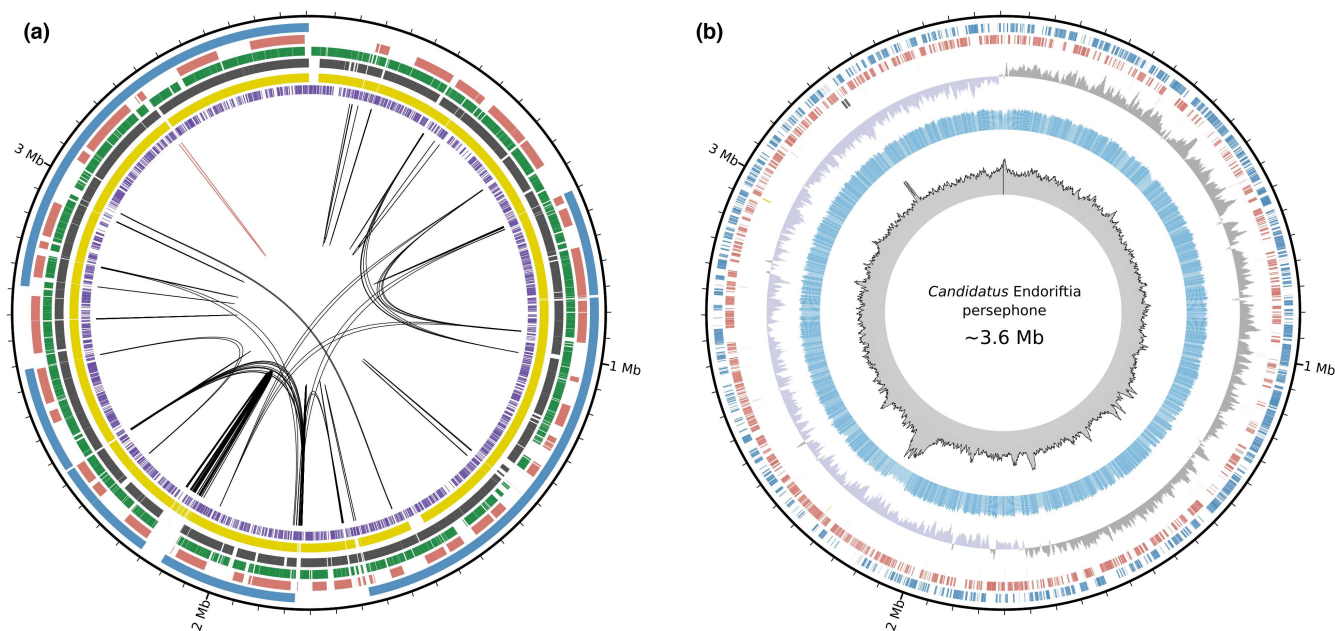

FIGURE 1 Overview of the complete and closed genome of Endoriftia and publicly available drafts. (a) The ~3.6 Mb closed genome of *Candidatus* Endoriftia persephone. The six distinct publicly available Endoriftia drafts were mapped back to the closed genome presented herein. The concentrical circles from the centre to the periphery represent in purple (Robidart et al., 2008); in yellow and black (Gardebrecht et al., 2012); in green and maroon (Perez & Juniper, 2016) and in cyan (Polzin et al., 2019) the different draft metagenomes. The black and red lines in the middle of the figure represent repetitive regions >5 kpb and >500 pb in the endosymbiont closed genome, respectively. (b) Circos plot showing the PacBio coverage across the closed genome (grey histograms; ~2000× coverage). The GC content is represented by the blue histograms. GC skew data is shown by the grey and purple histograms. Blue and red boxes correspond to coding sequence regions in the forward and reverse strands of the closed Endoriftia genome, respectively. The two grey boxes correspond to the rRNA clusters in the closed *Ca.* Endoriftia genome
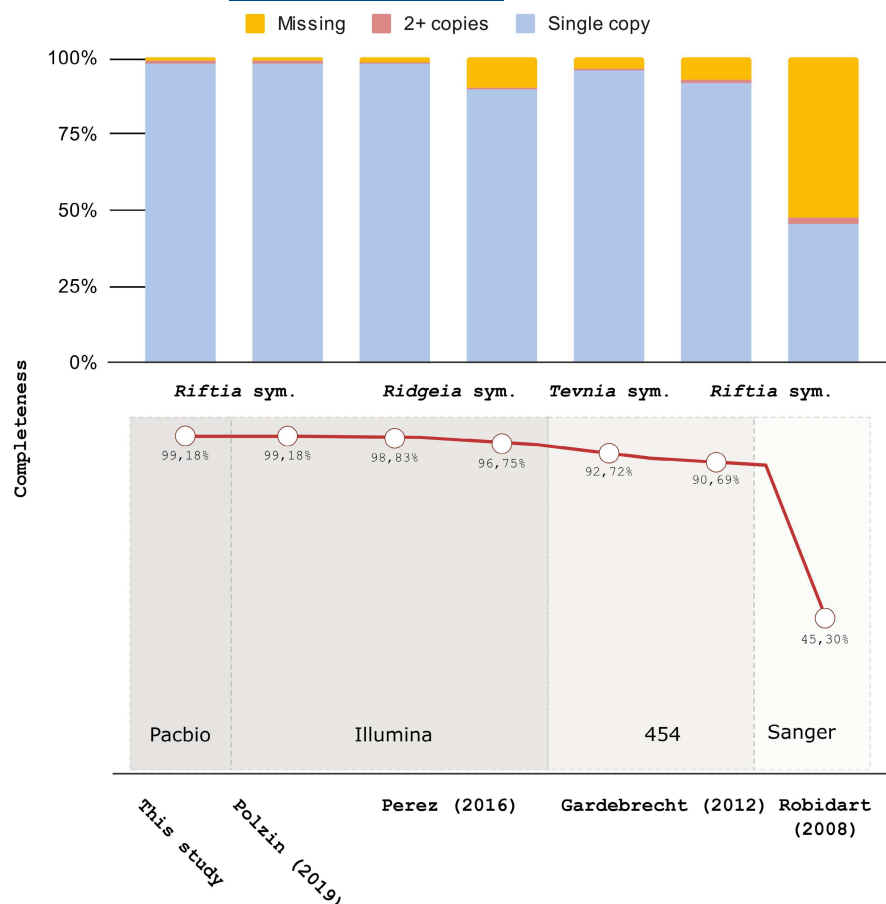
FIGURE 2 The completeness of the closed *Candidatus* Endoriftia persephone genome and publicly available drafts. The stacked proportional bar charts reflect the number of missing, multicopies, and single copy genes in the different genome drafts of Endoriftia as shown by CheckM analysis

Interestingly, two tandem rRNA gene clusters with the exact syntenic organization (including the intergenic tRNAs) were previously detected in a *Ridgeia*-associated raw metagenomic assembly (JGI's IMG-Mer database; GOLD analysis ID project: Ga0041824; contig Draft11:123922) (Perez & Juniper, 2016). Consistent with earlier studies (Perez et al., 2021; Perez & Juniper, 2016), but contradicting Gardebrecht et al. (2012) (*Riftia1* draft genome), we recovered two large and complete CRISPR (clustered regularly interspaced short palindromic repeat) regions composed of 12 and 39 direct repeats units, with respective sizes of ~9.4- and ~11.6-kb (Figure 3b). The two clusters belong to class I, type C and –E, respectively, with the conserved CRISPR2 region located ~370 bp upstream of the gene *purT* (phosphoribosylglycinamide formyltransferase 2), as recently described by Perez et al. (2021). It has been shown in a recent study (Perez et al., 2021) that CRISPR regions present in *Ridgeia*-associated Endoriftia contain a higher genetic diversity than housekeeping genes. In our analyses, we did not observe in the closed Endoriftia genome any intragenomic conservation of spacer sequences (Data S1), pointing as well to a high genetic variability of these spacer sequences. Since the dynamics and evolution of bacterial adaptive immunity are shaped by context-dependent environmental factors (e.g. local virome) and different bacterial strains often harbour distinct CRISPR loci (Westra et al., 2016), CRISPR-based genotyping could improve the final strain-level characterization of uncultured *Riftia*-associated (and free-living) Endoriftia populations.

Functional annotation of the closed Endoriftia genome using eggnog-mapper version 2 revealed that 2899 predicted genes (~89.9%) could be assigned to 20 distinct broad cluster of orthologous genes (COG) categories, with the categories "function unknown (S)", "energy production and conversion (C)" and "signal transduction mechanisms (T)" containing the greatest number of genes (Table S1). The percentage of uncharacterised predicted genes (i.e., genes with either unknown function or that remain unannotated) in Endoriftia genome (797 genes/25% of the total) and in the most complete genome of cold-seep endosymbiont available to date (endosymbiont of *Lamellibrachia barhami*; 1239/27%) (Breusing et al., 2020) is similar. This indicates that the function of a large number of genes in the tubeworm's endosymbiont genomes remains unknown.

After detecting positive selection and identifying particular changes in patterns of amino acid conservation (i.e., signs of positive selection at a protein/codon level), we identified a small percentage of genes in the Endoriftia closed genome showing signatures of adaptative evolution (p-value < 0.05; 223 genes /6.93%) in comparison to cold-seep tubeworm endosymbionts (*positive selection set*; $N = 7$) (*Lamellibrachia*, *Paraescarpia*, *Seepiophila)* and the free-living closely related bacterium *Sedimenticola* (Table S1). The positively selected genes are involved in a wide range of biological activity including cell cycle (e.g. *ftsZ*, *ftsY*, *ftsK*, *flgD*, *fliK*), DNA replication/repair (e.g. *holA*, *uvrA*, *parE*, *gyrA*, *smc2*), stress response (e.g. *lepA*, *hscB*), and cofactor biosynthesis (e.g. *moaB*, *btuF*, *hemF*, *hemY*). Furthermore, gene ontology (GO) analyses performed on the positively selected genes show

TABLE 1 Overview of the publicly available Endoriftia metagenomes and the complete and closed genome based on PROKKA version 1.14.0 annotation (Seemann, 2014)

Assembly name	Number of contigs	Total length	Largest contig	N_{50}	GC (%)	Gene	CDS	rRNA	Repeat region	tRNA	tmRNA
This_study	1	3,604,761	3,604,761	3,604,761	58.59	3282	3217	6	2	49	1
Riftia sym. (Polzin et al., 2019)	12	3,534,855	1,660,857	531,644	58.77	3262	3197	6	2	49	1
Ridgeia sym. 1 (Perez & Juniper, 2016)	97	3,441,033	236,298	83,967	58.88	3223	3162	3	1	47	1
Ridgeia sym. 2 (Perez & Juniper, 2016)	693	3,417,427	40,802	7630	58.87	3485	3428	3	0	43	1
Tevnia sym. (Gardebrecht et al., 2012)	184	3,637,102	248,702	92,701	58.16	3447	3389	4	4	44	1
Riftia sym. (Gardebrecht et al., 2012)	197	3,481,040	95,370	29,688	58.82	3462	3407	3	4	42	1
Riftia sym. (Robidart et al., 2008)	2170	3,203,254	10,451	1953	57.87	4845	4805	3	3	30	1

an enrichment of distinct molecular function terms related to binding (GTP, folic acid, and purine ribonucleoside), aminoacyl-tRNA hydrolase, ATP hydrolysis and peptidase activities (Figure S1). Due to the low nucleotide sequence divergence among the different Endoriftia populations within mid-ocean ridge systems (Perez & Juniper, 2016), only two genes with signs of positive selection were identified in the complete closed genome in comparison to cold-seep tubeworm endosymbionts (*Lamellibrachia*, *Paraescarpia*, *Seepiophila*), the free-living closely related bacterium *Sedimenticola thiotaurini* and the different Endoriftia draft genomes (*phylogenomic set*; *N* = 13; Table S1). These genes, *mreC* (cell shape-determining protein) and *hemB* (delta-aminolaevulinic acid dehydratase), are involved in cell division/shape (van den Ent et al., 2006) and haem biosynthesis (Choby & Skaar, 2016), respectively. Although more adequate metrics exist to detect positive selection in closely related bacterial populations (pN/pS), the previous results might indicate sympatric adaptations in the complete closed genome herein described and other Endoriftia populations (Table S1).

3.2 | Metabolic capabilities of Endoriftia

To further explore the potential metabolic capabilities of Endoriftia we combined multiple functional annotation tools and performed an exhaustive manual curation (Table S2). Our results corroborate most previous findings of genes involved in autotrophy, N metabolism, sulphur oxidation and motility (Gardebrecht et al., 2012; Kleiner et al., 2012; Markert et al., 2007; Perez & Juniper, 2016; Robidart et al., 2008) (Figure 4), in addition to novel genes and potential new metabolic capabilities in Endoriftia. Genes related to two carbon-fixation pathways were present in the genome, the Calvin-Benson-Bassham cycle (Cbb) and the reductive TCA cycle (rTca) (Felbeck, 1985; Hinzke et al., 2019; Minic & Hervé, 2004). Cbb is performed by a form II RuBisCO (Badger & Bek, 2008) and no carboxysome genes were found (Scott et al., 1999). As previously described, a CO_2 concentration mechanism was indicated by the presence of carbonic anhydrase genes belonging to the alpha and beta classes (Robidart et al., 2008). We, additionally, identified another carbonic anhydrase gene in the closed Endoriftia that falls into the gamma class (discussed more in details below). The reductive TCA cycle is supported by the presence of the two genes *aclA* and *aclB* (Leonard et al., 2021), based in the conserved domain composition of *aclA* (Nunoura et al., 2018), and the gene cluster synteny with *Thioflavicoccus mobilis* (Rubin-Blum et al., 2019) and phylogenetic inferences (Figure S2). A contiguous gene cluster *korDABC* encoding for the tetrameric version of 2-oxoglutarate:ferrodoxin oxidoreductase was also found upstream, and in the vicinity, of other genes involved in the reductive TCA cycle (Rubin-Blum et al., 2019). Two copies of dimeric versions *korAB* are also present in the genome and are thought to be capable of acting in both oxidative and reductive directions (see note S2 in Rubin-Blum et al., 2019). We found genes involved in the glycogen synthesis for carbon storage (Glg) (Sorgo et al., 2002) and cyanophycin synthesis for carbon and nitrogen storage (Cph) (Gardebrecht et al., 2012).
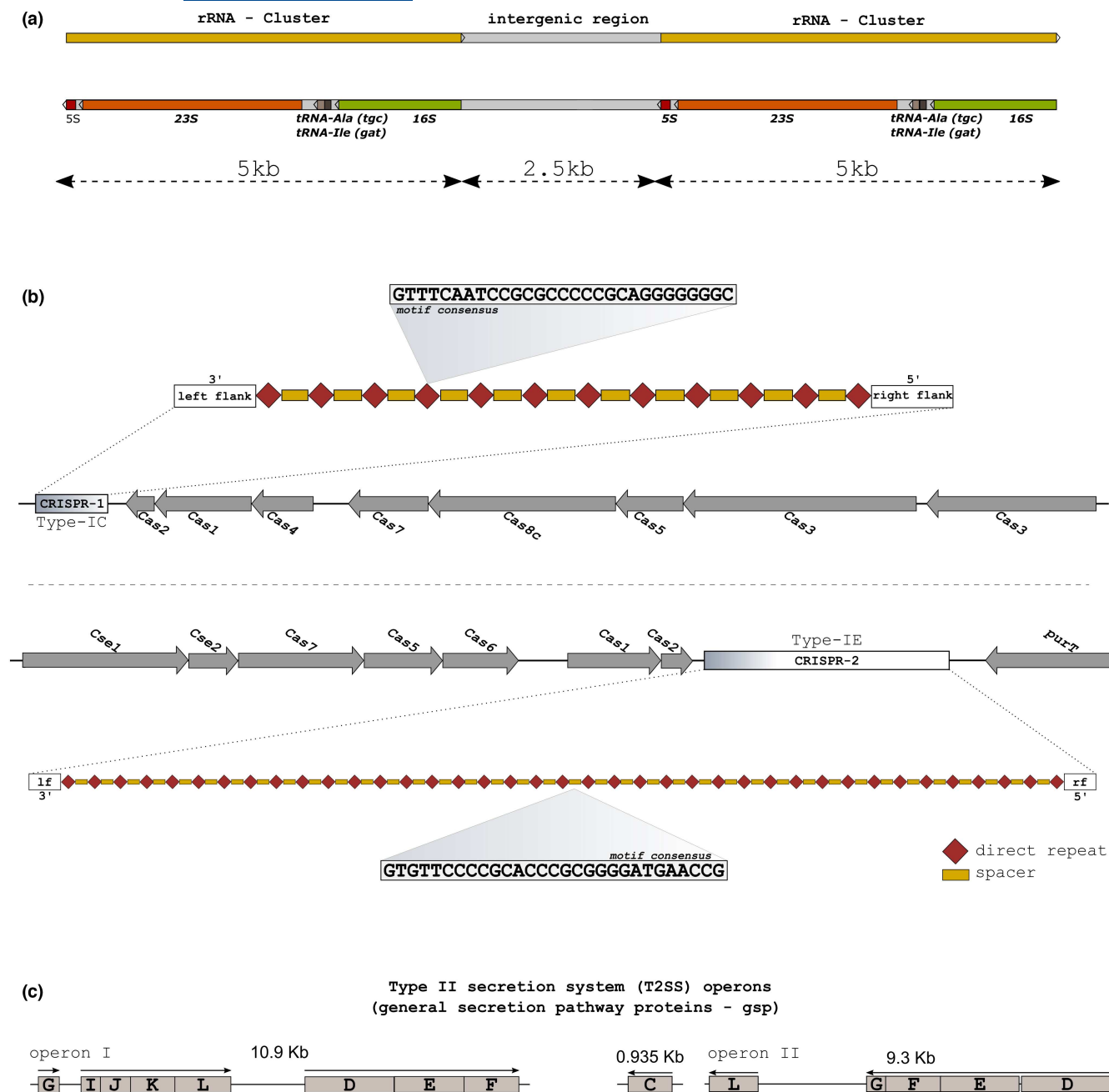
(a)

(b)

(c)

FIGURE 3 Genomic features obtained from the closed Endoriftia genome. (a) Two identical rRNA operons located in the closed Endoriftia genome. (b) Two large CRISPR (clustered regularly interspaced short palindromic repeat) regions composed of 12 and 39 direct repeats units, with respective sizes of ~9.4- and ~11.6 k present in the closed Endoriftia genome. (c) Type II secretion system (T2SS) operons in the closed Endoriftia genome

Genes for the oxidative direction of the TCA cycle are present as well (TcaC) (Markert et al., 2007). The presence of the gene cluster of *ccoNOQP* is indicative of cytochrome cbb$_3$ based oxygen respiration, able to function at low oxygen concentrations (CytCBB3) (Pitcher & Watmough, 2004). Similarly, we found the *petABC* gene cluster for cytochrome bc$_1$ complex mediated electron transport (Pet) (Trumpower, 1990).

[NiFe] hydrogenase (Hup) genes were also identified in the closed genome, pointing to hydrogen oxidation capability. Recently, however, incubation experiments did not support this hypothesis

(Mitchell et al., 2019). The closed genome harbours the genes of four main nitrogen processes: (1) denitrification (nitrate reduction to nitrite either performed in the periplasm by NapAB or in the cytoplasm by NarGHI, followed by the successive reductions until dinitrogen by NirS, NorCB and NosZ symbolized together here as Nirors (Gardebrecht et al., 2012; Zumft, 1997); (2) dissimilatory nitrate reduction (reduction to nitrate by NapAB or by NarGHI and electron transfer though the NADH ubiquinone oxidoreductase chain (Gardebrecht et al., 2012); (3) assimilatory nitrate reduction (symbolized here as AsN) (Girguis et al., 2000; Moreno-Vivián et al., 1999);
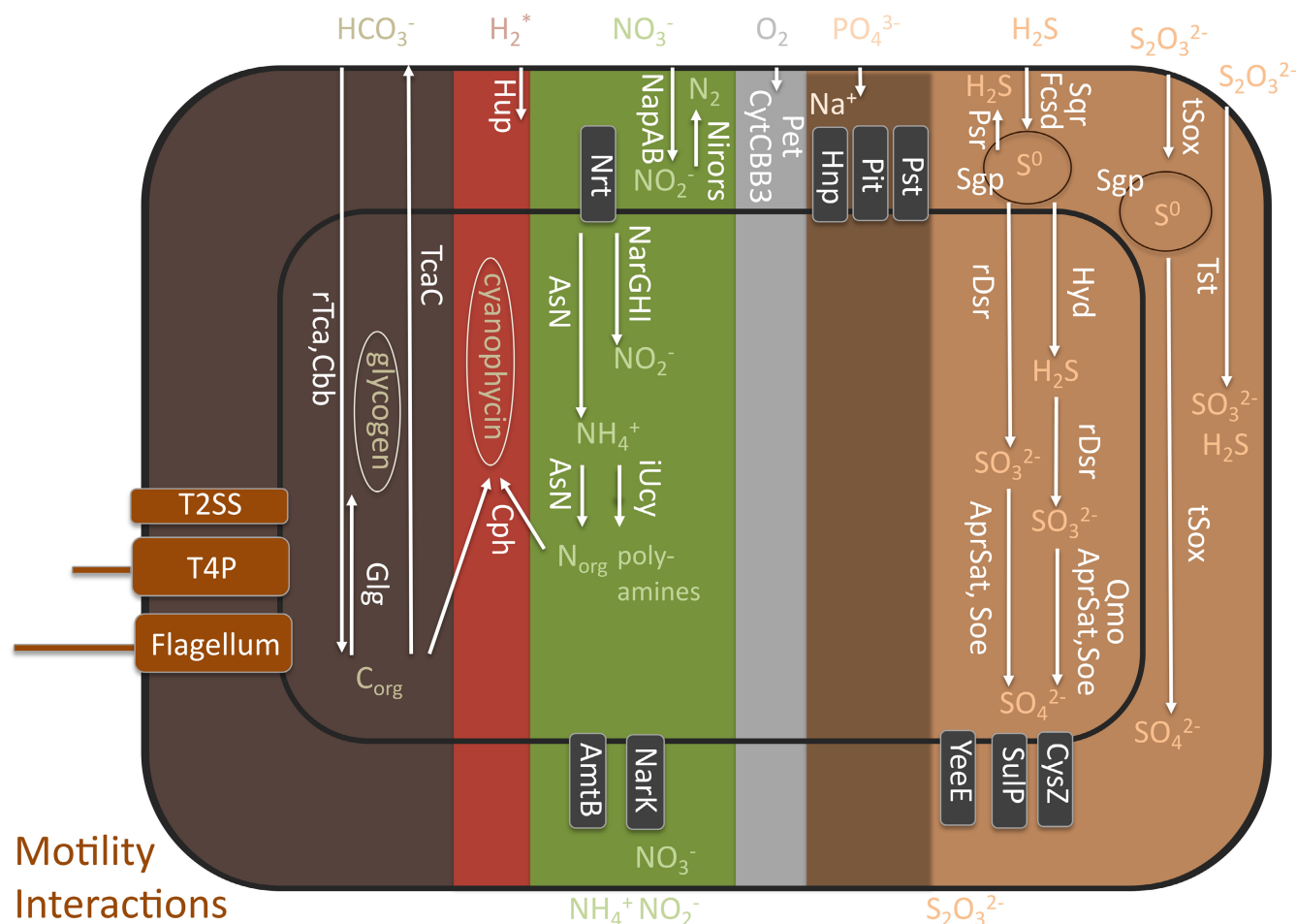
FIGURE 4 Major metabolic capabilities found in the closed Endoriftia genome. Selected relevant potential functional capabilities of *Candidatus* Endoriftia persephone inferred from its closed genome are shown (for simplicity not all transporters are depicted in the figure). Predicted and functionally annotated genes are grouped in metabolic pathways. Functional traits are features such as single metabolic pathways or composites of them that affect the organism fitness. Structural features such as transporters or secretion systems, and storage capabilities are also considered as traits. Trait labels are generally in white fonts and in vertical orientation, except for the motility and interactions on the left. Compound labels are horizontally oriented. Storage compartments are indicated with ellipses. AmtB, amonium transporter; AprSat, sulphate adenylyltransferase and adenylylsulphate reductase sulphite oxidation; AsN, assimilatory nitrate reduction; Cbb, Calvin-Benson-Basham cycle; Cph, cyanophycin biosynthesis; CysZ, sulphate transporter; CytCBB3, cytochrome cbb₃ based oxygen respiration; Fcsd, flavocytochrome c sulphide dehydrogenase sulphide oxidation; Glg, glycogen biosynthesis; Hnp, high affinity sodium-phosphate symporter; Hup*, putative hydrogen oxidation (Mitchell et al., 2019 found uptake of hydrogen apparently does not serve to fuel carbon fixation, neither was hydrogenase activity measured); Hyd, sulhydrogenase elemental sulphur oxidation; iUcy, incomplete urea cycle lacking last step arginase gene; NapAB, periplasmic nitrate reduction to nitrite; NarGHI, cytoplasmic nitrate reduction to nitrite; NarK, nitrate-nitrite antiporter; Nirors, sequential oxidation from nitrate to dinitrogen by nirS, norBC and nosZ as final steps of the denitrification process; Nrt, nitrate transporter; Pet, cytochrome bc₁ complex mediated electron transport chain; Pit, low affinity phosphate transporter; Psr, polysulphide reductase elemental sulphur reduction; Pst, high affinity phosphate transporter; Qmo, quinone-interacting membrane-bound oxidoreductase mediated sulphite oxidation; rDsr, reverse dissimilatory sulphate reductase mediated sulphur oxidation; rTca, reductive TCA cycle; Sgp, sulphur globule proteins; Soe, sulphite-oxidation enzyme sulphite oxidation; Sqr, sulphide:quinone oxydoreductase sulphide oxidation; SulP, sulphate permease; T2SS, type II secretion system; T4P, type IV pilus; TcaC, TCA cycle; tSox, truncated Sox mediated sulphur oxidation; Tst, thiosulphate disproportionation; YeeE, thiosulphate transporter

and, (4) an incomplete urea cycle (iUcy) lacking the last step gene for arginase. While genes encoding for ammonium transporter (AmtB), nitrate transporter (Nrt), and nitrate-nitrite antiporter (NarK) (Gardebrecht et al., 2012), were found, four of the five urea transporter subunits-encoding genes were absent. Consequently, uptake

of urea waste from the host as previously hypothesized by Robidart et al. (2008), does not seem possible (de Oliveira et al., 2021).

We found that Endoriftia is more versatile regarding sulphur metabolism than previously reported in *Riftia*-, and *Tevnia*-endosymbiont associated studies (Gardebrecht et al., 2012; Kleiner

116

et al., 2012; Robidart et al., 2008). Genes for two different mechanisms of sulphide oxidation to elemental sulphur are present: flavocytochrome c sulphide dehydrogenase (Fcsd) (Kleiner et al., 2012; Sorokin et al., 1998), and sulphide:quinone oxidoreductase (Sqr) (Dahl, 2017; Kleiner et al., 2012). Genes encoding for sulphur globule proteins, previously confirmed by electron energy loss spectrography (Pflugfelder et al., 2005), are also present in the genome (Sgp) (Dahl, 2017). Elemental sulphur from these globules could be mobilized back through the action of a polysulphide reductase (Psr; newly reported here), for sulphide supply (Robidart et al., 2008). Same function can be performed by a sulfhydrogenase in the cytoplasm (Hyd; newly reported here) (Ng et al., 2000). Additionally, both elemental sulphur and sulphide can undergo a reverse dissimilatory sulphate reductase mediated oxidation to sulphite in the cytoplasm (rDsr) (Dahl, 2017; Gardebrecht et al., 2012; Kleiner et al., 2012; Robidart et al., 2008). The resulting cytoplasmic sulphite can finally be oxidized to sulphate either by a membrane-bound quinone-interacting oxidoreductase (Qmo) (Dahl, 2017; Kleiner et al., 2012), by another sulphite-oxidizing enzyme (Soe; newly reported here) (Dahl, 2017), or by the combined action of sulphate adenylyltransferase and adenylylsulphate reductase (AprSat) (Dahl, 2017; Gardebrecht et al., 2012; Robidart et al., 2008). Genes encoding for a permease and a transporter are identified in the genome to export sulphate from the cytoplasm (SulP and CysZ) (Hryniewicz et al., 1990; Zolotarev et al., 2008). Furthermore, a gene encoding for a sulphite transporter is also detected (*TauE/SafE*). Genes for a truncated Sox pathway are also present (tSox) (Welte et al., 2009) oxidizing thiosulphate to elemental sulphur and to sulphite, in the periplasm. The presence of putative sulphane sulphurtransferase genes (Tst; newly reported here) (Aird et al., 1987) can indicate thiosulphate disproportionation to sulphite and sulphide in the periplasm. A gene encoding for the recently characterized thiosulphate uptake protein YeeE (Tanaka et al., 2020) was also identified in the genome. Whether thiosulphate then is used for cysteine synthesis as described (Tanaka et al., 2020) needs to be further investigated.

The presence of five sets of TRAP transporter (TAXI and Dct) subunits-encoding genes and tripartite tricarboxylate transporter Tct family subunits-encoding genes in the genome supports the idea of organic acid internalization in the symbiont cells (Kleiner et al., 2012). *Riftia pachyptila*'s circulating fluids and tissues contain high concentration of nonessential amino acids like alanine, glutamate, glycine and serine (Cian et al., 2000). The identification of sodium/glutamate symporter-, sodium-glycine/alanine symporter-, sodium/proline symporter- and SLC6 subfamily, as well as acetate permease-, citrate permease-, OprB family carbohydrate-selective porin-, PEP: sugar phosphotransferase system subunits-, and oligopeptide ABC transporter-encoding genes, suggest the possibility of amino acid transportation and independent ways of organic compound acquisition other than CO_2 fixation in Endoriftia. Genes for three phosphate transporters were found: a low affinity transporter (Pit), a high affinity transporter (Pst), and a high affinity sodium dependent symporter (here symbolized as Hnp). Finally, we have identified the presence of complete gene set related to type-II

secretion system in the closed Endoriftia genome (Figure 3c) (Perez & Juniper, 2016), and confirmed the presence of the type IV pilus and flagellum complete gene sets (Gardebrecht et al., 2012).

3.3 | Comparative genomics, phylogenetics and phylogenomics

To investigate the overall genomic similarity among the 12 different vestimentiferan endosymbionts found in cold-seep and vent environments, we calculated with OrthoANI (Lee et al., 2016) the average nucleotide identity indexes using the aligned genomic regions present in the tubeworm endosymbiont genomes (Table S1). Pairwise comparisons of endosymbiont genomes revealed that the gammaproteobacteria phylotype "Candidatus Endoriftia persephone" is present in *Tevnia jerichonana*, *Ridgeia piscesae* and *Riftia pachyptila* (Gardebrecht et al., 2012; Perez & Juniper, 2016; Robidart et al., 2008), as revealed by OrthoANI score values greater than 97%. These results are in accordance with Perez and Juniper (2016). Considerably lower ANI values between 73% and 74% show that the seep endosymbionts of *Lamellibrachia luymesi*, *Lamellibrachia barhami*, *Paraescarpia echinospica*, *Seepiophila jonesi*, and *Escarpia spicata* indeed diverge from Endoriftia as previously shown by 16S rRNA similarity (McMullin et al., 2003; Reveillaud et al., 2018; Vrijenhoek, 2010) and more recent genomic studies (Breusing et al., 2020; Yang et al., 2020).

Phylogenomic and phylogenetic 16S analyses of vestimentiferan symbionts revealed the presence of two distinct and fully supported clades, one containing the hydrothermal vent "Candidatus Endoriftia persephone" and the other containing the cold seep representatives, in agreement with previous reports (Breusing et al., 2020; McMullin et al., 2003; Reveillaud et al., 2018; Vrijenhoek, 2010; Yang et al., 2020) (Figure S3). The ingroup relationships within the Endoriftia and "seep endosymbionts" clades differ in the phylogenomic and 16S trees, however, it is clear that *Ridgeia* endosymbionts form their own clade sister group to *Tevnia* and *Riftia* endosymbionts, as shown in previous studies (Chao et al., 2007; Feldman et al., 1997; McMullin et al., 2003; Perez & Juniper, 2016). Based on the phylogenomics/phylogenetics data, a paraphyly was observed with the endosymbionts of *Lamellibrachia luymesi* and *L. barhami*, indicating that at least two distinct gammaproteobacterial chemoautotrophic bacteria are able to infect the cold-seep *Lamellibrachia* tubeworms, as previously reported (McMullin et al., 2003; Reveillaud et al., 2018). As a matter of fact, the OrthoANI score value for the *Lamellibrachia* endosymbiont pair is much lower (~92%) than the values herein reported for the different Endoriftia genomes (>97%), indicating that seep endosymbionts are more genetically divergent (Table S1).

A comparison of the genome sizes among vestimentiferan endosymbionts and free-living relatives revealed that Endoriftia's closed genome (~3.6 Mb/3217 coding sequence genes (CDS)) is considerably smaller harbouring fewer CDS than that of *Sedimenticola thiotaurini* (~3.9 Mb/3739 CDS) and *S. selenatireducens* (~4.6 Mb/4276 CDS) (Flood et al., 2015; Louie et al., 2016). Therefore, the theoretical

prediction of enlarged genome sizes related to facultative symbionts (Sachs et al., 2011) clearly does not hold true for Endoriftia. The genome size, GC content, and number of genes among the publicly available Endoriftia draft genomes, and the complete and closed genome herein described, are comparable (Table 1). The only exception is Robidart et al. (2008) draft genome, which presents an elevated number of predicted genes caused mainly by the fragmented nature of the assembly and possibly contamination. In fact, pairwise nucleotide similarity searches revealed distinct numbers of unmapped genomic segments in the fragmented drafts in relation to the closed genome. These unmapped genomic segments harbour many transposase, CRISPR-Cas, and secretion system related genes. As previously reported, genes involved in the type IV and type VI secretion systems were identified in *Ridgeia-Riftia-Tevnia*-associated Endoriftia (Gardebrecht et al., 2012; Perez & Juniper, 2016) (Table S1), but not in the closed genome herein described (where only the type II was identified). Protein secretion is key to modulate the interaction between bacteria and their environment (Tseng et al., 2009) and type II and type VI secretion systems have been recognized in other tubeworm endosymbionts. The diversity of secretion systems in Endoriftia may indicate lineage-specific adaptations towards the free-living and host-associated life stages in the different populations.

Orthology inferences performed with the distinct Endoriftia genomes revealed the presence of 1882 orthogroups shared by all the seven genomes, from which 1544 (~82%) were composed of single-copy genes (Figure 5a; Table S1). Only a small number of species-specific orthogroups were identified (i.e., paralogous groups; 32 groups), reinforcing the idea of homogeneity between the different Endoriftia populations (Gardebrecht et al., 2012). The complete and closed genome herein described, as well as the drafts obtained from Polzin et al. (2019) and Gardebrecht et al. (2012), did not contain any lineage-specific paralogous groups. Furthermore, only 18 putative genes present in the complete Endoriftia genome, mostly composed of short repetitive sequences without any sequence similarity against the NCBI nr or eggnog databases, were not assigned to any group.

3.4 | Pangenome of *Ca.* Endoriftia persephone

Since horizontal gene transfer events are pervasive in bacteria, the gene toolkit of an individual bacterial strain or subpopulations is much more restrained than the genetic repertoire of a species (Medini et al., 2005; Mira et al., 2010). The pangenome of Endoriftia based on the publicly available draft genomes and the closed genome (Gardebrecht et al., 2012; Perez & Juniper, 2016; Polzin et al., 2019; Robidart et al., 2008) presents a conserved core (i.e., persistent) represented by ~51% of all endosymbiont orthogroups (3048 genes) (Figure 5b). The shell and cloud orthogroup sets (non-core orthogroups present in more than one endosymbiont genome or lineage-specific genes, respectively), comprise 16.3% (966) and 32.3% (1917) of the total pangenome (Figure 5c). Compared to the previous estimates of Perez and Juniper (2016), the Endoriftia

pangenome described herein presents a higher proportion of shell and cloud genes. Only a small part of the closed Endoriftia genome (1.8%), as well as the draft genome obtained from Polzin et al. (2019) (0.9%), is composed of more phyletically restricted genes. Most of the shell genes belongs to the *Ridgeia piscesae* endosymbionts, whereas the cloud results certainly reflect the overall low quality of the initial Endoriftia draft genome assemblies (>96% of the cloud was unique to Robidart et al. (2008) draft genome; Figure 5c) rather than *bona fide* lineage-specific genes acquired by horizontal gene transfer. Overall, our results indicate that the relatively large size of the variable genomic regions is due to sequencing and assembling biases rather than true biological variability among the different Endoriftia population, as previously discussed by Perez and Juniper (2016).

3.5 | Mobilome of *Ca.* Endoriftia persephone

The acquisition of mobile genetic elements (MGEs) is known to contribute to the evolution of novel traits in bacteria (Ochman et al., 2000). MGEs are important drivers of the genomic plasticity in bacteria and could potentially facilitate host/symbiont interactions (Dietel et al., 2018; Finan, 2002; Newton & Bordenstein, 2011; Ochman & Moran, 2001; Siguier et al., 2014). Here, we fully characterize the mobilome in the closed Endoriftia genome (Figure 6).

We identified signs of a phage infection in the closed Endoriftia genome containing an incomplete ~15.2 kb prophage region that harbours seven phage-like protein interspersed by 11 hypothetical genes without any know function (Figures 6a, S4). Sensitive taxonomic identification of the prophage region pointed to a Caudovirales infection, the most abundant phage order found at hydrothermal vents (Castelán-Sánchez et al., 2019). Therefore, the presence of a single small and incomplete prophage sequence in the closed Endoriftia genome is not surprising, since facultative endosymbiotic bacteria are directly exposed to bacteriophages in both free-living and intracellular environments (Metcalf & Bordenstein, 2012). It is important to stress, however, that low gene density regions containing transposases are present in the closed Endoriftia genome (as well as other Endoriftia genome drafts), which could be an indication of ancient bacteria-phage interactions that evaded software recognition due to sequence erosion. Moreover, we screened and annotated 77 insertion sequences (IS) belonging to known described 31 different IS classes (e.g. ISXac2, ISPsy43; Table S1), hitherto uncharacterised in the Endoriftia genome. Few of these genes possibly encode for functional proteins due to the presence of integrase, core-, and toprim-catalytic domains sequences. The great majority of transposons (mainly DDE-, HTH- classes) found in the closed Endoriftia genome are composed of truncated and degenerated sequences indicative of a lack of complete functional transposases. A comparative study performed with 384 bacterial genomes indicated that ~2.5% of total gene number in facultative intracellular bacteria corresponded to transposon elements (Newton & Bordenstein, 2011). Interestingly, Endoriftia does not harbour as high number transposon-encoding
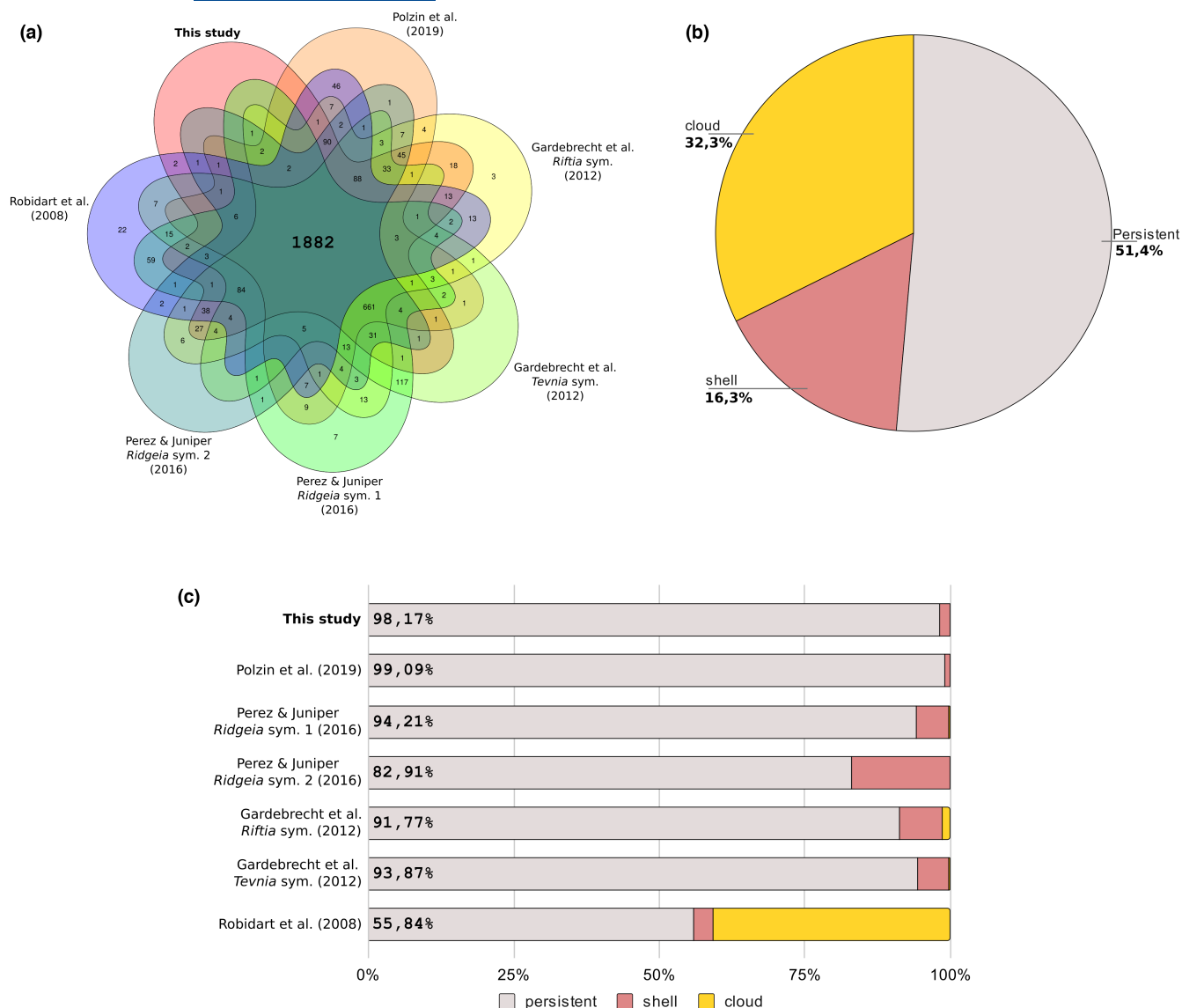
FIGURE 5 Venn diagram and pangenome of *Candidatus* Endoriftia persephone based on six publicly available drafts and the closed genome. (a) Seven set Venn diagram showing the shared orthologous groups among the six publicly available Endoriftia draft genomes and the closed genome herein described. (b) Pangenome of *Candidatus* Endoriftia persephone highlighting the persistent, shell, and cloud gene partitions. (c) Relative number of present in the three different partitions in the seven Endoriftia genomes

sequences in its genome (57 genes/~1.73% of the total number of genes) (Table S1) as would be expected to occur in facultative intracellular endosymbionts (Metcalf & Bordenstein, 2012; Newton & Bordenstein, 2011).

Despite a previous characterization of a putative plasmid containing F-type conjugative proteins (*tra* locus) in *Riftia* 1 endosymbiont genome draft (Gardebrecht et al., 2012), the closed Endoriftia genome, as well as the remaining five investigated draft genomes, do not possess any *tra*-related proteins. It is known that *tra* genes encode a transfer-apparatus that aids conjugative transfer of mobile genetic elements between bacteria, despite the high energetic demand to maintain such system in a cell (Zatyka & Thomas, 1998). This finding calls for questioning this mechanism concerning the possible horizontal gene transfers among the different populations of

Endoriftia. Additionally, we did not identify any extrachromosomal elements in our long-read assembly, as reported in other studies (Gardebrecht et al., 2012; Nelson et al., 1984; Robidart et al., 2008). Finally, we found a gene that encodes a putative reverse transcriptase in the closed Endoriftia genome, which raises the possibility of foreign DNA integration into the bacterial genome.

To complement our mobilome screenings and enrich the catalogue of putative horizontally acquired genes in the closed Endoriftia genome, we employed three different methods of detecting genomic islands (i.e., large genomic regions arisen by horizontal gene transfer) (Langille et al., 2010) (Figure 6a). The number of putative horizontally acquired genomic clusters in the closed genome varies between seven (IslandViewer4) and 22 (alien hunter), ranging from 100 to 225 coding sequence genes (Table S1). Since it is well-described

in the literature that the accuracy of different genomic island prediction methods greatly varies (da Silva Filho et al., 2018; Langille et al., 2010; Lu & Leong, 2016), and many nonoverlapping predictions (Figures 6b,c) were obtained, we focused our discussion on the results supported by more than one method.

We did not identify any lineage-specific genes (i.e., cloud genes) located in the genomic islands of the closed genome. In fact, the genes located in the genomic islands are present in nearly all six Endoriftia draft genomes, indicating that the acquisition of this putative foreign DNA predates the geographical dispersal of the different Endoriftia populations. Genes encoded in the islands contain transposition machinery, electron carrier-, transporter, nutrition-related, signal transduction, stress, and toxin combating, membrane-associated, DNA modification, regulatory, and sulphur metabolism protein-encoding genes. Nearly 45% of the predicted genes present on the genomic islands could not be assigned to any functional category and remain hypothetical in nature (Table S1).

Among these genes, we can highlight the presence of an alternative sigma factor (*algU*), which is involved in the integration of the horizontally acquired genes into the regulatory network of the bacterium host (Huang et al., 2012; Panyukov & Ozoline, 2013), and two copies of carbonic anhydrase (CA): β-CA cytoplasmic –and α-CA periplasmic. We identified a third carbonic anhydrase gene in the persistent genome of Endoriftia, which codes for a γ-CA type. These three known classes are important catalysts for CO_2 hydration reaction in bacteria responsible for not only regulating the intracellular pH (Supuran & Capasso, 2017), but also for the carbon fixation through the Calvin-Benson cycle. They do not present any transmembrane domains and only the α-CA harbours a signal peptide, based upon TMHMM2 and signalP-5.0 predictions, indicating a periplasmatic location. The discovery, sequence characterization and phylogeny of CA genes in Endoriftia genome answers a long-standing hypothesis (De Cian et al., 2003) (Figure 6d), which suggested an orchestration of cytosolic and membrane-bound CA genes in the endosymbiont to efficiently incorporate CO_2 from the external bacteriocyte into the bacterial cytoplasm. Our data clearly shows that Endoriftia lacks membrane-associated CA genes to enhance CO_2 diffusion across the cell membrane. Surprisingly, we could not locate the genes encoding for α- and β-CA on the genomic islands present in the *Ridgeia* draft genomes (Perez & Juniper, 2016) (Figures 6d, S5). However, due the important role of these genes in the host-associated and free-living environments, this absence is probably linked to assembly biases and completeness, rather than secondary losses in this specific Endoriftia population (see Figure 6 legend for more details).

3.6 | Absence of DNA methylation in host associated Endoriftia

Single molecule real time sequencing (SMRT) also provides information on the presence or absence of methyl modification of the genome at adenine or cytosine sites. In fact, DNA methylation is a process involved in a several biological processes in prokaryotes

including regulation of DNA replication, swift responses towards environmental stresses, and host-symbiont interactions (Casadesús & Low, 2006). Here, we investigated the base modification signals corresponding to the m4C and m6A DNA methylation in the closed Endoriftia genome. The modification quality value (QV) data indicated very low values and none of the conserved methylation motifs were detected, which points towards the absence of methylation in the host associated closed Endoriftia genome during our sampling conditions (Figure S6). However, we cannot completely rule out other symbiont subpopulations found in alternative sources (e.g. different parts of the trophosome, symbionts at the free-living stage) that may contain signs of methylation in their genome.

Additionally, we identified in the closed Endoriftia genome an operon containing three contiguous and fragmented N-6 adenine-specific methyltransferase gene copies with different levels of N6_Mtase domain conservation (revealed by hmmsearch analysis against PF02384 model). Neighbouring these three genes is the presence of a gene fragment containing an inactive DDE-type transposase suggesting a phage-mediated gene inactivation. Similarly, bacteria possess restriction-modification (R-M) system to reduce the chance of invading phages (Murray, 2000). Functional type I restriction modification (RM) system comprises three subunits: HsdR, HsdM and HsdS (Murray, 2000). Interestingly, the *hsdS* gene is missing from the closed Endoriftia genome, and the RM system appears to be dysfunctional due the fragmentation of one *hsdM* and two *hsdR* genes. Furthermore, a genomic island of Endoriftia contains a putative 5-methylcytosine-specific restriction endonuclease McrA- and DNA-cytosine methyltransferase Dcm-encoding genes, among which the amino acid sequence of *dcm* gene could not conclusively reveal presence of any active site according to PFAM searches. Overall, the absence of methylation signals indicates that the partial methyltransferase genes are not active in the closed Endoriftia genome described herein due a series of phage transposons insertions. These results hint towards a strong dependency of Endoriftia upon CRISPR-Cas machinery to cope with viral infections.

4 | CONCLUSION

This study reports the closed genome of the facultative generalist *Candidatus* Endoriftia persephone from deep-sea hydrothermal vents. We explored the closed Endoriftia genome to fully characterize the metabolic potential of *Riftia*'s endosymbiont based in a broad comparative approach focused on functional traits. This methodology enabled us to complement and link previous genomic/proteomic studies improving our understanding of Endoriftia's physiology and evolution. Additionally, due the deep long-read sequencing we were able to uncover the full genomic content of Endoriftia allowing the correct identification of many hitherto unknown structural variations and repetitive elements, which will be a valuable resource for genetic diversity studies of uncultured bacterial taxa. The closed
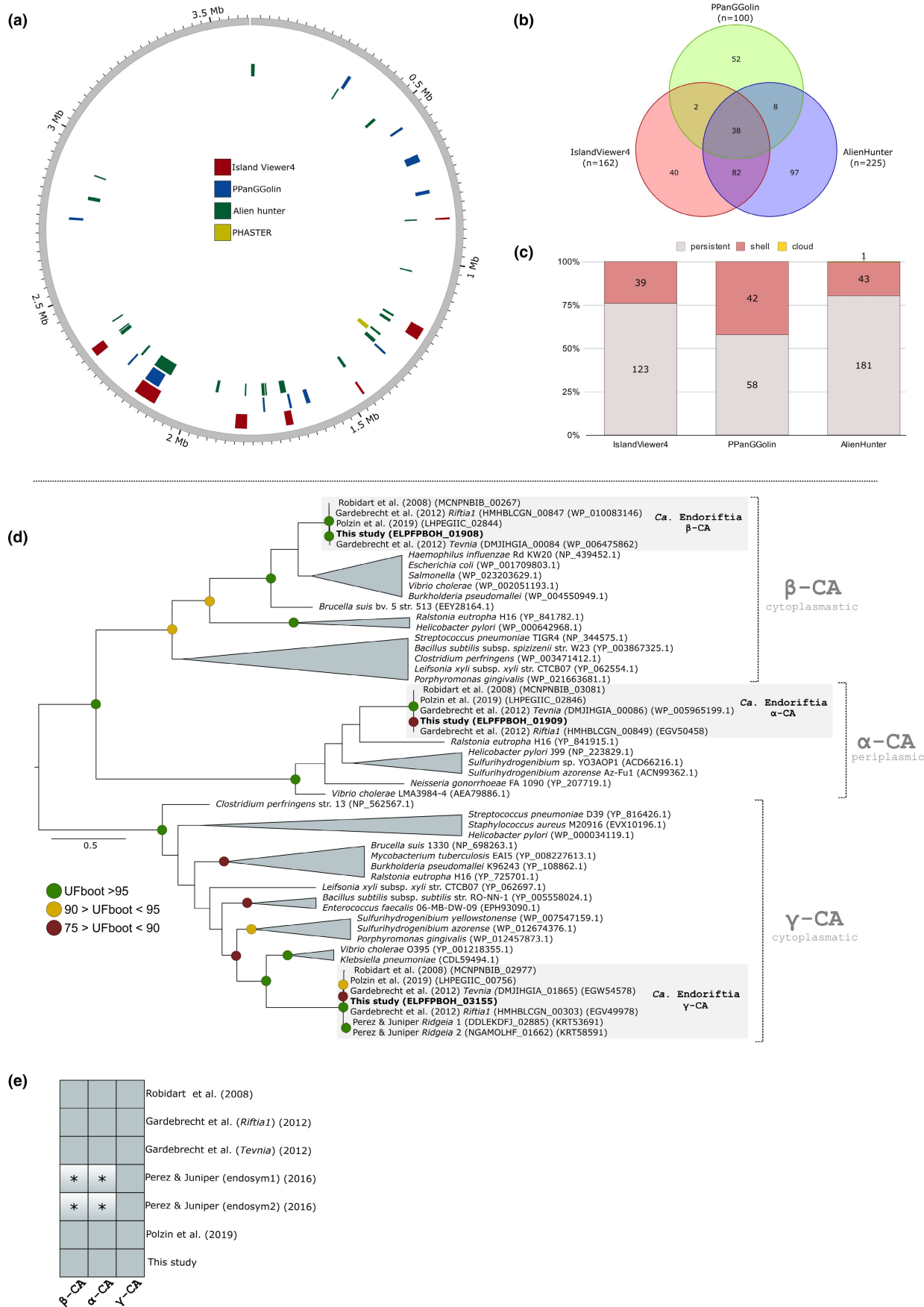
FIGURE 6 The mobilome of *Candidatus* Endoriftia persephone. (a) Genomic islands, and prophage regions identified in the closed Endoriftia genome. (b) Venn diagram depicting the overlapping genomic regions identified in the closed genome using IslandViewer4, alien_hunter and PPanGGOLin. (c) Number of persistent, shell and cloud genes located in the predicted genomic islands. (d) Maximum-likelihood phylogenetic tree of carbonic anhydrase genes using 1000 ultrafast bootstrap replicates. Internal (generated by our annotation pipeline) and external (NCBI accession numbers) Endoriftia proteins ids are displayed in the leaves of the phylogenetic tree. (e) Distribution of carbonic anhydrase genes in the closed Endoriftia genome and in the five publicly available draft genomes. Note that despite we did not identify the genes encoding for α- and β-CA in the *Ridgeia* draft genomes, these genes are indeed present in the raw metagenomic assemblies publicly available at JGI's IMG-Mer database (GOLD analysis ID project: Ga0041824; Draft11_123875, Draft11_123872)

Endoriftia genome also enabled us to identify and annotate genomic regions linked to horizontally transferred events and to analyse the epigenetic landscape in this bacterium, raising interesting questions about the evolution of the methylome and mobilome in facultative endosymbiotic systems. To conclude, the Endoriftia genome is the first closed endosymbiont genome obtained from a vestimentiferan tubeworm and will be valuable for a plethora of comparative physiological and evolutionary studies within the vestimentiferan-microbe mutualism field, as well as many in other metazoan-symbiont systems.

CONFLICT OF INTEREST

The authors declare no conflict of interest.

OPEN RESEARCH BADGES

DATA AVAILABILITY STATEMENT

The raw long-read sequencing data (accession no. SRR15838435) and the complete closed genome (accession no. CP090569) have been deposited in the SRA and GenBank databases under the BioProject PRJNA762254. The CRISPR spacers found in the closed Endoriftia genome, the protein coding sequences, and annotation files generated for the closed Endoriftia genome, as well as intermediary files and in-house bioinformatic scripts used in this manuscript are available in the Data S1.

ORCID

André Luiz De Oliveira https://orcid.org/0000-0003-3542-4439
Abhishek Srivastava https://orcid.org/0000-0002-8459-471X
Salvador Espada-Hinojosa https://orcid.org/0000-0001-9569-409X
Monika Bright https://orcid.org/0000-0001-7066-1363

REFERENCES

Aird, B. A., Heinrikson, R. L., & Westley, J. (1987). Isolation and characterization of a prokaryotic sulfurtransferase. *Journal of Biological Chemistry*, 262(36), 17327–17335.

Alexa, A., Rahnenfuhrer, J., & Lengauer, T. (2006). Improved scoring of functional groups from gene expression data by decorrelating GO graph structure. *Bioinformatics*, 22(13), 1600–1607. https://doi.org/10.1093/bioinformatics/btl140

Anisimova, M., Nielsen, R., & Yang, Z. (2003). Effect of recombination on the accuracy of the likelihood method for detecting positive selection at amino acid sites. *Genetics*, 164(3), 1229–1236. https://doi.org/10.1093/genetics/164.3.1229

Arndt, D., Grant, J. R., Marcu, A., Sajed, T., Pon, A., Liang, Y., & Wishart, D. S. (2016). PHASTER: A better, faster version of the PHAST phage search tool. *Nucleic Acids Research*, 44(W1), W16–W21. https://doi.org/10.1093/nar/gkw387

Badger, M. R., & Bek, E. J. (2008). Multiple Rubisco forms in proteobacteria: Their functional significance in relation to CO_2 acquisition by the CBB cycle. *Journal of Experimental Botany*, 59(7), 1525–1541. https://doi.org/10.1093/jxb/erm297

Bertelli, C., Laird, M. R., Williams, K. P., Fraser University Research Computing Group, S, Lau, B. Y., Hoad, G., Winsor, G. L., & Brinkman, F. S. (2017). IslandViewer 4: Expanded prediction of genomic islands for larger-scale datasets. *Nucleic Acids Research*, 45(W1), W30–W35. https://doi.org/10.1093/nar/gkx343

Bosch, C., & Grassé, P.-P. (1984). Cycle partiel des bactéries chimioautotrophes symbiotiques et leurs rapports avec les bactériocytes chez *Riftia pachyptila* Jones (Pogonophore Vestimentifère). I: Le trophosome et les bactériocytes. *Comptes Rendus Des Séances de l'Académie Des Sciences. Série 3, Sciences de La Vie*, 299(9), 371–376.

Breusing, C., Schultz, D. T., Sudek, S., Worden, A. Z., & Young, C. R. (2020). High-contiguity genome assembly of the chemosynthetic gammaproteobacterial endosymbiont of the cold seep tubeworm

Lamellibrachia barhami. *Molecular Ecology Resources*, 20(5), 1432–1444. https://doi.org/10.1111/1755-0998.13220

Bright, M., & Bulgheresi, S. (2010). A complex journey: Transmission of microbial symbionts. *Nature Reviews Microbiology*, 8(3), 218–230. https://doi.org/10.1038/nrmicro2262

Bright, M., Keckeis, H., & Fisher, C. R. (2000). An autoradiographic examination of carbon fixation, transfer and utilization in the *Riftia pachyptila* symbiosis. *Marine Biology*, 136(4), 621–632. https://doi.org/10.1007/s002270050722

Bright, M., & Lallier, F. (2010). The biology of vestimentiferan tubeworms. In R. N. Gibson, R. J. A. Atkinson, & J. D. M. Gordon (Eds.), *Oceanography and Marine Biology: An animal review* (Vol. 48, pp. 213–265). CRC Press-Taylor & Francis Group. https://hal.archives-ouvertes.fr/hal-01250932

Bright, M., & Sorgo, A. (2003). Ultrastructural reinvestigation of the trophosome in adults of *Riftia pachyptila* (Annelida, Siboglinidae). *Invertebrate Biology*, 122(4), 347–368. https://doi.org/10.1111/j.1744-7410.2003.tb00099.x

Bull, J. J., & Rice, W. R. (1991). Distinguishing mechanisms for the evolution of co-operation. *Journal of Theoretical Biology*, 149(1), 63–74. https://doi.org/10.1016/s0022-5193(05)80072-4

Camacho, C., Coulouris, G., Avagyan, V., Ma, N., Papadopoulos, J., Bealer, K., & Madden, T. L. (2009). BLAST+: Architecture and applications. *BMC Bioinformatics*, 10(1), 421. https://doi.org/10.1186/1471-2105-10-421

Casadesús, J., & Low, D. (2006). Epigenetic gene regulation in the bacterial world. *Microbiology and Molecular Biology Reviews*, 70(3), 830–856. https://doi.org/10.1128/MMBR.00016-06

Castelán-Sánchez, H. G., Lopéz-Rosas, I., García-Suastegui, W. A., Peralta, R., Dobson, A. D. W., Batista-García, R. A., & Dávila-Ramos, S. (2019). Extremophile deep-sea viral communities from hydrothermal vents: Structural and functional analysis. *Marine Genomics*, 46, 16–28. https://doi.org/10.1016/j.margen.2019.03.001

Chao, L. S.-L., Davis, R. E., & Moyer, C. L. (2007). Characterization of bacterial community structure in vestimentiferan tubeworm *Ridgeia piscesae* trophosomes. *Marine Ecology*, 28(1), 72–85.

Childress, J. J., & Girguis, P. R. (2011). The metabolic demands of endosymbiotic chemoautotrophic metabolism on host physiological capacities. *Journal of Experimental Biology*, 214(2), 312–325. https://doi.org/10.1242/jeb.049023

Choby, J. E., & Skaar, E. P. (2016). Heme synthesis and acquisition in bacterial pathogens. *Journal of Molecular Biology*, 428(17), 3408–3428. https://doi.org/10.1016/j.jmb.2016.03.018

Cian, M. D., Regnault, M., & Lallier, F. H. (2000). Nitrogen metabolites and related enzymatic activities in the body fluids and tissues of the hydrothermal vent tubeworm *Riftia pachyptila*. *Journal of Experimental Biology*, 203(19), 2907–2920.

Couvin, D., Bernheim, A., Toffano-Nioche, C., Touchon, M., Michalik, J., Néron, B., Rocha, E. P. C., Vergnaud, G., Gautheret, D., & Pourcel, C. (2018). CRISPRCasFinder, an update of CRISRFinder, includes a portable version, enhanced performance and integrates search for Cas proteins. *Nucleic Acids Research*, 46(W1), W246–W251. https://doi.org/10.1093/nar/gky425

da Silva Filho, A. C., Raittz, R. T., Guizelini, D., De Pierri, C. R., Augusto, D. W., dos Santos-Weiss, I. C. R., & Marchaukoski, J. N. (2018). Comparative analysis of genomic island prediction tools. *Frontiers in Genetics*, 9, 1–15. https://www.frontiersin.org/article/10.3389/fgene.2018.00619

Dahl, C. (2017). Sulfur metabolism in phototrophic bacteria. In P. C. Hallenbeck (Ed.), *modern topics in the phototrophic prokaryotes: metabolism, bioenergetics, and omics* (pp. 27–66). Springer International Publishing. https://doi.org/10.1007/978-3-319-51,365-2_2

Darling, A. E., Mau, B., & Perna, N. T. (2010). progressiveMauve: Multiple genome alignment with gene gain, loss and rearrangement. *PLoS ONE*, 5(6), e11147. https://doi.org/10.1371/journal.pone.0011147

De Cian, M., Andersen, A. C., Toullec, J., Biegala, I. C., Caprais, J., Shillito, B., & Lallier, F. (2003). Isolated bacteriocyte cell suspensions from the hydrothermal-vent tubeworm *Riftia pachyptila*, a potent tool for cellular physiology in a chemoautotrophic symbiosis. *Marine Biology*, 142, 141–151. https://doi.org/10.1007/s00227-002-0931-5

de Oliveira, A. L., Mitchell, J., Girguis, P., & Bright, M. (2021). Novel insights on obligate symbiont lifestyle and adaptation to chemosynthetic environment as revealed by the giant tubeworm genome. *Molecular Biology and Evolution*, msab347, 1–20. https://doi.org/10.1093/molbev/msab347

Di Meo, C. A., Wilbur, A. E., Holben, W. E., Feldman, R. A., Vrijenhoek, R. C., & Cary, S. C. (2000). Genetic variation among endosymbionts of widely distributed vestimentiferan tubeworms. *Applied and Environmental Microbiology*, 66(2), 651–658. https://doi.org/10.1128/AEM.66.2.651-658.2000

Didelot, X., & Wilson, D. J. (2015). ClonalFrameML: Efficient inference of recombination in whole bacterial genomes. *PLOS Computational Biology*, 11(2), e1004041. https://doi.org/10.1371/journal.pcbi.1004041

Dietel, A.-K., Kaltenpoth, M., & Kost, C. (2018). Convergent evolution in intracellular elements: plasmids as model endosymbionts. *Trends in Microbiology*, 26(9), 755–768. https://doi.org/10.1016/j.tim.2018.03.004

Douglas, A. E. (2010). *The symbiotic habit*. Princeton University Press. https://press.princeton.edu/books/paperback/9780691113425/the-symbiotic-habit

Emms, D. M., & Kelly, S. (2019). OrthoFinder: Phylogenetic orthology inference for comparative genomics. *Genome Biology*, 20(1), 238. https://doi.org/10.1186/s13059-019-1832-y

Felbeck, H. (1985). CO_2 fixation in the hydrothermal vent tube worm *Riftia pachyptila* (Jones). *Physiological Zoology*, 58(3), 272–281.

Felbeck, H., & Jarchow, J. (1998). Carbon release from purified chemoautotrophic bacterial symbionts of the hydrothermal vent tubeworm *Riftia pachyptila*. *Physiological Zoology*, 71(3), 294–302. https://doi.org/10.1086/515931

Feldman, R. A., Black, M. B., Cary, C. S., Lutz, R. A., & Vrijenhoek, R. C. (1997). Molecular phylogenetics of bacterial endosymbionts and their vestimentiferan hosts. *Molecular Marine Biology and Biotechnology*, 6(3), 268–277.

Finan, T. M. (2002). Evolving insights: Symbiosis islands and horizontal gene transfer. *Journal of Bacteriology*, 184(11), 2855–2856. https://doi.org/10.1128/JB.184.11.2855-2856.2002

Fletcher, J. A., & Doebeli, M. (2009). A simple and general explanation for the evolution of altruism. *Proceedings of the Royal Society B: Biological Sciences*, 276(1654), 13–19. https://doi.org/10.1098/rspb.2008.0829

Flood, B. E., Jones, D. S., & Bailey, J. V. (2015). Complete genome sequence of *Sedimenticola thiotaurini* strain SIP-G1, a polyphosphate- and polyhydroxyalkanoate-accumulating sulfur-oxidizing gammaproteobacterium isolated from salt marsh sediments. *Genome Announcements*, 3(3), 1–2. https://doi.org/10.1128/genomeA.00671-15

Gardebrecht, A., Markert, S., Sievert, S. M., Felbeck, H., Thürmer, A., Albrecht, D., Wollherr, A., Kabisch, J., Le Bris, N., Lehmann, R., Daniel, R., Liesegang, H., Hecker, M., & Schweder, T. (2012). Physiological homogeneity among the endosymbionts of *Riftia pachyptila* and *Tevnia jerichonana* revealed by proteogenomics. *ISME Journal*, 6(4), 766–776. https://doi.org/10.1038/ismej.2011.137

Gautreau, G., Bazin, A., Gachet, M., Planel, R., Burlot, L., Dubois, M., Perrin, A., Médigue, C., Calteau, A., Cruveiller, S., Matias, C., Ambroise, C., Rocha, E. P. C., & Vallenet, D. (2020). PPanGGOLiN: Depicting microbial diversity via a partitioned pangenome graph. *PLOS Computational Biology*, 16(3), e1007732. https://doi.org/10.1371/journal.pcbi.1007732

Genkai-Kato, M., & Yamamura, N. (1999). Evolution of mutualistic symbiosis without vertical transmission. *Theoretical Population Biology*, 55(3), 309–323. https://doi.org/10.1006/tpbi.1998.1407

Girguis, P. R., Lee, R. W., Desaulniers, N., Childress, J. J., Pospesel, M., Felbeck, H., & Zal, F. (2000). Fate of nitrate acquired by

the tubeworm *Riftia pachyptila*. *Applied and Environmental Microbiology*, *66*(7), 2783–2790. https://doi.org/10.1128/AEM.66.7.2783-2790.2000

Green, J. L., Bohannan, B. J. M., & Whitaker, R. J. (2008). Microbial biogeography: From taxonomy to traits. *Science.*, *320*, 1039–1043. https://doi.org/10.1126/science.1153475

Hand, S. C. (1987). Trophosome ultrastructure and the characterization of isolated bacteriocytes from invertebrate-sulfur bacteria symbioses. *Biological Bulletin*, *173*(1), 260–276. https://doi.org/10.2307/1541878

Harmer, T. L., Rotjan, R. D., Nussbaumer, A. D., Bright, M., Ng, A. W., DeChaine, E. G., & Cavanaugh, C. M. (2008). Free-living tube worm endosymbionts found at deep-sea vents. *Applied and Environmental Microbiology*, *74*(12), 3895–3898. https://doi.org/10.1128/AEM.02470-07

Heath, K. D., & Stinchcombe, J. R. (2014). Explaining mutualism variation: A new evolutionary paradox? *Evolution: International Journal of Organic Evolution*, *68*(2), 309–317. https://doi.org/10.1111/evo.12292

Hinzke, T., Kleiner, M., Breusing, C., Felbeck, H., Häsler, R., Sievert, S. M., Schlüter, R., Rosenstiel, P., Reusch, T. B. H., Schweder, T., & Markert, S. (2019). Host-microbe interactions in the chemosynthetic *Riftia pachyptila* symbiosis. *Host–Microbe Interactions in the Chemosynthetic Riftia pachyptila Symbiosis*, *10*(6), 20.

Hinzke, T., Kleiner, M., Meister, M., Schlüter, R., Hentschker, C., Pané-Farré, J., Hildebrandt, P., Felbeck, H., Sievert, S. M., Bonn, F., Völker, U., Becher, D., Schweder, T., & Markert, S. (2021). Bacterial symbiont subpopulations have different roles in a deep-sea symbiosis. *eLife*, *10*, e58371. https://doi.org/10.7554/eLife.58371

Hoang, D. T., Chernomor, O., von Haeseler, A., Minh, B. Q., & Vinh, L. S. (2018). UFBoot2: Improving the ultrafast bootstrap approximation. *Molecular Biology and Evolution*, *35*(2), 518–522. https://doi.org/10.1093/molbev/msx281

Hryniewicz, M., Sirko, A., Pałucha, A., Böck, A., & Hulanicka, D. (1990). Sulfate and thiosulfate transport in *Escherichia coli* K-12: Identification of a gene encoding a novel protein involved in thiosulfate binding. *Journal of Bacteriology*, *172*(6), 3358–3366. https://doi.org/10.1128/jb.172.6.3358-3366.1990

Hua, X., Liang, Q., Deng, M., He, J., Wang, M., Hong, W., Wu, J., Lu, B., Leptihn, S., Yu, Y., & Chen, H. (2021). BacAnt: A combination annotation server for bacterial dna sequences to identify antibiotic resistance genes, integrons, and transposable elements. *Frontiers in Microbiology*, *12*, 2015. https://doi.org/10.3389/fmicb.2021.649969

Huang, Q., Cheng, X., Cheung, M. K., Kiselev, S. S., Ozoline, O. N., & Kwan, H. S. (2012). High-density transcriptional initiation signals underline genomic islands in bacteria. *PLoS ONE*, *7*(3), e33759. https://doi.org/10.1371/journal.pone.0033759

Huerta-Cepas, J., Forslund, K., Coelho, L. P., Szklarczyk, D., Jensen, L. J., von Mering, C., & Bork, P. (2017). Fast genome-wide functional annotation through orthology assignment by eggNOG-Mapper. *Molecular Biology and Evolution*, *34*(8), 2115–2122. https://doi.org/10.1093/molbev/msx148

Huerta-Cepas, J., Szklarczyk, D., Heller, D., Hernández-Plaza, A., Forslund, S. K., Cook, H., Mende, D. R., Letunic, I., Rattei, T., Jensen, L. J., von Mering, C., & Bork, P. (2019). eggNOG 5.0: A hierarchical, functionally and phylogenetically annotated orthology resource based on 5090 organisms and 2502 viruses. *Nucleic Acids Research*, *47*(D1), D309–D314. https://doi.org/10.1093/nar/gky1085

Jones, P., Binns, D., Chang, H.-Y., Fraser, M., Li, W., McAnulla, C., McWilliam, H., Maslen, J., Mitchell, A., Nuka, G., Pesseat, S., Quinn, A. F., Sangrador-Vegas, A., Scheremetjew, M., Yong, S.-Y., Lopez, R., & Hunter, S. (2014). InterProScan 5: Genome-scale protein function classification. *Bioinformatics*, *30*(9), 1236–1240. https://doi.org/10.1093/bioinformatics/btu031

Kalyaanamoorthy, S., Minh, B. Q., Wong, T. K. F., von Haeseler, A., & Jermiin, L. S. (2017). ModelFinder: Fast model selection for accurate phylogenetic estimates. *Nature Methods*, *14*(6), 587–589. https://doi.org/10.1038/nmeth.4285

Kichenaradja, P., Siguier, P., Pérochon, J., & Chandler, M. (2010). ISbrowser: An extension of ISfinder for visualizing insertion sequences in prokaryotic genomes. *Nucleic Acids Research*, *38*(Database issue), D62-68. https://doi.org/10.1093/nar/gkp947

Klassen, J. L., & Currie, C. R. (2012). Gene fragmentation in bacterial draft genomes: Extent, consequences and mitigation. *BMC Genomics*, *13*, 14. https://doi.org/10.1186/1471-2164-13-14

Kleiner, M., Petersen, J. M., & Dubilier, N. (2012). Convergent and divergent evolution of metabolism in sulfur-oxidizing symbionts and the role of horizontal gene transfer. *Current Opinion in Microbiology*, *15*(5), 621–631. https://doi.org/10.1016/j.mib.2012.09.003

Klose, J., Polz, M. F., Wagner, M., Schimak, M. P., Gollner, S., & Bright, M. (2015). Endosymbionts escape dead hydrothermal vent tubeworms to enrich the free-living population. *Proceedings of the National Academy of Sciences*, *112*(36), 11,300–11,305. https://doi.org/10.1073/pnas.1501160112

Kolmogorov, M., Yuan, J., Lin, Y., & Pevzner, P. A. (2019). Assembly of long, error-prone reads using repeat graphs. *Nature Biotechnology*, *37*(5), 540–546. https://doi.org/10.1038/s41587-019-0072-8

Krzywinski, M., Schein, J., Birol, İ., Connors, J., Gascoyne, R., Horsman, D., Jones, S. J., & Marra, M. A. (2009). Circos: An information aesthetic for comparative genomics. *Genome Research*, *19*(9), 1639–1645. https://doi.org/10.1101/gr.092759.109

Kück, P., & Meusemann, K. (2010). FASconCAT: Convenient handling of data matrices. *Molecular Phylogenetics and Evolution*, *56*(3), 1115–1118. https://doi.org/10.1016/j.ympev.2010.04.024

Langille, M. G. I., Hsiao, W. W. L., & Brinkman, F. S. L. (2010). Detecting genomic islands using bioinformatics approaches. *Nature Reviews Microbiology*, *8*(5), 373–382. https://doi.org/10.1038/nrmicro2350

Lee, I., Ouk Kim, Y., Park, S.-C., & Chun, J. (2016). OrthoANI: An improved algorithm and software for calculating average nucleotide identity. *International Journal of Systematic and Evolutionary Microbiology*, *66*(2), 1100–1103. https://doi.org/10.1099/ijsem.0.000760

Leonard, J. M., Mitchell, J., Beinart, R. A., Delaney, J. A., Sanders, J. G., Ellis, G., Goddard, E. A., Girguis, P. R., & Scott, K. M. (2021). Cooccurring activities of two autotrophic pathways in symbionts of the hydrothermal vent tubeworm *Riftia pachyptila*. *Applied and Environmental Microbiology*, *87*(17), e0079421. https://doi.org/10.1128/AEM.00794-21

Li, Y., Liles, M. R., & Halanych, K. M. (2018). Endosymbiont genomes yield clues of tubeworm success. *ISME Journal*, *12*(11), 2785–2795. https://doi.org/10.1038/s41396-018-0220-z

Li, Y., Tassia, M. G., Waits, D. S., Bogantes, V. E., David, K. T., & Halanych, K. M. (2019). Genomic adaptations to chemosymbiosis in the deep-sea seep-dwelling tubeworm Lamellibrachia luymesi. *BMC Biology*, *17*(1), 91. https://doi.org/10.1186/s12915-019-0713-x

Louie, T. S., Giovannelli, D., Yee, N., Narasingarao, P., Starovoytov, V., Göker, M., Klenk, H.-P., Lang, E., Kyrpides, N. C., Woyke, T., Bini, E., & Häggblom, M. M. (2016). High-quality draft genome sequence of *Sedimenticola selenatireducens* strain AK4OH1T, a gammaproteobacterium isolated from estuarine sediment. *Standards in Genomic Sciences*, *11*(1), 66. https://doi.org/10.1186/s40793-016-0191-5

Lu, B., & Leong, H. W. (2016). Computational methods for predicting genomic islands in microbial genomes. *Computational and Structural Biotechnology Journal*, *14*, 200–206. https://doi.org/10.1016/j.csbj.2016.05.001

Markert, S., Arndt, C., Felbeck, H., Becher, D., Sievert, S. M., Hügler, M., Albrecht, D., Robidart, J., Bench, S., Feldman, R. A., Hecker, M., & Schweder, T. (2007). Physiological proteomics of the uncultured endosymbiont of *Riftia pachyptila*. *Science*, *315*(5809), 247–250. https://doi.org/10.1126/science.1132913

Mcullin, E., Hourdez, S., Schaeffer, S., & Fisher, C. (2003). Phylogeny and biogeography of deep sea vestimentiferan tubeworms and their bacterial symbionts. *Symbiosis*, *34*, 1–41.

Medini, D., Donati, C., Tettelin, H., Masignani, V., & Rappuoli, R. (2005). The microbial pan-genome. *Current Opinion in Genetics & Development*, *15*(6), 589–594. https://doi.org/10.1016/j.gde.2005.09.006

Metcalf, J. A., & Bordenstein, S. R. (2012). The complexity of virus systems: the case of endosymbionts. *Current Opinion in Microbiology*, *15*(4), 546–552. https://doi.org/10.1016/j.mib.2012.04.010

Minic, Z., & Hervé, G. (2004). Biochemical and enzymological aspects of the symbiosis between the deep-sea tubeworm *Riftia pachyptila* and its bacterial endosymbiont: *Riftia pachyptila* and its bacterial endosymbiont. *European Journal of Biochemistry*, *271*(15), 3093–3102. https://doi.org/10.1111/j.1432-1033.2004.04248.x

Mira, A., Martín-Cuadrado, A. B., D'Auria, G., & Rodríguez-Valera, F. (2010). The bacterial pan-genome:a new paradigm in microbiology. *International Microbiology: The Official Journal of the Spanish Society for Microbiology*, *13*(2), 45–57. https://doi.org/10.2436/20.1501.01.110

Mitchell, J. H., Leonard, J. M., Delaney, J., Girguis, P. R., & Scott, K. M. (2019). Hydrogen does not appear to be a major electron donor for symbiosis with the deep-sea hydrothermal vent tubeworm *Riftia pachyptila*. *Applied and Environmental Microbiology*, *86*(1), e01522–e01519. https://doi.org/10.1128/AEM.01522-19

Moreno-Vivián, C., Cabello, P., Martínez-Luque, M., Blasco, R., & Castillo, F. (1999). Prokaryotic nitrate reduction: Molecular properties and functional distinction among bacterial nitrate reductases. *Journal of Bacteriology.*, *181*, 6573–6584. https://doi.org/10.1128/JB.181.21.6573-6584.1999

Moriya, Y., Itoh, M., Okuda, S., Yoshizawa, A. C., & Kanehisa, M. (2007). KAAS: An automatic genome annotation and pathway reconstruction server. *Nucleic Acids Research*, *35*(Web Server), W182–W185. https://doi.org/10.1093/nar/gkm321

Murray, N. E. (2000). Type I restriction systems: Sophisticated molecular machines (a legacy of Bertani and Weigle). *Microbiology and Molecular Biology Reviews: MMBR*, *64*(2), 412–434. https://doi.org/10.1128/MMBR.64.2.412-434.2000

Nelson, D. C., Waterbury, J. B., & Jannasch, H. W. (1984). DNA base composition and genome size of the prokaryotic symbiont in *Riftia pachyptila* (Pogonophora). *FEMS Microbiology Letters*, *24*(2–3), 267–271. https://doi.org/10.1111/j.1574-6968.1984.tb01317.x

Nelson, K., & Fisher, C. R. (2000). Absence of cospeciation in deep-sea vestimentiferan tube worms and their bacterial endosymbionts. *Symbiosis*, *28*(1), 1–15.

Newton, I. L. G., & Bordenstein, S. R. (2011). Correlations between bacterial ecology and mobile DNA. *Current Microbiology*, *62*(1), 198–208. https://doi.org/10.1007/s00284-010-9693-3

Ng, K. Y., Kamimura, K., & Sugio, T. (2000). Production of hydrogen sulfide from tetrathionate by the iron-oxidizing bacterium *Thiobacillus ferrooxidans* NASF-1. *Journal of Bioscience and Bioengineering*, *90*(2), 193–198. https://doi.org/10.1016/s1389-1723(00)80109-7

Nguyen, L.-T., Schmidt, H. A., von Haeseler, A., & Minh, B. Q. (2015). IQ-TREE: A fast and effective stochastic algorithm for estimating maximum-likelihood phylogenies. *Molecular Biology and Evolution*, *32*(1), 268–274. https://doi.org/10.1093/molbev/msu300

Novikoff, A. B. (1945). The concept of integrative levels and biology. *Science*, *101*(2618), 209–215.

Nunoura, T., Chikaraishi, Y., Izaki, R., Suwa, T., Sato, T., Harada, T., Mori, K., Kato, Y., Miyazaki, M., Shimamura, S., Yanagawa, K., Shuto, A., Ohkouchi, N., Fujita, N., Takaki, Y., Atomi, H., & Takai, K. (2018). A primordial and reversible TCA cycle in a facultatively chemolithoautotrophic thermophile. *Science*, *359*(6375), 559–563. https://doi.org/10.1126/science.aao3407

Nurk, S., Meleshko, D., Korobeynikov, A., & Pevzner, P. A. (2017). metaSPAdes: A new versatile metagenomic assembler. *Genome Research*, *27*(5), 824–834. https://doi.org/10.1101/gr.213959.116

Nussbaumer, A. D., Fisher, C. R., & Bright, M. (2006). Horizontal endosymbiont transmission in hydrothermal vent tubeworms. *Nature*, *441*(7091), 345–348. https://doi.org/10.1038/nature04793

Ochman, H., Lawrence, J. G., & Groisman, E. A. (2000). Lateral gene transfer and the nature of bacterial innovation. *Nature*, *405*(6784), 299–304. https://doi.org/10.1038/35012500

Ochman, H., & Moran, N. A. (2001). Genes lost and genes found: Evolution of bacterial pathogenesis and symbiosis. *Science*, *292*(5519), 1096–1099. https://doi.org/10.1126/science.1058543

Panyukov, V. V., & Ozoline, O. N. (2013). Promoters of *Escherichia coli* versus promoter Islands: Function and structure comparison. *PLoS ONE*, *8*(5), e62601. https://doi.org/10.1371/journal.pone.0062601

Parks, D. H., Imelfort, M., Skennerton, C. T., Hugenholtz, P., & Tyson, G. W. (2015). CheckM: Assessing the quality of microbial genomes recovered from isolates, single cells, and metagenomes. *Genome Research*, *25*(7), 1043–1055. https://doi.org/10.1101/gr.186072.114

Perez, M., Angers, B., Young, C. R., & Juniper, S. K. (2021). Shining light on a deep-sea bacterial symbiont population structure with CRISPR. *Microbial Genomics*, *7*(8), 000625. https://doi.org/10.1099/mgen.0.000625

Perez, M., & Juniper, S. K. (2016). Insights into symbiont population structure among three vestimentiferan tubeworm host species at eastern pacific spreading centers. *Applied and Environmental Microbiology*, *82*(17), 5197–5205. https://doi.org/10.1128/AEM.00953-16

Pflugfelder, B., Fisher, C. R., & Bright, M. (2005). The color of the trophosome: elemental sulfur distribution in the endosymbionts of Riftia pachyptila (Vestimentifera; Siboglinidae). *Marine Biology*, *146*(5), 895–901.

Pitcher, R. S., & Watmough, N. J. (2004). The bacterial cytochrome cbb3 oxidases. *Biochimica Et Biophysica Acta*, *1655*(1–3), 388–399. https://doi.org/10.1016/j.bbabio.2003.09.017

Polzin, J., Arevalo, P., Nussbaumer, T., Polz, M. F., & Bright, M. (2019). Polyclonal symbiont populations in hydrothermal vent tubeworms and the environment. *Proceedings of the Royal Society B: Biological Sciences*, *286*(1896), 1–9. https://doi.org/10.1098/rspb.2018.1281

Queller, D. C. (1985). Kinship, reciprocity and synergism in the evolution of social behaviour. *Nature*, *318*(6044), 366–367. https://doi.org/10.1038/318366a0

Reveillaud, J., Anderson, R., Reves-Sohn, S., Cavanaugh, C., & Huber, J. A. (2018). Metagenomic investigation of vestimentiferan tubeworm endosymbionts from Mid-Cayman Rise reveals new insights into metabolism and diversity. *Microbiome*, *6*(1), 19. https://doi.org/10.1186/s40168-018-0411-x

Robidart, J. C., Bench, S. R., Feldman, R. A., Novoradovsky, A., Podell, S. B., Gaasterland, T., Allen, E. E., & Felbeck, H. (2008). Metabolic versatility of the *Riftia pachyptila* endosymbiont revealed through metagenomics. *Environmental Microbiology*, *10*(3), 727–737. https://doi.org/10.1111/j.1462-2920.2007.01496.x

Rubin-Blum, M., Dubilier, N., & Kleiner, M. (2019). Genetic evidence for two carbon fixation pathways (the calvin-benson-bassham cycle and the reverse tricarboxylic acid cycle) in symbiotic and free-living bacteria. *MSphere*, *4*(1), e00394–e00318. https://doi.org/10.1128/mSphere.00394-18

Sachs, J. L., Essenberg, C. J., & Turcotte, M. M. (2011). New paradigms for the evolution of beneficial infections. *Trends in Ecology & Evolution*, *26*(4), 202–209. https://doi.org/10.1016/j.tree.2011.01.010

Sachs, J. L., Kembel, S. W., Lau, A. H., & Simms, E. L. (2009). In situ phylogenetic structure and diversity of wild Bradyrhizobium communities. *Applied and Environmental Microbiology*, *75*(14), 4727–4735. https://doi.org/10.1128/AEM.00667-09

Scott, K. M., Bright, M., Macko, S. A., & Fisher, C. R. (1999). Carbon dioxide use by chemoautotrophic endosymbionts of hydrothermal vent vestimentiferans: Affinities for carbon dioxide, absence of carboxysomes, and δ 13 C values. *Marine Biology*, *135*(1), 25–34. https://doi.org/10.1007/s002270050597

Seemann, T. (2014). Prokka: Rapid prokaryotic genome annotation. *Bioinformatics*, *30*(14), 2068–2069. https://doi.org/10.1093/bioinformatics/btu153

Siguier, P., Gourbeyre, E., & Chandler, M. (2014). Bacterial insertion sequences: Their genomic impact and diversity. *FEMS Microbiology Reviews*, *38*(5), 865–891. https://doi.org/10.1111/1574-6976.12067

Siguier, P., Perochon, J., Lestrade, L., Mahillon, J., & Chandler, M. (2006). ISfinder: The reference centre for bacterial insertion sequences. *Nucleic Acids Research*, *34*(Database issue), D32-36. https://doi.org/10.1093/nar/gkj014

Sorgo, A., Gaill, F., Lechaire, J., Arndt, C., & Bright, M. (2002). Glycogen storage in the *Riftia pachyptila* trophosome: Contribution of host and symbionts. *Marine Ecology Progress Series*, *231*, 115–120. https://doi.org/10.3354/meps231115

Sorokin, D. Y., de Jong, G. A., Robertson, L. A., & Kuenen, G. J. (1998). Purification and characterization of sulfide dehydrogenase from alkaliphilic chemolithoautotrophic sulfur-oxidizing bacteria. *FEBS Letters*, *427*(1), 11–14. https://doi.org/10.1016/s0014-5793(98)00379-2

Supuran, C. T., & Capasso, C. (2017). An overview of the bacterial carbonic anhydrases. *Metabolites*, *7*(4), 56. https://doi.org/10.3390/metabo7040056

Suyama, M., Torrents, D., & Bork, P. (2006). PAL2NAL: Robust conversion of protein sequence alignments into the corresponding codon alignments. *Nucleic Acids Research*, *34*(Web Server), W609–W612. https://doi.org/10.1093/nar/gkl315

Tanaka, Y., Yoshikaie, K., Takeuchi, A., Ichikawa, M., Mori, T., Uchino, S., Sugano, Y., Hakoshima, T., Takagi, H., Nonaka, G., & Tsukazaki, T. (2020). Crystal structure of a YeeE/YedE family protein engaged in thiosulfate uptake. Science. *Advances*, *6*(35), eaba7637. https://doi.org/10.1126/sciadv.aba7637

Trumpower, B. L. (1990). Cytochrome bc1 complexes of microorganisms. *Microbiological Reviews*, *54*(2), 101–129. https://doi.org/10.1128/mr.54.2.101-129.1990

Tseng, T.-T., Tyler, B. M., & Setubal, J. C. (2009). Protein secretion systems in bacterial-host associations, and their description in the Gene Ontology. *BMC Microbiology*, *9*(1), S2. https://doi.org/10.1186/1471-2180-9-S1-S2

Van den Ent, F., Leaver, M., Bendezu, F., Errington, J., De Boer, P., & Löwe, J. (2006). Dimeric structure of the cell shape protein MreC and its functional implications. *Molecular Microbiology*, *62*(6), 1631–1642. https://doi.org/10.1111/j.1365-2958.2006.05485.x

Vrijenhoek, R. C. (2010). Genetics and evolution of deep-sea chemosynthetic bacteria and their invertebrate hosts. In S. Kiel (Ed.), *The vent and seep biota: Aspects from microbes to ecosystems* (pp. 15–49). Springer Netherlands. https://doi.org/10.1007/978-90-481-9572-5_2

Welte, C., Hafner, S., Krätzer, C., Quentmeier, A., Friedrich, C. G., & Dahl, C. (2009). Interaction between Sox proteins of two physiologically distinct bacteria and a new protein involved in thiosulfate oxidation. *FEBS Letters*, *583*(8), 1281–1286. https://doi.org/10.1016/j.febslet.2009.03.020

Wenger, A. M., Peluso, P., Rowell, W. J., Chang, P.-C., Hall, R. J., Concepcion, G. T., Ebler, J., Fungtammasan, A., Kolesnikov, A., Olson, N. D., Töpfer, A., Alonge, M., Mahmoud, M., Qian, Y., Chin, C.-S., Phillippy, A. M., Schatz, M. C., Myers, G., DePristo, M. A., … Hunkapiller, M. W. (2019). Accurate circular consensus long-read sequencing improves variant detection and assembly of a human genome. *Nature Biotechnology*, *37*(10), 1155–1162. https://doi.org/10.1038/s41587-019-0217-9

Westra, E. R., Dowling, A. J., Broniewski, J. M., & van Houte, S. (2016). Evolution and ecology of CRISPR. *Annual Review of Ecology, Evolution, and Systematics*, *47*, 307–331.

Wollenberg, M. S., & Ruby, E. G. (2009). Population structure of *Vibrio fischeri* within the light organs of Euprymna scolopes squid from Two Oahu (Hawaii) populations. *Applied and Environmental Microbiology*, *75*(1), 193–202. https://doi.org/10.1128/AEM.01792-08

Yang, Y., Sun, J., Sun, Y., Kwan, Y. H., Wong, W. C., Zhang, Y., Xu, T., Feng, D., Zhang, Y., Qiu, J.-W., & Qian, P.-Y. (2020). Genomic, transcriptomic, and proteomic insights into the symbiosis of deep-sea tubeworm holobionts. *ISME Journal*, *14*(1), 135–150. https://doi.org/10.1038/s41396-019-0520-y

Yang, Z. (2007). PAML 4: Phylogenetic analysis by maximum likelihood. *Molecular Biology and Evolution*, *24*(8), 1586–1591. https://doi.org/10.1093/molbev/msm088

Zatyka, M., & Thomas, C. M. (1998). Control of genes for conjugative transfer of plasmids and other mobile elements. *FEMS Microbiology Reviews*, *21*(4), 291–319. https://doi.org/10.1111/j.1574-6976.1998.tb00355.x

Zhang, J., Nielsen, R., & Yang, Z. (2005). Evaluation of an improved branch-site likelihood method for detecting positive selection at the molecular level. *Molecular Biology and Evolution*, *22*(12), 2472–2479. https://doi.org/10.1093/molbev/msi237

Zhang, R., Mirdita, M., Levy Karin, E., Norroy, C., Galiez, C., & Söding, J. (2021). SpacePHARER: Sensitive identification of phages from CRISPR spacers in prokaryotic hosts. *Bioinformatics*, *37*(19), 3364–3366. https://doi.org/10.1093/bioinformatics/btab222

Zhou, Y., Liang, Y., Lynch, K. H., Dennis, J. J., & Wishart, D. S. (2011). PHAST: A fast phage search tool. *Nucleic Acids Research*, *39*(Web Server issue), W347–W352. https://doi.org/10.1093/nar/gkr485

Zolotarev, A. S., Unnikrishnan, M., Shmukler, B. E., Clark, J. S., Vandorpe, D. H., Grigorieff, N., Rubin, E. J., & Alper, S. L. (2008). Increased sulfate uptake by *E. coli* overexpressing the SLC26-related SulP protein Rv1739c from *Mycobacterium tuberculosis*. *Comparative Biochemistry and Physiology. Part A, Molecular & Integrative Physiology*, *149*(3), 255–266. https://doi.org/10.1016/j.cbpa.2007.12.005

Zumft, W. G. (1997). Cell biology and molecular basis of denitrification. *Microbiology and Molecular Biology Reviews: MMBR*, *61*(4), 533–616. https://doi.org/10.1128/mmbr.61.4.533-616.1997

SUPPORTING INFORMATION

Additional supporting information can be found online in the Supporting Information section at the end of this article.

Conclusions and Outlook

Microbe - eukaryote mutualisms are remarkably diverse with respect of the number of microbial partners. The human gut harbors a microbial community of 10^{13} microbial cells with more than 2000 species (Sender et al. 2016, Thursby and Juge 2017). In contrast, a *Zoothamnium niveum* colony is covered by a population of around half a million bacterial cells of a single microbial phylotype, *Candidatus* Thiobius zoothamnicola, not counting the possible unspecific overgrowth at the base of its acellular stalk. According to evolutionary game theory, we consider that the relationship between *Zoothamnium niveum* and *Candidatus* Thiobius zoothamnicola is a one-to-one, binary relationship. This most simple situation is by far the exception rather than the rule in nature, but allows to develop better theoretical models to assess the effect of one partner on the other.

In **Chapter 2** we demonstrated that *Candidatus* Thiobius zoothamnicola performs carbon fixation when exposed to sulfide and oxygen, and part of the fixed carbon is transferred to the *Zoothamnium niveum* colonies hosting them on their surfaces. This happens through both milking and farming. In the milking process, the bacterial cell passively leaks part of the low molecular weight organic carbon resulting from its chemosynthetic activity and the host acquires it. In the farming process, detached symbiont cells are ingested by the filter feeding host. While farming benefits the host, it is costly for the symbiont. In contrast, the milking process is considered a byproduct the symbiont provides to the host at no extra costs. We further found that the leakage to the host remains stable regardless of environmental conditions. This indicates that neither symbiont nor host are able to control the transfer of byproducts.

In **Chapter 3**, we disrupt the environment by shutting down sulfide supply, a naturally occurring perturbation in the giant ciliate habitat. Ultimately the colony dies, and the fate of the symbiont still covering the dead colony remains to be further followed, but prior death the host releases its next generation. We observed, however, a reduction in efficiency in the reproductive effort of the ciliate, because the colony must produce a surplus of new macrozooids to keep pace with the release of swarmers for granting chance to seed a new

generation. Ten new macrozooids have to be produced under sulfide starvation for the effective release of six swarmers, in comparison with a one-to-one ratio of macrozooids and swarmers in the presence of sulfide. Overall, this association is well adapted to its notoriously instable environment.

In **Chapter 4** we discovered that the host *Zoothamnium niveum* retains the possibility to play the loner strategy when losing the symbiont in the swarmer dispersal stage, showing a polyphenism in which the aposymbiotic host resembles the ancestral colony shape of the *Zoothamnium* genus, broader and shorter than the symbiotic morph, with more zooids in each branch. This is to our knowledge the first time polyphenism has been shown in a mutualism, being induced by the presence of the symbiont. The taller shape of the symbiotic colonies could be adaptive as it could better mix sulfidic and oxic seawater and provide better access of these chemicals to the symbionts. In a sense the symbiotic *Zoothamnium niveum* colonies act as skyscrapers for their thiotrophic symbiont. Because the host has been detected already also in the environment in very low numbers, this retained capability of the host to live aposymbiotically, opens new questions about its potential capability to reacquire the symbionts. As of yet we have not discovered a free-living symbiont population but other possibilities such as horizontal transfer from others symbiotic colonies may be possible. Additionally, we observed a negative effect of sulfide in the maximal size of the aposymbiotic colonies compared to the size of aposymbiotic colonies grown under oxic conditions. This indicates a possible effect of sulfide detoxification by the symbiont as an additional byproduct commodity to the host.

In **Chapters 5 and 6**, applying genomics and metagenomics, we addressed two contrasting bacterial symbionts, *Candidatus* Thiobius zoothamnicola and *Candidatus* Endoriftia persephone, both belonging to the same family Sedimenticolaceae. *Candidatus* Thiobius zoothamnicola is a vertically transmitted, obligate ectosymbiont, *Candidatus* Endoriftia persephone is a horizontally transmitted, facultative endosymbiont. While vertically transmitted endosymbionts have smaller genomes than their free-living relatives due to transmission bottlenecks reducing the purifying activity of natural selection (Moran 1996, Mira and Moran 2002) and due to trait loss compensated by their symbiotic partner (Ellers 2012), horizontally transmitted symbionts exhibit larger genomes than their free-living

relatives. The hypothesis here is an alternance of symbiotic and free-living lifestyles requires more evolutionary adaptations, i.e., more traits, than a strictly symbiotic lifestyle (only adaptation to the host is needed) or a free-living lifestyle (facing competition and predation) (Sachs et al. 2011). Whereas the prediction holds for the ectosymbiont *Candidatus* Thiobius zoothamnicola, unexplainably, it does not for the endosymbiont *Candidatus* Endoriftia persephone.

In direct comparison, *Candidatus* Thiobius zoothamnicola has a smaller genome size with less genes and less traits than *Candidatus* Endoriftia persephone. They share many genes for the following functional traits: Calvin-Bensom-Bassham cyle and the caboxysomes, sulfide oxidation sulfide quinone reductase, sulfide dehydrogenase (flavocytochrome C), truncated SOX pathway, reverse dissimilatory sulfate reduction pathway, adenylylsulfate reductase, sulfate adenlylyltransferase, sulfite oxidation enzyme, a sulfate transporter and the sulfur globules, polyphosphate usage and the high-affinity phosphate transporter, assimilatory nitrate reduction, an incomplete urea cycle and a nitrate transporter, type 2 secretion system and type IV pilus. They differ in their preference for oxygen concentration in the habitat. Endoriftia is adapted to low oxygen concentrations, while Thiobius cytochrome terminal oxidases requires high oxygen concentrations.

Overall, *Candidatus* Endoriftia persephone contains many more genes for the following functional traits, revealing higher versatility in carbon, sulfur, phosphorous and nitrogen metabolism: a second possibility for carbon fixation with the presence of genes for reductive TCA cycle, glycogen for carbon storage, rhodanese mediate thiosulfate disproportionation, a sulfhydrogenase, a quinone-interacting membrane-bound oxidoreductase and two more transporters (a sulfate permease and a thiosulfate transporter), dissimilatory nitrate reduction and denitrification traits, a phosphate transporter, and all genes for a flagellum (Robidart et al. 2008, Gardebrecht et al. 2012, Perez and Juniper 2016).

Candidatus Thiobius zoothamnicola instead has genes for polyhydroxyalcanoates storage but otherwise mostly shares the trait potentials with *Candidatus* Endoriftia persephone.

Remarkably, the ciliate ectosymbiont exhibits the potential for lactate utilization and possible lactate and acetate transporters, coupled with the presence of the glyoxylate cycle. Further, it shows the potential for urease and the presence of a urea transporter. All these potential traits remain to be experimentally tested, but their gene presence in the genome indicate the possibility of additional byproduct benefits for the symbiont using nitrogen waste or fermentative products from the host.

At the beginning of my PhD project, the exchange of commodities between *Zoothamium nuveum* and *Candidatus* Thiobius zoothamnicola was proposed as consisting in the nourishment of the former by the later with leaked organic carbon in exchange to a better access to oxygen and sulfide (figure 11 in Chapter 1). At the end of my PhD, we consider the *Zoothamnium niveum – Candidatus* Thiobius zoothamnicola a nutritional mutualism, with a facultative host and a obligate ectosymbiont, specifically associating with each other, and providing as byproduct benefit organic carbon to the host and detoxifying sulfide, and a host providing a better access to oxygen and sulfide as a byproduct benefit to the symbiont, in addition to a potential of the host providing further byproducts to the symbiont in form on fermentative and nitrogen waste, as indicated by the symbiont genome.

We have the opportunity now to culture the mutualism and aposymbiotic hosts. We also have available genomes of both partners (in the meantime the host genome has also been sequenced in our lab) to study experimentally the exchange of commodities in this system. With bacterial genomic evidence we can test now whether lactate, acetate and/or urea are cost-free byproducts from the host to the symbiont. Such work could include the use of isotopically labeled molecules applying NanoSIMS and running in parallel transcriptomics and other omics. Ultimately, a bipartite flux balance analysis could be at reach, enabling bottom-up costs estimates. The aposymbiotic host additionally offers other experimental possibilities to generate controls and to disentangle symbiont effects on the host. The maintenance mechanism of the association is a further topic of interest that is ripe to be addressed. The possibility to produce metrics for fitness related parameters for both partners of the binary association enable experimental designs to interrogate for the action of partner fidelity feedback in comparison with alternatives such as punishments, by creating situations in which one partner resembles a situation of cheating (e.g. symbiont not

performing carbon fixation) and determining if there are costly actions from the other partner to punish the cheater, or if the coupling between fitness of the partners produce a synergistic surplus of fitness favoring the maintenance of the association (Weyl et al. 2010, Archetti et al. 2011).

A humble binary system of two mutualists, a bacterium and a colonial ciliate, is now ready for further elucidation of the mechanisms to come and to stay together, from coupling of functions in ecology to the evolutionary forces at work in interspecific cooperation. Just as this bacterial species learned to live on top of their larger host without harming it or being excessively harmed, we can learn to recognize the factors that will enable us to inhabit our host, the planet Earth in a sustainable way.

References

Archetti, Marco, István Scheuring, Moshe Hoffman, Megan E. Frederickson, Naomi E. Pierce, and Douglas W. Yu (2011). "Economic game theory for mutualisms and cooperation". Ecology Letters 14: 1300–1312. doi:10.1111/j.1461-0248.2011.01697.x.

Ellers, Jacintha, E. Toby Kiers, Cameron R. Currie, Bradon R. McDonald, and Bertanne Visser (2012). "Ecological interactions drive evolutionary loss of traits". Ecology Letters 15(10):1071–1082. doi:10.1111/j.1461-0248.2012.01830.x.

Gardebrecht, Antje, Stephanie Markert, Stefan M. Sievert, Horst Felbeck, Andrea Thürmer, Dirk Albrecht, Antje Wollherr, et al. (2012). "Physiological homogeneity among the endosymbionts of *Riftia pachyptila* and *Tevnia jerichonana* revealed by proteogenomics". The ISME Journal 6: 766–776. doi:10.1038/ismej.2011.137.

Mira, A. and Moran, N. A. (2002). "Estimating population size and transmission bottlenecks in maternally transmitted endosymbiotic bacteria". Microbial Ecology 44(2):137–143. doi: 10.1007/s00248-002-0012-9.

Moran, N. A. (1996). "Accelerated evolution and Muller's rachet in endosymbiotic bacteria". Proceedings of the National Academy of Sciences of USA 93(7):2873–2878. doi: 10.1073/pnas.93.7.2873.

Perez M., Juniper S. K. (2016). "Insights into symbiont population structure among three vestimentiferan tubeworm host species at Eastern Pacific spreading centers". Applied and Environmental Microbiology 82. doi:10.1128/AEM.00953-16

Robidart, Julie C., Shellie R. Bench, Robert A. Feldman, Alexey Novoradovsky, Sheila B. Podell, Terry Gaasterland, Eric E. Allen, and Horst Felbeck (2008). "Metabolic versatility of the *Riftia pachyptila* endosymbiont revealed through metagenomics". Environmental Microbiology 10(3):727–737. doi:10.1111/j.1462-2920.2007.01496.x

Sachs, Joel L., Carla J. Essenberg, and Martin M. Turcotte (2011). "New paradigms for the evolution of beneficial infections". TRENDS in Ecology and Evolution 26(4):202–209. doi:10.1016/j.tree.2011.01.010.

Thursby E, Juge N. (2017). "Introduction to the human gut microbiota". Biochemical Journal 474(11):1823-1836. doi: 10.1042/BCJ20160510.
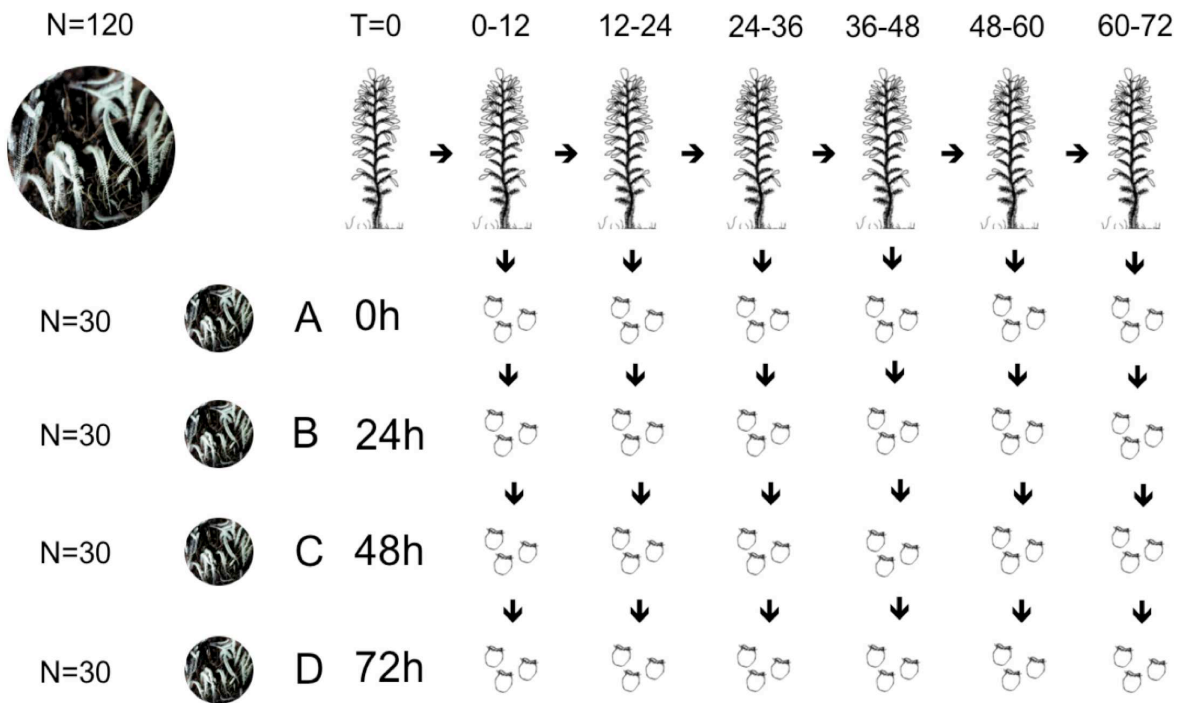
Weyl, E. Glen, Megan E. Frederickson, Douglas W. Yu, and Naomi E. Pierce (2010). "Economic contract theory tests models of mutualism". Proceedings of the National Academy of Sciences of USA 107(36): 15712–15716. doi: 10.1073/pnas.1005294107.

Annex. Supplementary information of chapters 3, 4, 5 and 6

(it does not include excel file big tables)

Chapter 3. Host-symbiont stress response to lack-ofsulfide in the giant ciliate mutualism. Supplementary material
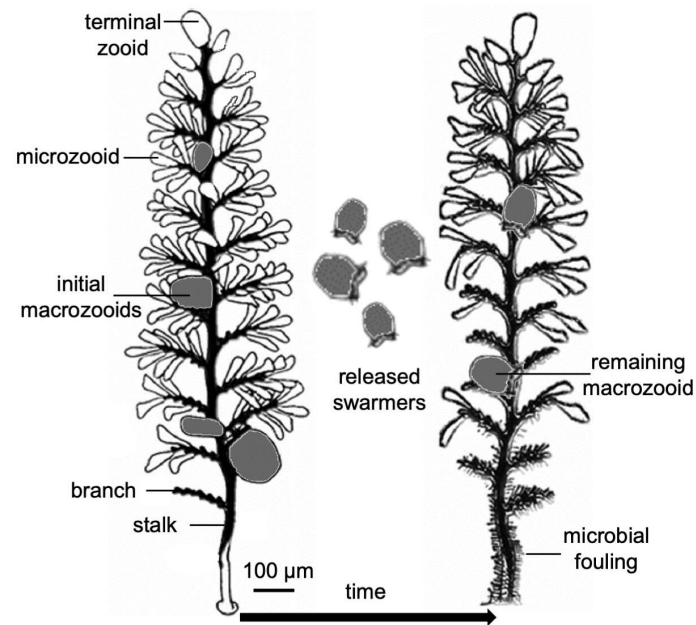

S1 Fig. Scheme of colony. The colony iscomposed of astalk with alternate branches and three different cell types–terminal zooids for division, microzooids for nutrition, and macrozooids for asexual reproduction. The size of the colony iscounted in number of branches. Acolony with initial macrozooids present at the start of the experiment and remaining macrozooids at the end of experiment isshown. During experimental time the release of swarmers was also counted.

S2 Fig. Time schedule of the sulfide starvation experiment. Colonies (n =120) were monitored every 12 h(horizontal time line). Released swarmers from each of this time points were divided in 4cohorts (A, B, C, D; vertical time line).

S3 Fig. Comparison of colonies from Sv. Jernej and Strunjan. All Wilcoxon-Mann-Whitney tests fail to reject the null hypothesis of equal medians: (A) colony size (p =0.72), (B) number of initial macrozooids per colony (p =0.49), (C) number of swarmers (released macrozooids) per colony (p =0.46) and (D) size of swarmers (p =0.41).
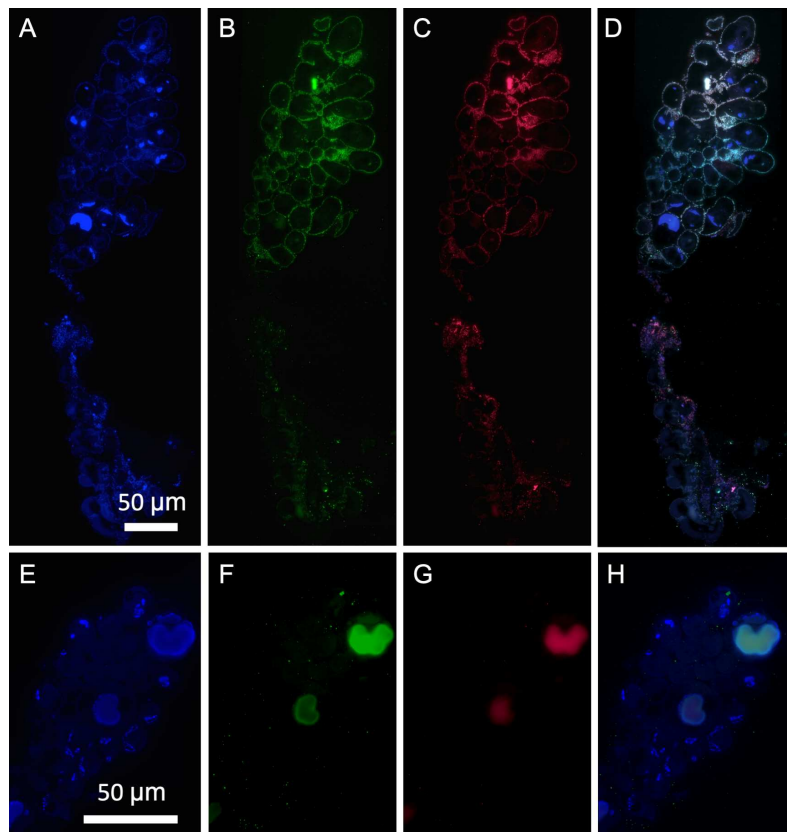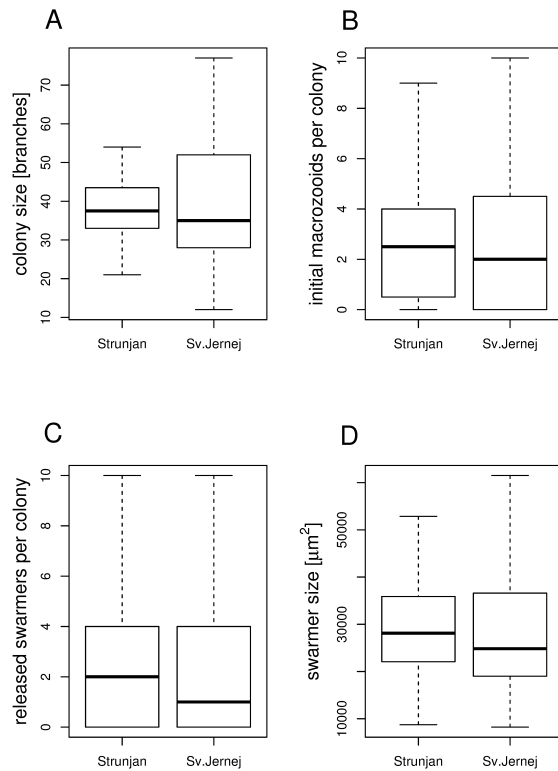
S4 Fig. FISH micrographs colonies. Colony alive after 48 h(A) DAPI staining (blue), (B) symbiont-specific probe (green), (C) EUBmix and Archea probes (red) (D) composite of A, B, C; note the increase in microbial fouling from top to bottom. Colony alive after 72 hwith very few symbionts left (E) DAPI staining (blue), (F) symbiont-specific probe (green), (G) EUBmix and Archea probes (red), (H) composite of E, Fand G.

S1 Table. Collections and abiotic parameters measured prior collection at wood surface. Samples listed according to type of experiment, applied technique, time series of experiment, site, date of collection, number of wood, and abiotic parameters: depth, temperature, salinity, and pH. Abiotic parameters were measured using a Multi 340i sensor WTW.

experiments	technique	site	date	wood #	depth (m)	temperature (°C)	salinity	pH	time series (h)
host sulfide starvation	microscopy	Sv. Jernej	03.07.2015	86	0.3	28.3	35	8.2	0 - 72
	microscopy	Strunjan	25.07.2015	100	0.5	30.5	36	8.3	0 - 72
host sulfidic condition	microscopy	Strunjan	20.07.2021	121	0.5	28.4	34	8.3	0 - 108
symbiont sulfide starvation	FISH	Sv. Jernej	09.-14.7.2014	60-68	03-1.0	23.5-28.2	30-31	7.8-8.1	24 - 72
	SEM micrographs/analyses		03.10.2012	6	0.4	20.0-20.7	34	8.1	0 (in situ)
symbiont sulfide starvation	SEM micrographs/analyses	Sv. Jernej	21.10.2012	25, 28, 29	0.4	20.0-20.7	34	8.1	0 - 48
	SEM micrographs		07.07.2013	41	0.5	28.1	34	8.1	48

S2 Table. Abiotic parameters measured at the start (and at the end) of experiments. Abiotic parameters: temperature, salinity, pH and oxygen and sulfide concentrations (mean ± standard deviation). Temperature, salinity, pH were measured using a Multi 340i sensor WTW. Oxygen concentration was measured using a PreSenS Flow-through Cell FTC-PSt3. Sulfide concentration was measured photometrically according to Cline (1969).

| experiments	water	temperature (°C)	salinity	pH	oxygen (% saturation)	ΣH_2S (µM)
host sulfide starvation	new	26.0 ± 0.9	36 ± 0	8.0 ± 0.1	97 ± 6	N/A
	removed	25.5 ± 0.6	36 ± 1	7.7 ± 0.2	99 ± 4	N/A
host sulfidic condition	new	26.8 ± 0.5	35 ± 0	7.4 ± 0.1	4 ± 4	448 ± 11
	removed	25.4 ± 0.6	36 ± 1	7.6 ± 0.4	89 ± 10	6 ± 5
symbiont sulfide starvation	FISH start	24.2 ± 0.5	32 ± 0	8.1 ± 0.0	101 ± 2	N/A
	SEM & analyses start	22.1 ± 0.1	34 ± 0	8.1 ± 0.0	123 ± 0	N/A
	SEM start	25.3 ± 1.0	36 ± 0	8.1 ± 0.0	101 ± 3	N/A

Chapter 4. Thiotrophic bacterial symbiont induces polyphenism in giant ciliate host *Zoothamnium niveum*. Supplementary material
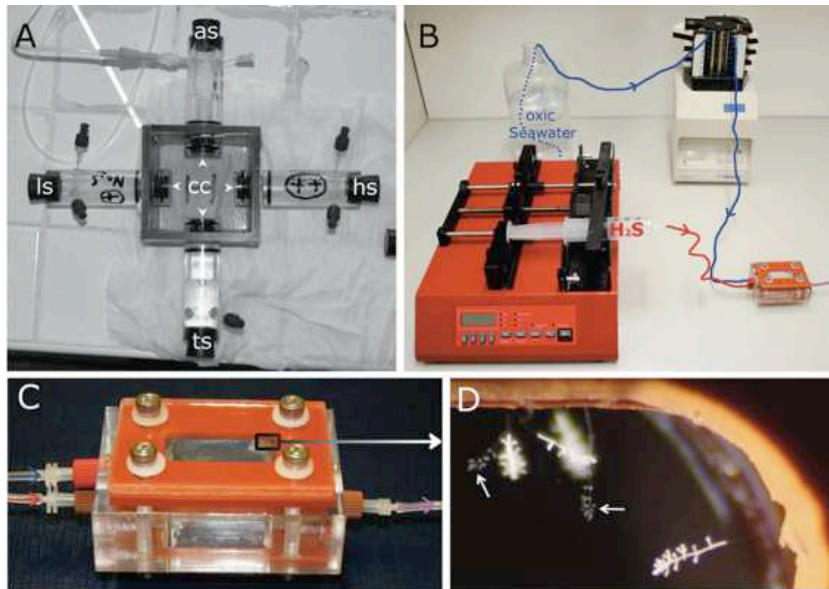
Supplementary Figure S1

(**a**) Hard PVC preference chamber with central cube (cc) and four attached vials with gas-permeable membranes (arrowheads) to allow gas diffusion and swarmer settlement. Two cylinders were filled with low (ls) and high (hs) sulphide concentrations, the third cylinder with thiosulphate (ts) solution, and the fourth cylinder with anoxic seawater (as). (**b**) Flow-through system with 8-channel peristaltic pump providing constant seawater flow to the plexiglas chamber through the upper inlet, and syringe pump providing sulfide to the chamber through the lower inlet. (**c**) Chamber with upper and lower inlet and outlet. (**d**) Close-up at the upper corner of the chamber showing both white symbiotic colonies and pale aposymbiotic colonies (arrows) growing next to each other.
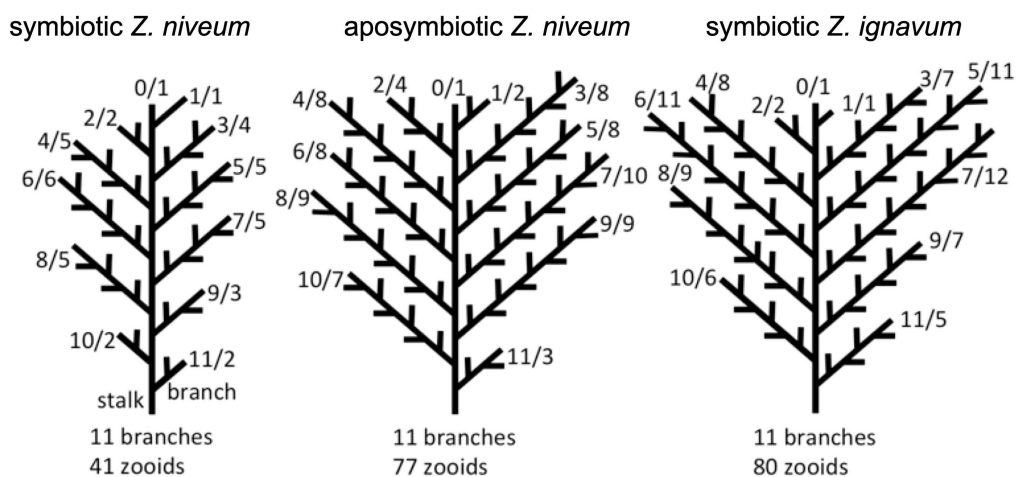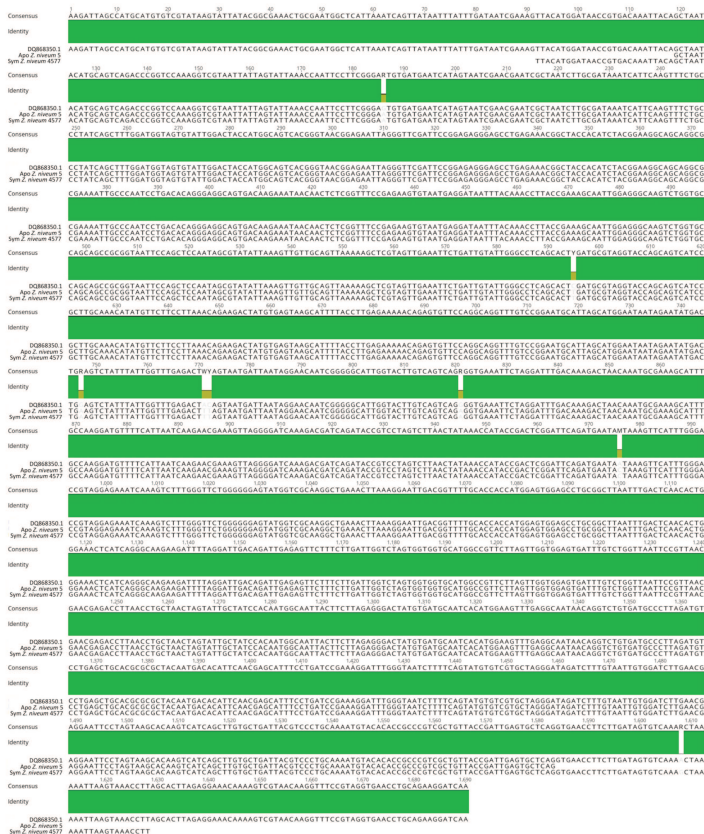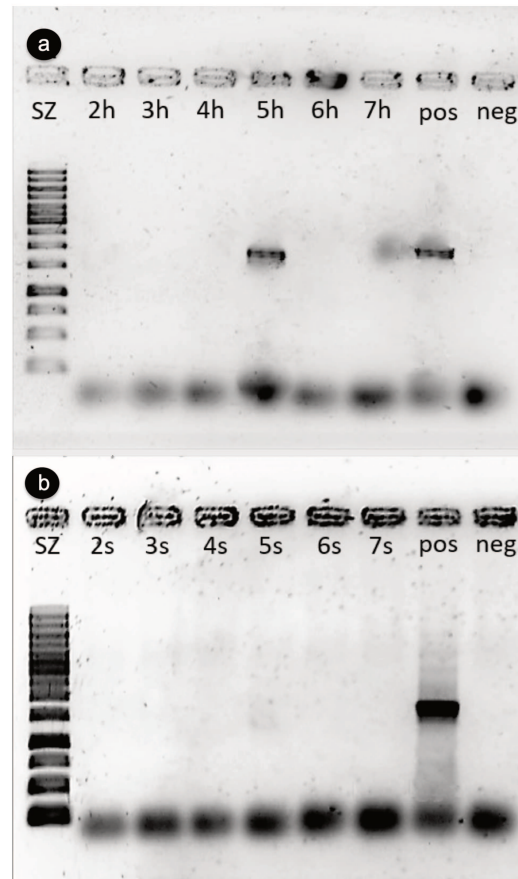

Supplementary Figure S2

Illustration of growth form of symbiotic and aposymbiotic *Z. niveum* and symbiotic *Z. ignavum*. Note that all three colonies exhibit 11 branches, but differ the number of zooids on each branch. First number = branch number, second number = number of zooids on this branch; each ending delineates a zooid, which is not drawn.

Supplementary Figure S3
Gel electrophoresis pictures showing PCR products of 18S (**a**) and 16S (**b**) rRNA genes (SZ = size marker = Gene ruler™ 1kb DNA Ladder, Waltham, Massachusetts, USA; colonies collected in the field resembled aposymbiotically grown morph (# 4697/2-5): 2-5h = host, 2-5s = symbiont; pos = positive control of colony (# 4577) collected in field resembled symbiotically grown morph; neg = negative control).

Supplementary Figure S4
Alignment of 18S rRNA gene from *Zoothamnium niveum*: aposymbiotic morph (# 4697/5, NCBI accession number MN535886) and symbiotic morph (# 4577, NCBI accession number MN535887) from Piran, Slovenia and *Z. niveum* (DQ868350.1) from Fort Pierce, FL, USA.

Supplementary Figure S5

Micrograph of colonies grown on submerged wood.

Replicates	1	2
Sampling wood number	41	61 -63
Sampling location	Sv. Jernej	Sv. Jernej
Latitude	45.498286 N	45.498286 N
Longitude	13.59352 E	13.593521E
Depth (m)	0.5	0.5 - 1.5
Sampling date	7 July 2013	9 July 2014
Colonies used for swarmer release	10	120
Number of initial swarmers	15	240
Incubation time (h)	**Number of swarmers analysed with SEM**	
4	3	8
24	6	10
48	4	10

Supplementary Table S1: Swarmers during dispersal

Replicate 1 and 2 with wood number from with colonies were retrieved, sampling location with latitude and longitude, depth, and sampling date; number of colonies used for producing swarmers in embryo dishes, number of initial swarmers that were incubated under oxic conditions between 4 and 48 h and analyzed with SEM.

Supplementary Table S2: Swarmer recruitment to sulfide in preference chambers

(a) Sampling location, latitude, longitude, depth, and sampling date of colonies from two concrete blocks surrounded by seagrass *Posidonia oceanica* debris used for producing swarmers in embryo dishes under oxic conditions for settlement preference experiment with six replicates, showing number of colonies used for swarmer release, initial number of swarmers and settlement of swarmers exclusively colonizing membranes emitting high and low sulphide within 24 hours.

Sampling						
Sampling location	concrete blocks, Bay of Stareso, Corse					
Latitude	42.58047 N					
Longitude	8.72438 E					
Depth	7 - 10 m					
Sampling date	September 2003					
Colonies used for swarmer release	50					
Replicates	**1**	**2**	**3**	**4**	**5**	**6**
Number of initial swarmers	40	40	50	50	30	30
Number of settled swarmers						
Low sulphide	5	5	3	8	1	4
High sulphide	3	5	1	2	8	4

Replicate chemistry	time	ΣH_2S (µmol L^{-1})	O_2 (µmol L^{-1})	T (°C)	Salinity	pH
In chamber	0 h	0	211	19.4	32	8.2
	24 h	0	167	19.1	33	8.3
Low sulphide	1 - 24 h	112 ± 45	54 ± 18			
High sulphide	1 - 24 h	386 ± 25	23 ± 11			
Thiosulphate	1 - 24 h	0	186 ± 20			
N$_2$ - bubbled	1 - 24 h	0	< 1			

(b) The experiment was repeated without swarmers in October 2018 to measure the abiotic conditions (sulphide, oxygen, temperature, salinity, pH) in the chamber at the beginning (0h) and after 24h; sulfide and oxygen concentrations were measured at the four membranes facing the chamber after 1h, 5 h, 18 h, and 24 h (mean ± standard deviation).

139

Supplementary Table S3: Swarmer recruitment in flow-through chambers
Wood number from which colonies were sampled, Sampling location with latitude and longitude, depth, and sampling date of colonies from submerged wood used for producing swarmers in embryo dishes incubated under oxic conditions and transferred to flow-through chambers for recruitment experiment under oxic condition between 2 and 22 hours; 17 replicates with replicate number provided; for each replicate time of settlement of swarmers, initial number of swarmers, total number of settled swarmer, and number of settled symbiotic and aposymbiotic swarmers are provided; aposymbiotic and symbiotic swarmers were counted after settlement.

Sampling wood number	Sampling location	Latitude	Longitude	Depth (m)	Sampling date	Replicate number	Time of settle-ment (h)	Number of initial swarmers	Total number of settled swarmers	Number of symbiotic settled swarmers	Number of apo-symbiotic settled swarmers
59	Sv. Jernej	45.49829 N	13.59352 E	1.5	4 July 2014	70	**2**	120	46	11	35
59	Sv. Jernej	45.49829 N	13.59352 E	1.5	4 July 2014	71	**2.5**	120	48	45	3
41	Sv. Jernej	45.49829 N	13.59352 E	0.5	7 July 2013	43	**3.5**	227	90	35	55
61 -63	Sv. Jernej	45.49829 N	13.59352 E	0.7	9 July 2014	77	**7.5**	120	75	59	16
70	Sv. Jernej	45.49829 N	13.59352 E	1.0	16 July 2014	79	**7.5**	150	79	67	21
70	Sv. Jernej	45.49829 N	13.59352 E	1.0	16 July 2014	78	**9**	120	61	48	13
72-76	Strunjan	45.52810 N	13.60406 E	0.7 - 1.5	22 July 2014	84	**9**	90	59	50	9
72-76	Strunjan	45.52810 N	13.60406 E	0.7 - 1.5	22 July 2014	86	**9.5**	90	26	9	17
72-76	Strunjan	45.52810 N	13.60406 E	0.7 - 1.5	22 July 2014	87	**9.5**	90	36	28	8
72-76	Strunjan	45.52810 N	13.60406 E	0.7 - 1.5	22 July 2014	88	**9.5**	150	40	14	26
60 - 63	Sv. Jernej	45.49829 N	13.59352 E	0.3 - 0.7	9 July 2014	74	**11**	160	51	34	17
60 - 63	Sv. Jernej	45.49829 N	13.59352 E	0.3 - 0.7	9 July 2014	75	**12.3**	200	97	61	36
70	Sv. Jernej	45.49829 N	13.59352 E	1.0	16 July 2014	83	**12.5**	105	35	10	25
56 - 58	Sv. Jernej	45.49829 N	13.59352 E	0.5 - 1.0	29 June 2014	68	**13**	132	129	91	38
41	Sv. Jernej	45.49829 N	13.59352 E	0.5	7 July 2013	39	**21**	220	105	80	25
41	Sv. Jernej	45.49829 N	13.59352 E	0.5	7 July 2013	41	**23**	218	158	144	14
41	Sv. Jernej	45.49829 N	13.59352 E	0.5	7 July 2013	42	**22**	218	105	80	25

Supplementary Table S4. Effects of sulphide and food supply on aposymbiotic host traits
Sampling location and date of collection of colonies from submerged wood (wood number and depth) used for producing swarmers in embryo dishes used as inoculum (number of total swarmers, number of settled aposymbiotic swarmers, time of settlement); experiments under environmental conditions (ΣH_2S and O_2 concentration, temperature, salinity, pH, water flow through chambers, microbial abundance in seawater shown as median and Q_{25} and Q_{75}) used for growing aposymbiotic colonies for seven days; colony size as number of branches, number of colonies, colony survival at day 7 are counted; life span, maximal colony size and time when maximal colony size is reached are estimated; numbers of colonies analyzed with scanning electron microscopy (SEM) and fluorescent in situ hybridisation (FISH) at the end of the experiment are shown.

Experiment	77	75	68	72	78	83
Sampling						
Wood number	61 - 63	61 - 63	56 - 58	59	70	70
Sampling location Sv. Jernej (date)	9 July 2014	9 July 2014	29 June 2014	4 July 2014	16 July 2014	16 July 2014
Depth (m)	0.7	0.7	0.5 - 1.0	1.5 m	1.0 m	1.0 m
Swarmer inoculum						
Number of total swarmers	120	200	132	120	120	105
Number of settled aposymb. swarmers	16	36	38	N/A	13	25
Time of settlement (h)	7.5	12.3	13.0	2.5	9.0	12.5
Experimental conditions						
ΣH_2S ($\mu mol\ L^{-1}$)	21 ± 6	0	19 ± 7	0	24 ± 3	0
O_2 ($\mu mol\ L^{-1}$)	215 ± 7	221 ± 4	216 ± 5	216 ± 4	218 ± 4	212 ± 8
Temperature (°C)	25.3 ± 0.5	24.1 ± 0.4	25.1±0.6	25.0 ± 0.6	25.3 ± 0.3	25.5 ± 0.3
Salinity	32.9 ± 1.2	32.8 ± 0.7	31.8 ± 0.5	32.2 ± 0.7	33.1 ± 1.0	33.8 ± 1.2
pH	8.2 ± 0.0	8.1 ± 0.0	8.2 ± 0.0	8.1 ± 0.0	8.2 ± 0.0	8.2 ± 0.1
Flow (mL h^{-1})	84 ± 2	81 ± 4	63 ± 21	79 ± 6	82 ± 5	76 ± 13
Microbial abundance ($x10^5\ mL^{-1}$)	2.0 (1.8, 2.9)	3.0 (2.4, 3.8)	7.9 (7.6, 8.0)	7.5 (7.3, 7.8)	11.5 (9.3, 15.2)	16.5 (15.6, 17.2)
Colony growth and survival						
Colony size, day 7 (no. of branches)	6 (6, 7)	3 (2, 3)	6 (6,7)	3 (2, 4)	8 (8, 9)	0
Number of colonies on day 7	5	25	21	30	9	0
Colony survival on day 7 (%)	28	25	100	30	64	0
Estimated lifespan (d)	12.3	8.0	13.2	8.1	17.4	6.4
Estimated maximal colony size	5.9	6.1	5.8	7.2	7.7	7.3
Estimated time of maximal colony size (d)	6.0	4.0	6.4	4.0	8.5	3.2
Methods applied at end of experiment						
SEM (n)	N/A	N/A	4	8	4	N/A
FISH (n)	4	6	6	5	5	N/A

Supplementary Table S5. The symbiotic and aposymbiotic *Z. niveum* phenotypes

Data of symbiotic and aposymbiotic morphs grown in the same chamber (number 68) are presented as median and interquartile range of estimated number of branches and survival on day 7, and estimated life span, estimated number of branches at the estimated time of vertex. Fitness drop measured as relative reduction in number of branches between symbiotic and aposymbiotic colonies.

	Experiment 68 Symbiotic morphs	Experiment 68 Aposymbiotic morphs
Number of branches	22 (18, 29) n=21	6 (5, 6) n=21
Estimated number of zooids	107	24
Survival (%)	66 n=32	100 n=46
Estimated lifespan (days)	-	13.2
Estimated max. number of branches	-	5.8
Estimated time of vertex (day)	-	6.4
Fitness (relative growth reduction)	100	27

Chapter 5.
Comparative genomics
of a vertically
transmitted
thiotrophic bacterial
ectosymbiont and its
close free-living
relative.
Supplementary
information
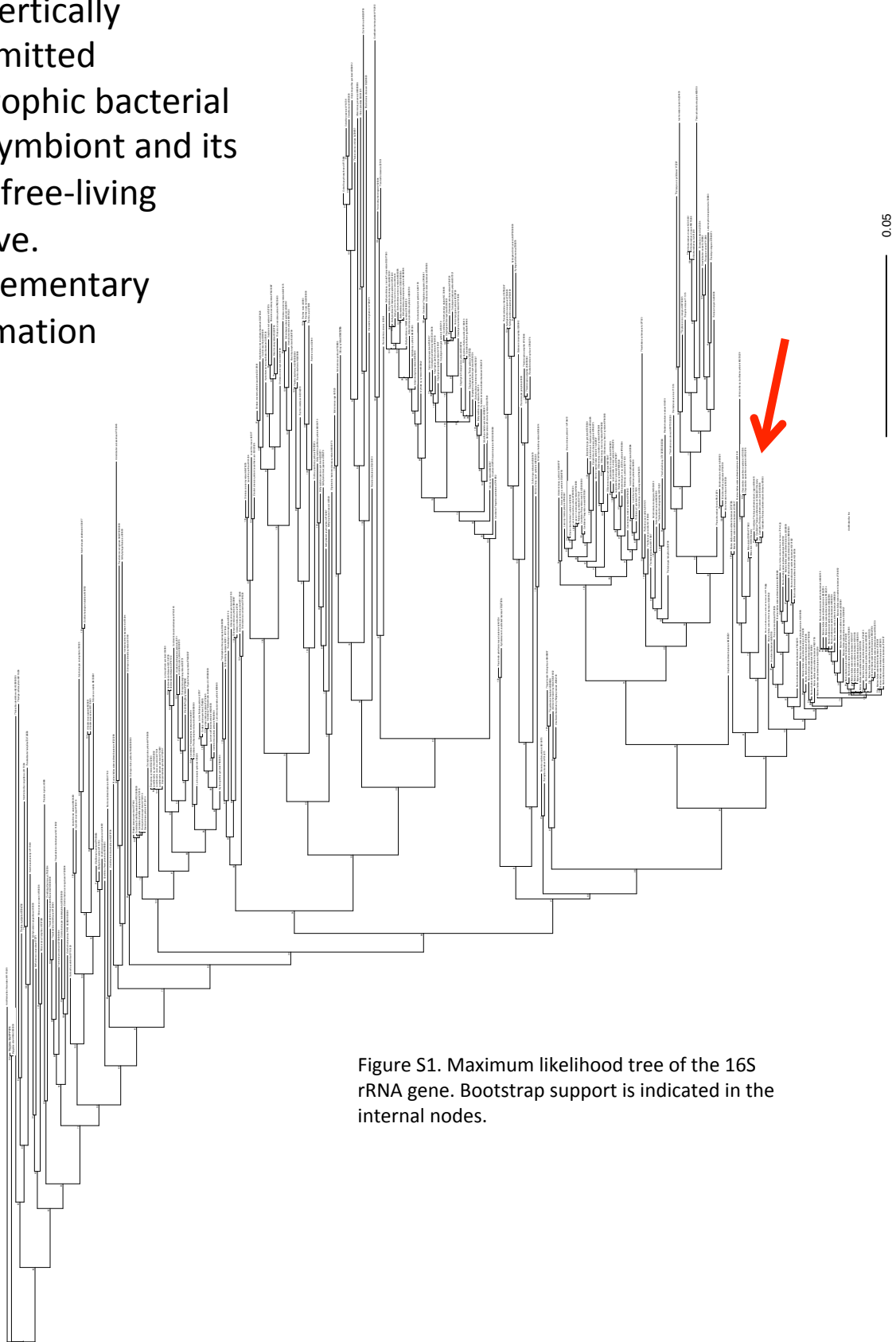
Figure S1. Maximum likelihood tree of the 16S
rRNA gene. Bootstrap support is indicated in the
internal nodes.
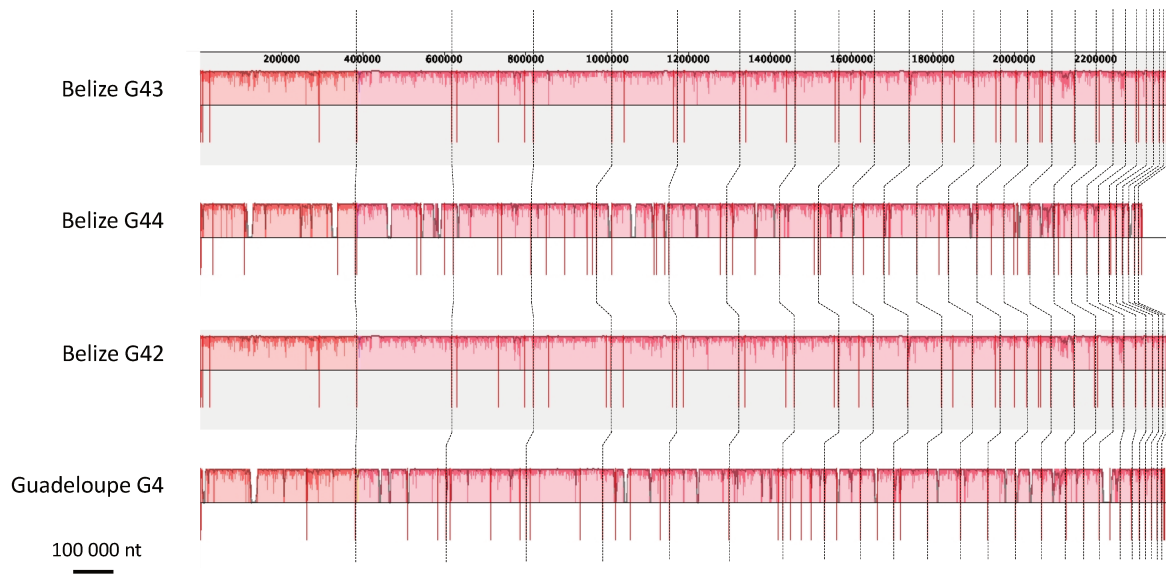
Figure S2. Mauve synteny plot of the four Thiobius MAGs, showing full reconciliation of contig ordering. Vertical dashed lines indicate the limits of the clusters of contiguity. The clusters of contiguity are ordered by decreasing length of the block.
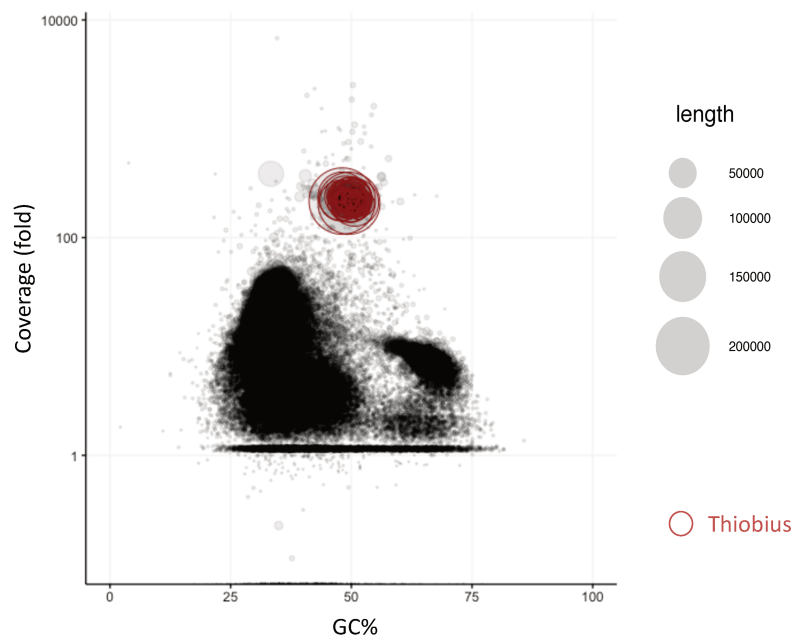
Figure S3. Binning outcome of *Zoothamnium niveum* Belize G43 sample, as organized by coverage (in logarithmic scale) and GC content. Thiobius bin location is indicated by the red color of the contigs.
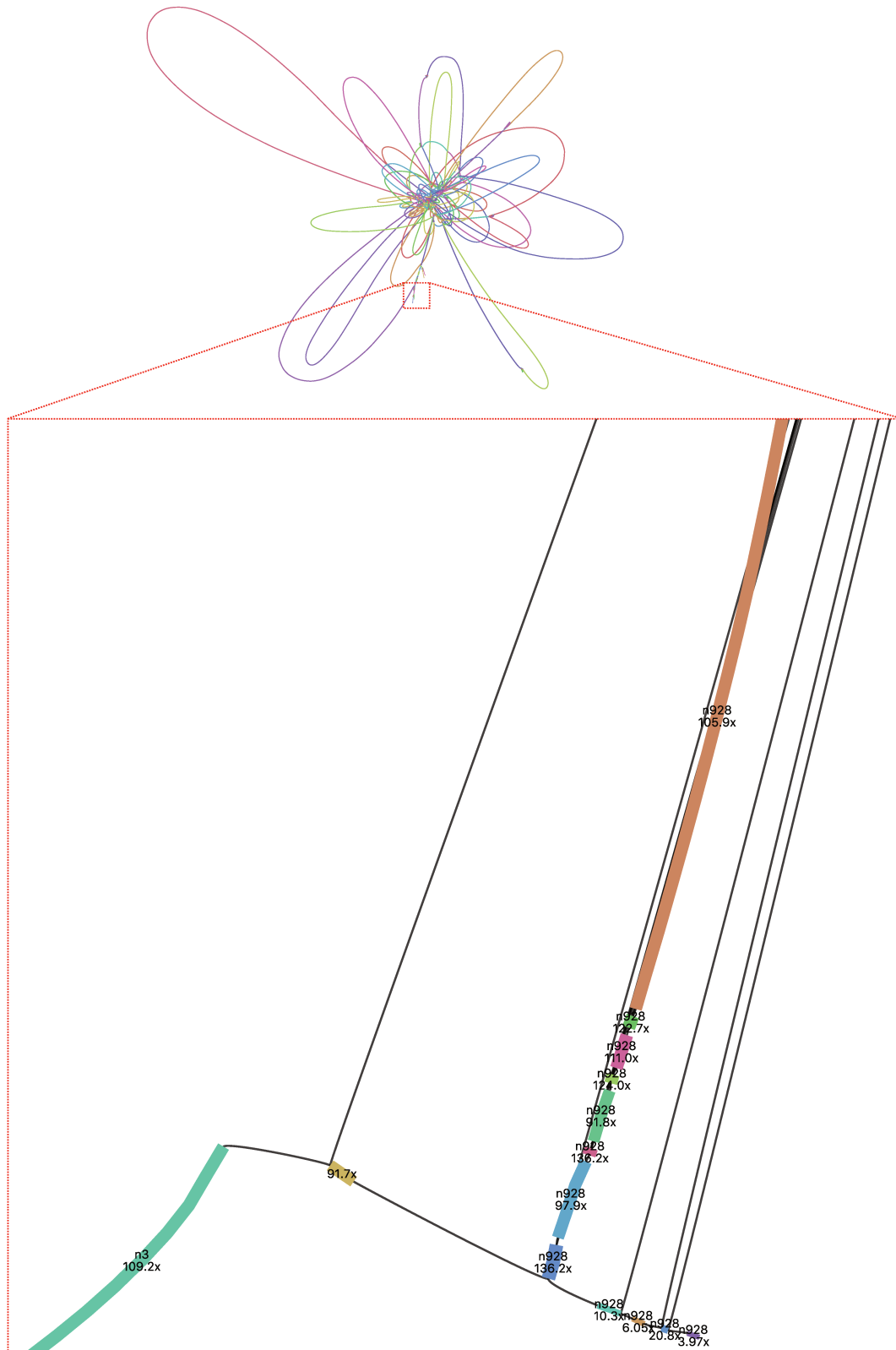
Figure S4. Linkage analysis of Thiobius G43 SPAdes assembly with Bandage, showing the incorrect extension of contig n928 that disrupts the contiguity of the 16S rRNA gene in the stringent quality threshold read refinement assembly (G43.1). The misassembled nodes in the bottom right part show a lower coverage and are likely contamination from a different organism with a lower presence in the sample. A slight variation in the workflow consisting in a more permissive read filtering threshold provides a contig that overcomes this trouble. The bridging node from the de Bruijn graph has a coverage of 92x that is consistent with the rest of the stretches.
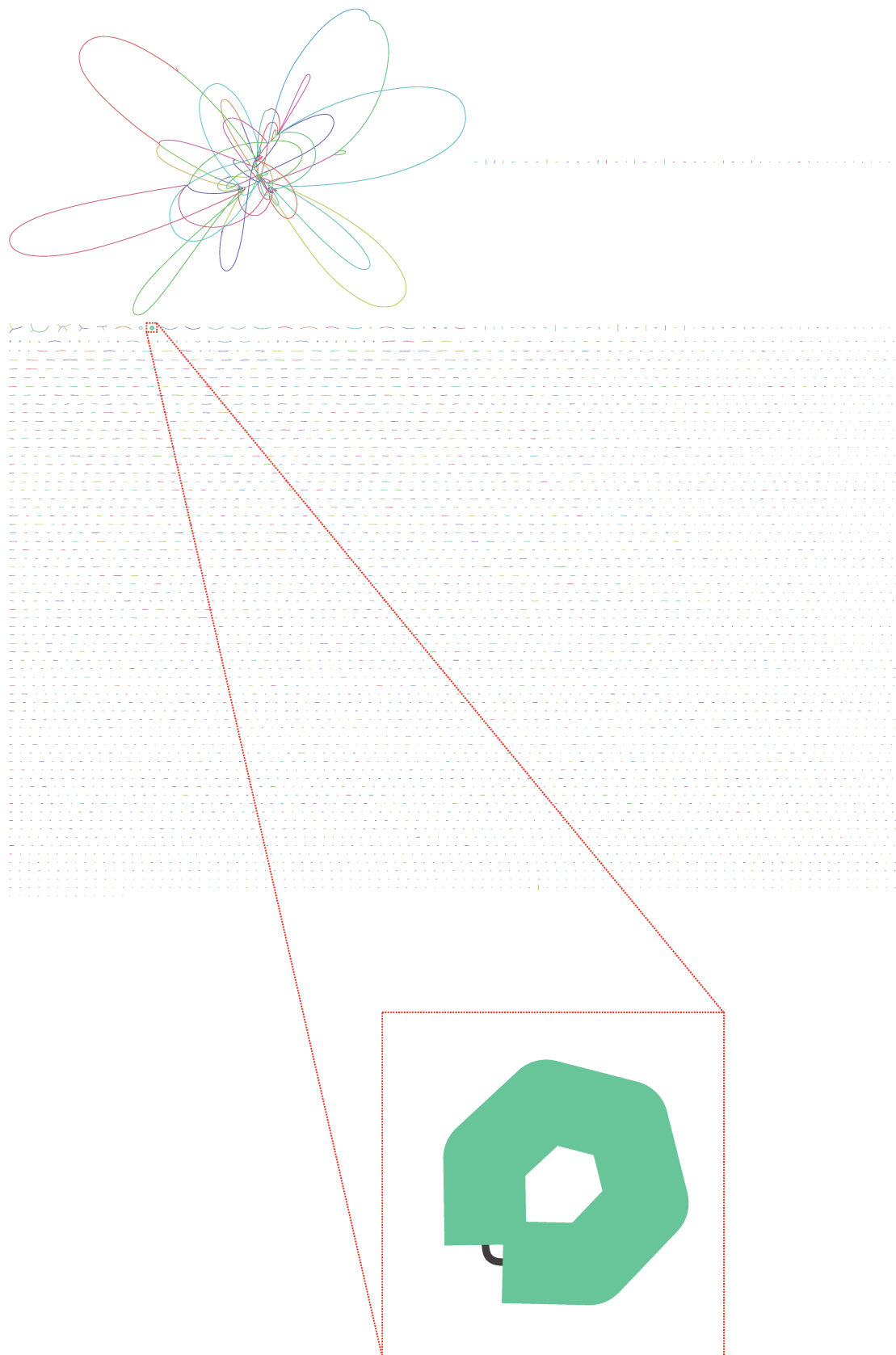
Figure S5. ODIII6 initial assembly contained a contig that shows only annotation of bacteriophage proteins. A SPAdes reassembly of ODIII6 allows the Bandage visualization of the DeBruijn graph, showing that the contaminating contig is circular, and is disconnected from the main component that contains all other contigs of the assembly.
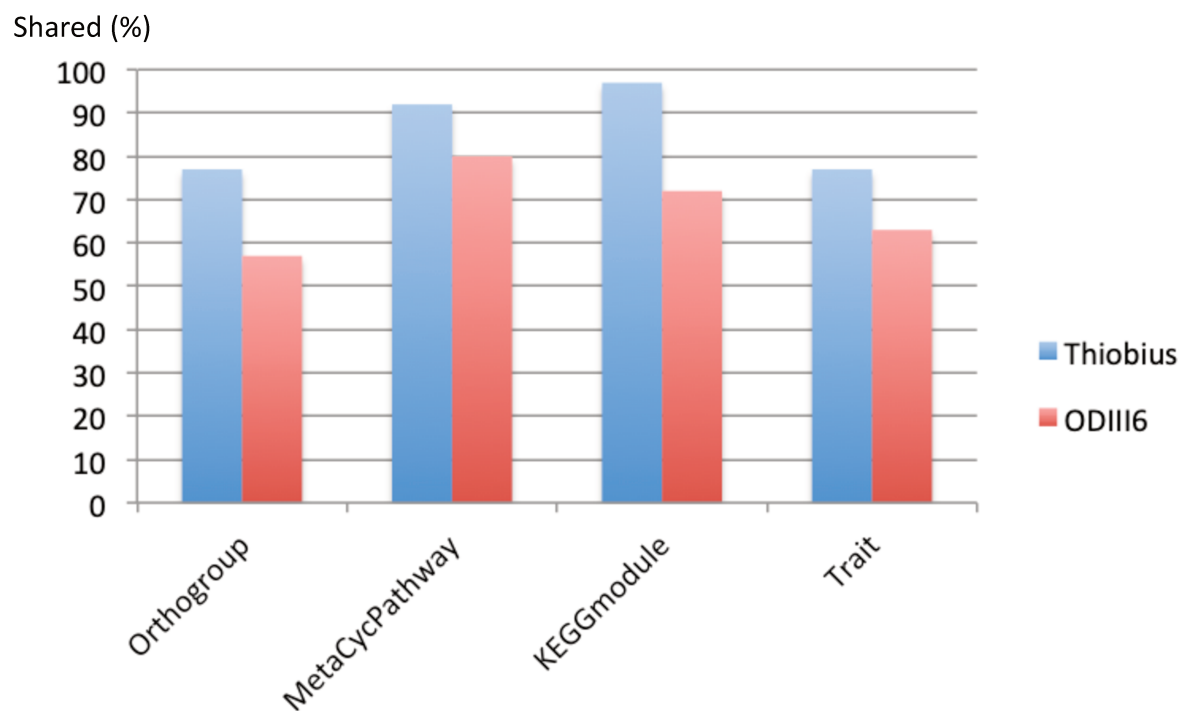
Figure S6. The shared part of the genomes is represented differently with the varying levels of integration. From finer to coarser grain: genes (orthogroup), pathway (either MetaCyc or KEGG module), and trait.
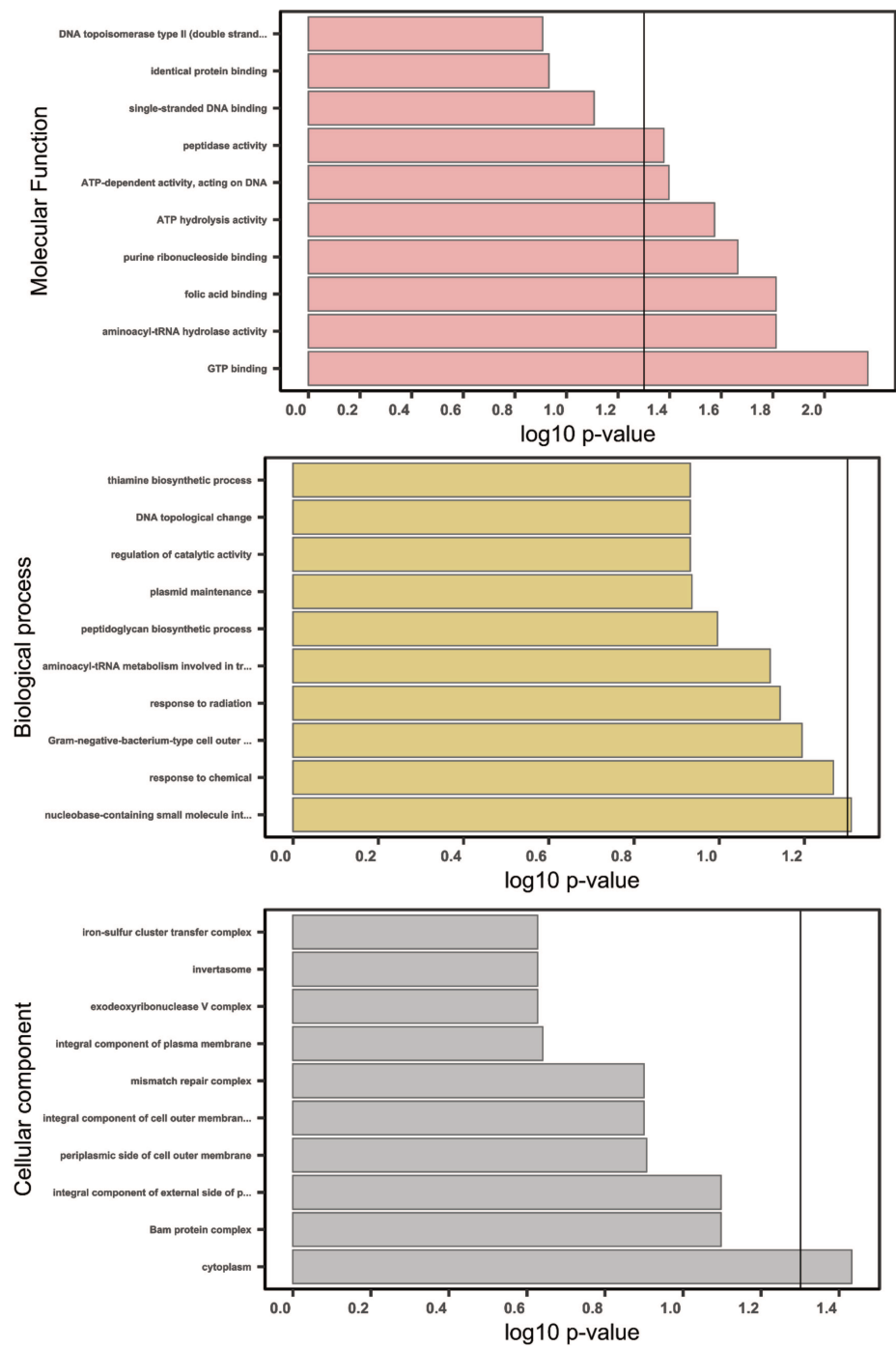
Supplementary Figure 1 - Gene ontology (GO) enrichment analyses for the positively selected genes identified in the complete and closed Endoriftia genome. The graphs correspond to three domains of ontologies: molecular function (MF), biological process (BP), and cellular component (CC). The selected genes were analysed for enrichment in specific GO categories using the TopGO program against the background (all coding sequence genes). Y axis corresponds to enriched GO terms found in the respective domains (BP, MF and CC). X axis correspond to the log function of Fisher p-values obtained for each one of the enriched terms. The back line denotes a p-value = 0.05. P-values greater than 1,30 (log 0,05) indicate statistically significant enriched term.
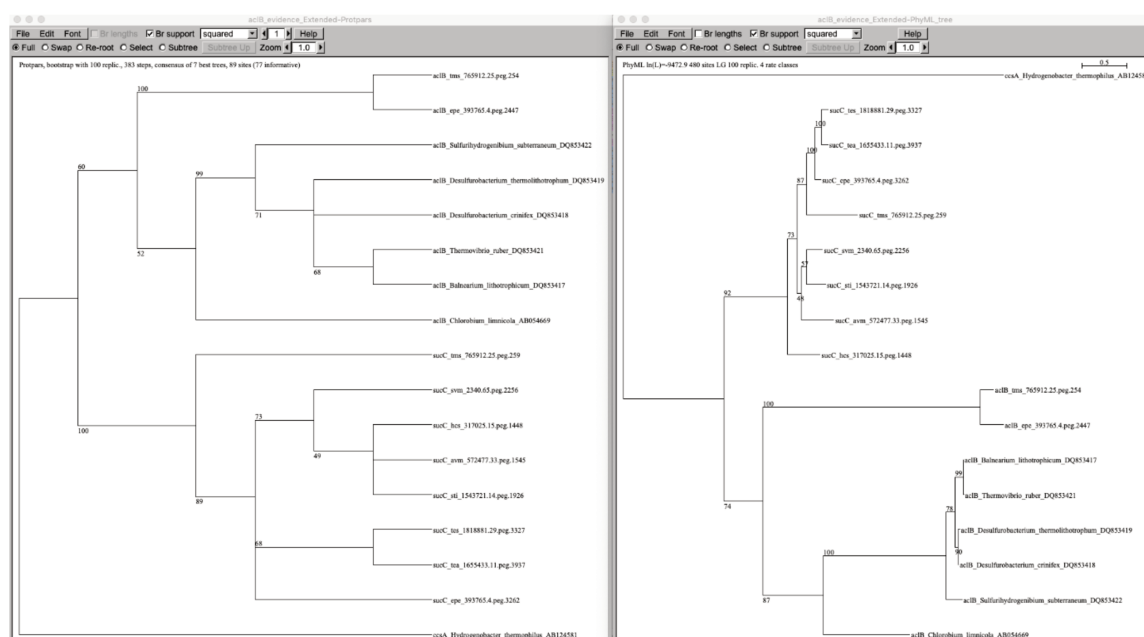
Supplementary Figure 2 - Maximum parsimony (left) and maximum likelihood gene tree (right) reconstructions with several gene orthologs of *aclB* and *sucC*. The gene trees corroborate that the *aclB* and *sucC* Endoriftia genes cluster with their respective homologs. epe, *Candidatus* Endoriftia persephone; tes, *Candidatus* Thiodiazotropha endoloripes; tea, *Candidatus* Thiodiazotropha endolucinida; hcs, *Hydrogenovibrio* crunogenus; sti, *Sedimenticola thiotaurini*; svm, *Solemya velum*; tms, *Thioflavicoccus mobilis*. Both trees were calculated over a Muscle alignment in SeaView v4.5.4 with default parameters and 100 non-parametric bootstraps).
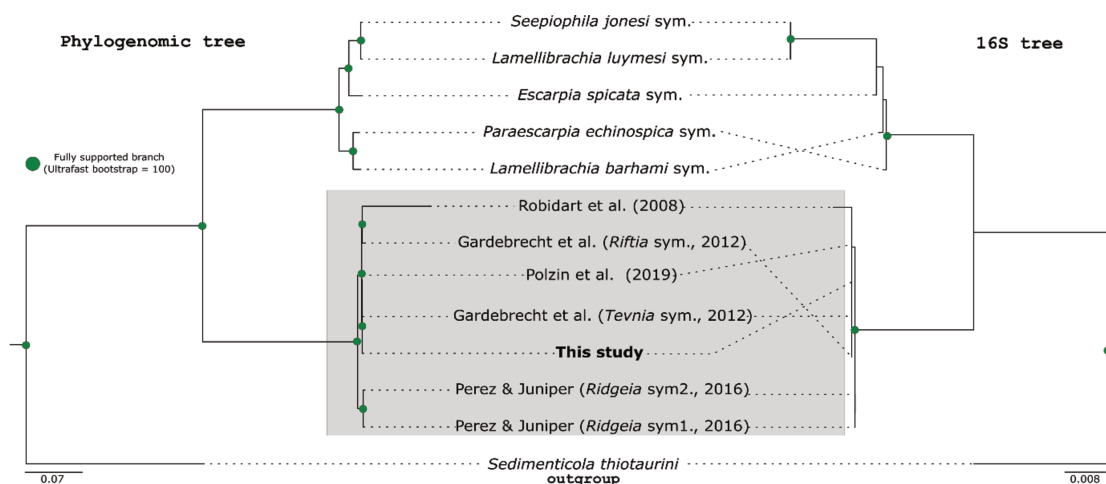
Supplementary Figure 3- Rooted maximum-likelihood phylogenomic (left) / phylogenetic 16S (right) trees of tubeworm endosymbionts using 1000 rapid bootstrap and SH-aLRT test replicates. The supermatrix was generated concatenating 1,879 shared orthogroups. 16S sequences were obtained from the different drafts by sequence similarity searches using the reference sequences obtained from the complete and closed genome. Node supports correspond to SH-aLRT and bootstrap values. The grey box indicates the unique endosymbiont phylotype of *Tevnia*, *Ridgeia* and *Riftia* tubeworms. Fully supported nodes are indicated by green circles in the tree nodes.

148
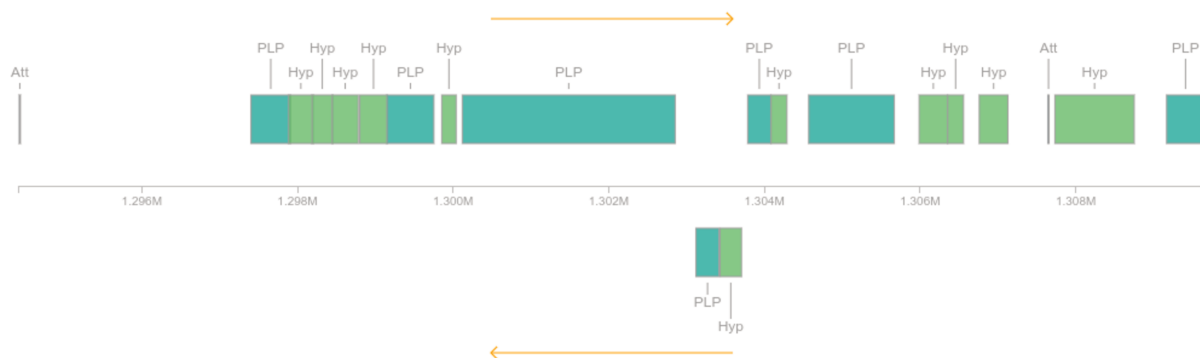
Supplementary Figure 4 – Prophage region identified in the complete and closed Endoriftia genome. The 15,2 kb incomplete phage region located in the closed genome of Endoriftia. Sensitive similarity searches identified a Caudovirales infection.
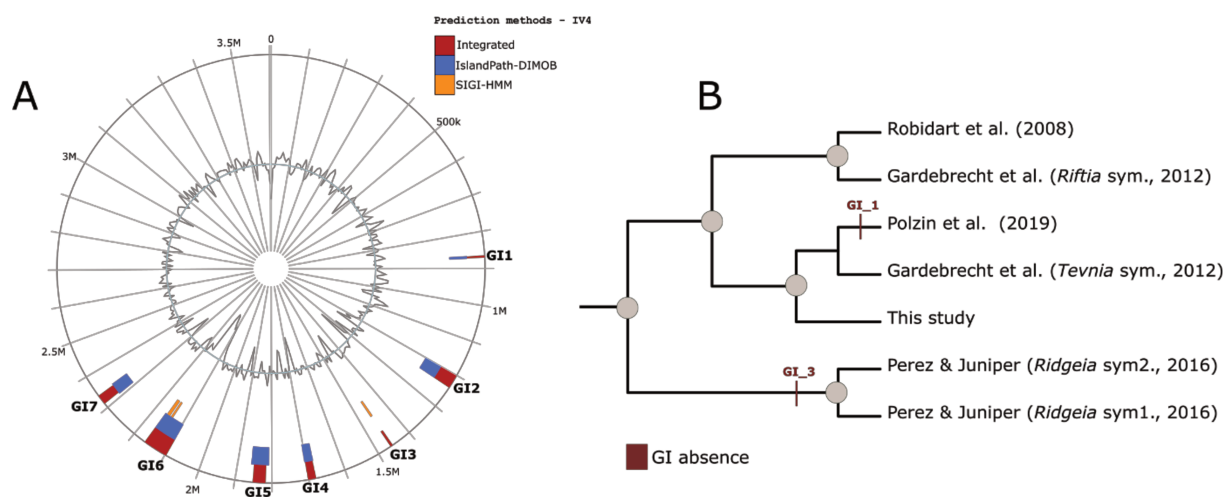

Supplementary Figure 5 – Genomic islands identified by IslandViewer4 and their distribution in the seven Endoriftia genomic datasets. A, IslandViewer4 identified seven genomic islands present in the complete and closed Endoriftia genome harbouring 162 coding sequences. **B,** Genomic islands 1 and 3 identified in the complete and closed genome are missing in the Polzin et al. (2019) and Perez & Juniper (2016) Endoriftia drafts.
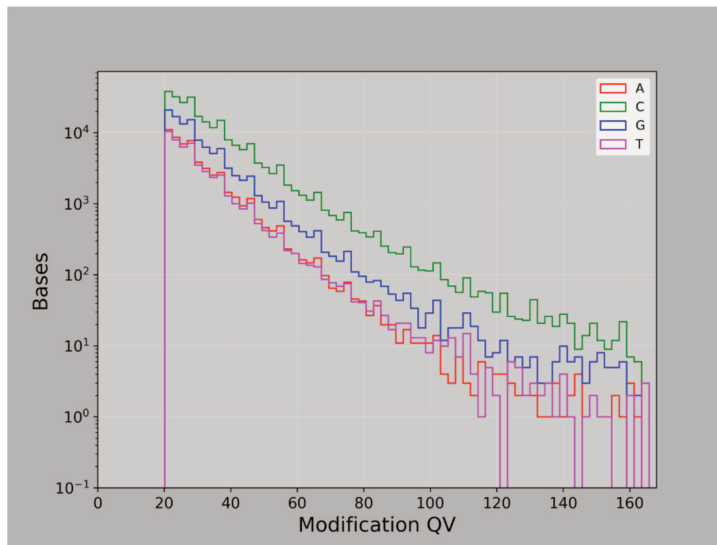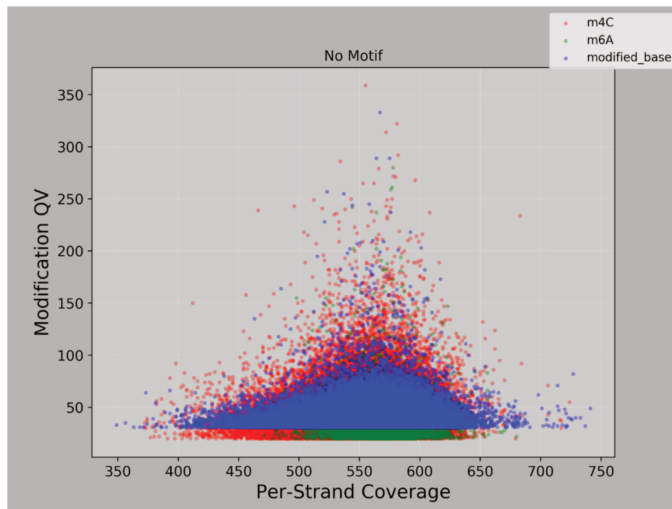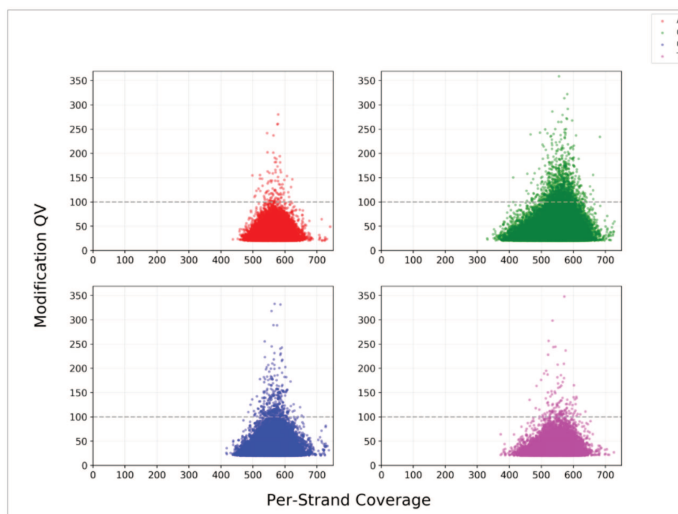
Supplementary Figure 6 – Modification quality value (QV) and scatter plots of sequencing coverage with the identified motif sites. The low QV **(A)**, absence of conserved methylation motifs **(B-C)**, as well as the incomplete methyltransferase domains identified in important genes related to epigenetic regulation in Endoriftia (see main text) suggest a lack of methylation in the host-associated Endoriftia genome herein described.

Synopsis of the publications

Chapter	Citation	Status	Contribution
1	Bright, Monika, Salvador Espada-Hinojosa, Ilias Lagkouvardos, and Jean-Marie Volland (2014). "The giant ciliate *Zoothamnium niveum* and Its thiotrophic epibiont *Candidatus* Thiobios zoothamnicoli: A model system to study interspecies cooperation." Frontiers in Microbiology 5. doi:10.3389/fmicb.2014.00145.	Published	Coauthor
2	Volland, Jean-Marie, Arno Schintlmeister, Helena Zambalos, Siegfried Reipert, Patricija Mozetič, Salvador Espada-Hinojosa, Valentina Turk, Michael Wagner, and Monika Bright (2018). "NanoSIMS and tissue autoradiography reveal symbiont carbon fixation and organic carbon transfer to giant ciliate host." The ISME Journal 12(3):714–727. doi:10.1038/s41396-018-0069-1.	Published	Coauthor
3	Espada-Hinojosa, Salvador, Judith Drexel, Julia Kesting, Edwin Kniha, Iason Pifeas, Lukas Schuster, Jean-Marie Volland, Helena C. Zambalos, and Monika Bright (2022). "Host-symbiont stress response to lack-of-sulfide in the giant ciliate mutualism." PLOS ONE 17(2): e0254910. doi:10.1371/journal.pone.0254910.	Published	First author
4	Bright, Monika, Salvador Espada-Hinojosa, Jean-Marie Volland, Judith Drexel, Julia Kesting, Ingrid Kolar, Denny Morchner, et al. (2019). "Thiotrophic bacterial symbiont Induces polyphenism in giant ciliate host *Zoothamnium niveum*." Scientific Reports 9(1):15081. doi:10.1038/s41598-019-51511-3.	Published	Coauthor
5	Espada-Hinojosa, Salvador, Clarissa Karthäuser, Abhishek Srivastava, Lukas Schuster, Teresa Winter, André Luiz De Oliveira, Frederik Schulz, Matthias Horn, Stefan Sievert, and Monika Bright (2024). "Comparative genomics of a vertically transmitted thiotrophic bacterial ectosymbiont and its close free-living relative." Molecular Ecology Resources 24(1): e13889. doi:10.1111/1755-0998.13889.	Published	First author
6	De Oliveira, André Luiz, Abhishek Srivastava, Salvador Espada-Hinojosa, and Monika Bright (2022). "The complete and closed genome of the facultative generalist *Candidatus* Endoriftia persephone from deep-sea hydrothermal vents." Molecular Ecology Resources 22(8): 3106–3123. doi:10.1111/1755-0998.13668.	Published	Coauthor